NASA Contractor Report 3510

Turbulent Boundary Layer Heat Transfer Experiments: Convex Curvature Effects Including Introduction and Recovery

T. W. Simon, R. J. Moffat,
J. P. Johnston, and W. M. Kays

GRANTS NSG-3124 and NAG 3-3
FEBRUARY 1982

NASA Contractor Report 3510

Turbulent Boundary Layer Heat Transfer Experiments: Convex Curvature Effects Including Introduction and Recovery

T. W. Simon, R. J. Moffat,
J. P. Johnston, and W. M. Kays
Stanford University
Stanford, California

Prepared for
Lewis Research Center
under Grants NSG-3124 and NAG 3-3

National Aeronautics
and Space Administration

**Scientific and Technical
Information Branch**

1982

TABLE OF CONTENTS

Nomenclature

A^+	Effective sublayer thickness in the Van Driest model.
$C_f/2$	Skin-friction coefficient, $\tau_w/\rho U_{pw}^2$.
C_p	Static pressure coefficient, $(P_s - P_{s,ref}) \Big/ \frac{1}{2} \rho U_{pw}^2$.
c_p	Specific heat.
F	Blowing fraction, $\rho_w V_w / \rho_\infty U_\infty$.
H	Shape factor, δ_1/δ_2.
HF	Heat flux meter signal.
i	Enthalpy.
K	Acceleration parameter, $\nu/U_{pw}^2 (dU_{pw}/ds)$.
K_i	Heat flux meter calibration constant.
k	Inverse radius of curvature, $1/R$.
ℓ	Mixing length.
ℓ_o	Flat-wall mixing length.
M	Mach number.
n	Distance normal to the test wall.
n^+	Nondimensional distance normal to the test wall, nu_τ/ν.
P'	An independent parameter.
P, P_s	Static pressure.
Pr	Prandtl number.
Pr_t	Turbulent Prandtl number.
P_t	Total pressure.
P_{sw}	Wall static pressure.
$\dot{q}''$	Heat flux.
q^2	Turbulent kinetic energy, $\overline{u'^2} + \overline{v'^2} + \overline{w'^2}$.
R	Radius of curvature.
R_{eff}	Effective radius of curvature.

$Re_x(Re_s)$ x(s)-Reynolds number, $U_{pw}x/\nu$ ($U_{pw}s/\nu$).

Re_{δ_2} Momentum thickness Reynolds number, $U_{pw}\delta 2/\nu$.

Re_{Δ_2} Enthalpy thickness Reynolds number, $U_{pw}\Delta_2/\nu$.

Ri Richardson number.

s Streamwise distance referenced to start of curvature.

S' Sensitivity coefficient (see App. A).

S_i Streamwise conductance for plate-plate heat flux.

S Stability parameter, $U/R/(\partial U/\partial n)$.

St Stanton number, $\dot{q}''/\rho C_p U_{pw}(T_w-T_\infty)$.

T Temperature.

T^+ Dimensionless temperature, $(T_w-T)u_\tau/(\dot{q}_w''/\rho c_p)$.

T_o Stagnation temperature.

U Mean streamwise velocity.

U^+ Nondimensional streamwise velocity, U/u_τ.

u' Fluctuating streamwise velocity.

u_τ Shear velocity, $\sqrt{\tau_w/\rho}$.

V Mean velocity normal to test wall.

v' Fluctuating velocity normal to the test wall.

w' Fluctuating cross-stream velocity.

y Distance normal to test wall.

Y_{crit} Distance from wall where $S = S_{crit}$.

Y_{sl} Distance from wall where extrapolated shear stress equals zero.

z Distance in spanwise direction.

Greek Letters

β Empirical constant in curvature mixing-length correlation.

β' Empirical constant in turbulent Prandtl number model.

γ The value of the turbulent Prandtl number for plane flow.

δ_{sl} Shear layer thickness (see Sec. 1.1).

δ^*_{sl} Displacement thickness integrated to δ_{sl}.

δ_{99} Thickness of boundary layer, where mean velocity is 99% of the potential for mean velocity.

δ_{995} Thickness of boundary layer, where mean velocity is 99.5% of the potential flow mean velocity.

δ_1 Displacement thickness, $\int_o^\infty ((U_p-U)/U_{pw})\, dn$.

δ_2 Momentum thickness, $\int_o^\infty (1+kn)U(U_p-U)/U_{pw}^2 dn$.

$\delta( )$ Uncertainty in ( ).

Δ_2 Enthalpy thickness (see App. B).

ε_H Turbulent diffusivity of thermal energy.

ε_M Turbulent diffusivity of momentum.

θ Angle of turn from start of curvature.

κ Karman constant, 0.41.

λ Mixing length proportionality factor.

P' An independent parameter.

ρ Density.

τ Total shear stress.

τ_w Surface shear stress.

Subscripts

p Of the potential flow.

pw Of the potential flow at the wall.

ref Reference.

w At the wall.

P' Of an independent parameter P'.

∞ In the free stream.

Chapter 1
INTRODUCTION

Turbulent boundary layers on convexly curved walls are encountered in many engineering applications: the forward part of a blunt body, leading edges of air intakes, blade passages of turbomachinery, aircraft wings, and rocket nozzles. Curved boundary layers with high heat transfer rates are encountered on gas turbine blades, where accurate prediction of and design for turbine blade heat loads are critical to the reliability and efficiency of modern high-performance engines. There is ample evidence that curvature affects heat transfer. Some of this effect has been attributed to the extra rates of strain associated with streamwise curvature which significantly affect the structure of turbulent boundary layers [2,35] and the heat transfer rates [13,32].

The primary objective of this experiment was to measure the effect of convex curvature on the heat transfer rate over a representative domain of initial and boundary conditions. The work was undertaken as part of an ongoing series of projects at Stanford University sponsored by NASA-Lewis Labs. The motivating problem was the need to understand the mechanisms and accurately predict the heat transfer rates on gas turbine blades.

When the curvature project began, the state of the art for design heat-load calculations was the computer code STAN5 [1]. This code solves the partial differential equations which govern transport of thermal energy and momentum in boundary layers. The quality of the predictions it makes is dependent upon the applicability of the Reynolds stress model it uses. Though the stress modeling of STAN5 is quite simple, it is a trusted program for use within its data base, because its Reynolds stress model is supported with empirical input from twelve years of careful experimentation at Stanford. STAN5 accurately accounts for streamwise acceleration or deceleration and/or transpiration blowing or suction. Presently, however, it does not account for streamwise curvature. The purpose of the Stanford curvature program is to add curvature to its useful domain.

During the course of the work, numerous colleagues made significant contributions. Dr. J. Gillis had a major role in the construction and qualification of the facility. Robin A. Birch aided in the design and construction of much of the facility, resulting in a very reliable apparatus. Kokichi Furuhama, Michael Glass, and Vanessa MacLaren assisted with the qualification of the facility and the updating of the data-reduction programs. Professor Shinji Hinami, a Visiting Professor, made many helpful suggestions.

1.1 Previous Research

A comprehensive survey of the literature on curvature effects, prior to 1972, was given by Bradshaw (2). He pointed out that the effect of curvature is about ten times as strong as one would predict from a thin shear layer, eddy-viscosity model by simply adding the extra rate of strain $\partial V/\partial x$ to the existing strain field.

Experimental work on the effects of curvature dates back to the days of Ludwig Prandtl. One early study by Wilcken [3], a student of Prandtl, was the first documented study of curvature effects where the facility was designed to keep secondary flow effects to a minimum. At that time, Prandtl had put forth a stability argument for curvature, Wilcken was to test it.

> "Because the various parts of the boundary layer are variously affected by centrifugal force in the presence of a curved surface, a concave surface produces a tendency to force the fast parts of the flow toward the surface and the slow parts away from it. This tendency favors the exchange of the slow layers next to the surface with the faster ones on the inside of the flow. Thus, it reinforces the already existing turbulent exchange procedure. The contrary is the case for the convex faces. Here the centrifugal force has a stabilizing effect, reducing the turbulence.

Prandtl also had developed the early form of a mixing length model, then called "free path," for a flat plate. Wilcken, though admitting some secondary flow influence, found that curvature significantly affected

the "free path lengths." He stated, "Boundary layer events on curved surfaces should be ascribed more importance than has generally been the case up to the present." Curved flow research continued under Prandtl at the Kaiser Wilhelm Institute for Flow Research with the studies of Wendt [4] and Schmidbauer [5]. The general conclusion was that, even for weak curvature, the boundary layer hydrodynamics are significantly affected.

The next documented study was in a curved channel, where the flow could become fully developed. This study by Wattendorf [6] in 1934 showed that the fully developed flow was significantly influenced by curvature, although the overall pressure drop was not. Wattendorf also found, from his mean velocity and wall static pressures measurements, that the power, n, in the power-law velocity profile, $U^+ = cy^{+1/n}$, decreases with stronger convex curvature and increases for stronger concave curvature. His descriptor of the strength of curvature was the parameter ν/Ru_τ, where R was positive for concave curvature.

In 1937, Clauser and Clauser [7] investigated the effect of curvature on the transition from laminar to turbulent flow. This is the first time that hot-wire anemometry had been applied to curved flows. They found that stabilizing convex curvature increased the critical Reynolds number and delayed transition. Their observations showed that, on typical airfoils of the time, convex curvature might double the critical Reynolds number. Hans Liepmann [8] extended the study of the effect of curvature on transition to very weak curvature ($0 < \delta_2/R < 0.001$). In this range it was found that transition was not affected by convex curvature but was affected by concave curvature. This indicated that the process of transition was different for the concave wall than for the flat or convex wall.

In 1955, Frank Kreith [9] performed a clever heat transfer test that showed quite conclusively that the heat transport from a concave wall was considerably more than from a convex wall. For his channel flow, he concluded that curvature effects scaled on U/r, the forced vortex parameter. No measurements of local heat transfer rates were taken. The hydrodynamics of a fully developed, curved, turbulent channel flow similar to the Kreith facility were studied in detail by

Eskinazi and Yeh [10]. Using hot-wire anemometry, they measured the downstream development of profiles of streamwise velocity fluctuations and, for the fully developed flow, measured the profiles of $\overline{u'^2}$, $\overline{v'^2}$, and $\overline{u'v'}$. They stated that one of the most important influences of curvature is on the $\overline{v'^2}$-production term $-\overline{u'v'}(U/r)$. They noted that near the convex wall $\overline{u'v'}$ was positive, indicating a suppression (negative production) of $\overline{v'^2}$. Their spectral measurements of $\overline{u'^2}$ and $\overline{v'^2}$ showed that the decrease in turbulent mixing activity was largest in the low-wave-number range.

The first curved-flow heat transfer test with wall-measured heat flux data was that of Schneider and Wade [11]. With plug-type heat flow transducers they measured local heat fluxes on a convex wall that were 50% of the predicted flat-wall values and considerably less than would be predicted by the model of Kreith [9]. Their tunnel aspect ratio was 1.0, so considerable contamination by secondary flow was probable.

V. C. Patel [12] studied the hydrodynamics of the flow through a 90° curved duct similar to the facility used in the Schneider and Wade study, except that the aspect ratio was 5.0. No attempt was made to separate streamwise acceleration and deceleration from the other effects of streamwise curvature, and there was some confusion about whether the change in the mean velocity profiles was due to curvature or the local acceleration and deceleration within the bend. Patel measured only mean quantities, which, even with the increased aspect ratio, may have been influenced by secondary flows. He noted that curvature affects the shape factor and, therefore, the rate of entrainment.

Also in 1968, Thomann [13], at the Aeronautical Research Institute of Sweden, made detailed local heat transfer measurements on surfaces that were straight and convexly and concavely curved. The Thomann study was performed in a wind tunnel with a freestream Mach number of 2.5, uniform static pressure on the test wall, and a boundary layer thickness-to-radius of curvature ratio of $\delta_{99}/R \approx 0.02$. The resultant effect of curvature was found to be an increase in convective heat flux of $\approx$ 20% for the concave case and a decrease of $\approx$ 15% for the convex case with respect to the flat-wall case (see Fig. 1-1). Since the

Thomann study was done in a supersonic freestream, significant compressible effects were present. As discussed by Bradshaw [2], compression or dilation produces strong extra rate-of-strain effects in the boundary layer which may alter the turbulent transport process in much the same fashion as does curvature.

In 1969, Bradshaw [14] discussed the analogy between streamwise curvature and buoyancy in turbulent shear flow and introduced a modification of the Richardson number used in meteorological work to curved and rotating flow computation. The gradient Richardson number for curved flows is written: $R_i = 2S(1+S)$ where S is the stability parameter, $S = (U/R)/(\partial U/\partial n)$, positive for the convex wall and negative for the concave wall. He then proposed [14,15] that the Monin-Obouhkov formula for the correlation of the apparent mixing length with small buoyancy effects $\ell/\ell_o = 1 - \beta Ri$ could be used to model the effects of weak curvature. This approach met with considerable success. In fact, the value of the constant β could be inferred by analogy from meteorological experiments in stably and unstably stratified boundary layers. It is generally agreed to be the order 10.

So and Mellor [16,17,18] published results from a very detailed hydrodynamic experiment on curved-wall boundary layers. In their experiment, the ratio of boundary layer thickness to radius of curvature ratio was $\delta_{99}/R \approx 0.07$, and the aspect ratio was ~ 8.0. Because of an imaginative design which employed wall jets, secondary flows were kept acceptably small. Profiles of all the Reynolds stresses were measured. On the convex wall it was found that the turbulent shear stress was "turned off" in the outer half of the boundary layer. Over the concave wall, they found evidence of a stationary system of longitudinal vortices, analogous to those formed between rotating cylinders. Wall shear stress was inferred from a Clauser plot technique, but the turbulent shear stress profile was not measured close enough to the wall to enable them to check the wall value by extrapolation. The Clauser plot technique has since become an accepted method for inferring wall shear stress and has been verified by later experimenters, e.g., Gillis [35].

Ellis and Joubert [19] of the University of Melbourne measured profiles of mean velocity in boundary layers of a curved duct. They

noted that the width of the logarithmic zone was curvature-dependent. Convex curvature caused the velocity profile to become wake-like at a lower value of n^+ and the opposite for concave. They searched for, but could not find, similarity of the mean flow, as represented by a defect type law for either the fully developed, curved, turbulent channel flow or the outer regions of convex wall boundary layers. On the concave surface, Ellis and Joubert found evidence of Taylor-Görtler vortices.

During the 1970s, Bradshaw undertook a series of experiments on curvature effects. The first experiment was one of very weak curvature ($\delta_{995}/R = 0.01$). The early results were presented by Meroney [20] and the final results by Hoffmann [21]. Mean and turbulence data were taken in a curved duct of 30° bend and aspect ratio of 6.0. No attempt was made to separate the weak acceleration/deceleration effects. The data consisted of mean quantities and the important higher-order quantities through order 4. Spanwise variations of skin friction due to weak Taylor-Görtler cellular activity were observed on the concave wall; they measured variations of 20% in local skin-friction coefficient. Later experiments on curvature at the Imperial College included the recovery from an "impulse" of curvature in a curved duct (Smits, Young, and Bradshaw [22]) and in an axisymmetric flare (Smits, Eaton, and Bradshaw [23]). The second case showed the combined effects of sustained lateral divegence and recovery from curvature. It was found that Taylor-Görtler cells were established in the curved duct but not in the axisymmetric flare, indicating an effect of lateral divergence. In both studies, mean data and fluctuating data through order 4 were taken. During this same time, Castro and Bradshaw [24] were studying the convexly curved, free-mixing layer.

Effects of mild curvature were studied by Ramaprian and Shivaprashad [25,26,27,28]. Their test facility was very similar to the Hoffmann and Bradshaw facility, with the notable exception of an aspect ratio of 2.5. They did not observe Taylor-Görtler cells on the concave wall, contrary to the findings of Hoffmann and Bradshaw. The authors admit that this difference may be attributed to significant secondary flows.

Detailed measurements of the hydrodynamics of a curved channel flow were made by Hunt and Joubert [29] in 1979. The data for this study were taken in an apparatus in which a duct downstream of the nozzle could be straight or bent into a large-radius curve. The channel was shallow, allowing the convex and concave boundary layers to merge about 40% of the distance around the 45° bend. The curve started at the exit of the nozzle, so the ratio of boundary layer thickness to radius of curvature was extremely small ($\delta_{99}/R \simeq 0.005$) at the start of curvature, then grew rapidly around the bend. The aspect ratio was large, 13.2 to 1.0, to minimize secondary flow effects. Roll-cell vortices of the Taylor-Görtler type were observed in the channel just off the concave wall. These cells resulted in variations in skin friction across the span of ± 4%. Data taken included mean velocity profiles and profiles of the important Reynolds stresses. It was found that the measured Reynolds shear stress extrapolated to the convex wall agreed with skin friction values found with the Clauser plot technique. Profiles at the end of the test region were fully developed in the mean quantities and nearly fully developed in the turbulence quantities.

In 1977, Brinich and Graham [30] measured mean velocity and temperature profiles and wall heat transfer rates in a curved channel similar to the one in which Eskinazi and Yeh [10] took hydrodynamic data. The heat transfer facility, however, had an aspect ratio of 6.0, and considerable secondary flow influence was observed. Nevertheless, they noted an increase in the heat transfer rate on the outer (concave) wall and a slight decrease on the inner (convex) wall. Their temperature profiles reached an asymptotic shape characterized by a skew of the peak toward the concave wall, giving a much steeper temperature gradient on the concave than on the convex wall. Temperature profiles were not plotted in inner coordinates, so it is not known whether they showed a log-law relationship.

R. M. C. So [31] continued his curvature work beyond the hydrodynamic studies discussed earlier [16,17,18] with an analytical prediction of the effect of curvature on the turbulent Prandtl number. He developed the rather simple relationship:

$$\frac{\varepsilon_M}{\varepsilon_H} = \frac{1 - \frac{1}{2}\beta' Ri\left(1 - \frac{1}{4\gamma^2}\right)}{1 - \frac{1}{8}\beta'\left(\sqrt{1+4Ri} - 1\right)\left(1 + \frac{1}{2\gamma}\right)}$$

where γ is the value of the turbulent Prandtl number of a corresponding plane flow. The value $\beta' = 6.0$ has been found to give the best correlations with curved-flow data, swirling-flow data, and meteorological data [55,56,57]. This equation gives an increase of $\varepsilon_M/\varepsilon_H$ for $Ri > 0$ (convex) and $Pr < 1$. This ratio will decrease if either one of the two inequalities is reversed. For air flowing over a convex wall, the diffusivity of thermal energy decreases faster than the eddy diffusivity. Since the Prandtl number for air is nearly unity, the deviation from Reynolds analogy ($\varepsilon_M/\varepsilon_H = 1$) is predicted by the above equation to be small.

Recently, Mayle, Blair, and Kopper [32] measured local heat transfer rates in a curved duct which had an aspect ratio of 4.25. Their study was with low-velocity air ($M \simeq 0.06$ as opposed to the high-velocity study of Thomann [13]), in which the test wall static pressure and temperature were uniform. The ratio of boundary layer thickness to radius of curvature at the start of the curve was ~ 0.01. Their findings (see Fig. 1-2), confirming those of Thomann, showed a decrease in the wall heat flux of $\approx 20\%$ for the convex wall and an increase of $\approx 33\%$ for the concave wall relative to the flat-wall heat flux prediction of Reynolds, Kays, and Kline [33].

Previous heat transfer studies dealt only with the curved region, none reported results of recovery downstream of the curve. The present investigation is the first time the effects on heat transfer of both the introduction of and recovery from curvature have been investigated. When looking at the problem of gas turbine blade cooling or many other applications where curvature effects on heat transfer are significant, one realizes that the regions of strong curvature are often followed by regions of weak or no curvature, so the recovery effects are as pertinent as the effects of the introduction of curvature.

The present heat transfer results are from a program studying both the heat transfer and fluid mechanics of a convexly curved flow. Since heat transport is by turbulent motion, the hydrodynamic study is an essential input to the heat transfer study. Detailed results of the hydrodynamic study have been reported by Gillis and Johnston [34,35]. Their work was performed on essentially the same tunnel configuration as the present study (see Fig. 2-1) and with boundary layer thickness-to-radius of curvature ratios of 0.10 and 0.05, two of the cases presented herein. The Gillis and Johnston results are summarized in Figs. 1-3 through 1-7. Fig. 1-3 shows the effect of convex curvature on skin friction, as calculated using a Clauser plot. The initial response to the introduction of curvature was fast, and the behavior was seemingly near-asymptotic. At the end of the curved region ($\simeq$ 16 boundary layer thicknesses downstream from the start of curvature for the δ_{99}/R = 0.10 case), the skin friction reached a value $\sim$ 30% less than the flat-wall predicted value. In the recovery region, the return of the skin friction was slow. After $\sim$ 20 boundary layer thicknesses from the start of the recovery region, the skin friction was still $\sim$ 20-25% below the flat-wall value. They also found that, though the boundary layer thickness at the beginning of curvature differed by a factor of two for the two experiments, the variation of $C_f/2$ with distance within the curved region was surprisingly similar for the two cases. Fig. 1-4, a typical plot of mean velocity profiles in wall coordinates, shows that the log region shortens within the curved section but is always discernibile. The effect of convex curvature on profiles of the turbulence quantities ($\overline{u'^2}$, $\overline{q^2}$, and $\overline{u'v'}$) is shown on Figs. 1-5, 1-6, and 1-7, respectively. Within the curved region, the turbulence activity declined quickly throughout the boundary layer, but especially in the outer regions, to a near self-similar profile. The recovery to a normal flat-wall profile was slow and appears to be by propagation from the wall. The slow growth of the turbulence profiles in the recovery region may be responsible for the slow return of the skin friction to flat-wall values. Fig. 1-7 shows that, at the beginning of curvature, the shear stress in the outer portion of the boundary layer changes sign for a short distance. This term is linked to the production of TKE, a sign-reversal indicates a negative production of TKE in this region.

Gillis and Johnston identified a parameter called the "shear layer thickness," the n-distance of the extrapolated shear stress profile (see Fig. 1-8) labeled "δ_{sl}." They proposed a model by which to visualize the strongly curved boundary layer: a two-layer model shown in Fig. 1-9. The inner layer is characterized by non-zero TKE and shear stress, a typical boundary layer, but constrained in thickness to δ_{sl}, which remains essentially constant within the curve. The outer layer is characterized by non-zero TKE but essentially zero shear stress. The outer layer is the decaying residue of the upstream boundary layer. At the beginning of the recovery region, the restriction on δ_{sl} due to curvature is lifted and the inner layer grows within what remains of the outer layer. The results of the present heat transfer study are consistent with this model.

The hydrodynamic study of Gillis and Johnston is part of an overall program involving heat transfer rates on smooth, convexly curved surfaces. The present experiments build upon their study of the hydrodynamic processes, investigating the heat transfer processes through structurally similar, but heated, boundary layers.

1.2 Objectives

The final objective of the Stanford curvature program is to add curvature to the list of effects that can be appropriately predicted with turbulent boundary layer prediction programs, e.g., STAN5 [1]. With this goal in mind, the objectives of the present study were to:

1. Accurately measure wall heat transfer rates from a smooth, convexly curved wall and downstream flat recovery plate over a large enough domain of carefully controlled initial and boundary conditions so that the eventual model can be used with minimal extrapolation.
2. Build upon the understanding of the curved boundary layer gained during the Gillis and Johnston study [35] and others listed in Section 1.1. For this study a series of 15 runs were made with differing initial and boundary conditions to learn about the sensitivity of the curvature effect to various parameters thought to be important. This will aid in developing a prediction model based on maximum physical insight.

3. Test the preliminary prediction model proposed by Gillis and Johnston [35], making changes where appropriate.
4. Construct a heat transfer facility that is sufficiently flexible to accomplish the above objectives and future objectives of the overall program, specifically, convex curvature with discrete jet injection, which simulates modern gas turbine film-cooling geometries.

1.3 The Experiment

In the following experiment, thermal and hydrodynamic boundary layers were grown on a flat preplate, then were introduced to a 90°, 45 cm radius of curvature convex wall, followed by a recovery wall. The wall temperature was maintained uniform, and the static pressure on the test wall was controlled to a prescribed function of downstram distance, either uniform or constant $K\ (\nu/U_{pw}^2 \cdot dU_{pw}/ds)$. Detailed wall heat flux data as well as profiles of velocity and temperature were measured in the developing, curved, and recovery regions. The initial and boundary conditions were varied to determine sensitivity to various parameters. The 15 cases in the present study investigated the sensitivity of the effect of convex curvature on heat transfer to:

a) Initial boundary layer thickness.
b) Magnitude of free-stream velocity.
c) Free-stream acceleration.
d) Location of the beginning of heating with respect to the beginning of curvature or the beginning of recovery.
e) Maturity of the momentum boundary layer at the beginning of curvature.

One other parameter which should be varied systematically is the radius of curvature of the test wall. The cost and complexity of a test facility with such flexibility precluded this entry.

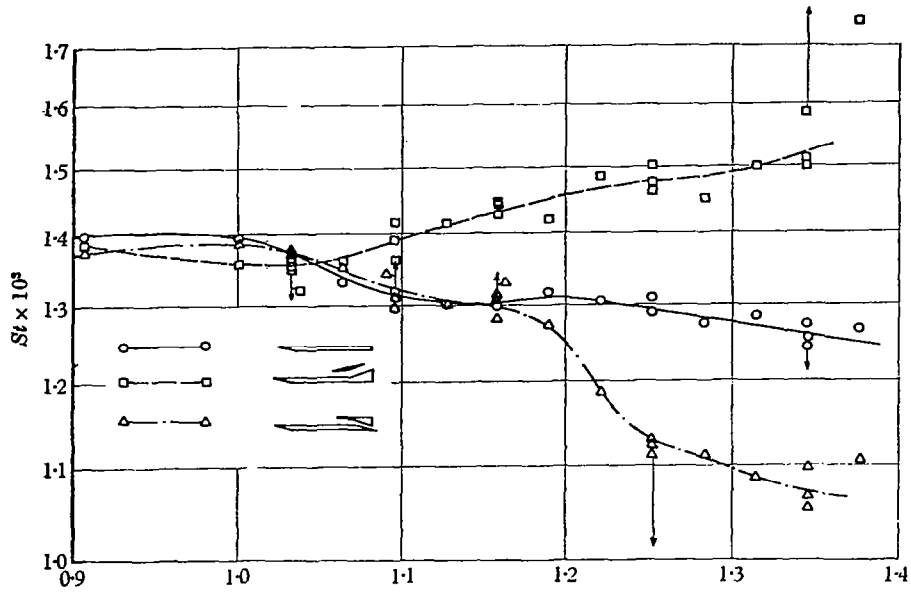

Fig. 1-1. Stanton number versus streamwise distance, M = 2.5, $T_o - T_w$ = 77.5 K , from Thomann [13].

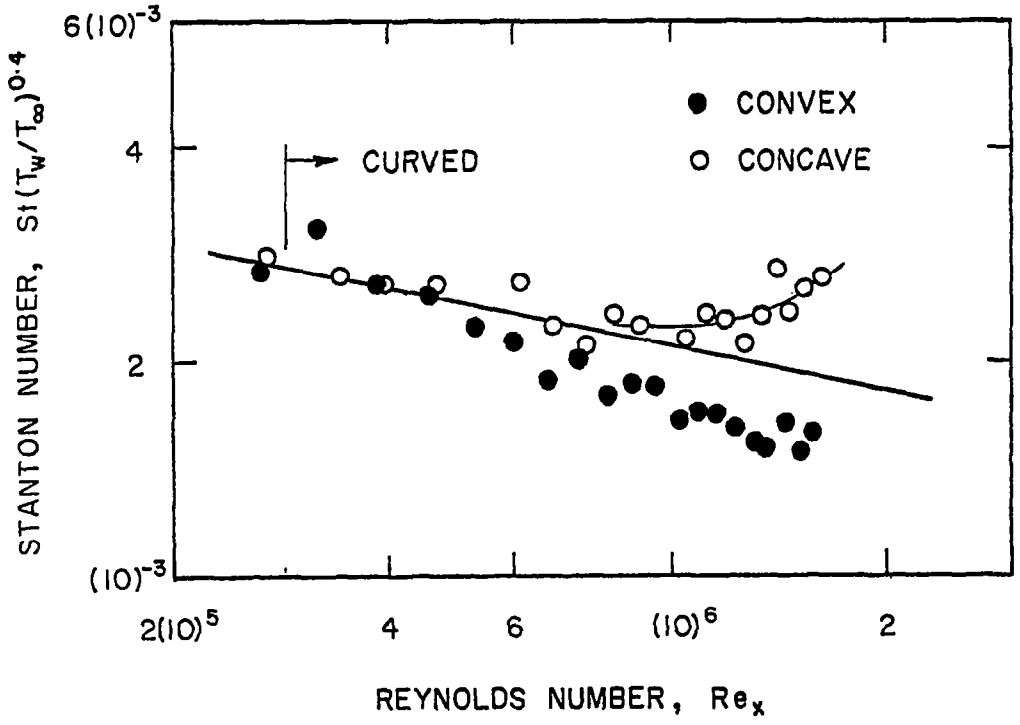

Fig. 1-2. Stanton number versus x-Reynolds number, from Mayle, Blair, and K opper [32].

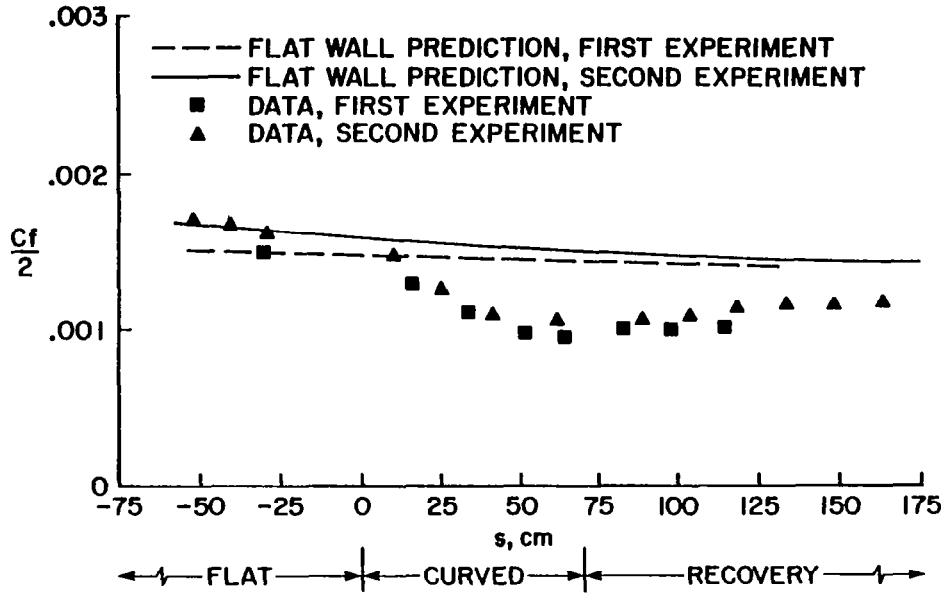

Fig. 1-3. Skin friction versus streamwise distance, δ_{99}/R = 0.10, from Gillis and Johnston [35].

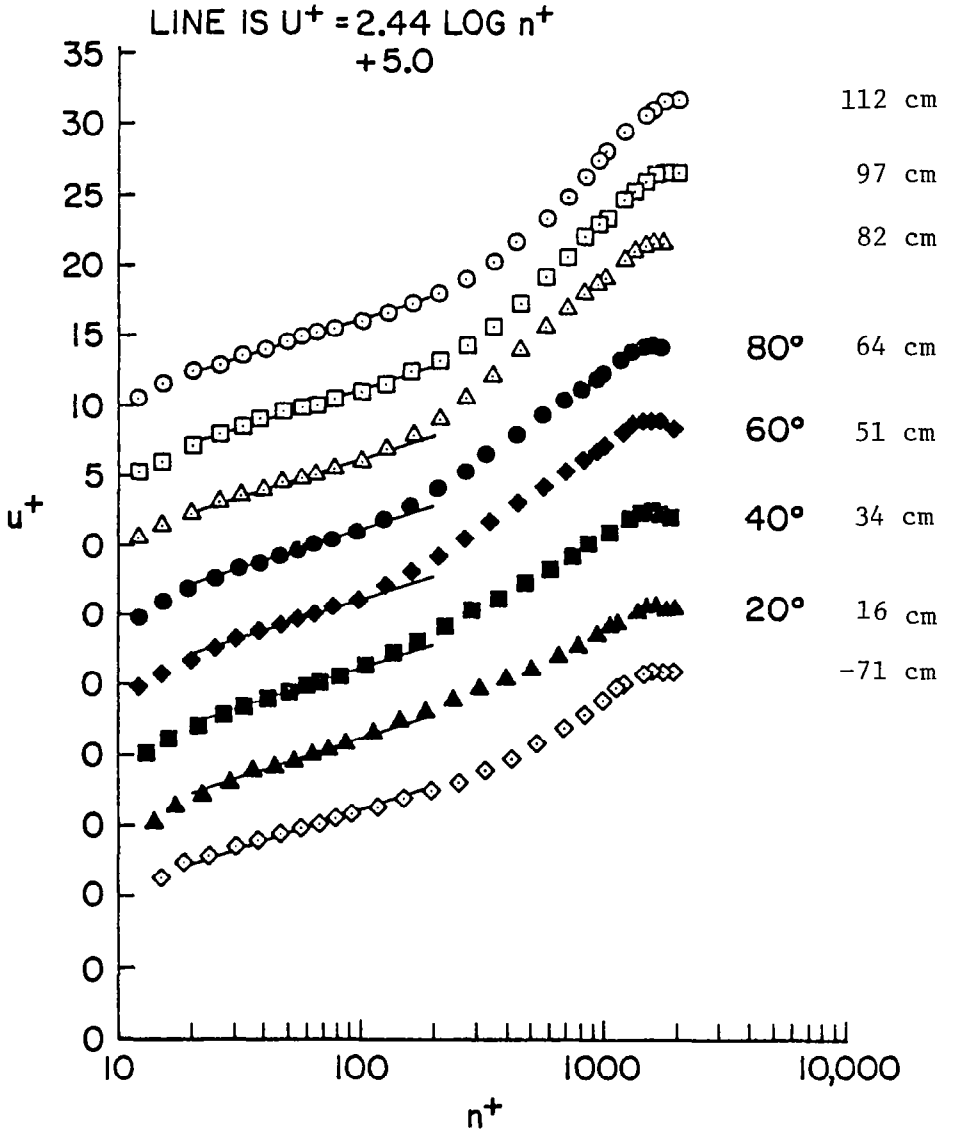

Fig. 1-4. Mean velocity profiles in wall coordinates, δ_{99}/R = 0.10, from Gillis and Johnston [35].

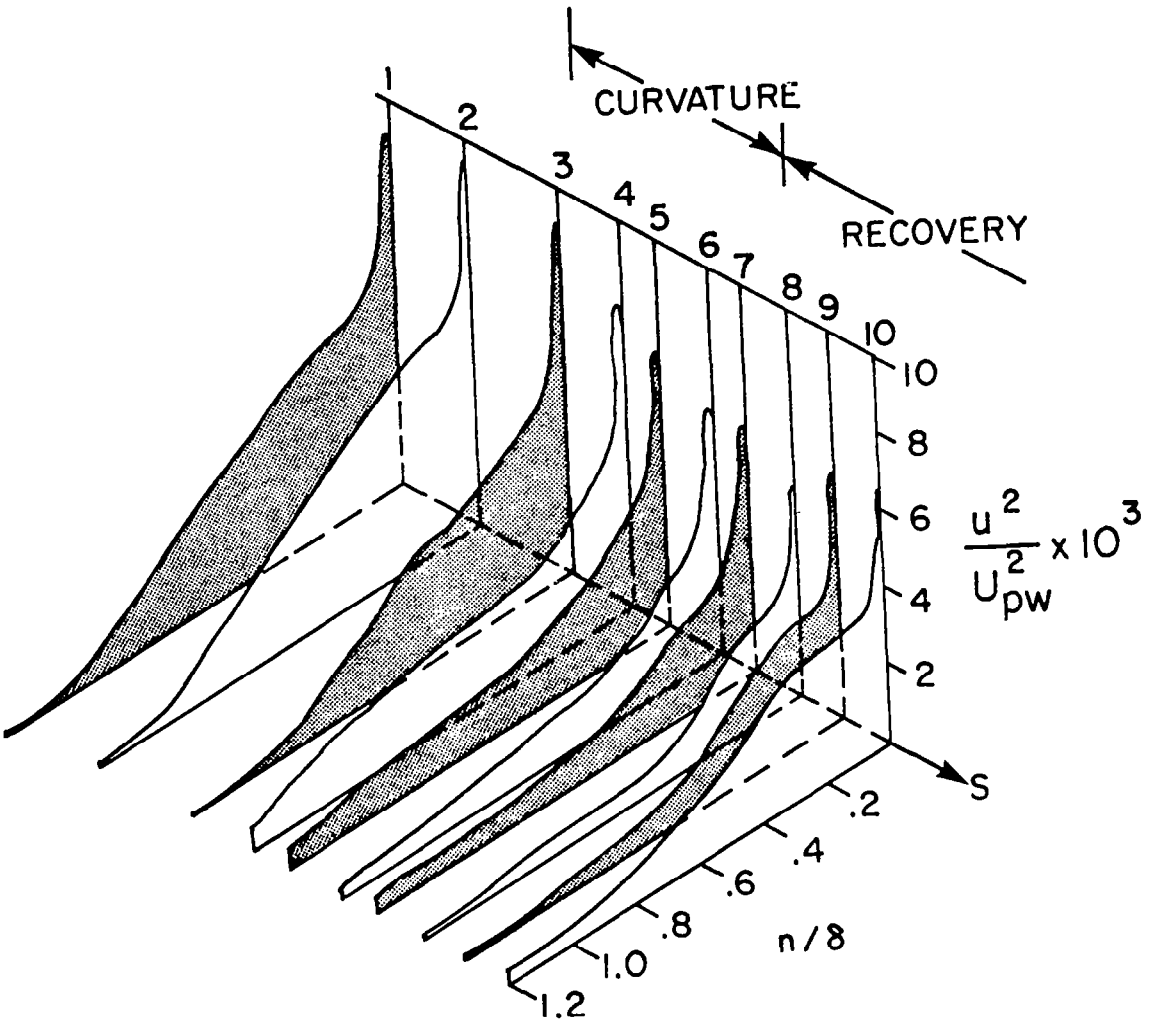

Fig. 1-5. Streamwise turbulence intensity profiles versus distance in the streamwise direction, $\delta_{99}/R = 0.10$, from Gillis and Johnston [35].

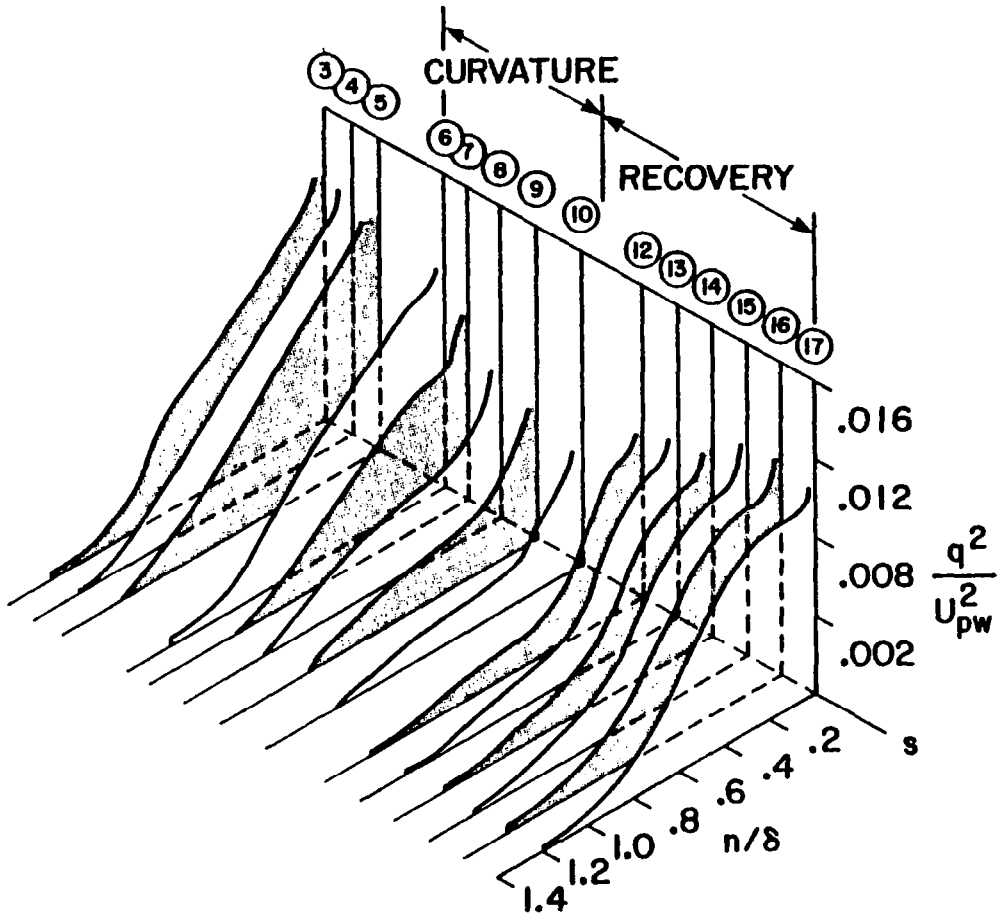

Fig. 1-6. T.K.E. profiles versus distance in the streamwise direction, $\delta_{99}/R = 0.10$, from Gillis and Johnston [35].

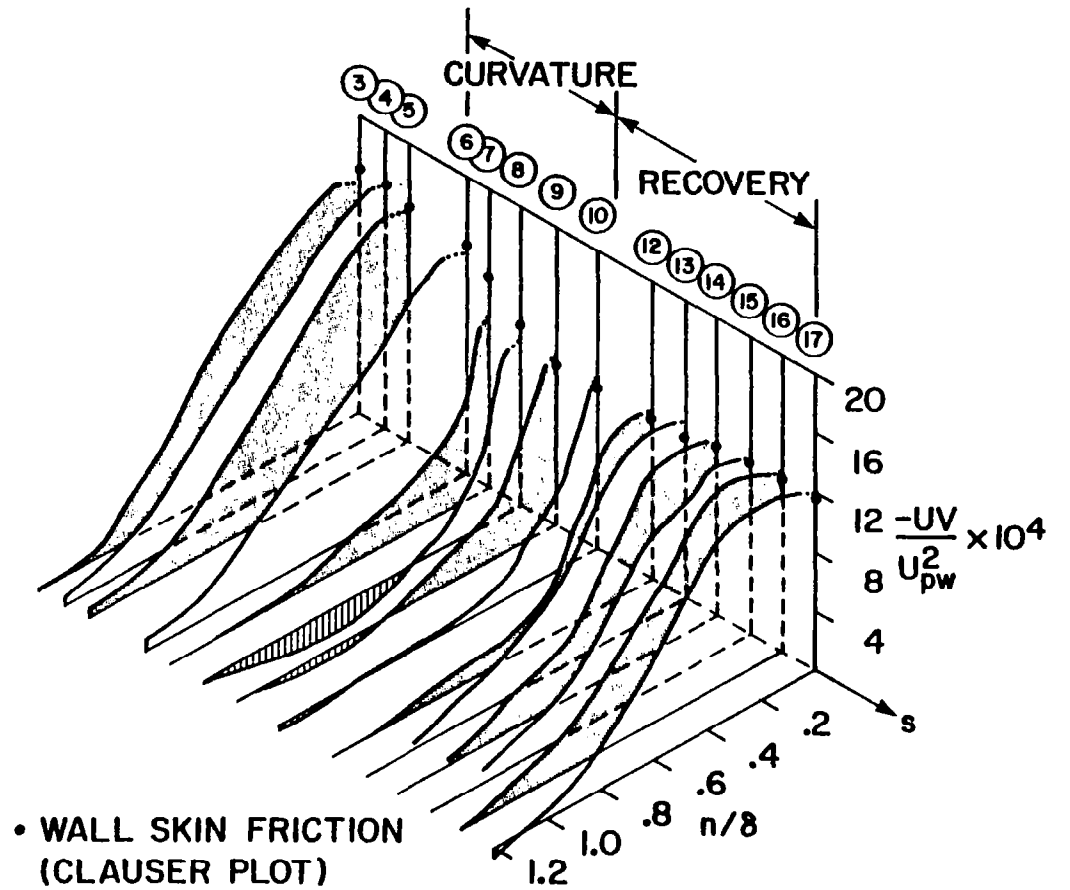

Fig. 1-7. Reynolds shear stress profiles versus distance in the streamwise direction, $\delta_{99}/R = 0.10$, from Gillis and Johnston [35].

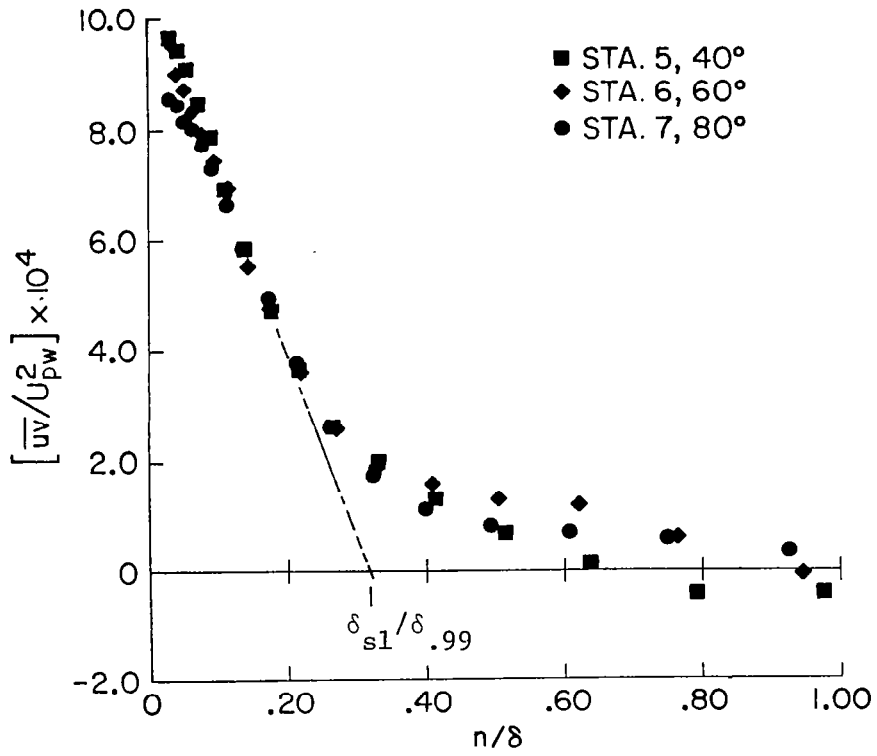

Fig. 1-8. Reynolds shear stress profile showing "δ_{sl}", from Gillis and Johnston [35].

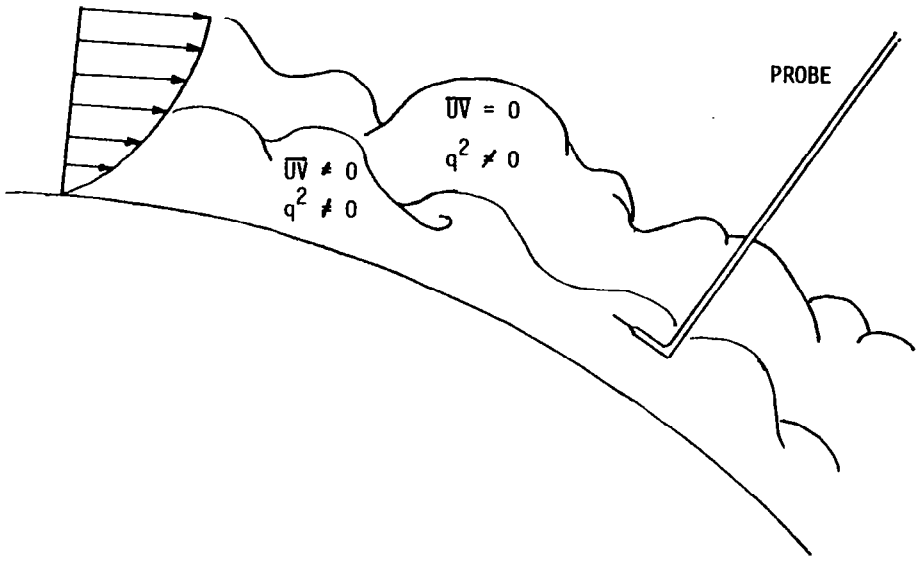

Fig. 1-9. Two-layer curved boundary layer structure, from Gillis and Johnston [35].

Chapter 2
THE EXPERIMENTAL APPARATUS

The test facility used in the present heat transfer study was used in the hydrodynamic study of Gillis and Johnston* [35]. The hydrodynamic aspects of the tunnel, discussed in detail in Ref. 35, are summarized below. Systems added to the facility to broaden the hydrodynamic operating domain and systems specific to the heat transfer measurements are discussed in detail.

2.1 General Description

A curved-wall heat transfer facility has been constructed (Fig. 2-1) that allows development of a smooth, flat-wall, heated boundary layer upstream of a 90° bend of 45 cm radius of curvature followed by a flat-wall recovery. There were five circuits to the facility:

(1) The main loop: from the main fan, through the return ducting, oblique header, heat exchanger and screen pack and contraction nozzle combination, then into the test regions and back to the main fan via a plenum box.

(2) The charging loop: discharge flow to the room via louvres and slots then return to the tunnel via the filter box and charging blower.

(3) The suction loop: suction from the preplate, reinjected to the plenum box via the suction fan.

(4) The cooling water loop for the heat exchanger: a 303ℓ capacity water tank, water supply, and discharge lines to and from the tank, for circulation and for make-up.

(5) The hot water loop: heated the preplate and recovery walls, using two temperature-controlled water heaters.

*Cases 2 and 3 of Ref. 35.

2.2 Hydrodynamic Aspects of the Facility

The main flow was driven by a fan which delivered air to an oblique header that turned the flow into a heat exchanger. The flow passed through the exchanger, a screen pack, and an 11:1 contraction nozzle before entering the tunnel test region. Details of the screen pack and nozzle can be found in Ref. 44. Flow exited the test region into a plenum box, which supplied the main fan. The tunnel velocity was controlled by changing pulleys and belts on the fan and motor, and could be varied from 3.5 m/s to 26 m/s.

The developing region was 16.5 cm by 56 cm in cross section and ~ 200 cm long. The outer wall was straight and adjustable by pivoting about its upstream edge so that the static pressure could be made nearly uniform, allowing the growth of a normal flat-wall (non-accelerated) boundary layer. A 15 cm section of the test wall in the preplate beginning ~ 84 cm upstream of the start of curvature was constructed with ~ 2000-1/16 inch diameter holes uniformly spaced across the span and connected to an auxiliary fan (Fig. 2-1a) allowing boundary layer suction. This system extended the operating domain to thinner boundary layers and very low momentum thickness Reynolds number laminar and transitional boundary layers. When a thick, fully turbulent, two-dimensional boundary layer was desired at the beginning of curvature, the boundary layer was tripped just downstream of the nozzle. When the suction fan was operating to produce thinner boundary layers, the trip was located downstream of the suction holes.

Within the curved region, the flexible outer (concave) wall was adjusted so that the static pressure on the convex test wall followed the desired function of streamwise distance, usually uniform. When the static pressure on the test wall was uniform, there was no streamwise acceleration of the inner region of the boundary layer. Cases with acceleration were set up by trial and error until a nearly constant K was achieved within the curve. Twenty-six 0.025-inch (0.6 mm) diameter static pressure tap holes distributed in both the streamwise and spanwise directions were used for these adjustments. The tunnel was maintained slightly above ambient pressure with the charging blower (Fig. 2-1a), which took air from the room via a filter box. Because the

tunnel was pressurized, separation of the boundary layer on the concave wall, upon entering the curved region, could be prevented by discharge of the boundary layer fluid through a series of seven spanwise louvres. Secondary flows in and downstream of the bend were reduced by peeling off the sidewall boundary layers upon entry to the bend, by using sidewall slots within the bend, and by installing boundary layer fences on the convex surface near the side walls beyond the heated portion of the span. The secondary flow control was developed by J. C. Gillis. The details of the evolution and a more thorough discussion of the final design are presented in Ref. 35.

The recovery region was a straight tunnel of dimensions 15 cm by 53 cm and approximately 125 cm long. Boundary layer fences continued downstream of the curve for the first 60 cm of recovery length.

The outer walls were constructed so that profile data could be taken at five stations in the developing region, six stations within the curve, and six stations within the recovery region. Stations typically had seven spanwise positions for checking two-dimensionality.

2.3 Heat Transfer Aspects of the Facility

The test wall was constructed of copper and segmented and instrumented so that the local heat flux could be measured on the preplate, the convexly curved wall and the recovery wall.

The preplate was divided into 48 segments, each 2.5 cm long in the streamwise direction and each instrumented with an embedded iron-constantan thermocouple. The last 24 segments were heated with circulating hot water (Fig. 2-1b) and were instrumented for direct heat flux measurement. Each segment consisted of a 3 mm thick copper plate backed with 3-0.5 mm thick bakelite sheets, the center one containing a silver-constantan thermopile at the centerline location. The thermopile signal was correlated with heat flux by calibration (see Appendix C for calibration details). The heated water circulated through a 1.2 × 2.5 cm copper waveguide channel behind the bakelite sheets. This wall was constructed in 1960 and had been used in the studies of Refs. 43 through 47. Although the circulating water was isothermal, a film buildup over the years prevented the test wall from being perfectly isothermal.

Small segment-to-segment temperature differences existed, typically smaller than 0.2°C, which resulted in scatter of the Stanton number data of approximately 2%. This scatter was not considered in the uncertainty analysis. The plate-to-plate streamwise conductance for each gap within the preplate was measured during the heat flux meter calibration. These values were then used in the data-reduction program to correct for small plate-to-plate heat flows.

The convex wall was constructed of 6 mm thick copper stock segmented into 5 cm lengths in the streamwise direction. Each segment was electrically heated, allowing steady-state measurement of the spanwise-averaged wall heat flux by energy-balance techniques. Data reduction included correction for: plate-to-plate heat conduction, losses to the support assembly, and radiation losses. The plate-to-plate conductances were calculated. Gap conductances at the ends of the plates and for the preplate/curve and curve/recovery wall gaps were measured during preliminary tests where the temperature drop across the gap under study was made artificially large and the other heat flow paths were insulated or controlled to zero ΔT. The power delivered to each plate, less corrections for other losses, was presumed to be conducted across the gap with the measured ΔT. Gap-conductance uncertainties were incorporated into the uncertainty analysis; they are typically small contributors to the overall uncertainty. The 14 segments of the curved wall were supported by ten circumferential phenolic ribs. The ends of the ribs were held by a large aluminum frame. The curve was cut by first adding aluminum ribs (see Fig. 2-2) for additional support then turning the entire assembly while cutting the 90° arc with a single-point cutting tool. After the machining operation, the aluminum support ribs and side rail spacers were removed. The center used for the machining operation was part of the frame and was the center of rotation of an arm used for traversing the various boundary layer probes. The heating elements for each curved wall segment were two 46 cm lengths of AWG #28 chromel wire embedded into parallel heater grooves and epoxy-bonded. At one end of each plate, the two embedded wires were connected by a large copper bus bar and at the other end were connected to the output terminal of a variable transformer. The overall heater resistance was about 8 Ω.

To have well-stabilized power to the plates, the building power was passed through two voltage regulators in series. The output of the second regulator was connected to the input of a step-down transformer. This reduced the voltage to typically ~ 40 volts AC. Next in line were powerstats that controlled each test plate power. This arrangement allowed individual control of the power over a wide range with accuracy. All electrical power cables were enclosed inside conduit to minimize interference with instrumentation cables. A switching arrangement permitted the insertion of a precision wattmeter into each circuit.

Constructed into the test facility but not used for the present study was a system for injecting 1 cm diameter discrete jets of air through the last 13 plates of the curved wall at a 30° injection angle. These will be used in future curved-wall, film-cooling experiments [48] which are a continuation of the Stanford flat-wall studies [43,44,45]. For the present study, the injection holes were filled with balsa wood plugs before the surface was sanded and polished.

Each plate had three iron-constantan thermocouples distributed across the span for redundancy and to detect spanwise variation of temperature. For most cases, the output of the three thermocouples was nearly the same, indicating two-dimensionality, but for cases where transition occurred within the curved section, the convective heat transfer coefficient was significantly higher near the ends of the plates where corner secondary flows promoted earlier transition. For these cases, a simple spanwise heat-conduction model was necessary that could be used to estimate the centerline heat flux from the measured spanwise average heat flux. This model was tested by comparison to measurements of centerline heat flux using stick-on heat flux meters (see Section 2.5.c). Although this correction was small for cases where transition was complete at the beginning of the curve, it was used in reducing the data of all the heat transfer runs. the uncertainty of this correction was included in the overall uncertainties given in Appendix G. The embedded thermocouples were laid into milled slots so that there was a long contact length ($L/D > 20$) to minimize conduction error, following the techniques of Moffat [49]. The aluminum frame section near the ends of the copper plates was heated with hot circulating

water to minimize end losses. The copper tubes for ducting this heating water were crushed against the aluminum with the side-rail blocks shown in Fig. 2-2. The side-rail, frame, and tube assembly was filled with high-conductivity grease before crushing. The large support drum was heated with patch heaters that were controlled to a specified temperature.

The recovery wall was the same as the preplate wall, so that the test surface was symmetric about the center of the curve.

To minimize the radiation heat transfer from the heated copper walls, they were sanded with progressively finer sandpaper then polished with commercial copper polish. After polishing, the surface was shiny enough that details of the surroundings could be examined in the reflection on the surface. The surface was regularly polished to remove oxide buildup. With these precautions, the surface emissivity was held to an estimated 0.05 to 0.15.

2.4 Instrumentation for Hydrodynamic Measurements

Mean velocity profile measurements were taken using a total pressure probe and wall static pressure ports. The outside diameter of the total pressure probe was 0.7 mm. The wall-static pressure and total-to-static pressure differences were read from a Statham model PM-97 transducer calibrated to assure linearity to within ± 0.25% of full-scale output. Output was read with a Hewlett-Packard integrating digital voltmeter model 2401C using a 33-second integration time. Before each test, a two-point recalibration against a Combist micromanometer was made. Pressure differences less than approximately 0.25 mm of water were read directly off the Combist micromanometer. In the curved region, the static pressure was read at the wall. The local velocity was then calculated from the formula:

$$U = \frac{2}{\rho} (Pt(n) - Ps(n))^{1/2}$$

where $Pt(n)$ was the measured local total pressure and $Ps(n)$, the local static pressure, was calculated from Psw as

$$Ps(n) = Psw + \frac{\rho U_{pw}^2}{2}\left(1 - \frac{1}{(1+kn)^2}\right)$$

which presumes the potential velocity distribution:

$$U_p = \frac{U_{pw}}{(1+kn)}$$

Flow angles were measured with a Conrad probe constructed with 45° bevels and an indicator to measure relative angles. Convergence angles in the boundary layer were referenced to the potential core flow direction at the same streamwise and spanwise position. The uncertainty of the angle measurement was an estimated 1°. The differential pressure across the two tubes of the probe was sensed with the Statham PM-97 transducer and read with the Hewlett-Packard Model 2401C integrating digital voltmeter.

2.5 Instrumentation for Heat Transfer Measurements

a. Temperature Measurements

All temperature measurements were taken with iron-constantan thermocouples, except for the boundary layer traversing thermocouple, which was chromel-constantan. Samples of the curved section iron-constantan thermocouples and the traversing chromel-constantan thermocouple were calibrated against a Hewlett-Packard Quartz Thermometer, which was accurate to within 0.02°C. The samples of iron-constantan showed the same calibration curve, at the beginning of the data-taking and near the end, to within 0.08°C. The calibration curves and the uncertainty of calibration were incorporated into the data-reduction program.

The embedded thermocouples in the preplate and recovery wall were calibrated at operating temperature by referencing them to a calibrated sample of iron-constantan wire. This was done by taping the reference wire onto the copper plate section over the thermocouple to be calibrated, then pressing a 2.5 cm thick by 15 cm wide by 53 cm high layer of styrofoam over the thermocouples so that they were centered. Outside the styrofoam was a full-area patch heater which was controlled so that the temperature difference across the styrofoam was less than ~ 0.1C.

After about 20 minutes, the entire assembly reached thermal equilibrium, with no temperature gradient across the copper and air gap separating the two thermocouple junctions. The calibration for each thermocouple in the preplate and recovery wall was then taken and incorporated into the data-reduction program.

All the thermocouple wires were brought together into an isothermal zone at the back of the console panel, where they were connected to rotary thermocouple selector switches leading to the display of the signal through a Hewlett-Packard digital voltmeter, Model 3465B. to avoid temperature gradients along the thermocouple wires, they were inserted into 1/8-in. polyflo tubing for a portion of their length and a metal cable tray thermally insulated on the inside for the remainder. The isothermal zone box was lined inside with 0.8 mm copper sheets to conduct away local hot spots and insulated on the outside with aluminum foil-backed rock wool insulation. An aluminum free-standing radiation shield was inserted between the isothermal zone box and power equipment in the lab. One diagnostic thermopile was installed from corner to corner within the zone box to test for thermal gradients. The output of this thermopile was typically less than 3-4 μV and never larger than 9 μV (~ 0.1°C). All the iron-constantan thermocouples shared the same ice bath reference junction.

Temperature traverses were made with a chromel-constantan thermocouple probe constructed with 0.08 mm wire and designed for minimum conduction error [50]. This probe was calibrated against the quartz thermometer and measured temperature of the flowing stream with an estimated uncertainty of ± 0.08C. Processing of the traverse data included correction for viscous heating, following Moffat [51], and for the effects on fluid properties of temperature and humidity. The output was read on a Hewlett-Packard integrating digital voltmeter Model 2401°C.

b. Embedded Heat Flux Meters

Surface heat flux for each preplate or recovery wall section was measured with a heat flux meter installed between bakelite laminates behind each 0.3 mm thick copper plate segment. Each meter is 5 cm wide

and 0.4 mm thick and is wound with multiple silver-constantan thermopiles to measure temperature difference across its thickness.

The embedded heat flux meter calibration was done with a specially constructed calibration heater. Power to the heater was measured with a Sensitive Research Galvanometric type precision wattmeter. After calibration, the heat flux meter constant was known to an estimated uncertainty of ± 3%. Details of the calibration and the uncertainty estimate are given in Appendix C. The heat flux meter output was connected to a selector switch via shielded instrument wire. The output was read on a Hewlett-Packard digital voltmeter model 3465B.

c. Stick-On Heat Flux Meters

Stick-on heat flux meters were used for spanwise uniformity studies and for coarse verification of the installed instrumentation. They were multi-junction copper-constantan thermopiles laminated into 0.08 mm thick sheets of Mylar and were attached with double-stick plastic tape. Since they were detachable, they could be moved from place to place during a test. They measured local heat flux with an estimated uncertainty of 5-10%. Though they were calibrated with the same procedure as with the embedded meters (App. C), the calibration changed slightly with each sticking and removing cycle--hence the larger uncertainty.

d. Electric Power

Power delivered to each plate of the curved section was measured with a single Sensitive Research galvanometric type precision AC wattmeter by switching it into the power circuit of each plate, one at a time. The wattmeter was calibrated in a DC mode against a standard to within 0.05 watt. The wattmeter calibration was incorporated into the data-reduction program. A correction was made within the data-reduction program for the wattmeter insertion losses. This correction is discussed in detail in Ref. 44.

2.6 Qualification of the Facility--Hydrodynamics

A detailed discussion of the hydrodynamic qualification of the flow was presented by Gillis and Johnston [35]; important points are summarized below.

The potential flow in the developing region was found to be uniform in velocity to typically ± 0.15 percent, and the level of turbulence intensity

$$\sqrt{\overline{u'^2}}/U_\infty$$

was typically less than 0.5%. The spanwise variation of the momentum thickness at the beginning of curvature was typically less than ± 5%.

Wherever there is streamline curvature, there is a cross-stream pressure gradient. If the flow is in a tunnel of finite dimensions, this pressure gradient will accelerate boundary layer fluid on the side walls from the concave surface to the convex. Streamlines on the convex surface then tend to converge toward the centerline as the secondary flows continue their spiral. Converging streamlines are inevitable; the designer of the curved tunnel must make the convergence acceptably small. Convergence angles, measured with a Conrad probe, were 2° over the central span of 13 cm and less than 5° over a span of 25 cm. Streamline convergence became perceptible after about 60° of curvature, and continued to grow throughout the remainder of the curve, then persisted down the recovery wall. An integral momentum balance using curved flow definitions of the integral parameters suggested by Honami [52] was presented in Ref. 37 and showed closure to within 5% for the baseline case. The influence of secondary flow is seen predominantly in the wake region of the boundary layer and is expected not to influence significantly the wall-measured data or extrapolations from the log region to the wall.

2.7 Qualification of the Facility--Heat Transfer

The flow in the developing region was found to be uniform in temperature to within 0.05C. It was monitored continuously during each run and controlled constant to within 0.05C. Temperature control of the

tunnel air was achieved by dumping a portion of the water circulating through the heat exchanger and replenishing with make-up water from a cold-water supply main. The spanwise uniformity of the heated boundary layer at the introduction of curvature was checked by measuring the local heat flux with stick-on heat-flux meters and by measuring the local enthalpy thickness at various spanwise stations. The enthalpy thickness non-uniformity was less than ± 5%, and the local heat-flux non-uniformity was of the order of, or less than the uncertainty of the meter.

Within the curved region, thermocouples distributed across the span of each plate indicated that spanwise non-uniformity of the wall temperature was typically less than 0.07C and as low as 0.03C when preplate wall suction was applied. Spanwise uniformity of the heat flux within the bend was tested with the stick-on heat-flux meters. In the first half of the bend, the heat flux was uniform to within the uncertainty of the stick-on heat flux meter. In the last half of curvature, a spiral vortex driven by secondary flow spilling over the top of each boundary layer fence was observed by using a tuft on a wand. This vortex was centered about 1 cm inboard of the fence and about 5 cm away from the wall. Measurements of the local heat flux using the stick-on heat-flux meters (Fig. 2-3) indicated that these vortices were augmenting the heat transfer over a 2 cm span at the end of each segment. These vortices are not believed to have influenced the average heat flux significantly, what little influence they may have had should have been accounted for by the spanwise conduction correction model incorporated into the data-reduction program. In the afterplate, the fences were located inboard 4 cm from the walls to catch this vortex, break it up, and contain it between the fence and the wall. The corner vortices are not believed to have influenced the afterplate data significantly, since these data were taken with heat flux meters embedded at the wall centerspan. A conduction analysis on the wall showed that the 3 mm thick copper plate separating the heat flux meter from the air averaged the heat flux over an effective span of only about 8 cm of the 40 cm fence-to-fence total span.

Since two different techniques were being used to measure the average heat flux, it seemed appropriate to measure, as a means of qualification, the heat flux on the preplate, curve, and recovery walls with a common instrument, i.e., a stick-on heat flux meter. During a representative run, this stick-on heat flux meter was moved progressively from the last of the preplate to the first of the curve, the last of the curve, and the first of the recovery wall. It was found that the built-in instruments and stick-on meters agreed to within their uncertainties.

The effect of small secondary flows on the wall-measured data or data found by extrapolation from the log region to the wall is expected to be minimal. An earlier design of the boundary layer fences allowed convergence angles in the recovery region that were about 50% more than those for the final design. Stanton number data taken before and after the modification were the same to within their uncertainty, indicating no significant sensitivity to small secondary flows. Secondary flows slightly influence the wake regions of the thermal and hydrodynamic boundary layers, however, making an integral energy or momentum balance along the tunnel centerline difficult.

Further qualification of the Stanton number data was made by comparison to the mean temperature profiles for the baseline cases. These profiles extended into the conduction layer to n^+ values as low as 4.0. They followed the curve $T^+ = Pr\ n^+$ (see Fig. 3-3), indicating accurate values of wall and fluid temperatures, Stanton number, and skin friction. Also, local heat flux values were calculated from the temperature profiles as

$$\dot{q}''_w = -k \frac{T - T_w}{n}$$

where T was taken a distance n away from the wall near $n^+ = 6.5$. This local heat flux was then used to calculate the local Stanton number, which was within 5% of the wall-measured values for all the stations except the last station of the recovery region, where the gradient-calculated value was ~ 9% higher.

The Stanton number data were repeatable within their uncertainty band. The baseline case was the last case run of the 15 cases discussed herein. The first qualified case to be run was ostensibly the same case, but was completed eight months prior to the baseline case. Although the tunnel had been set up in many different configurations in the interim, the Stanton number data for the two cases were the same to within 5%.

2.8 The Energy Balance

A final all-inclusive test of the hydrodynamic and heat transfer measurements is the energy balance. This was performed by taking detailed wall measurements and velocity and temperature profile measurements while the rig was carefully controlled to the same steady-state conditions. The wall measurements taken at each wall segment are shown in Fig. 2.4. The energy balance data are tabulated in Appendix G as case 100779 and are also plotted as Fig. 2.5 in St versus Re_{Δ_2} coordinates. Table 2.1 shows the excess flowing energy in the boundary layer per meter of span for various streamwise locations:

$$\int_0^\infty \rho u(i-i_\infty)\, dn = Re_{\Delta_2} \nu \rho_\infty C_p (T_w - T_\infty)$$

This was calculated for each of the spanwise positions by: (1) integrating the velocity and temperature profiles and (2) integrating the energy integral equation in the streamwise direction using wall-measured values of heat flux. If all measurements were perfectly certain and the streamlines were perfectly parallel, the agreement between the two methods would be exact.

The overall closure was 93%. This is reasonable; the closure for the momentum balance for the same case [35] was 95%, which is considered good [37]. Closure for the first 80% of the curve is better than 93%, indicating secondary flow effects only on the profiles taken downstream of the curve. This secondary flow effect is expected to be on the wake region of the profiles and is expected to have no significant effect on the wall-measured Stanton numbers.

Table 2.1

Energy Balance

S (cm)	-35	10	41	61	119
Flowing Energy (KJ/sec-m)		13°	52°	78°	
From Profiles	0.216	0.475	0.648	0.720	1.027
From Wall Measurements	0.227	0.506	0.663	0.746	0.981
Closure (%)		93	99	97	93

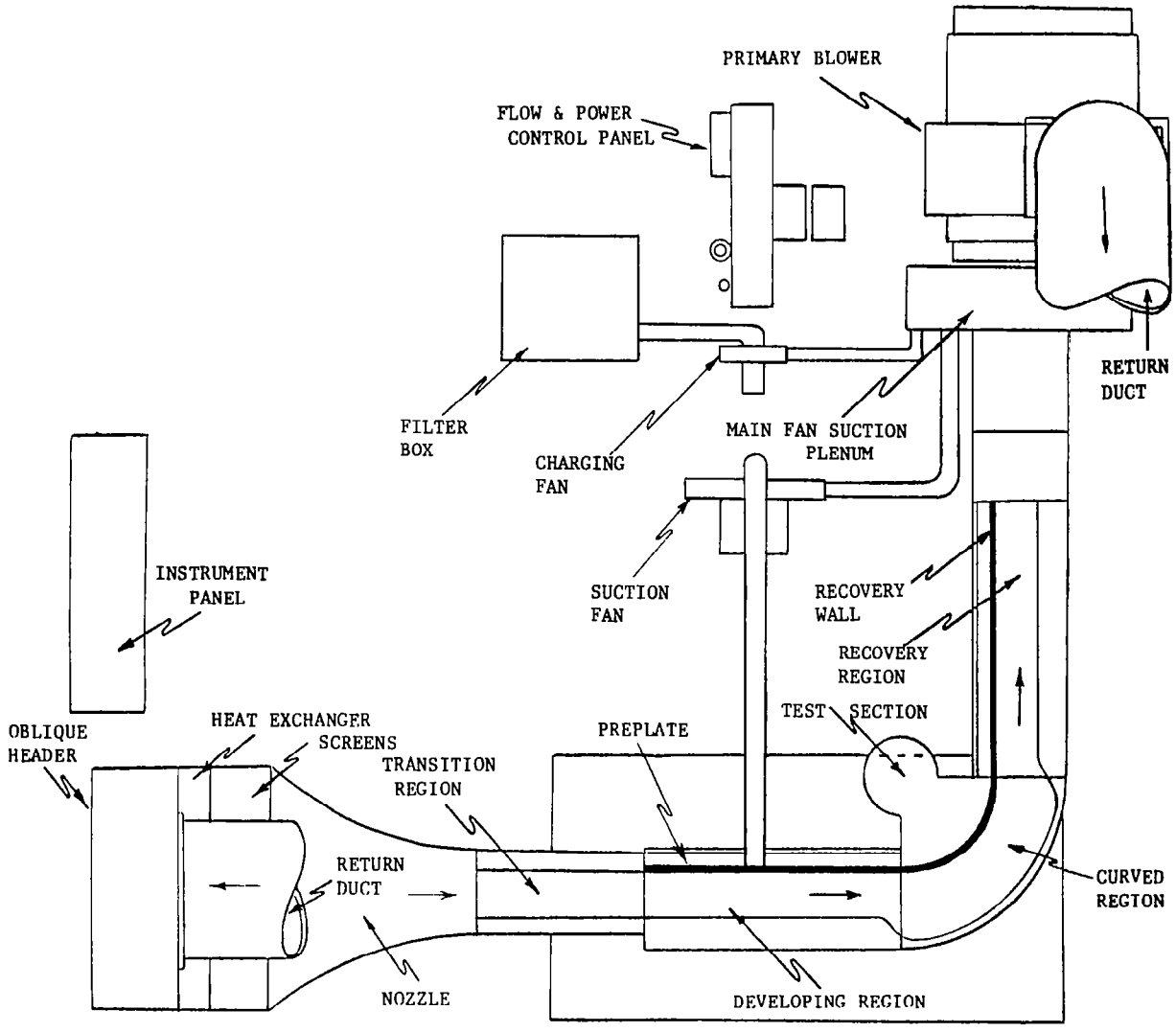

Fig. 2-1a. Plan view of the facility.

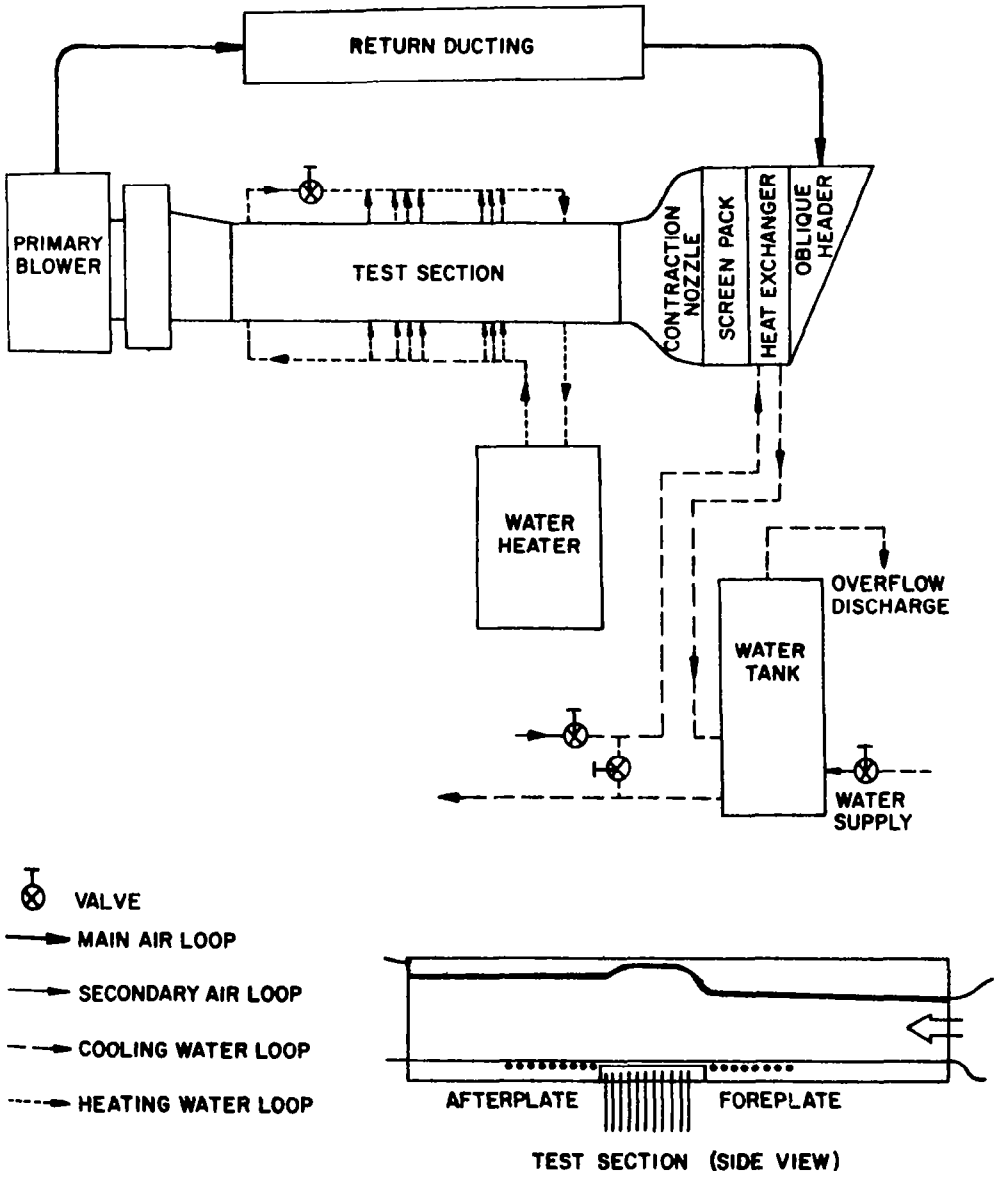

Fig. 2-1b. Schematic of the facility.

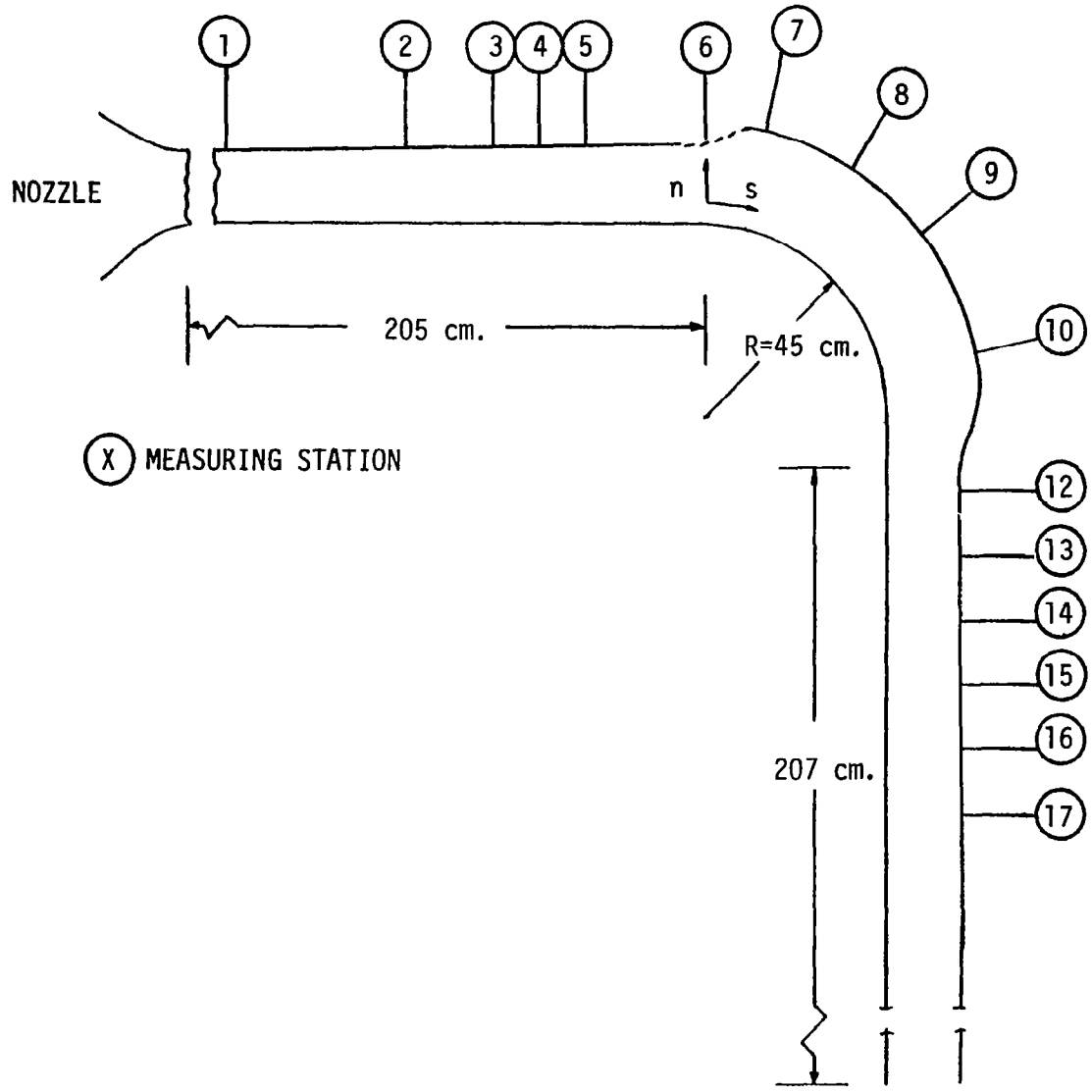

Fig. 2-1c. Location of measuring stations.

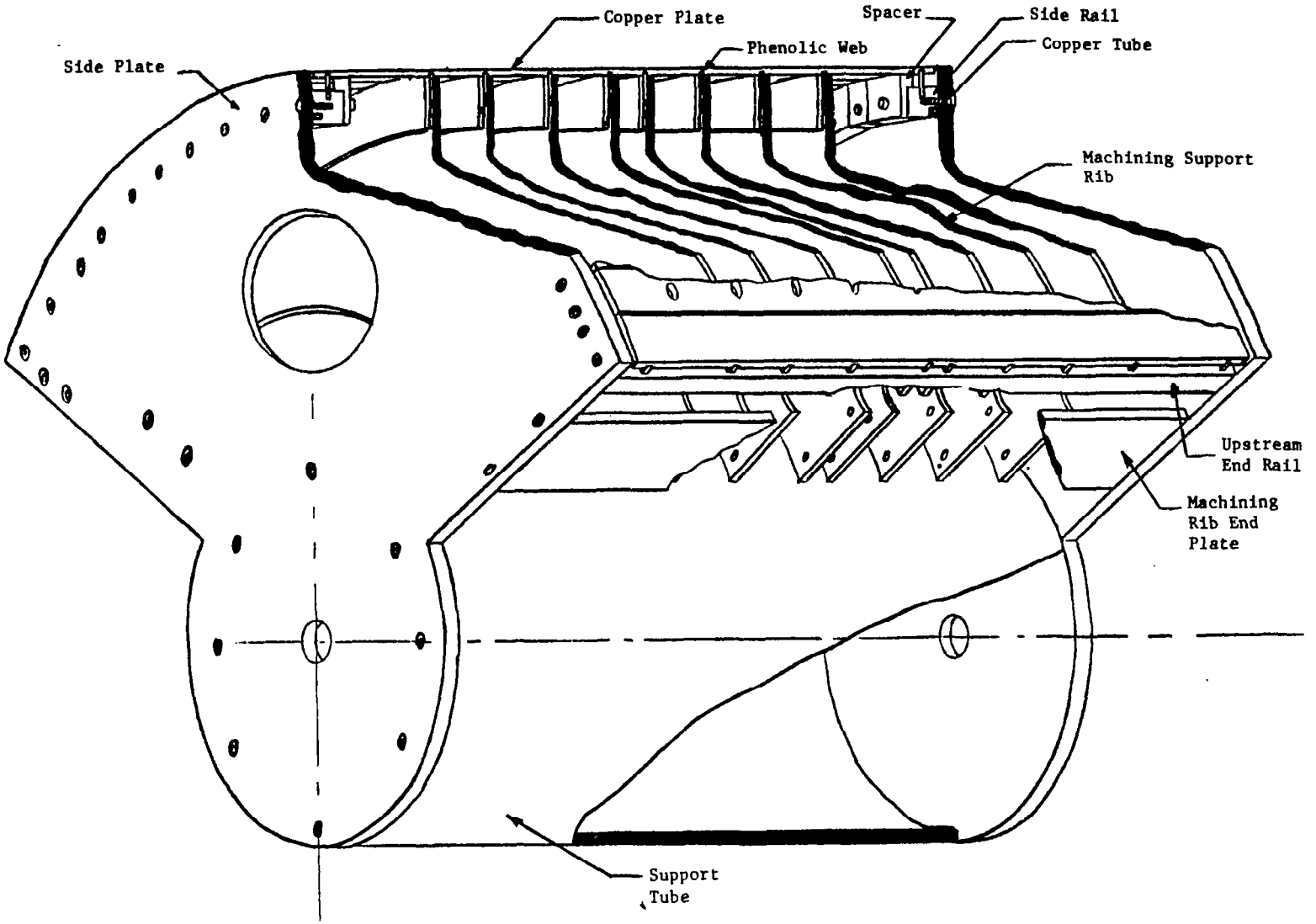

Fig. 2-2. Cutaway of the curved test section.

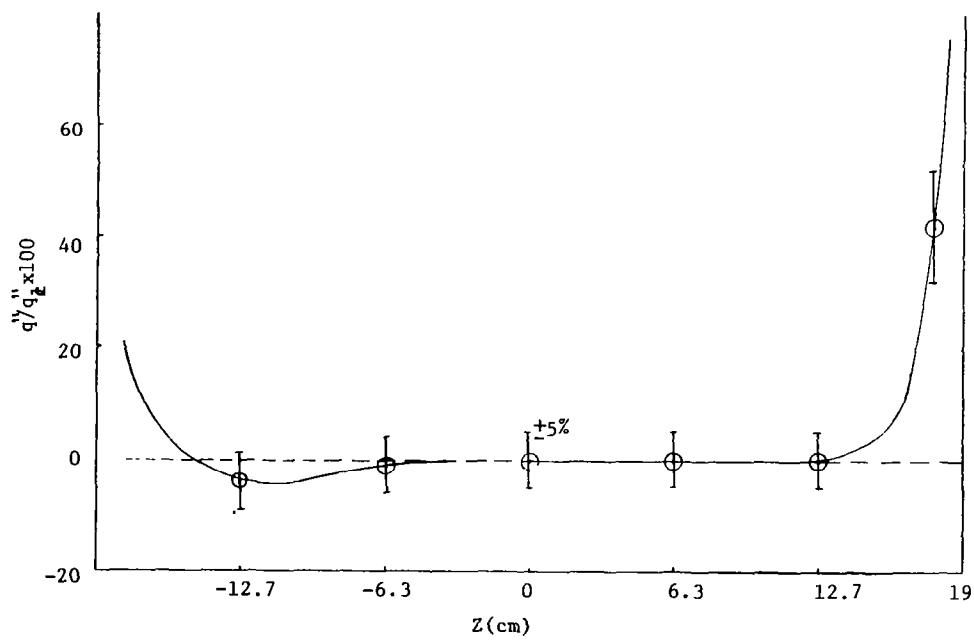

Fig. 2-3. Spanwise variation in local heat flux near the end of the curvature.

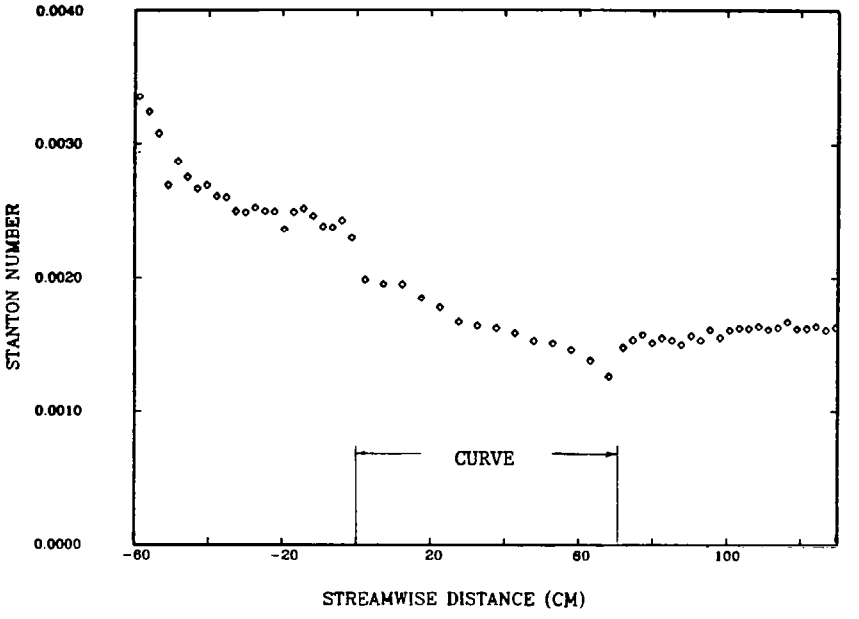

Fig. 2-4. Stanton number versus streamwise distance for the energy balance run.

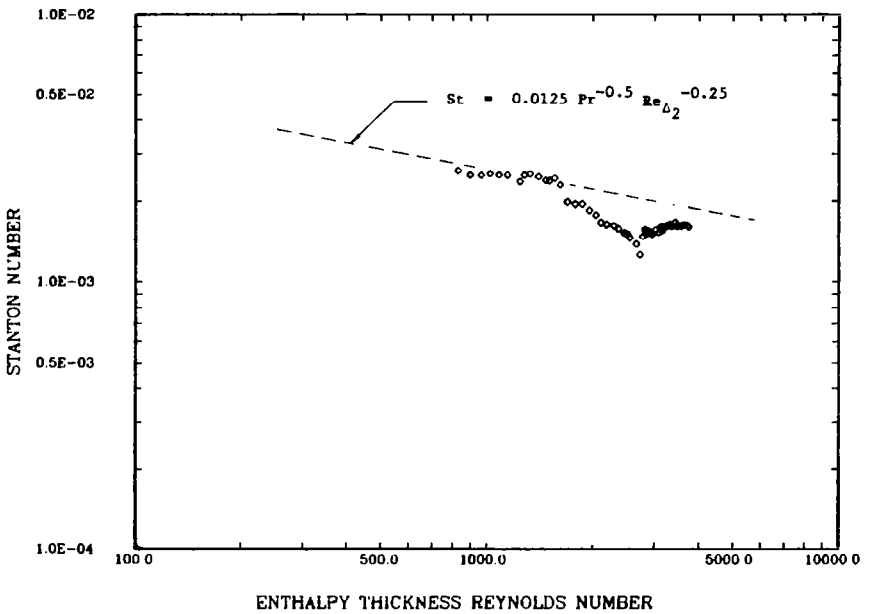

Fig. 2-5. Stanton number versus enthalpy thickness Reynolds number for the energy balance run.

Chapter 3

THE EXPERIMENTAL RESULTS

The following chapter first discusses a representative heat transfer run in some detail, then presents results of investigations of separate effects: cases similar to the baseline case but with varying values of a particular parameter.

3.1 The Baseline Case

The baseline case is a fully turbulent boundary layer responding to the introduction of, then withdrawal of, convex curvature subject to uniform wall static pressure and temperature. Data from this case are shown in Figs. 3-1 through 3-5.

3.1.1 Stanton Number versus Streamwise Distance

Figure 3-1 shows the local Stanton number versus distance in the streamwise direction for a ratio of boundary layer thickness-to-radius of curvature of $\delta_{99}/R \simeq 0.10$. The wall static pressure coefficient on the test surface, C_p, was held constant to within $\pm$ 0.02 and the wall-to-freestream temperature difference, nominally 17°C, was held constant to within $\pm$ 0.6°C. The Reynolds number based on momentum thickness at the beginning of curvature was 4173, and the shape factor was 1.41, indicating a mature turbulent boundary layer. The uncertainty of the Stanton number data was typically 3.3%, 4.8%, and 3.5% for the upstream developing region, the curved region, and the recovery region, respectively. These typical values are shown in Fig. 3-1. The 95% certainty band for each data point is listed with the data in Appendix G for all the cases discussed. The uncertainty analysis is presented in Appendix A. Small differences in temperature from segment to segment introduce variations in local Stanton number which appear as scatter. These variations are not considered in evaluating the uncertainty intervals.

Figure 3-1 shows that the effect of curvature on the heat transfer rate is quite dramatic. The wall heat flux decreases ~ 15% when the curvature is introduced and continues to decrease within the bend so that, at the end of the 90° curve, the Stanton number is ~ 35-40% below

the value that would be expected on a flat wall (dashed line). The recovery of the heat transfer rates on the flat wall downstream of the bend is extremely slow. After 60 cm of recovery length, the Stanton number is still ~ 15% below the flat-plate expected value. This behavior is the same as that of the skin friction shown in Fig. 1-3.

If Reynolds analogy held, the behavior of the turbulent transport of thermal energy ($\overline{v't'}$) would be similar to that of the Reynolds shear stress ($-\overline{u'v'}$) measured by Gillis and Johnston [35], Fig. 1-7. The shear stress profile at the beginning of curvature is dramatically altered. The shear stress is essentially shut off in the outer part of the boundary layer and reduced in the inner layer, resulting in reduced wall shear and heat flux and a steepening of the velocity and temperature profiles at the wall. Note also, from the shear-stress profiles (Fig. 1-7), that the turbulent mixing activity returns very slowly to flat-plate values in the recovery region--hence the slow recovery of skin friction and Stanton number.

3.1.2 Stanton Number versus Enthalpy Thickness Reynolds Number

There exists a definite relationship [36] between the Stanton number and the enthalpy thickness Reynolds number for a fully turbulent boundary layer on a flat plate with uniform wall temperature and static pressure and no unheated starting-length effect. This relationship is shown in Fig. 3-2, along with the data from the present baseline case. The preplate data join this correlation as the unheated starting length effect disappears, but, when curvature is introduced, the data begin to drop below the correlation. Shown also in Fig. 3-2 is the equivalent correlation for a laminar boundary layer. The slope of the laminar boundary layer correlation is -1.0, which is the same as the slope for the turbulent curved-wall data. This would lead one to think that stabilizing convex curvature is causing something similar to "relaminarization," a name used in connection with strongly accelerated turbulent boundary layers [36]. Turbulence measurements by Gillis and Johnston [35] and others, show that the curved turbulent boundary layer is still very much a turbulent boundary layer, but one in which the production of turbulence is contained to a thinner layer than if the streamlines were not curved. Their mean velocity profiles [35] also show no lasting

growth of the viscous sublayer with convex curvature.* Therefore, though the St versus Re_{Δ_2} trace appears similar to that of a laminar boundary layer, the boundary layer is not laminar nor is the sublayer growing significantly within the curve. In the recovery region, Fig. 3-2 shows the Stanton number slowly returning to the flat-plate correlation. After a sufficient downstream distance, the curvature effect becomes distant history and data should once again fall on the correlation (similar to the disappearance of the unheated starting length effect). Comparing the data to the flat-plate correlation of St versus Re_{Δ_2} seems a reasonable way of determining the degree of recovery from curvature. The Re_{Δ_2} correlation of Fig. 3-2 is based upon local conditions, whereas the Re_x correlation of Fig. 3-1 is based upon the virtual origin of the turbulent boundary layer, which is permanently altered by curvature. Viewing the data in terms of St versus Re_{Δ_2} allows one to see the effect of curvature without contamination by Reynolds number effects. Figure 3-2 shows that, at the end of the recovery section, the local Stanton number is still ~ 20% below the flat-plate correlation.

3.1.3 Mean Temperature Profiles

Figure 3-3 shows representative temperature profiles expressed in inner coordinates. One profile is taken from the preplate region, one at the beginning of the curve, four from the curved region, and three from the recovery region. The first profile in the recovery region was taken only 1.6 cm downstream of the end of the 90° bend. The profiles show that the effect of curvature is to increase the strength of the wake region. This is seen as a steepening of the temperature profiles in the outer part of the boundary layer. Curvature apparently does not result in a noticeable lasting change of the thickness of the conduction layer.

Since the mean velocity profiles (Fig. 1-4) had a discernible log region, both within the curved region and the recovery region, and since

---

*There appears to be a small, rapid increase of the sublayer thickness, followed by a quick return to normal as curvature is introduced [35].

local Reynolds analogy is expected to be approximately true , $\varepsilon_M/\varepsilon_H \simeq 1.0$ [31], one would expect the temperature profiles to have a log region as well. Figure 3-3 shows that there is indeed a log-linear region of the temperature profiles, though it becomes quite small within the curve (as with the mean velocity profiles). The thermal law-of-the-wall expression which was used is:

$$T^+ = 13.2\ Pr + \frac{Pr_t}{\kappa} \ell n \frac{n^+}{13.2} \qquad \text{(Ref. 36)} \qquad (1)$$

This expression was derived for a normal flat-wall turbulent boundary layer. Since the Stanton number and skin friction coefficients are measured independently, the only unknown available with which to force Eqn. (1) into the data is the average turbulent Prandtl number. The log-region dashed lines in Fig. 3-3 are from Eqn. (1), which fits acceptably well the log-linear region or each profile, except the one taken 1.6 cm downstream of the end of the curve. This boundary layer is apparently not in equilibrium. The mean velocity profiles used in deducing $C_f/2$ for Eqn. (1) (and making a recovery correction to the indicated temperature) were measured in the heated boundary layer with a pitot tube. The turbulent Prandtl numbers used to match Eqn. (1) to the data are plotted versus streamwise distance in Fig. 3-4. The introduction of curvature causes a slight increase in the turbulent Prandtl number, as predicted by R.M.C. So [31]. The rise in Pr_t when curvature is introduced is partly due to the disappearance of a weak unheated starting length effect and partly due to the introduction of curvature, so that the curvature effect would be slightly smaller than the total effect shown in Fig. 3-4. Shown also are Pr_t values found with the same technique, but for the case $\delta_{99}/R \simeq 0.05$. It is expected that the unheated starting length effect is insignificantly small by the first point (S = -35 cm) for the $\delta_{99}/R = 0.05$ case and by $\sim 30°$ of curvature for the $\delta_{99}/R = 0.10$ case.

The effect of the withdrawal of curvature on the turbulent Prandtl number is quite dramatic. When the turbulent activity begins to increase near the wall and propagate outward (as shown in Figs. 1-6 and 1-7), the transport of thermal energy apparently increases faster than the transport of momentum. It's not unreasonable to expect a violation

of Reynolds analogy with this rapidly changing boundary layer, since the two quantities in the ratio $\varepsilon_M/\varepsilon_H$ are fundamentally different, one a scalar and the other a vector. It is remarkable, however, that this violation persists so far downstream. The trend is similar to that seen in the strongly decelerating, but attached, turbulent boundary layer and is repeated for the $\delta_{99}/R = 0.05$ case.

3.1.3 Energy Balance

Since both detailed profiles and detailed wall data were taken for this example case, all the terms in the energy integral equation (Appendix B) are available.

A check on the data was made by comparing the growth of the enthalpy thickness Reynolds number, as calculated from the energy integral equation, to the enthalpy thickness Reynolds numbers for each profile. The comparison, Fig. 3-5, shows that they agree to within ~ 9%. The largest contributor to the lack of agreement is the influence of the small secondary flows on the wake of the boundary layer, as previously discussed. Secondary flows convect thermal energy toward the tunnel centerline on the convex wall, resulting in higher measured enthalpy thicknesses than predicted by integrating the energy equation along the centerline streamline. Agreement within 9% is reasonable [37]. Secondary flows are not expected to significantly influence the wall-measured Stanton number or the portions of the profiles between the wall and the wake.

The following sections present several studies made to investigate separate parameters. Descriptors of the baseline case and cases in the following studies are presented in Table 3-1.

3.2 The Effect of the Initial Boundary Layer Thickness

Three cases were compared for this study: the baseline case (δ_{99}/R (θ=0) = 0.10), a case with δ_{99}/R (θ=0) = 0.05, and a third case with δ_{99}/R (θ=0) = 0.02 (see Fig. 3-6). The data upstream of the curve differ slightly for the three cases because they have different virtual origins (Reynolds number effect). Within the curve, the data (Fig. 3-6) are similar for the three cases, in these coordinates, showing the

Table 3-1

HEAT TRANSFER RUN DESCRIPTORS

Case #	I.D.	U_{pw}(m/s) (ref.)	Re_{δ_2} (S = -35 cm)	Extrapolated to S = 0 Re_{δ_2}	δ_{99}/R	T.B.L. Virtual Origin (cm)	Re_{Δ_2} (Beginning Curve	Re_{Δ_2} (Beginning Recovery)
100779	Energy balance	15.1	3712	4270	0.10	-217	1641	2759
070280	$\delta_{99}/R(\theta=0) = 0.10$	14.8	3613	4173	0.10	-214	1775	2845
022680	$\delta_{99}/R(\theta=0) = 0.05$	14.5	1937	2563	0.05	-119	1825	2892
060480	$\delta_{99}/R(\theta=0) = 0.02$	24.2	464	1724	0.02	-39	1755	3572
112779	$\delta_{99}/R(\theta=0) = 0.05$ $U_{pw} = 26$ m/s	26.4	3826	4795	0.06	-142	2476	4368
011380	$\delta_{99}/R(\theta=0) = 0.08$ $U_{pw} = 7$ m/s, K = 0.0 Turbulent	7.0	1365	1696	0.08	-147	998	1496
113079	$\delta_{99}/R(\theta=0) = 0.05$ $\Delta_2/R(\theta=0) = 0$	14.5	1937	2563	0.05	-119	0	1498
030280	$\delta_{99}/R(\theta=0) = 0.05$ $\Delta_2/R(\theta=90°) = 0.0$	14.5	1937	2563	0.05	-119	0	0
010680	$U_{pw} = 7$ m/s Late transitional	7.0	689	1060	0.05	-81	697	1270
012480	$U_{pw} = 5.2$ m/s Transitional	5.2	618	874	0.06	-86	480	953
062880	Early transitional	12.4	322	724	0.02	-30	600	1109
062580	Very early transitional	7.0	238	275	0.02	-15	472	746
060980	$U_{pw} = 3.5$ m/s Transitional	3.5	145	222	0.02	-23	323	653
042280	$\delta_{99}/R(\theta=0) = 0.05$ $U_{pw} = 13$ m/s, K = .57E-6	13.3	1719	2313	0.05	-113	1560	2869
051080	$\delta_{99}/R(\theta=0) = 0.05$ $U_{pw} = 9$ m/s, K = 1.25E-6	9.0	883	1349	0.05	-85	1181	2038

first evidence of the way in which convex curvature organizes the data. The parameter δ_{99}/R, labeled the "strength of curvature," has been used as a curved-wall flow descriptor [2]. Figure 3-6 shows that, within the range $0.02 \leq \delta_{99}/R\ (\theta = 0) \leq 0.10$ and for the conditions tested, there is only a weak dependence on $\delta_{99}/R\ (\theta = 0)$ as viewed in these coordinates.

If the streamwise distance were scaled on the radius of curvature or shear layer thickness, δ_{sl}, the above conclusion about the effect of δ_{99} would again hold. If the streamwise distance were scaled on the boundary layer thickness (either the local value or the value at the beginning of the curve), one would reach a quite different conclusion. If the abscissa were S/δ_{99} the case with larger δ would have the abscissa compressed relative to those with smaller δ. One would then conclude that, for cases of larger $\delta_{99}(\theta=0)/R$, the effect of curvature is more than for cases of smaller $\delta_{99}(\theta=0)/R$ because the slope of St versus $S/\delta_{99}(\theta=0)$ is steeper. At this point, there is no strong reason to choose one scaling length over the others, so the data are left in terms of the dimensional quantity "S".

Figure 3-7 shows these data recast in the coordinates St versus enthalpy thickness Reynolds number. Eventually the Stanton number data for all three cases follow a line of -1 slope in these coordinates. The data of the $\delta_{99}/R = 0.10$ and 0.05 cases rapidly approach the -1 sloped line at the start of curvature. Because the cases of $\delta_{99}/R = 0.10$ and 0.05 immediately enter the asymptotic state, they can be considered to represent strong curvature. It appears that, once the curvature is sufficiently strong, the parameter δ_{99}/R is of minimal further significance. Gillis and Johnston [35] found that $\delta_{sl}/R = 0.03$ for both their cases ($\delta_{99}/R = 0.10$ and 0.05). Therefore, one could expect that, if no other parameter were changed from its test value but δ_{99}/R, cases with $\delta_{99}/R > 0.03$ would have their region of non-zero $\overline{u'v'}$ compressed to 0.03 R, whereas cases with $\delta_{99}/R < 0.03$ would show continued growth of the boundary layer until $\delta_{99}/R = 0.03$. The data of the $\delta_{99}/R = 0.02$ case is quite different from the above "strong" curvature cases. The asymptotic state is reached much more slowly, presumably because the initial boundary layer thickness is less

than the eventual shear layer thickness. The abrupt introduction of curvature results in an immediate decrease in Stanton number in this weak curvature case similar to that seen for the strong curvature cases, however. The minimum Stanton numbers for the three cases of Fig. 3.7 are 30-40% below the flat-wall correlation.

Within the 60 cm recovery length, the Stanton data for each case returns to within 10-15% of the Re_{Δ_2} correlation values. The rate of return of the Stanton number to the flat-wall turbulent boundary layer correlation seems to be proportional to the difference between the local Stanton number and the flat-plate Stanton number for the same enthalpy thickness Reynolds number.

3.3 The Effect of U_{pw}*

Figures 3-8 through 3-10 show the results of a study of the effect of U_{pw}. Figure 3-8 shows Stanton number versus distance in the streamwise direction for the baseline case, U_{pw} = 15 m/s, and for two other values of U_{pw}: 7 m/s and 26 m/s. The two high-velocity cases respond nearly the same (when corrected for the Reynolds number effect), while the low-velocity case seems to be approaching closely to the same state in the last 30° of the curve. Since U_{pw} appears in the denominator of Stanton number, this means that the wall heat flux at any position on the curve increases almost linearly with U_{pw}. The shear stress profiles from Gillis and Johnston (Fig. 1-7) display an asymptotic state for $\theta > 60°$. The cases of higher velocity (112779, 070280 in Fig. 3-8) show the Stanton number data rapidly locking into this curved flow state. The lower velocity case (011280) shows the data approaching the other data more slowly, and about 60° of the curve is needed for the low-velocity data to attain the curved boundary layer condition. In the last 30° of bend, one can find a very weak U_{pw} dependence as viewed in these coordinates; the data of the 26 m/s case (112779) is 8% below the baseline data (070380) and the U_{pw} = 7 m/s case (011380) data are 14% above.

*The velocity that would exist at the test wall, were there no boundary layer.

Figure 3-10 shows a three-dimensinal plot in which U_{pw} is used as the third axis. This allows one to visualize the surface more easily and provides space for insertion of a fourth case which has the intermediate velocity but a boundary layer thickness of $\delta_{99}/R = 0.05$ (see Table 3-1). In Fig. 3-10, the low- and high-velocity cases can each be compared with an intermediate case of nearly the same boundary layer thickness at the beginning of the curve, separating the effect of δ_{99}/R from the effect of U_{pw}.

The following paragraph exemplifies the difficulty in viewing data in these coordinates. The Stanton number data at any given S-location within the last 30° of bend are nearly the same for the three cases, the lower-velocity cases yield lower Re_x values and therefore higher predicted flat-wall Stanton numbers. The flat-wall Stanton number plane is shown in Fig. 3-10 as a nearly horizontal plane. The lower-velocity cases would therefore show a stronger effect of curvature in terms of St/St_o. The minima within the curve are 50%, 42%, and 39% below the flat-plate correlations for U_{pw} = 7, 15, and 26 m/s, respectively. If, in the asymptotic curved boundary layer, the Stanton number is dependent upon only local conditions, as now appears to be true, the history of the development of the boundary layer upstream of the bend is not important. Comparisons to flat-wall values in these coordinates, as done above and commonly done with curvature studies, are not appropriate. The Reynolds number effect must be separated from the curvature effect.

Figure 3-9 shows that the data within the curved region, for all three cases, eventually follow a -1 relationship with Re_{Δ_2}. Careful examination of the introduction of curvature shows that, for the low-velocity case, the data approach this -1 slope in the first 30-40% of the curve. In the mid-velocity case, the data quickly reach the -1 correlation (as observed in the previous study, Fig. 3-7) at the beginning of the curve. The data of the highest-velocity case drop below the -1 correlation, then approach this correlation in the first 20-30° of curvature. This seems to be the principal effect of U_{pw}: to change the shape of the St versus Re_{Δ_2} curve without changing its eventual -1 slope.

Figure 3-8 or 3-10 shows that the increase in Stanton number in the recovery region is faster in the lower-velocity cases. The reason for this becomes evident when the data are viewed in the coordinates of Fig. 3-9. The rate of return of Stanton number within the recovery region appears to be proportional to the distance from the flat-plate correlation (a first-order lag in these coordinates).

3.4 Effect of Freestream Acceleration

Figures 3-11 and 3-12 show the combined effects of streamwise curvature and acceleration. The curved region is the only region where there is freestream acceleration; $K \simeq 0.0$ for the preplate and recovery regions. In their discussion of the accelerating boundary layer, Kays and Moffat [38] point out that, for the asymptotic accelerated boundary layer, the momentum thickness Reynolds number reaches a constant value while the enthalpy thickness Reynolds number continues to increase. In the following study, the momentum thickness Reynolds number at the start of curvature was within 10% of the value they gave for the asymptotic state corresponding to the acceleration parameter K. Therefore, the momentum bnoundary layer was expected to lock into the asymptotic acceleration state at the start of curvature.

Three cases are compared for this study: $K = 0.0$, 0.57×10^{-6}, and 1.25×10^{-6}. The boundary layer thickness-to-radius of curvature ratio for all three cases was about 0.05. The $K = 1.25 \times 10^{-6}$ case of Fig. 3-12 shows a different Stanton number trace within the curved region than seen in the preceding figures or in the case of milder acceleration. There apparently is an acceleration effect which is as important as the curvature effect.

A considerable amount of work has been done on accelerating boundary layers on flat walls, (e.g., Ref. 38). The following is a very brief review: Examples of the effect of acceleration on smooth, flat-wall boundary layers [38] for $K = 0.57 \times 10^{-6}$ and $K = 1.45 \times 10^{-6}$ are shown in Figs. 3-13 and 3-14, respectively. Figure 3-13 shows that acceleration with $K = 0.57 \times 10^{6}$ does not significntly influence the heat transfer rates. Figure 3-14 shows that acceleration with $K = 1.45 \times 10^{-6}$ results in a dramatic dropoff of the Stanton number.

This is predominantly a result of the acceleration's thickening the viscous sublayer or conduction layer; that is, it is predominantly an inner-region effect. Figure 3-14 shows also that, for the strong acceleration cases studied, the slope of the Stanton number curve in these coordinates is between -0.25 and -1.0.

The combined case of curvature and acceleration (Fig. 3-12), shows a combination of two effects which act on different parts of the boundary layer, acceleration on the inner and curvature on the outer. The slope of Stanton number versus enthalpy thickness Reynolds number for the case of strong curvature with strong acceleration of $K = 1.25 \times 10^{-6}$ (Fig. 3-12) is approximately -2.0, which shows that both effects are significant and the two effects are additive. The case of $K = 0.57 \times 10^{-6}$ (Fig. 3-12) shows an eventual -1 slope, but there appears to be an effect of this lesser acceleration at the beginning of curvature.

A careful review of the data for this study shows an interaction of the effects of curvature and acceleration. Figure 3-13 shows that, on the flat wall, acceleration with $K = 0.57 \times 10^{-6}$ should not show an effect of acceleration. Figure 3-12 shows that $K = 0.57 \times 10^{-6}$ results in an effect of acceleration at the introduction of curvature that apparently disappears as the expected -1 slope appears. Figure 3-14 for the flat wall shows that $K = 1.45 \times 10^{-6}$ results in a -0.5 slope; a K value of 2.5×10^{-6} would be required to have a -1.0 slope. Figure 3-12 shows that $K = 1.25 \times 10^{-6}$ results in a -2 slope. It appears, therefore, that the curved boundary layer is more sensitive to the growth of the conduction layer than is the flat-wall boundary layer. This is similar to the interaction between acceleration and wall suction [38].

3.5 Effect of Unheated Starting Length

Figures 3-15 and 3-16 show the effect of the location of the beginning of heating with respect to (1) the virtual origin of the turbulent momentum boundary layer and (2) the beginning and ending of curvature.

The first comparison is to show that the unheated starting length is not influencing the studies already discussed. Cases 070280 and 060480 have heating beginning ~ 63 cm upstream of the beginning of cur-

vature. Case 070280 has heating beginning 154 cm downstream of the virtual origin of the turbulent momentum boundary layer, whereas case 060480 has heating beginning 24 cm upstream. The two cases are therefore quite different in unheated starting length. Figure 3-16 shows that, even for case 070280, where the unheated starting length is most severe, the effect of the unheated starting length disappears quickly and is gone before curvature is introduced, the Stanton number data are on the correlation. Differences in the Stanton number data from case to case for all the cases discussed thus far, therefore, cannot be attributed to the unheated starting length effect.

The second comparison is to show the effect of starting a thermal boundary layer inside of a well-developed turbulent momentum boundary layer in the vicinity of the curved section.

Case 113079 of Figs. 3-15 and 3-16 shows the effect of curvature where the thermal boundary layer began at the start of curvature. When curvature is introduced, the production of turbulence is confined to the inner part of the boundary layer, effectively reducing the scale of the layer. In the cases where heating begins within the curve, it is reasonable to assume that much of the added thermal energy is contained within the inner (active) region. If this is so, the thermal energy is not allowed to mix effectively to the outer region and the Stanton number drops fast at first, then quickly levels off. When viewed in the coordinates of Fig. 3-16, the data of the two cases where heating began upstream of the curve (cases 070280 and 060480) eventually reach the presumed asymptotic state characterized by the line of -1 slope. In the case where heating began at the beginning of curvature, the data again attain this -1 sloped line as well. Using the above scenario, this condition was eventually reached when the inner layer received a sufficient amount of thermal energy to establish an asymptotic temperature profile. Fig. 3-16 shows that the recovery for this case is similar to that of cases 070280 and 060480 characterized by a rate of return proportional to the difference between the local Stanton number and the correlation.

Case 030280 had the same hydrodymamic boundary layer as 113079, but the heating began at the beginning of the recovery section. In this

case, the thermal boundary layer began to grow as the shear layer of the Gillis and Johnston model began to recover to flat-wall conditions. The data finally attained a trajectory where its return to the correlation of Fig. 3-16 was at about the same rate as seen for the other cases, and was slower than would be expected in a normal flat-wall boundary layer.

There is evidence from this study that the state of the flow outside of the shear layer is not important in the recovery process. A comparison of cases 070280 and 030280 shows that they recover similarly after the unheated starting length effect of case 030280 disappears. However, the distributions of the thermal energy within the recovering layers for the two cases are quite different. Case 070280, in which heating began within the preplate region, would have a considerable amount of thermal energy as residue outside "δ_{sl}". Case 030280, in which heating began at the beginning of the recovery section, would have minimal thermal energy beyond "δ_{sl}". Since they recover in a similar fashion, this residual thermal energy must not be instrumental in the recovery process.

3.6 The Effect of the Maturity of the Momentum Boundary Layer

The results of a study showing the effect of the maturity of the momentum boundary layer at the start of curvature are shown in Figs. 3-17 through 3-21. The descriptor to identify the separate cases is the momentum thickness Reynolds number at the start of curvature.* For this study, Re_{δ_2} (θ=0) varies from 222, indicating a laminar-to-early transitional boundary layer, to the baseline case of 4173 indicating a fully turbulent boundary layer.

Figure 3-17 shows that, if the boundary layer is sufficiently turbulent, (cases 070280, 011380, 010680, and 012480), the convex curvature becomes an effective organizer of the data. Though the preplate data for the four cases are radically different, the traces of Stanton number versus streamwise distance within the curved region (Fig. 3-17) are

*A simple model has been devised for extrapolating the measured starting profile data to the beginning of the curve. This model is presented as Appendix D.

remarkably similar. A plausible explanation of this can be made by using the "shear layer" model proposed by Gillis and Johnston [35]. If the boundary layer is sufficiently turbulent, the thin layer (~ 30% of the original boundary layer), which will become the shear layer, has well established turbulent mixing activity. When curvature is introduced, the turbulence production is confined to this inner region, and the remainder of the boundary layer is of minor importance. A mature turbulent boundary layer would have large-scale turbulent mixing. In the asymptotic curved turbulent boundary layer, the scales become adjusted to the shear layer thickness. Within the shear layer, then, the asymptotic states of both transitional and fully turbulent cases are essentially the same. The history is contained in the outer layer, which apparently has a minor influence. These late transitional and turbulent cases, Fig. 3-18, display the slope -1, considered to be the asymptotic curved turbulent boundary layer state.

Figure 3-18 shows that the recovery data for cases of late transitional or turbulent boundary layers are similar to those of the mature turbulent boundary layer.

In contrast to the above four cases are those in which the boundary layer is laminar or early transitional at the start of curvature, Figs. 3-19 and 3-20, characterized by the nearness of the data to the laminar flat-plate correlation. For the nearly laminar cases (e.g., 062880 and 062580), the small amount of turbulent activity that may be present is not sufficient to force transition to continue in the face of stabilizing curvature. The data remain near the laminar correlation until the layer has matured: the convex curvature has therefore delayed transition. When transition finally begins, within the bend, it appears to be retarded by curvature. Figure 3-20 shows the transition, as seen by an increase of Stanton number toward the turbulent correlation, to be slow until the stabilizing convex curvature is removed and then to progress quickly.

A notable difference from the two cases discussed above is case 060980, a case with extremely low velocity and momentum thickness Reynolds numbers. In this case, although there appears to be some effect of curvature, particularly at the introduction, the curvature does not

seem to retard the transition as strongly as it did in the other cases and transition is nearly complete by the end of the curved region.

The laminar and early transitional cases in Fig. 3-20 show that the curvature did not prevent transition. The introduction of the stabilizing curvature resulted in a momentary return toward the laminar correlation, but transition effects dominated the trajectory within the curved region. At the very end of the curve, cases 060980 showed a trend similar to that observed in fully turbulent curved boundary layers (the -1 slope). This may be due to the growth of the boundary layer, as discussed above, in conjunction with the emergence of turbulence activity as the dominant transport mechanism. The uncertainty for these transitional data was as large as ± 10-13% (see App. G for details).

Figure 3-20 shows the recovery data for laminar-to-early-transitional boundary layers. The data return quickly to the turbulent flat-wall boundary layer correlation. The most significant effect of curvature was the delay and retardation of transition.

Figure 3-21 shows the combined plot of Figs. 3-17 and 3-19 as a three-dimensional view of Stanton number versus streamwise distance and momentum thickness Reynolds number at the beginning of the curve Re_{δ_2} (θ=0). The figure shows three distinct regimes. In the first, exemplified by the most distant curve, transition dominates the trajectory and curvature is only a mild retardant. In the second, the next two curves in order of increasing Re_{δ_2} (θ=0), curvature delays and retards the transition process and, when curvature is removed, the boundary layer returns to "normal" quickly. In the third regime, there is the typical response of a mature turbulent boundary layer to convex curvature.

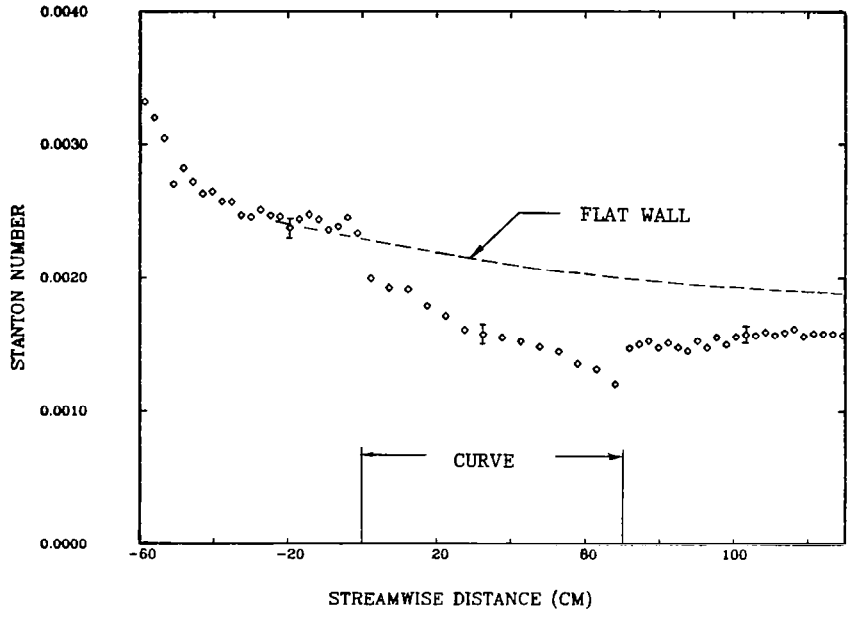

Fig. 3-1. Stanton number versus streamwise distance for the baseline case (070280) - Turbulent $\delta_{99}/R(\theta=0)$ = 0.10, U_{pw} = 14.8 m/s , K ≃ 0.0.

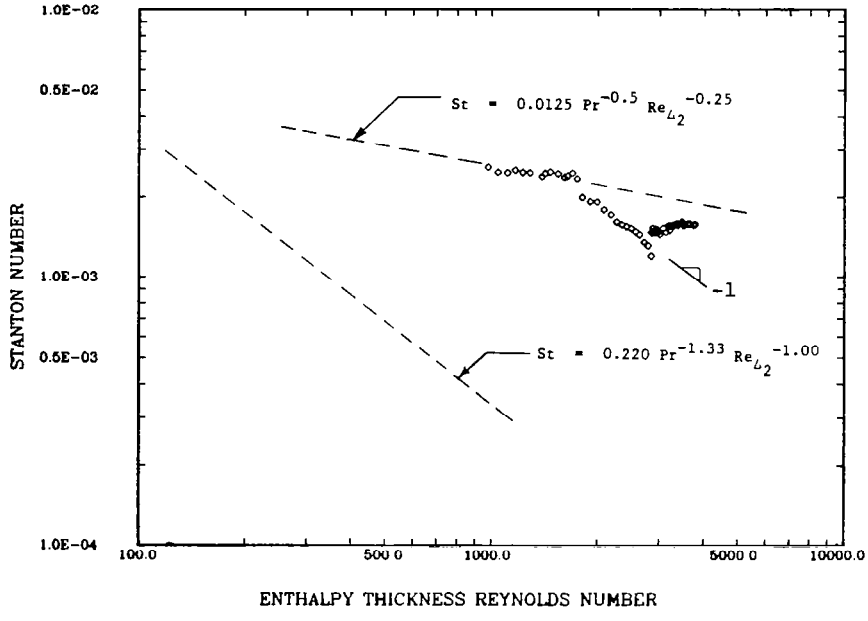

Fig. 3-2. Stanton number versus enthalpy thickness Reynolds number for the baseline case (070280) - Turbulent, $\delta_{99}/R(\theta=0)$ = 0.10, U_{pw} = 14.8 m/s , K ≃ 0.0.

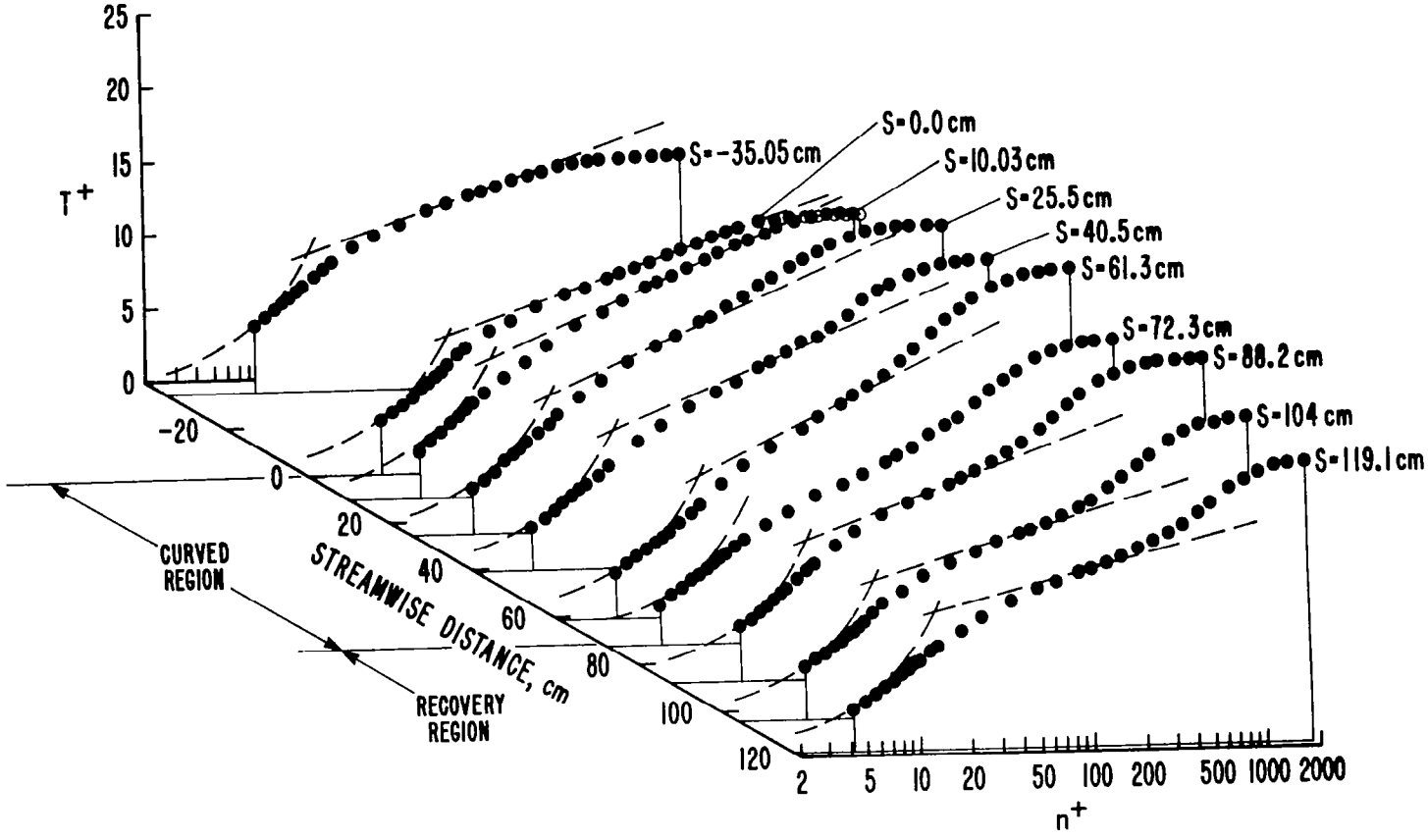

Fig. 3-3. Temperature profiles in inner coordinates for the baseline case (070280) - Turbulent, $\delta_{99}/R(\theta=0)$ = 0.10, U_{pw} = 14.8 m/s , K ≃ 0.0.

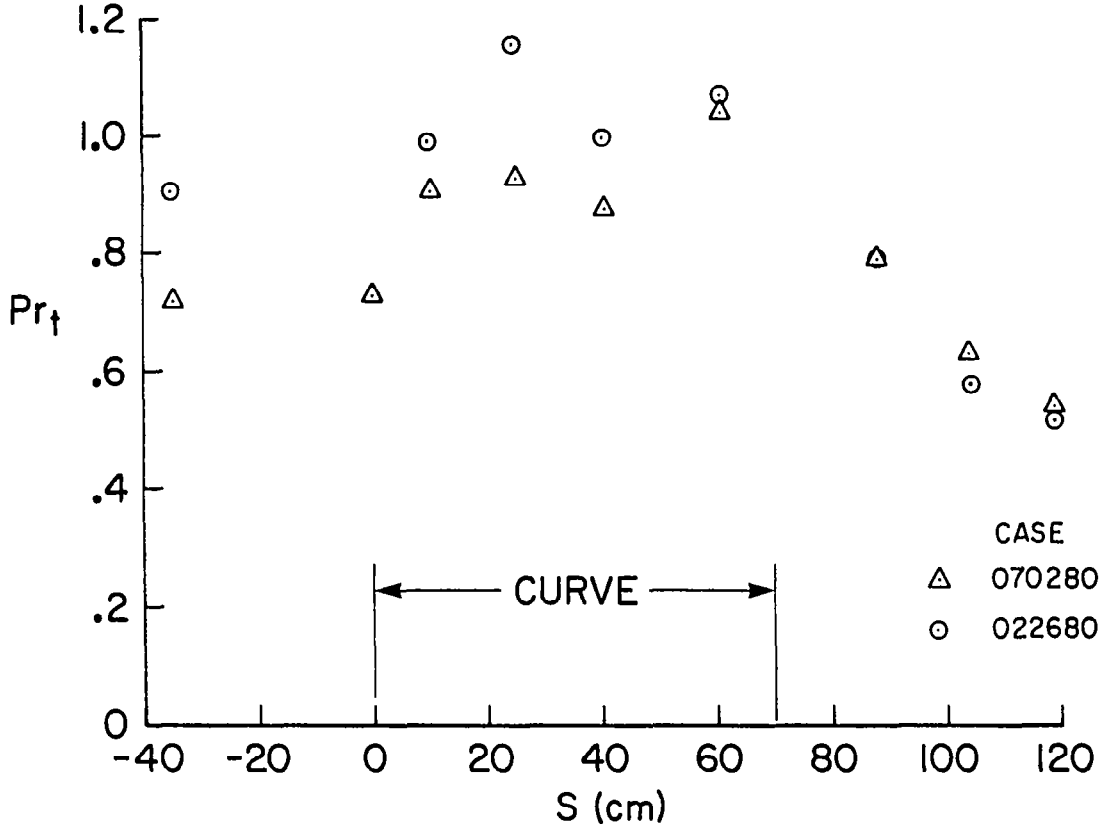

Fig. 3-4. Turbulent Prandtl number versus streamwise distance for the baseline case (070280) - Turbulent, $\delta_{99}/R(\theta=0) = 0.10$, $U_{pw} = 14.8$ m/s , $K \simeq 0.0$.

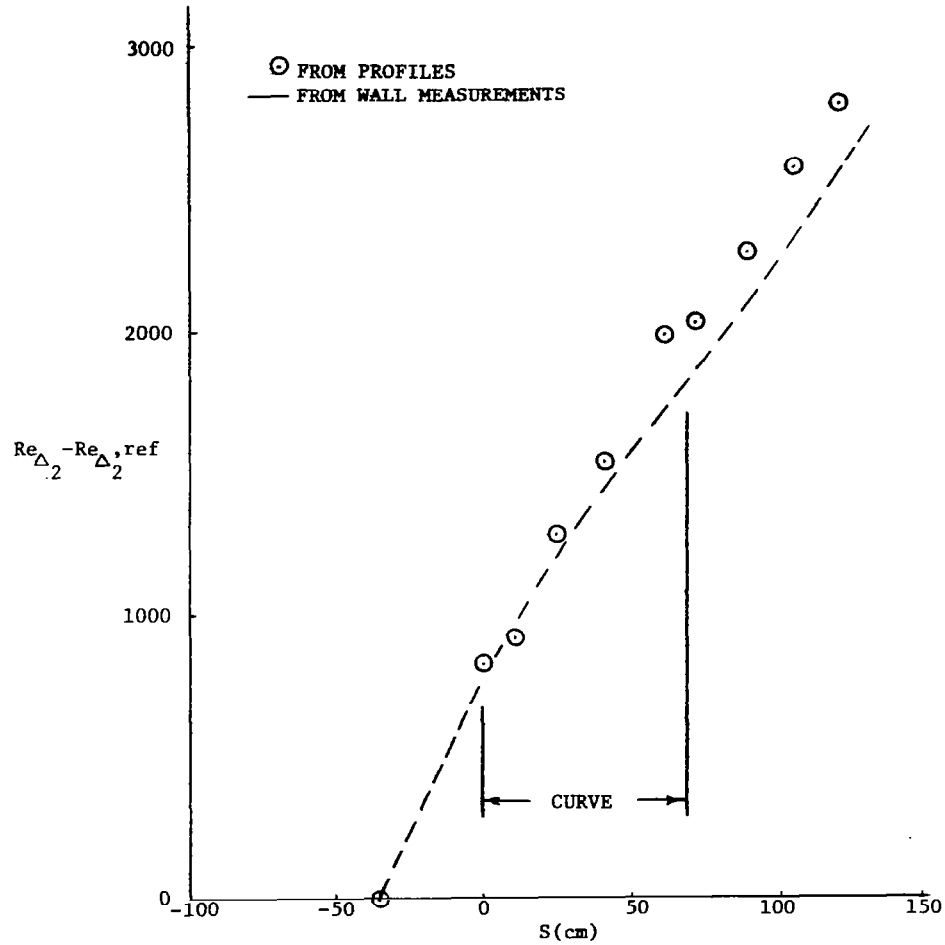

Fig. 3-5. Comparison of Re_{Δ_2} from the energy integral equation and Re_{Δ_2} from the measured profiles for the baseline case[2](070280) - Turbulent, $\delta_{99}/R(\theta=0)$ = 0.10, U_{pw} = 14.8 m/s , K ≃ 0.0.

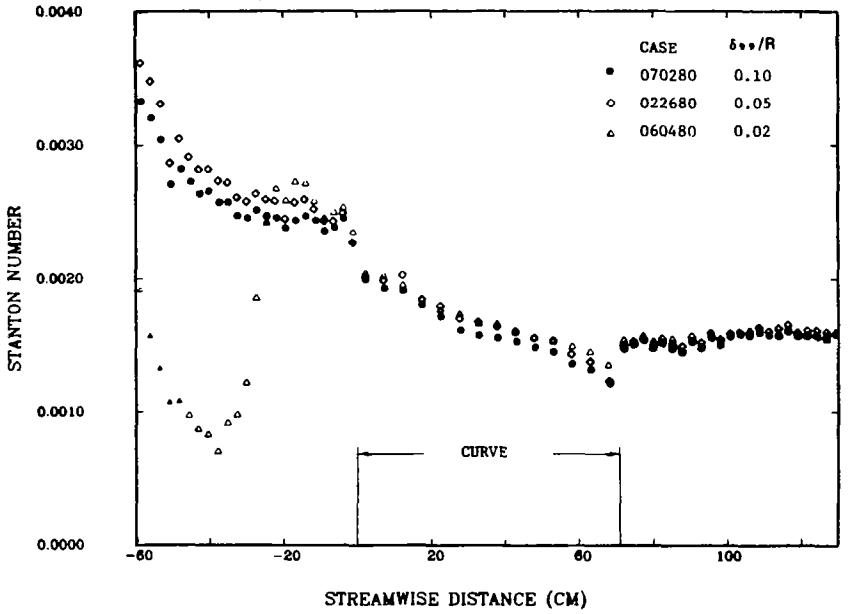

Fig. 3-6. The effect of initial boundary layer thickness - Stanton number versus streamwise distance.

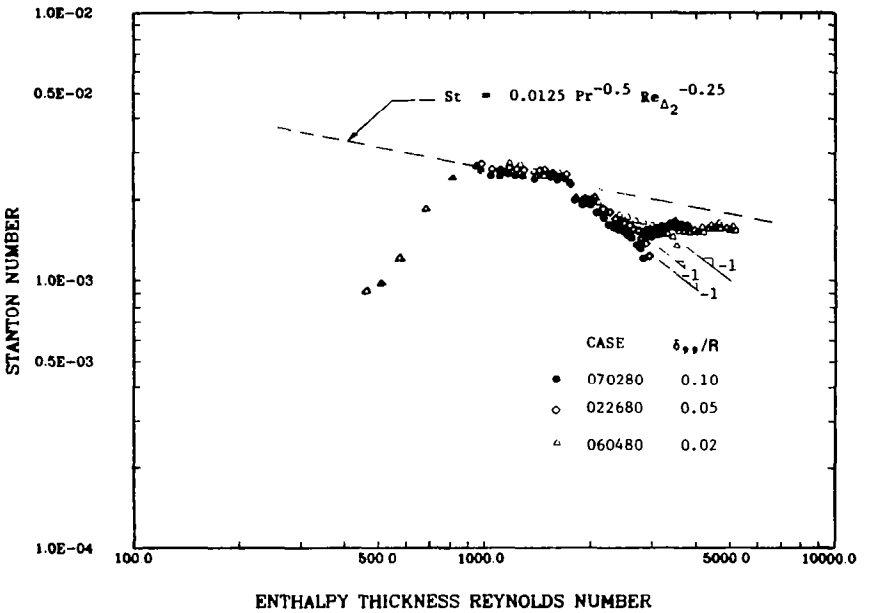

Fig. 3-7. The effect of initial boundary layer thickness - Stanton number versus enthalpy thickness Reynolds number.

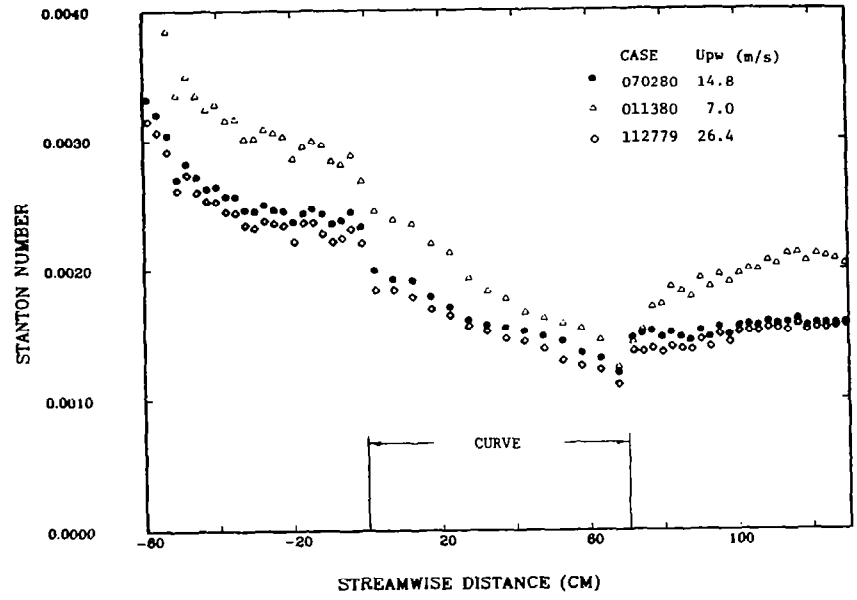

Fig. 3-8. The effect of U_{pw} - Stanton number versus streamwise distance

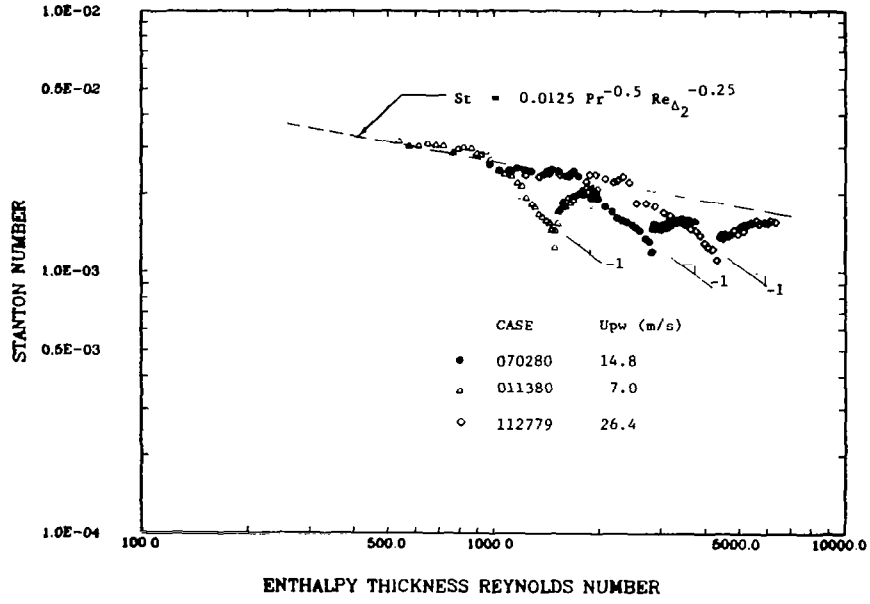

Fig. 3-9. The effect of U_{pw} - Stanton number versus enthalpy thickness Reynolds number.

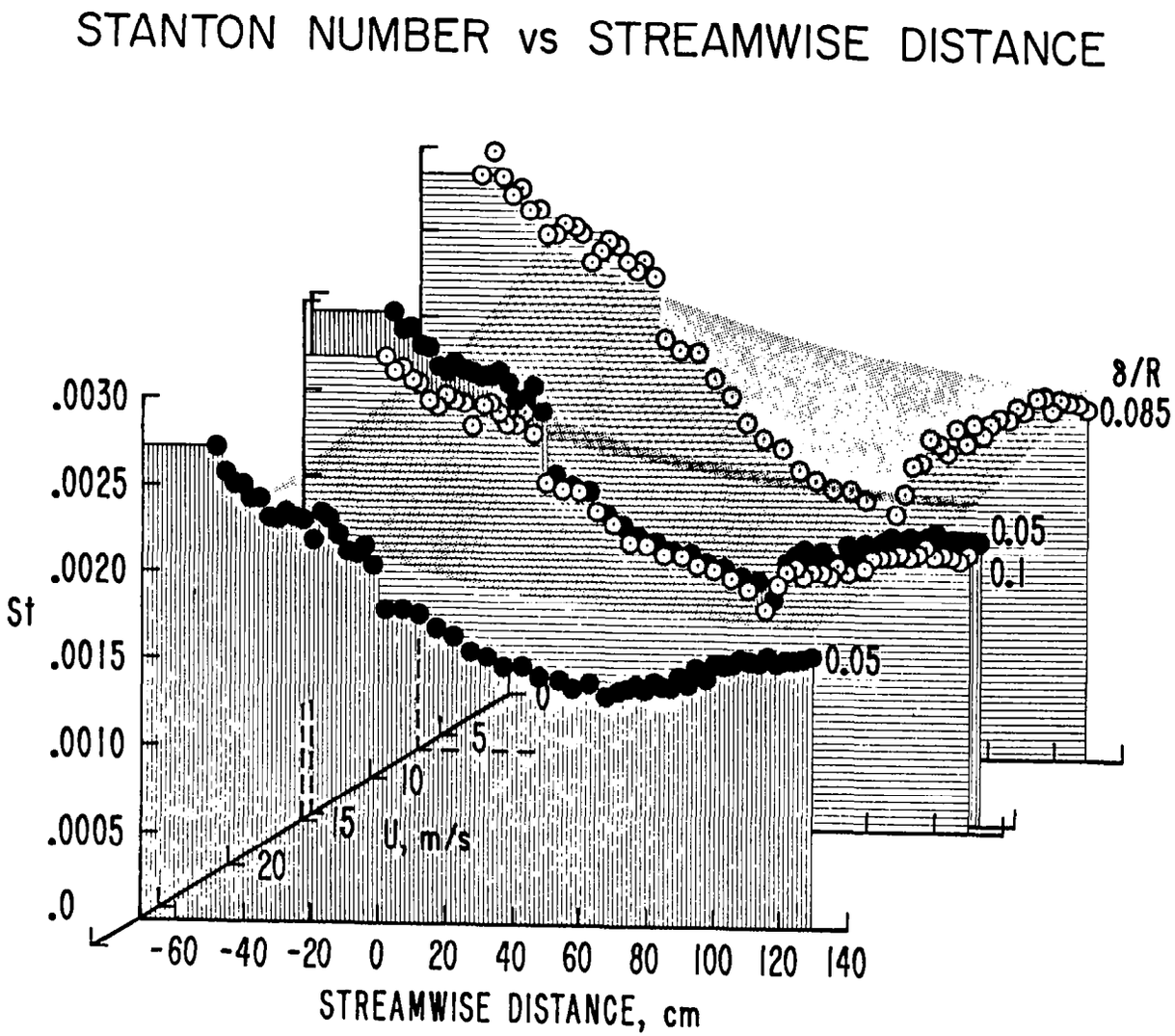

Fig. 3-10. The effect of U_{pw} - Stanton number versus streamwise distance and U_{pw} .

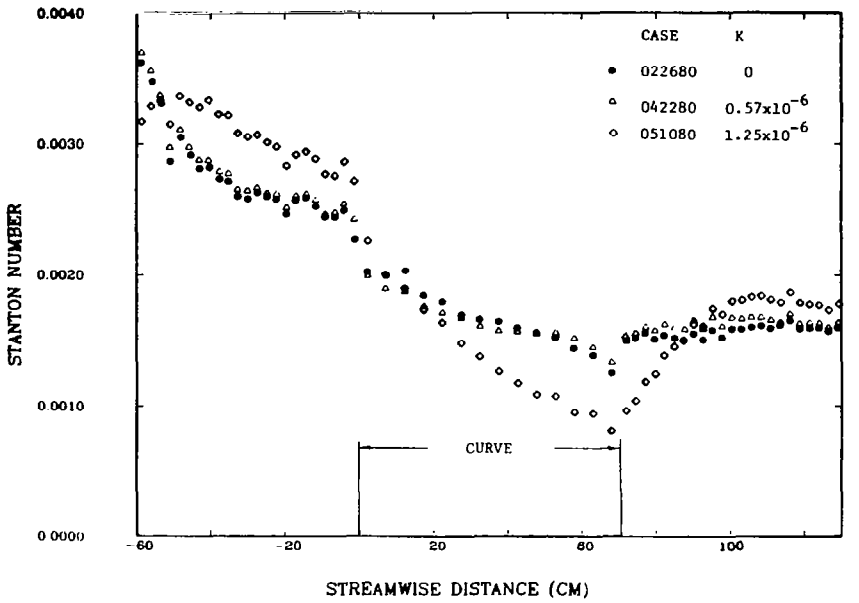

Fig. 3-11. The effect of free-stream acceleration on the curved boundary layer - Stanton number versus streamwise distance.

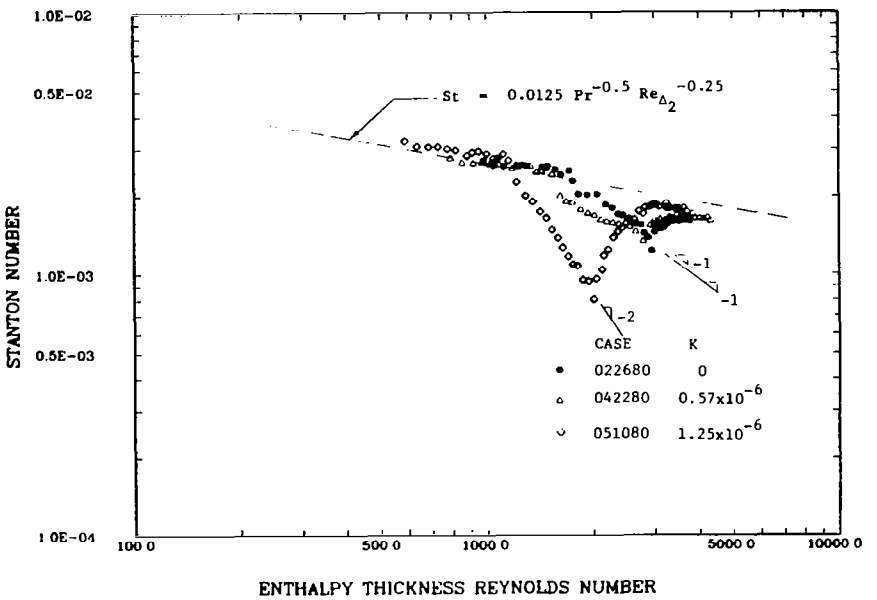

Fig. 3-12. The effect of free-stream acceleration on the curved boundary layer - Stanton number versus enthalpy thickness Reynolds number.

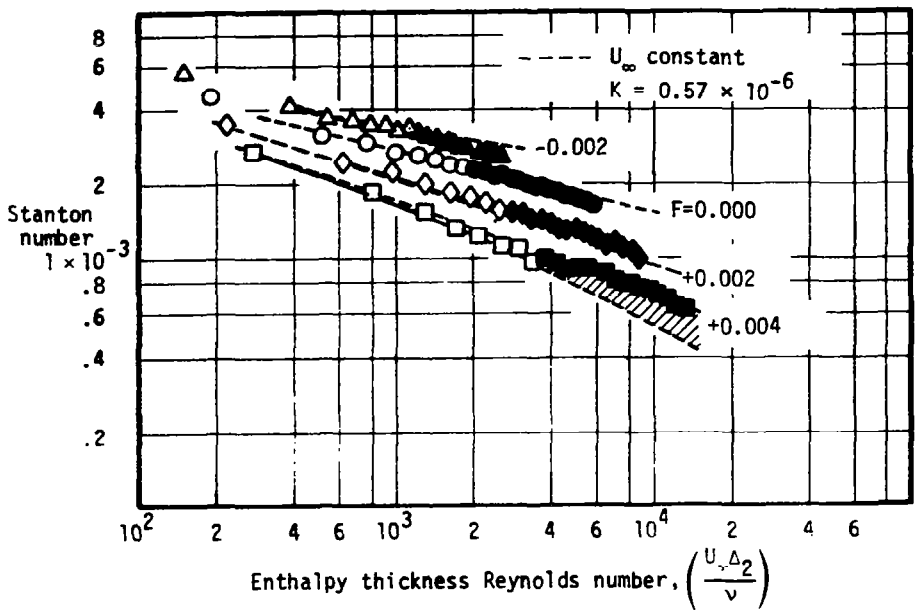

Fig. 3-13. The effect of mild free-stream acceleration (from Kays and Moffat [38]) - Stanton number versus enthalpy thickness Reynolds number.

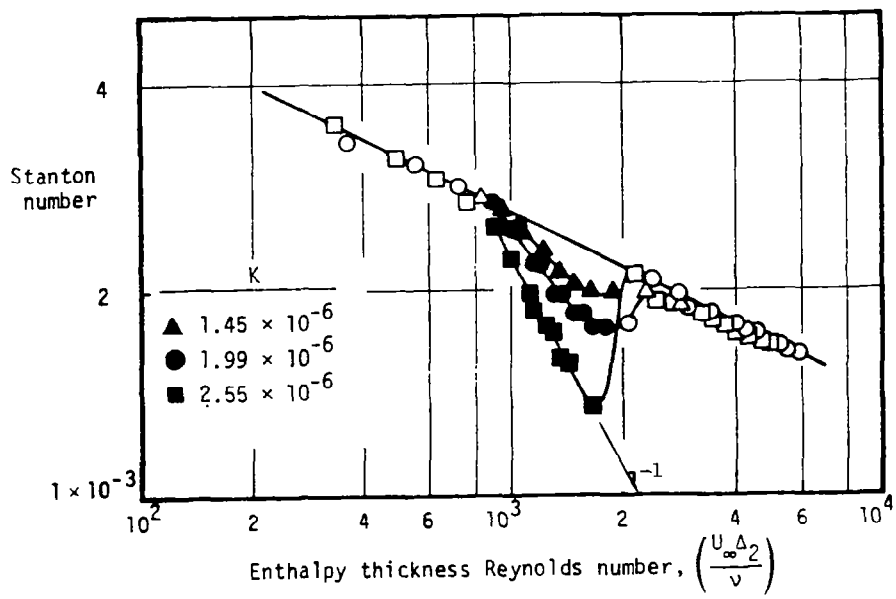

Fig. 3-14. The effect of strong free-stream acceleration (from Kays and Moffat [38]) - Stanton number versus enthalpy thickness Reynolds number.

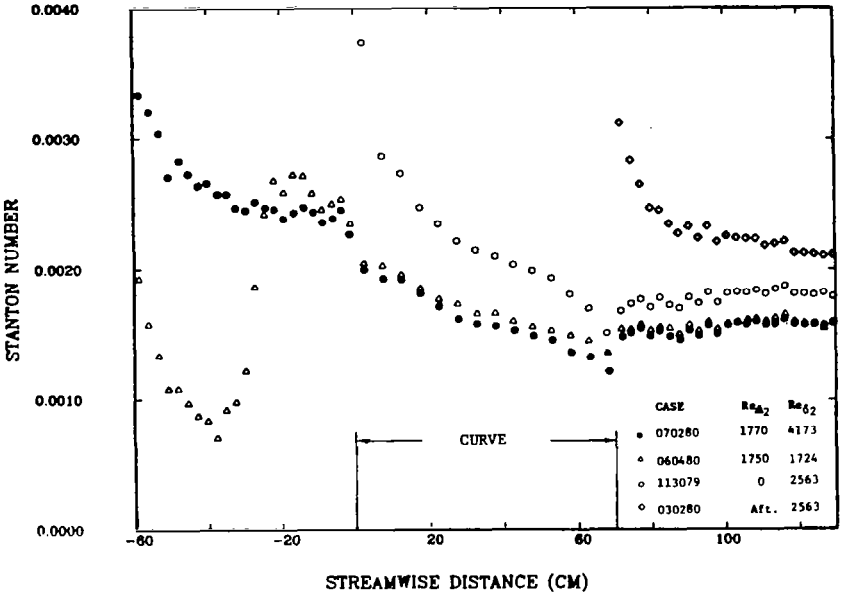

Fig. 3-15. The effect of unheated starting length - Stanton number versus streamwise distance.

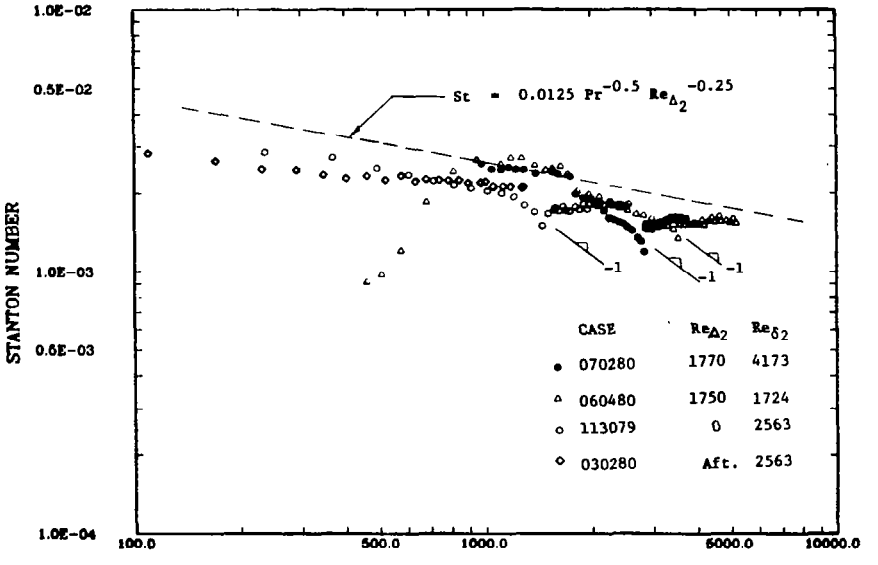

Fig. 3-16. The effect of unheated starting length - Stanton number versus enthalpy thickness Reynolds number.

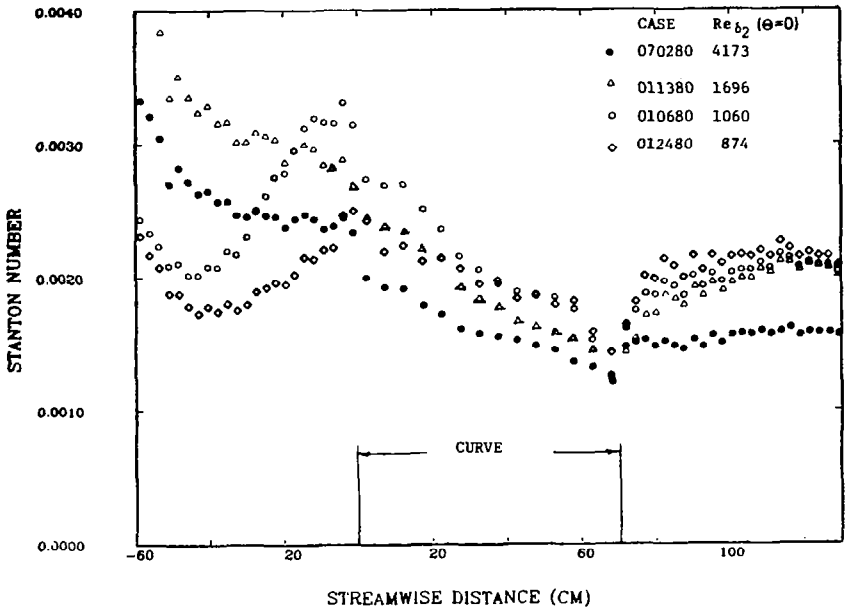

Fig. 3-17. The effect of the maturity of the momentum boundary layer - Stanton number versus streamwise distance for the late-transitional and turbulent cases.

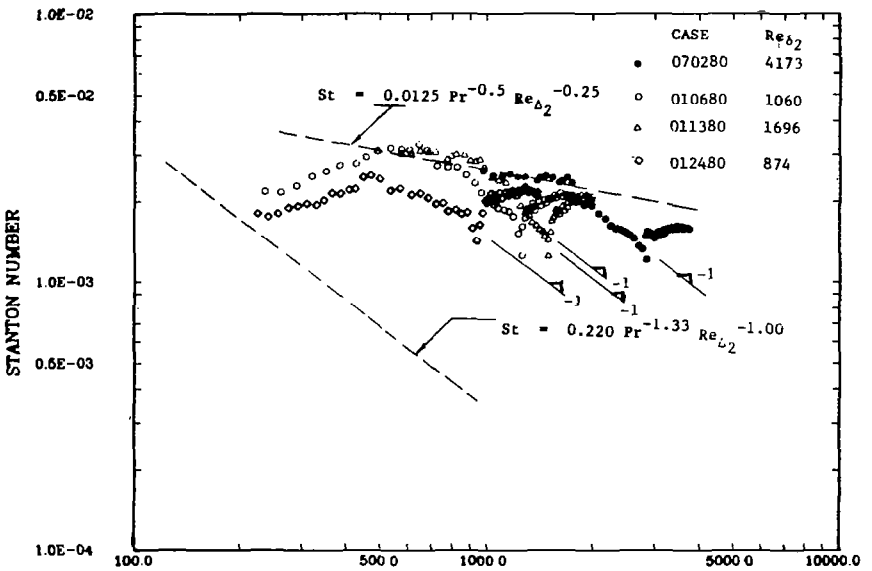

Fig. 3-18. The effect of the maturity of the momentum boundary layer - Stanton number versus enthalpy thickness Reynolds number for the late-transitional and turbulent cases.

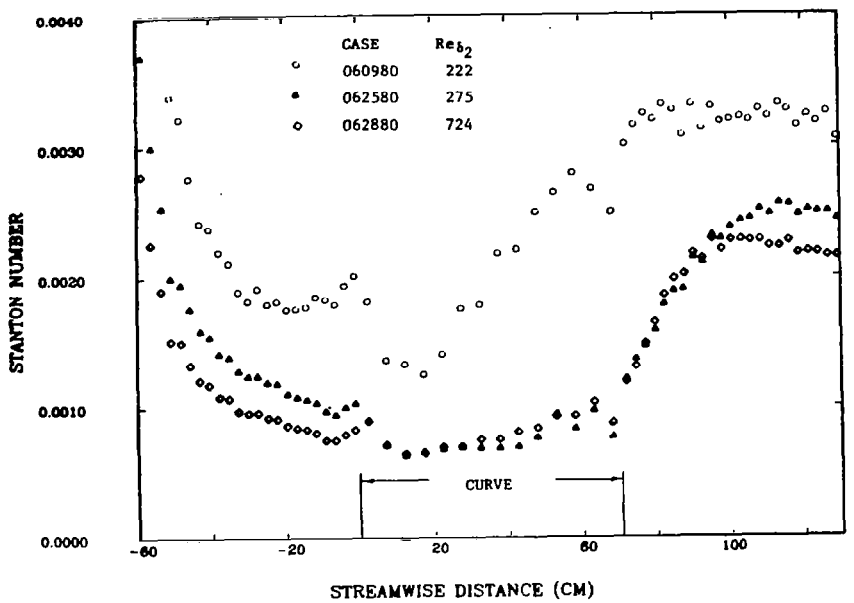

Fig. 3-19. The effect of the maturity of the momentum boundary layer - Stanton number versus streamwise distance for the laminar and early-transitional cases.

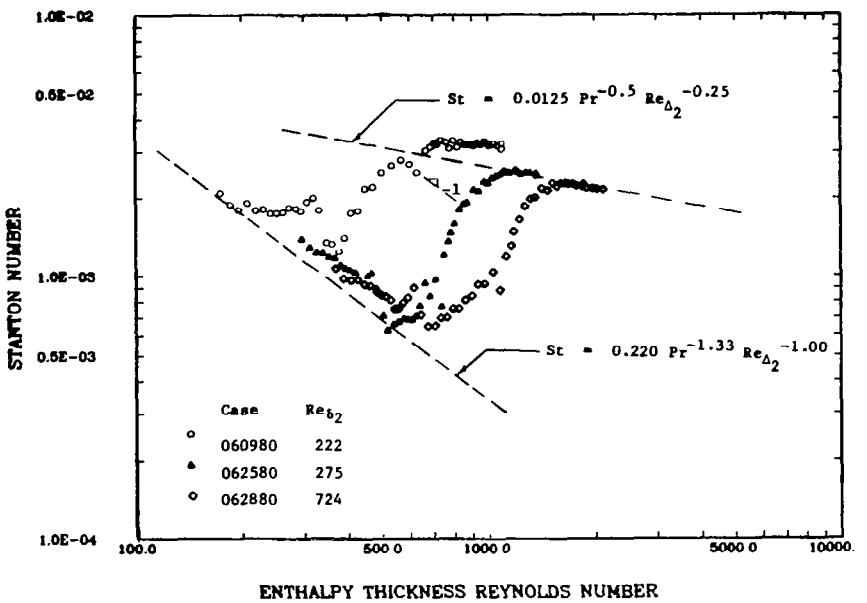

Fig. 3-20. The effect of the maturity of the momentum boundary layer - Stanton number versus enthalpy thickness Reynolds number for the laminar and early-transitional cases.

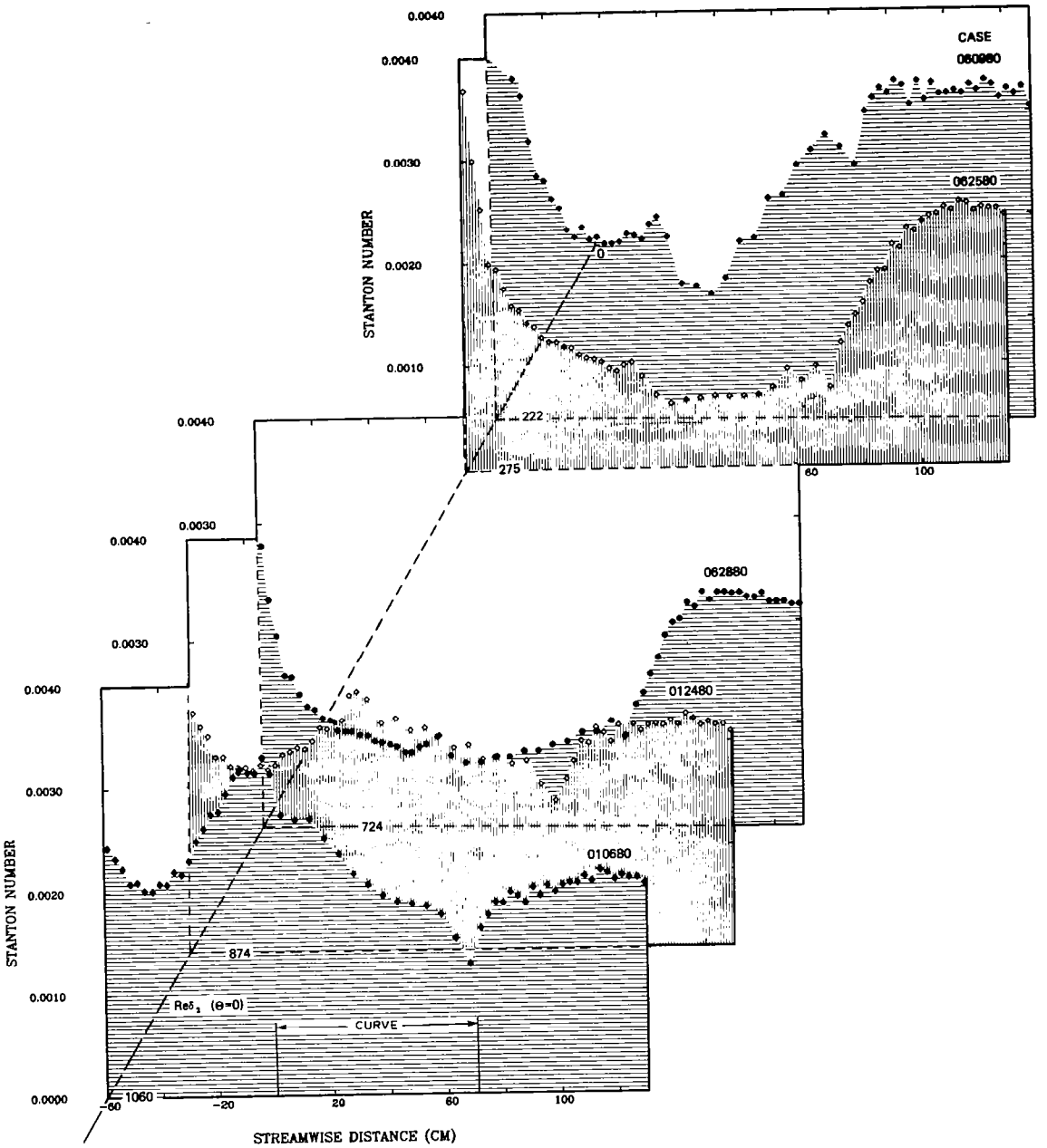

Fig. 3-21. The effect of the maturity of the momentum boundary layer - Stanton number versus enthalpy thickness Reynolds number and momentum thickness Reynolds number at the start of curvature.

Chapter 4
HEAT TRANSFER PREDICTIONS

One of the objectives of the curvature project was to develop a turbulence model for curved-wall heat transfer predictions that could be used for practical engineering calculations. This is, in fact, the most useful form in which to convey the results of these curvature experiments.

4.1 State of the Art

Prior to the beginning of the curved-wall studies at Stanford, the most prevalent curvature model was one which stemmed from a suggestion by Bradshaw [14] and was formulated and tested by Johnston and Eide [40]. Recently, Gillis and Johnston [35], with the benefit of their recovery data, proposed a second model consistent with their "shear layer" interpretation of the curved turbulent boundary layer. Both models are discussed below. They modified the distribution of the mixing length across the boundary layer to account for streamwise curvature.

Other, higher-order, models have been developed by Launder et al. [54], Irwin and Smith [39], and Gibson [53]. These models are quite good for mild curvature. Although higher-order models give more detail of the turbulence structure, they are generally more difficult to run and less useful as engineering tools. In order to make the results of the modeling effort most useful to industry, it was deemed desirable to keep the computation scheme simple--hence the mixing-length approach.

The mixing-length hypothesis uses an empirically prescribed length scale to relate the mean velocity gradient to the Reynolds shear stress, through the formula:

$$-\overline{uv} = \ell^2 \frac{\partial U}{\partial n} \left| \frac{\partial U}{\partial n} \right| \qquad (4\text{-}1)$$

A typical distribution of mixing length "ℓ" for a flat-wall boundary layer is:

$$\ell = \kappa n \left[1 - \exp(-n^+/A^+) \right] \qquad (4\text{-}2)$$

the modified van Driest model [36] for the inner portion of the boundary layer, where κ, the Karman constant, is 0.41. For the outer portion of the boundary layer, the typical flat-wall mixing length distribution has

$$\ell = 0.085\ \delta_{99} \qquad (4\text{-}3)$$

The smaller of (4-2) or (4-3) is used. The parameter A^+ identifies the thickness of the viscous sublayer and is affected by acceleration/deceleration or blowing/suction. The value for a flat-wall boundary layer with uniform freestream velocity and no transpiration is $A^+ = 25$.

The curvature model suggested by Bradshaw [14] modified this flat-wall distribution for curvature according to the relationship:

$$\ell = \ell_o(1 - \beta Ri) \quad ,$$

where ℓ_o is the local flat-wall mixing length and Ri is the local gradient Richardson number defined by

$$Ri = 2S(1 + S) \quad ,$$

where S, the stability parameter, is

$$S = \frac{U}{R_{eff}} \Big/ \frac{\partial U}{\partial n}$$

The parameter β is an empirical parameter generally of the order 10. The effective radius of curvature, R_{eff}, comes from a first-order lag model proposed by Johnston and Eide [41]:

$$\frac{d(1/R_{eff})}{dx} = \frac{1}{10\ \delta_{99}} \left[\frac{1}{Ro} - \frac{1}{R_{eff}} \right]$$

Ro is the wall radius of curvature. This mixing-length model was investigated in detail by Johnston and Eide [40,41]. Their recommendation for the value of the constant β was 6.0. Figure 4-1 shows its

performance for the baseline case. The prediction was initialized with starting profiles taken 35 cm upstream of the beginning of the curve. The test wall was isothermal and U_{pw} was uniform. No correction for the effect of curvature on turbulent Prandtl number was made. The response to the introduction of curvature was predicted quite well, but, after the curve, $C_f/2$ and St recovered far too quickly. If the turbulent Prandtl number were decreased in the recovery region according to the curve of Fig. 3-4, the recovery process would be even faster. This model was devised before recovery data had been taken. Since it is merely an empirical fit of curved and rotating wall mixing lengths, it is not surprising that the model's performance in the recovery region was poor.

Gillis and Johnston [35] improved the recovery prediction by devising a model in which the main effect of curvature was to confine the turbulent motions close to the wall and allow the previously existing large-scale motions to decay. In the recovery region, they modeled the regrowth of the inner boundary layer as a normal boundary layer growing on a flat plate within a velocity gradient. Their model follows.*

The mixing length in the outer portion of the boundary layer was modeled as:

$$\ell \propto \delta_{sl} - \delta^*_{sl}$$

where δ_{sl} is the width of the active shear layer and δ^*_{sl} is the displacement thickness of the boundary layer integrated out to the shear layer thickness δ_{sl}. The constant of proportionality was found to be 0.10. The shear layer thickness in the flat-wall preplate or recovery wall was found by extrapolating the linear portion of the shear stress profile to $\overline{uv} = 0$, as shown in Fig. 1-8. Within the curve, Gillis and Johnston use a proposal from Gibson [42], that there is a critical value of the stability parameter, S, defined as:

$$S = \frac{U/R}{\partial U/\partial n}$$

*See Ref. 35 for more details.

above which the shear stress cannot sustain itself. Gibson found that this critical value was approximately 0.17. Gillis and Johnston found that a critical value of 0.11 optimized the prediction of their data.

The model used in the following predictions of the heat transfer data is essentially the same model as presented in Ref. 35, with the exceptions of two changes made to the estimation of δ_{sl} within the curve.

To describe the first change, it is necessary to define the following two parameters:

Y_{crit} The n-distance away from the wall where $S = S_{crit}$.

Y_{sl} The n-distance away from the wall where the extrapolated shear stress equals zero.

In the Gillis and Johnston model,

$$\ell = 0.10 \quad (\delta_{sl} - \delta^*_{sl})$$

where $\delta_{sl} = Y_{sl}$ in the developing or recovery regions and $\delta_{sl} = Y_{crit}$ in the curved region. With their model it was found that the switchover at the beginning of curvature quickly altered the shear stress profile driving Y_{sl} down to a small fraction of Y_{crit}. But, as the change in the shear stress profile began to alter the mean velocity profile, Y_{sl} began to rebound, passing up through and finally well above Y_{crit}. This rebound eventually affected the mean velocity and temperature profiles, causing the calculated values of $C_f/2$ and St to increase in a manner much like recovery from curvature, though still within the curve. The critical stability argument states that, in the asymptotic curved state, the extrapolated shear layer thickness. Y_{sl}, equals the n-distance where $S = S_{crit}$, Y_{crit}. But in this model, Y_{sl} could be well above Y_{crit}, especially, it was found, when δ_{99}/R was small. The change in the model was to construct a "controller" that would not allow Y_{sl} to grow much above Y_{crit}. The new model calculated the δ_{sl} to be used in computing the curved-region mixing length profile as:

$$\delta_{sl} = Y_{crit} \quad \text{when} \quad Y_{sl} < Y_{crit}$$

$$\delta_{sl} = Y_{crit}\left(1.0 - 2.0\left(\frac{Y_{sl}}{Y_{crit}} - 1.0\right)\right)$$

when $Y_{sl} > Y_{crit}$ but $\delta_{sl}/Y_{crit} > 0.33$.

It is a stiff "controller" that drives δ_{sl} down when $Y_{sl} > Y_{crit}$ trying to force $Y_{sl} \approx Y_{crit}$ for the asymptotic curved boundary layer. Note that when $Y_{sl} < Y_{crit}$ the new instruction has no effect.

The second change to the model was developed when trying to predict the three cases of differing δ_{99}/R. It was found that the optimum value of S_{crit} was a function of δ_{99}/R. Fitting the optimum values for cases of $\delta_{99}/R = 0.10$, 0.05, and 0.02 with a smooth curve gave:

$$S_{crit} = \frac{(\delta_{99}/R)^{1/3}}{4}$$

Since the δ_{99}/R used in the model is the local value and not the value at the start of curvature, S_{crit} is continually updated as the boundary layer thickens. This correlation gives the correct trend with δ_{99}/R for the cases studied. It is not known, however, that it would do equally well if δ_{99}/R were changed from case to case by changing R while holding $\delta_{99}(\theta=0)$ constant.

In the following sections, predictions are made of many of the heat transfer runs presented earlier. In these predictions the turbulent Prandtl number was not changed as a result of curvature. Figure 3-4 shows that, within the curve, the change of turbulent Prandtl number is small and in a direction that would decrease the Stanton numbers slightly below the following predictions. A mild improvement to the model could be made, then, by incorporating a turbulent Prandtl number correction for the curved boundary layer. One possibility is the model developed by R.M.C. So [31] discussed in Chapter 1.

Figure 3-4 shows that there seems to be an effect of recovery on the turbulent Prandtl number. The following predictions, which make no such correction, are expected to show too slow a recovery. At present, no model exists for making this correction. Profiles of local $\overline{v't'}/\overline{u'v'}$ across the recovering boundary layer would be valuable in developing a model that accurately accounts for this effect.

The present model can be quite temperamental. The calculation of Y_{sl} is done by extrapolation of a linear portion of the shear stress profile to the wall. After some distance downstream of the beginning of curvature, the shear stress profile develops inflections that can cause Y_{sl} to jump a considerable distance from step to step. This usually results in variations in the slope of St versus Re_{Δ_2} (or s), oscillating about what appears to be a reasonable value. Occasionally the program will extrapolate to an extremely small Y_{sl} due to an inflection very near the wall. When this happens, the solution goes irreparably out of control. Because of this, the program can be quite frustrating and expensive to run. An improvement might be to calculate the shear layer thickness as an integral thickness:

$$Y_{sl} \text{ is a function of } \int_0^{n_o} \frac{\tau}{\tau_w} dn \quad ,$$

where n_o is the n-distance when the shear stress goes to zero. This would stabilize the model considerably.

The following sections demonstrate how well the above model with the above changes predicts the heat transfer cases discussed in Chapter 3.

4.2 Predicting the Effect of Curvature for the Baseline Case

Figures 4-2 and 4-3 show the prediction of the baseline case. The introduction of curvature rapidly decreases the skin friction and Stanton number. For this case the effect is strong enough to overshoot and oscillate for some time before settling down to the asymptotic curved state. The prediction of both the skin friction and the Stanton number within the curve is quite good. Note that a Pr_t correction would decrease St slightly near the end of the curve. The recovery is quite accurately predicted. Note that the Pr_t correction would increase the predicted St in the recovery region. To try to assess just how much the correction would increase St, the ratio of $St/(C_f/2)$ was calculated from the profile data for this case from Chapter 3, then multiplied by the predicted $C_f/2$ to get an estimated Stanton number with a recovery correction on Pr_t. This corrected Stanton number is shown in

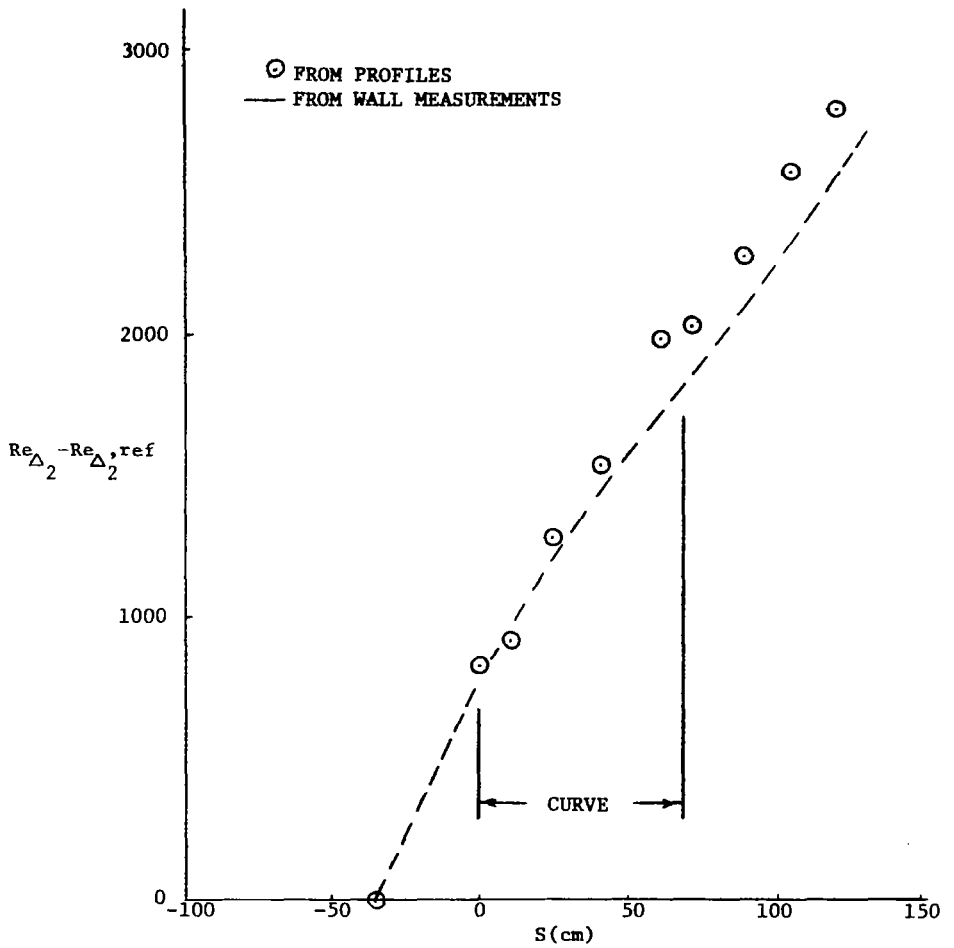

Fig. 3-5. Comparison of Re_{Δ_2} from the energy integral equation and Re_{Δ_2} from the measured profiles for the baseline case[2](070280) - Turbulent, $\delta_{99}/R(\theta=0)$ = 0.10, U_{pw} = 14.8 m/s , K ≃ 0.0.

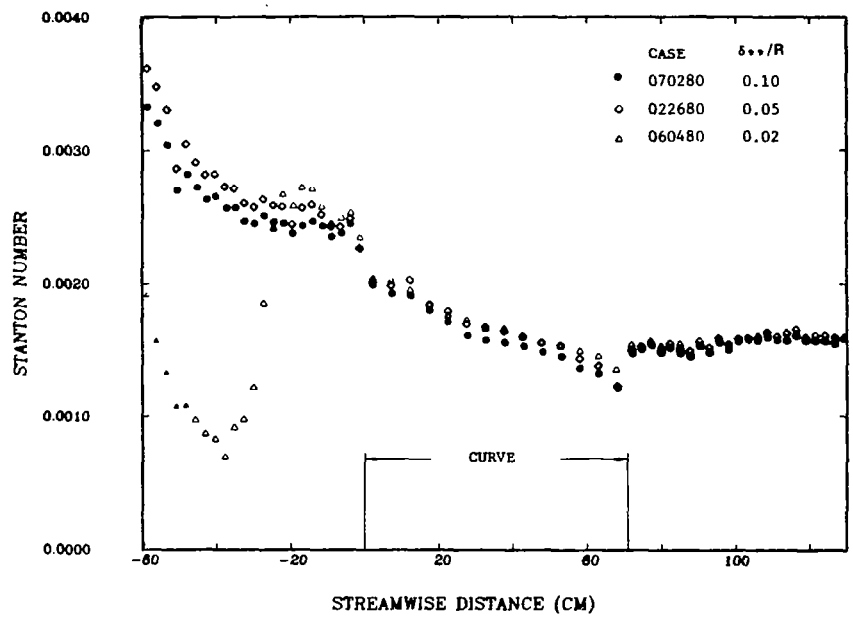

Fig. 3-6. The effect of initial boundary layer thickness - Stanton number versus streamwise distance.

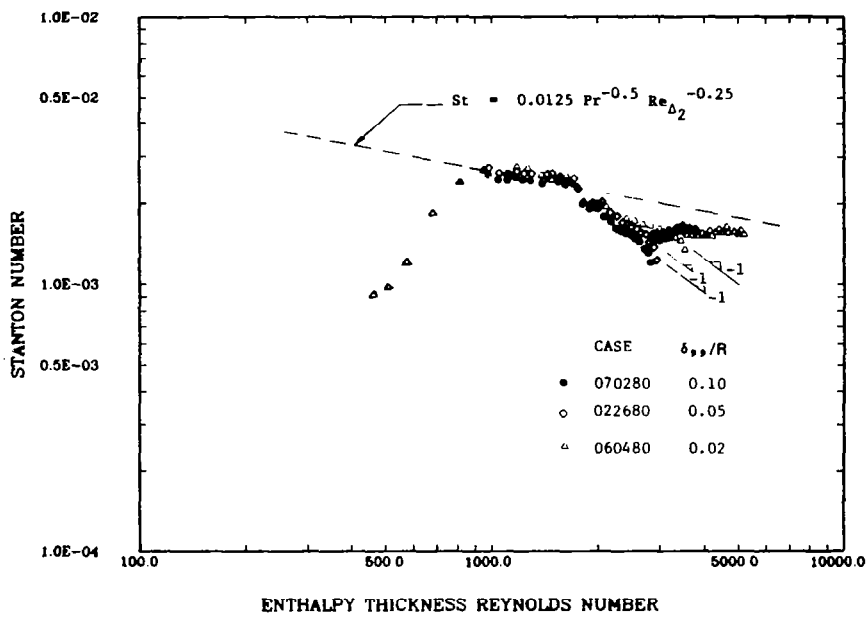

Fig. 3-7. The effect of initial boundary layer thickness - Stanton number versus enthalpy thickness Reynolds number.

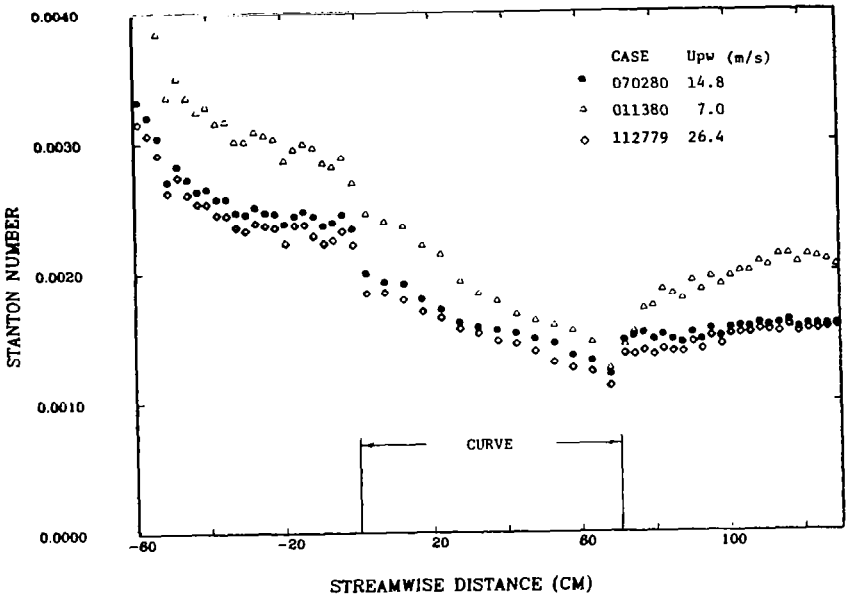

Fig. 3-8. The effect of U_{pw} - Stanton number versus streamwise distance

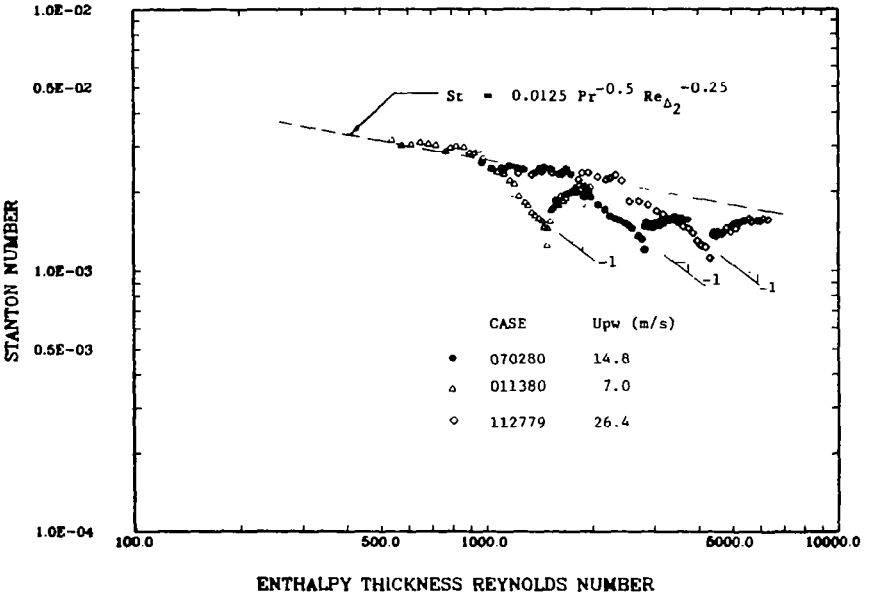

Fig. 3-9. The effect of U_{pw} - Stanton number versus enthalpy thickness Reynolds number.

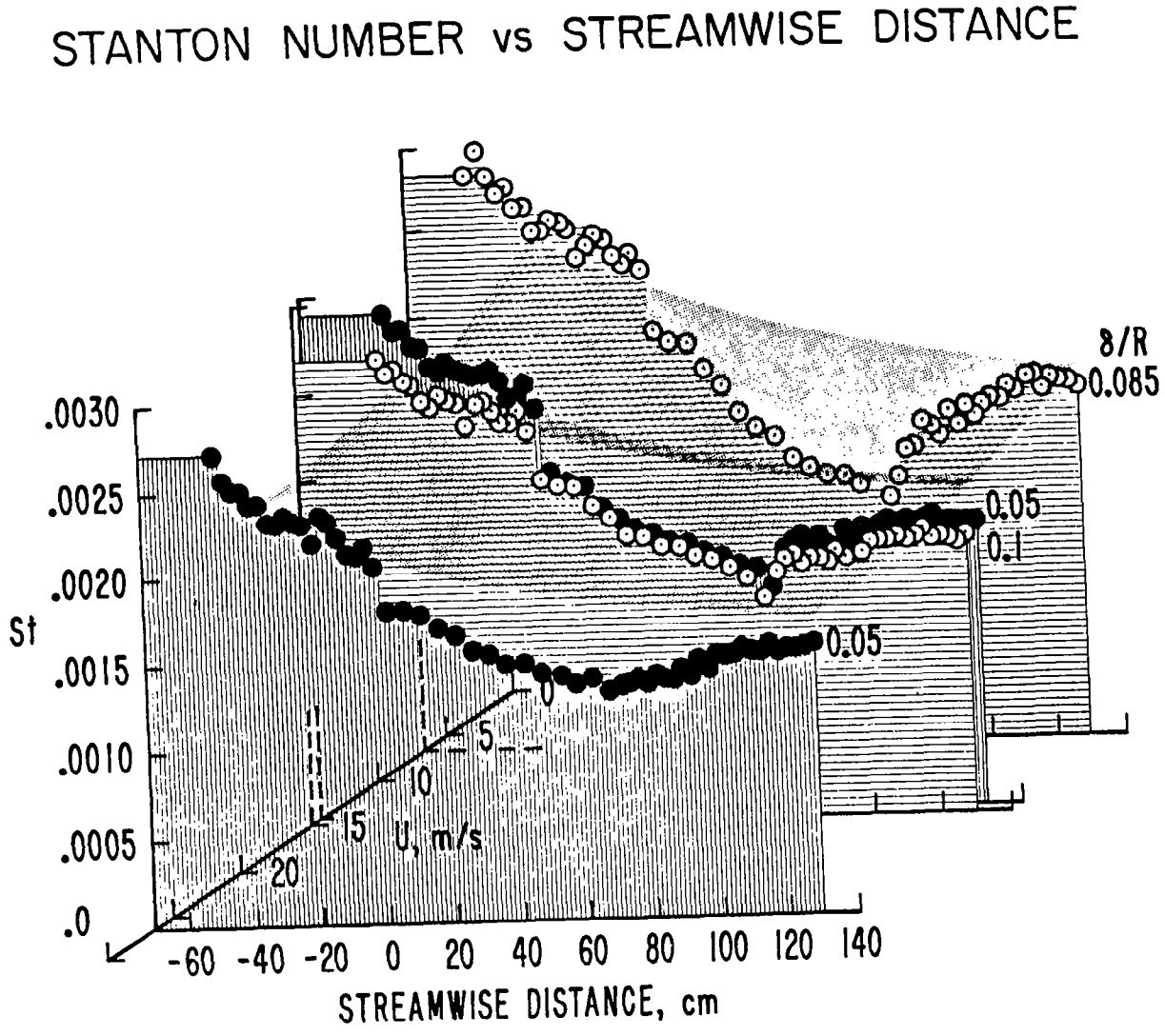

Fig. 3-10. The effect of U_{pw} - Stanton number versus streamwise distance and U_{pw} .

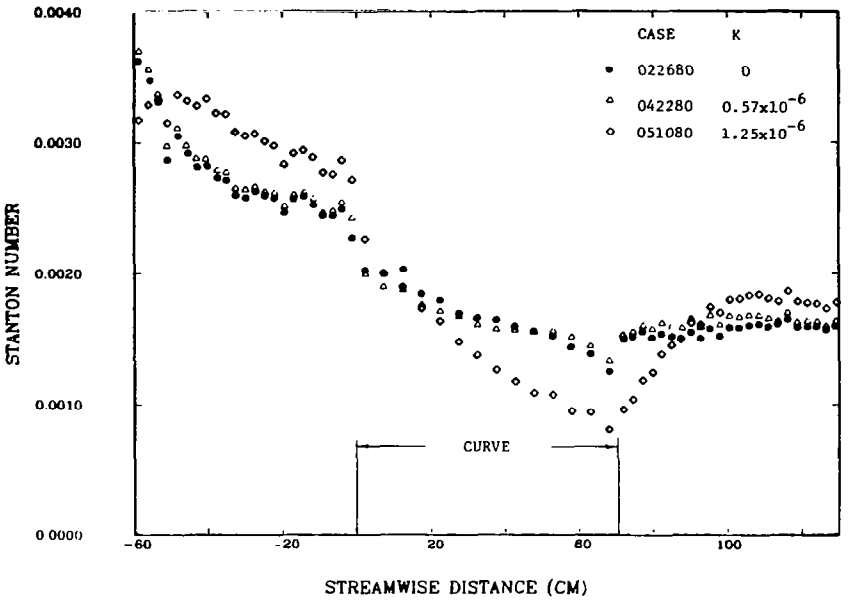

Fig. 3-11. The effect of free-stream acceleration on the curved boundary layer - Stanton number versus streamwise distance.

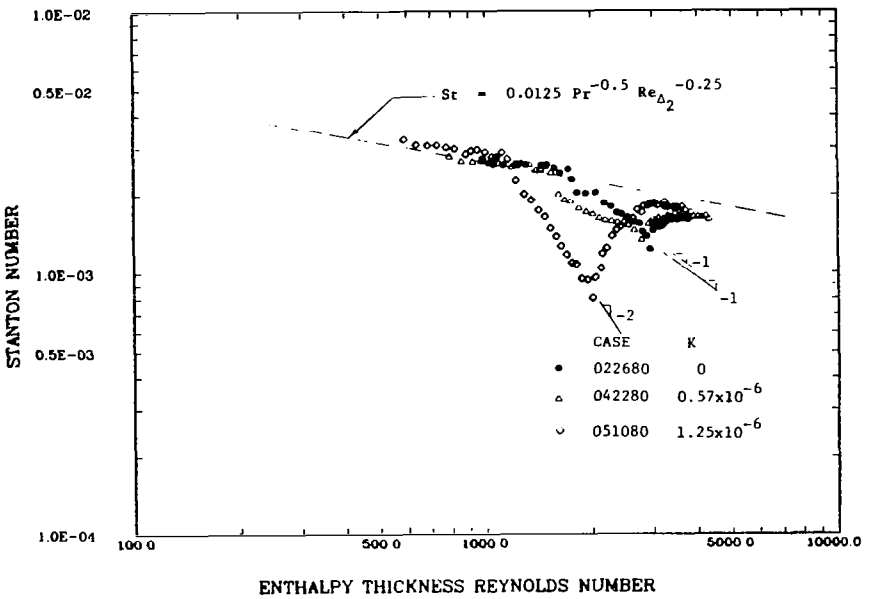

Fig. 3-12. The effect of free-stream acceleration on the curved boundary layer - Stanton number versus enthalpy thickness Reynolds number.

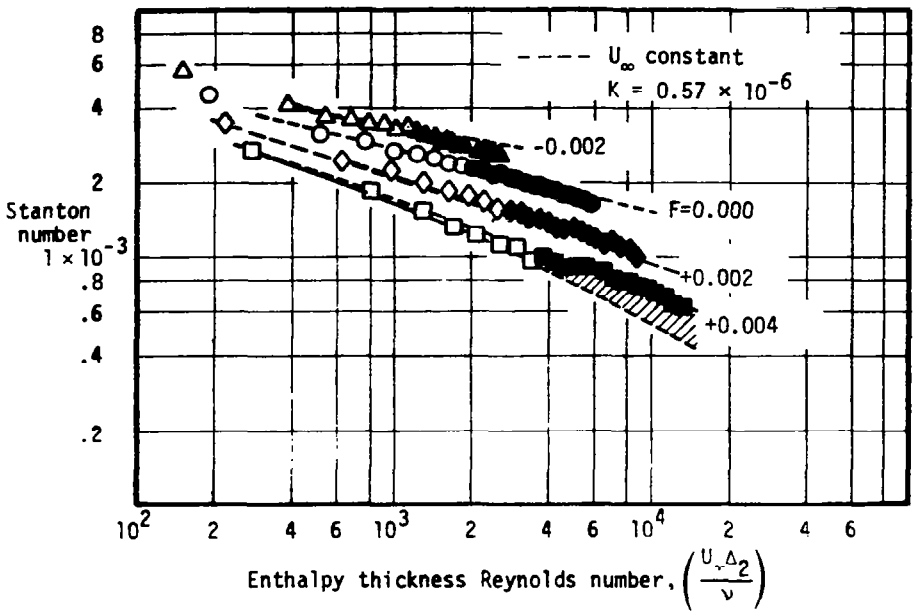

Fig. 3-13. The effect of mild free-stream acceleration (from Kays and Moffat [38]) - Stanton number versus enthalpy thickness Reynolds number.

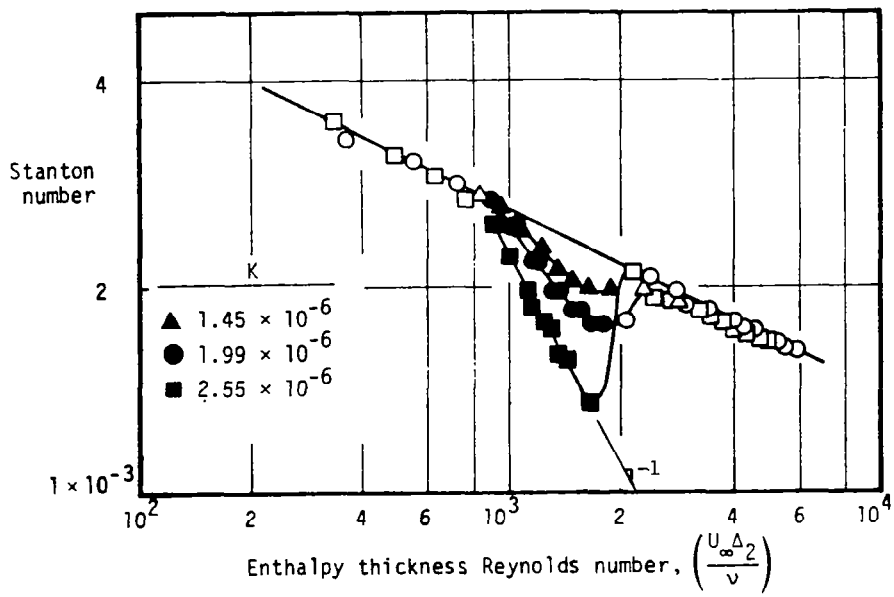

Fig. 3-14. The effect of strong free-stream acceleration (from Kays and Moffat [38]) - Stanton number versus enthalpy thickness Reynolds number.

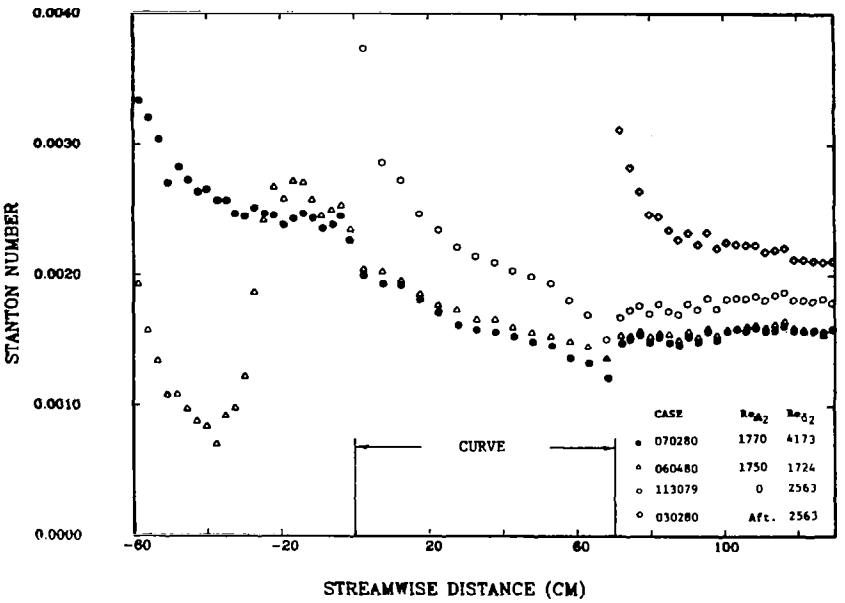

Fig. 3-15. The effect of unheated starting length - Stanton number versus streamwise distance.

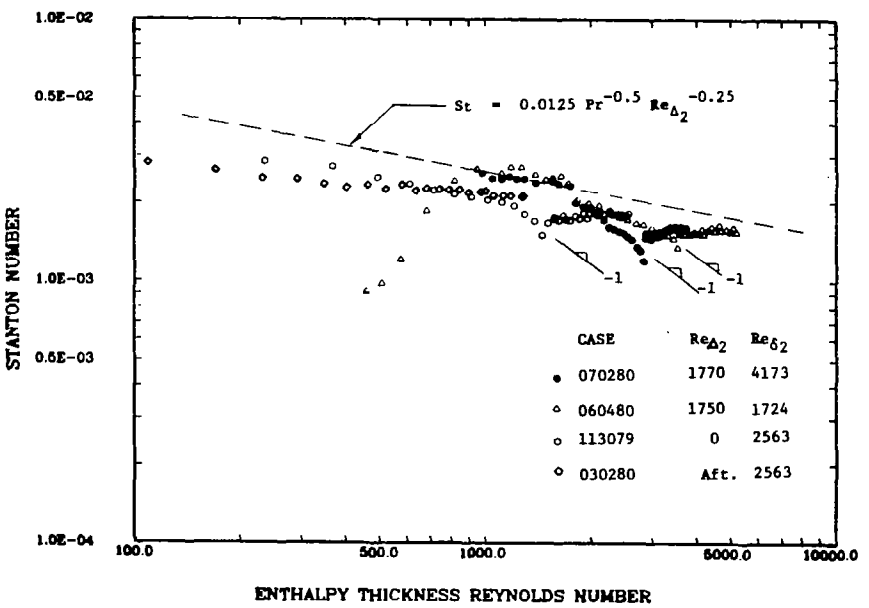

Fig. 3-16. The effect of unheated starting length - Stanton number versus enthalpy thickness Reynolds number.

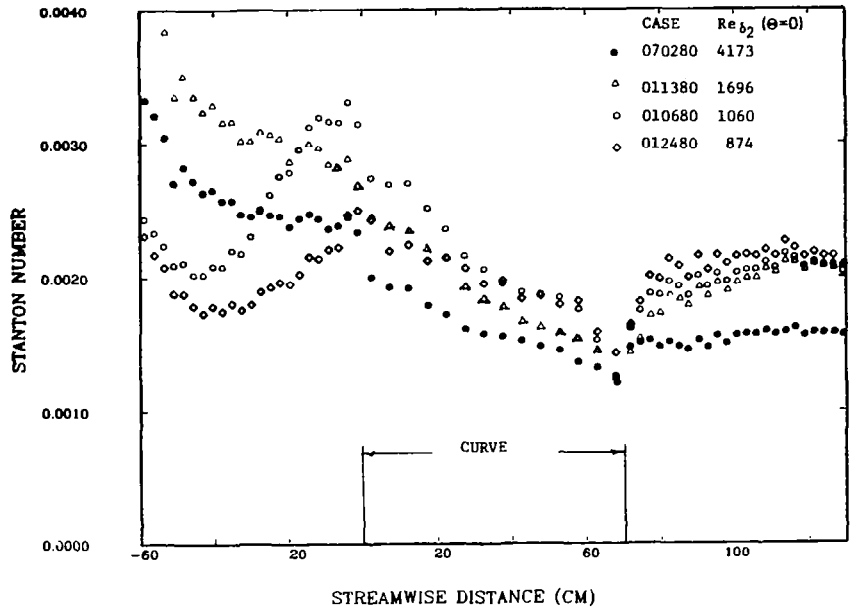

Fig. 3-17. The effect of the maturity of the momentum boundary layer - Stanton number versus streamwise distance for the late-transitional and turbulent cases.

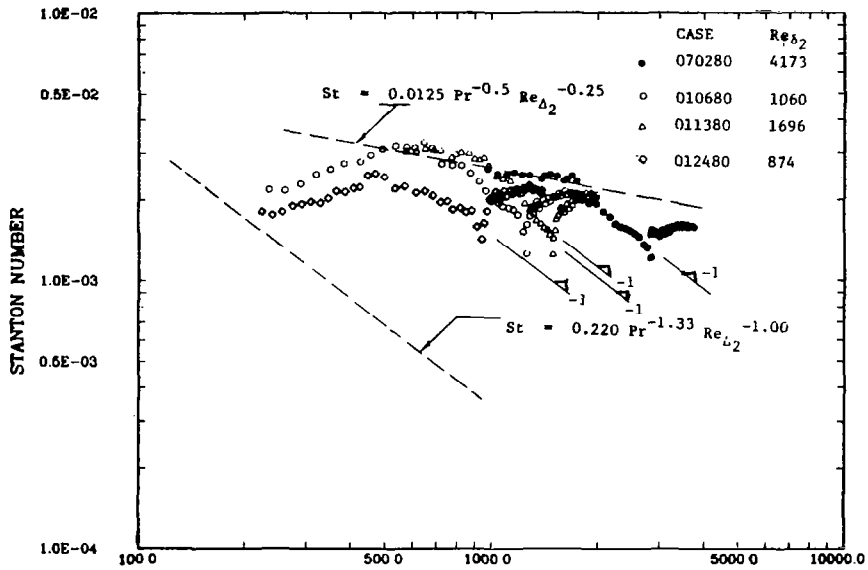

Fig. 3-18. The effect of the maturity of the momentum boundary layer - Stanton number versus enthalpy thickness Reynolds number for the late-transitional and turbulent cases.

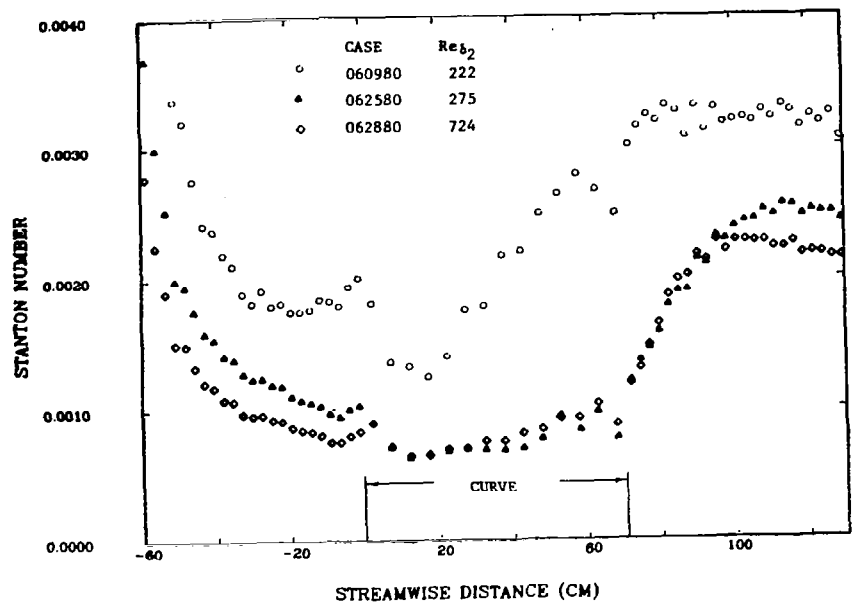

Fig. 3-19. The effect of the maturity of the momentum boundary layer - Stanton number versus streamwise distance for the laminar and early-transitional cases.

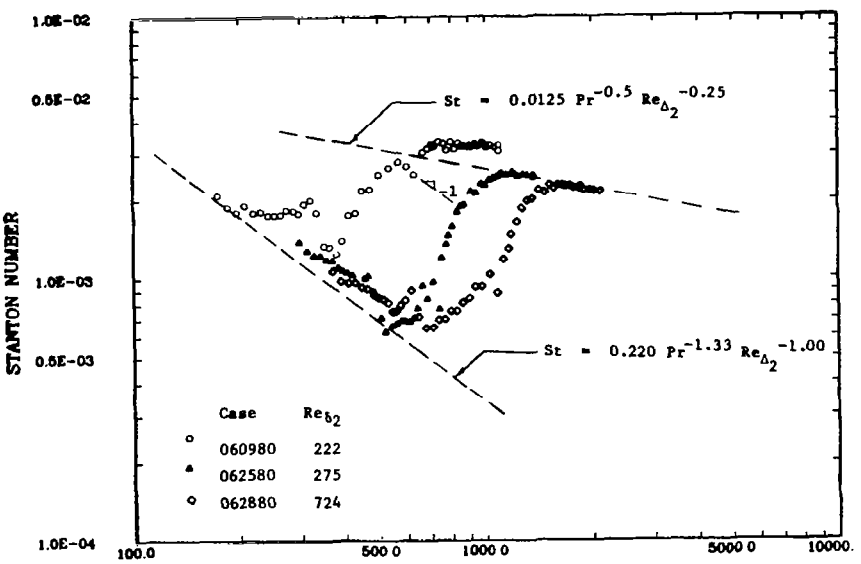

Fig. 3-20. The effect of the maturity of the momentum boundary layer - Stanton number versus enthalpy thickness Reynolds number for the laminar and early-transitional cases.

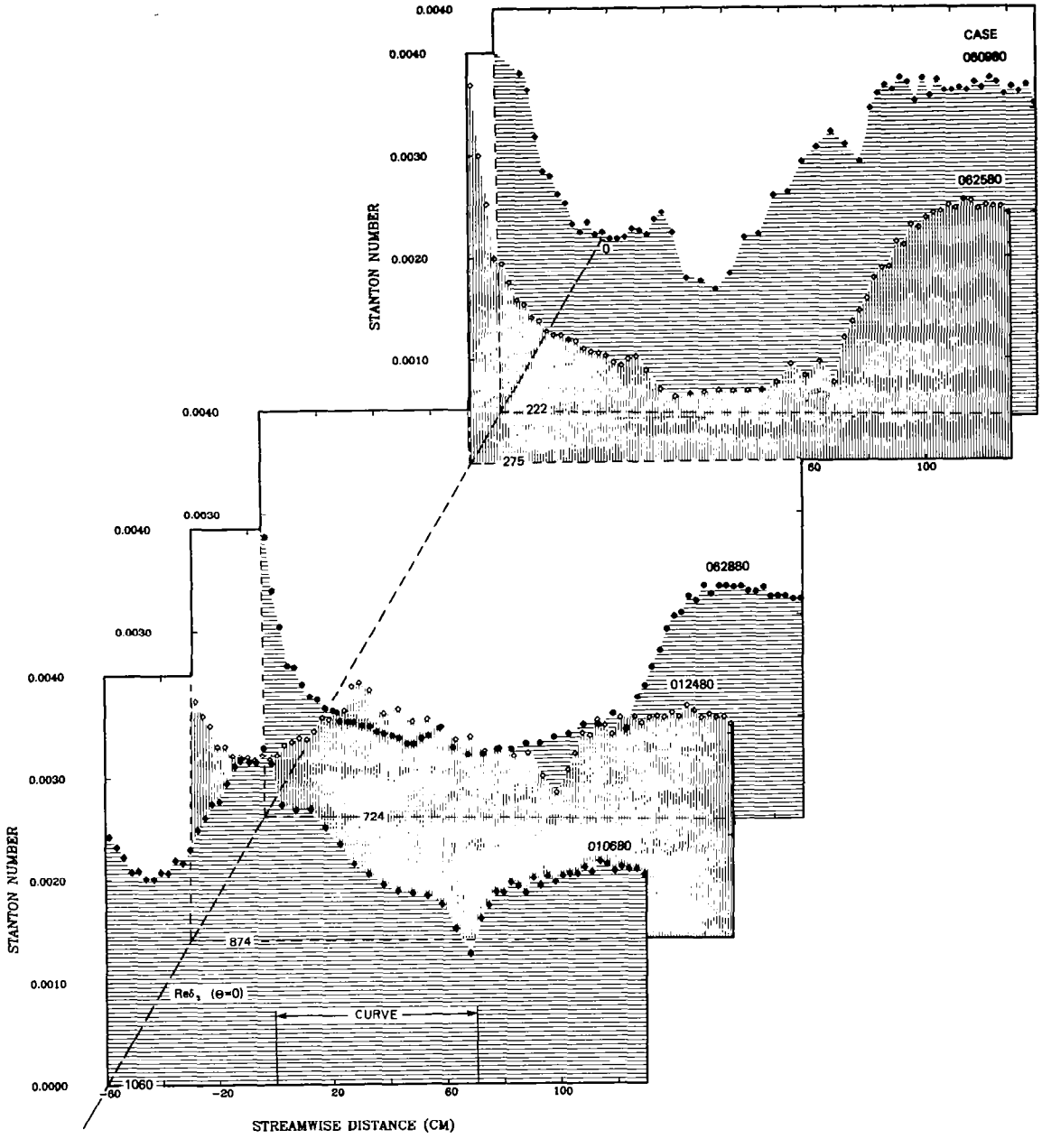

Fig. 3-21. The effect of the maturity of the momentum boundary layer - Stanton number versus enthalpy thickness Reynolds number and momentum thickness Reynolds number at the start of curvature.

Chapter 4
HEAT TRANSFER PREDICTIONS

One of the objectives of the curvature project was to develop a turbulence model for curved-wall heat transfer predictions that could be used for practical engineering calculations. This is, in fact, the most useful form in which to convey the results of these curvature experiments.

4.1 State of the Art

Prior to the beginning of the curved-wall studies at Stanford, the most prevalent curvature model was one which stemmed from a suggestion by Bradshaw [14] and was formulated and tested by Johnston and Eide [40]. Recently, Gillis and Johnston [35], with the benefit of their recovery data, proposed a second model consistent with their "shear layer" interpretation of the curved turbulent boundary layer. Both models are discussed below. They modified the distribution of the mixing length across the boundary layer to account for streamwise curvature.

Other, higher-order, models have been developed by Launder et al. [54], Irwin and Smith [39], and Gibson [53]. These models are quite good for mild curvature. Although higher-order models give more detail of the turbulence structure, they are generally more difficult to run and less useful as engineering tools. In order to make the results of the modeling effort most useful to industry, it was deemed desirable to keep the computation scheme simple--hence the mixing-length approach.

The mixing-length hypothesis uses an empirically prescribed length scale to relate the mean velocity gradient to the Reynolds shear stress, through the formula:

$$-\overline{uv} = \ell^2 \frac{\partial U}{\partial n} \left| \frac{\partial U}{\partial n} \right| \qquad (4\text{-}1)$$

A typical distribution of mixing length "ℓ" for a flat-wall boundary layer is:

$$\ell = \kappa n \left[1 - \exp(-n^+/A^+) \right] \qquad (4\text{-}2)$$

the modified van Driest model [36] for the inner portion of the boundary layer, where κ, the Karman constant, is 0.41. For the outer portion of the boundary layer, the typical flat-wall mixing length distribution has

$$\ell = 0.085\ \delta_{99} \qquad (4\text{-}3)$$

The smaller of (4-2) or (4-3) is used. The parameter A^+ identifies the thickness of the viscous sublayer and is affected by acceleration/deceleration or blowing/suction. The value for a flat-wall boundary layer with uniform freestream velocity and no transpiration is $A^+ = 25$.

The curvature model suggested by Bradshaw [14] modified this flat-wall distribution for curvature according to the relationship:

$$\ell = \ell_o(1 - \beta Ri) \quad ,$$

where ℓ_o is the local flat-wall mixing length and Ri is the local gradient Richardson number defined by

$$Ri = 2S(1 + S) \quad ,$$

where S, the stability parameter, is

$$S = \frac{U}{R_{eff}} \Big/ \frac{\partial U}{\partial n}$$

The parameter β is an empirical parameter generally of the order 10. The effective radius of curvature, R_{eff}, comes from a first-order lag model proposed by Johnston and Eide [41]:

$$\frac{d(1/R_{eff})}{dx} = \frac{1}{10\ \delta_{99}} \left[\frac{1}{Ro} - \frac{1}{R_{eff}} \right]$$

Ro is the wall radius of curvature. This mixing-length model was investigated in detail by Johnston and Eide [40,41]. Their recommendation for the value of the constant β was 6.0. Figure 4-1 shows its

performance for the baseline case. The prediction was initialized with starting profiles taken 35 cm upstream of the beginning of the curve. The test wall was isothermal and U_{pw} was uniform. No correction for the effect of curvature on turbulent Prandtl number was made. The response to the introduction of curvature was predicted quite well, but, after the curve, $C_f/2$ and St recovered far too quickly. If the turbulent Prandtl number were decreased in the recovery region according to the curve of Fig. 3-4, the recovery process would be even faster. This model was devised before recovery data had been taken. Since it is merely an empirical fit of curved and rotating wall mixing lengths, it is not surprising that the model's performance in the recovery region was poor.

Gillis and Johnston [35] improved the recovery prediction by devising a model in which the main effect of curvature was to confine the turbulent motions close to the wall and allow the previously existing large-scale motions to decay. In the recovery region, they modeled the regrowth of the inner boundary layer as a normal boundary layer growing on a flat plate within a velocity gradient. Their model follows.*

The mixing length in the outer portion of the boundary layer was modeled as:

$$\ell \propto \delta_{sl} - \delta^*_{sl}$$

where δ_{sl} is the width of the active shear layer and δ^*_{sl} is the displacement thickness of the boundary layer integrated out to the shear layer thickness δ_{sl}. The constant of proportionality was found to be 0.10. The shear layer thickness in the flat-wall preplate or recovery wall was found by extrapolating the linear portion of the shear stress profile to $\overline{uv} = 0$, as shown in Fig. 1-8. Within the curve, Gillis and Johnston use a proposal from Gibson [42], that there is a critical value of the stability parameter, S, defined as:

$$S = \frac{U/R}{\partial U/\partial n}$$

*See Ref. 35 for more details.

above which the shear stress cannot sustain itself. Gibson found that this critical value was approximately 0.17. Gillis and Johnston found that a critical value of 0.11 optimized the prediction of their data.

The model used in the following predictions of the heat transfer data is essentially the same model as presented in Ref. 35, with the exceptions of two changes made to the estimation of δ_{sl} within the curve.

To describe the first change, it is necessary to define the following two parameters:

Y_{crit} The n-distance away from the wall where $S = S_{crit}$.

Y_{sl} The n-distance away from the wall where the extrapolated shear stress equals zero.

In the Gillis and Johnston model,

$$\ell = 0.10 \quad (\delta_{sl} - \delta^*_{sl})$$

where $\delta_{sl} = Y_{sl}$ in the developing or recovery regions and $\delta_{sl} = Y_{crit}$ in the curved region. With their model it was found that the switchover at the beginning of curvature quickly altered the shear stress profile driving Y_{sl} down to a small fraction of Y_{crit}. But, as the change in the shear stress profile began to alter the mean velocity profile, Y_{sl} began to rebound, passing up through and finally well above Y_{crit}. This rebound eventually affected the mean velocity and temperature profiles, causing the calculated values of $C_f/2$ and St to increase in a manner much like recovery from curvature, though still within the curve. The critical stability argument states that, in the asymptotic curved state, the extrapolated shear layer thickness. Y_{sl}, equals the n-distance where $S = S_{crit}$, Y_{crit}. But in this model, Y_{sl} could be well above Y_{crit}, especially, it was found, when δ_{99}/R was small. The change in the model was to construct a "controller" that would not allow Y_{sl} to grow much above Y_{crit}. The new model calculated the δ_{sl} to be used in computing the curved-region mixing length profile as:

$$\delta_{sl} = Y_{crit} \quad \text{when} \quad Y_{sl} < Y_{crit}$$

$$\delta_{sl} = Y_{crit}\left(1.0 - 2.0\left(\frac{Y_{sl}}{Y_{crit}} - 1.0\right)\right)$$

when $Y_{sl} > Y_{crit}$ but $\delta_{sl}/Y_{crit} > 0.33$.

It is a stiff "controller" that drives δ_{sl} down when $Y_{sl} > Y_{crit}$ trying to force $Y_{sl} \approx Y_{crit}$ for the asymptotic curved boundary layer. Note that when $Y_{sl} < Y_{crit}$ the new instruction has no effect.

The second change to the model was developed when trying to predict the three cases of differing δ_{99}/R. It was found that the optimum value of S_{crit} was a function of δ_{99}/R. Fitting the optimum values for cases of $\delta_{99}/R = 0.10$, 0.05, and 0.02 with a smooth curve gave:

$$S_{crit} = \frac{(\delta_{99}/R)^{1/3}}{4}$$

Since the δ_{99}/R used in the model is the local value and not the value at the start of curvature, S_{crit} is continually updated as the boundary layer thickens. This correlation gives the correct trend with δ_{99}/R for the cases studied. It is not known, however, that it would do equally well if δ_{99}/R were changed from case to case by changing R while holding $\delta_{99}(\theta=0)$ constant.

In the following sections, predictions are made of many of the heat transfer runs presented earlier. In these predictions the turbulent Prandtl number was not changed as a result of curvature. Figure 3-4 shows that, within the curve, the change of turbulent Prandtl number is small and in a direction that would decrease the Stanton numbers slightly below the following predictions. A mild improvement to the model could be made, then, by incorporating a turbulent Prandtl number correction for the curved boundary layer. One possibility is the model developed by R.M.C. So [31] discussed in Chapter 1.

Figure 3-4 shows that there seems to be an effect of recovery on the turbulent Prandtl number. The following predictions, which make no such correction, are expected to show too slow a recovery. At present, no model exists for making this correction. Profiles of local $\overline{v't'}/\overline{u'v'}$ across the recovering boundary layer would be valuable in developing a model that accurately accounts for this effect.

The present model can be quite temperamental. The calculation of Y_{sl} is done by extrapolation of a linear portion of the shear stress profile to the wall. After some distance downstream of the beginning of curvature, the shear stress profile develops inflections that can cause Y_{sl} to jump a considerable distance from step to step. This usually results in variations in the slope of St versus Re_{Δ_2} (or s), oscillating about what appears to be a reasonable value. Occasionally the program will extrapolate to an extremely small Y_{sl} due to an inflection very near the wall. When this happens, the solution goes irreparably out of control. Because of this, the program can be quite frustrating and expensive to run. An improvement might be to calculate the shear layer thickness as an integral thickness:

$$Y_{sl} \text{ is a function of } \int_0^{n_o} \frac{\tau}{\tau_w} dn \quad ,$$

where n_o is the n-distance when the shear stress goes to zero. This would stabilize the model considerably.

The following sections demonstrate how well the above model with the above changes predicts the heat transfer cases discussed in Chapter 3.

4.2 Predicting the Effect of Curvature for the Baseline Case

Figures 4-2 and 4-3 show the prediction of the baseline case. The introduction of curvature rapidly decreases the skin friction and Stanton number. For this case the effect is strong enough to overshoot and oscillate for some time before settling down to the asymptotic curved state. The prediction of both the skin friction and the Stanton number within the curve is quite good. Note that a Pr_t correction would decrease St slightly near the end of the curve. The recovery is quite accurately predicted. Note that the Pr_t correction would increase the predicted St in the recovery region. To try to assess just how much the correction would increase St, the ratio of $St/(C_f/2)$ was calculated from the profile data for this case from Chapter 3, then multiplied by the predicted $C_f/2$ to get an estimated Stanton number with a recovery correction on Pr_t. This corrected Stanton number is shown in

Figs. 4-2 and 4-3. With this correction, the prediction and the data are quite close. Ideally, the prediction curve of Fig. 4-3 would follow the data with a -1 slope. The strong introduction results in a steeper slope. As the shear layer thickens, Y_{sl} continues to grow, and the slope decreases. When Y_{sl} becomes larger than Y_{crit}, the "controller" decreases δ_{sl}, trying to drive it to Y_{crit}, seen as a downward trend near the end of the curve. Runs made with sustained curvature show that the model predicts a continued decrease in St with nearly a -1.0 slope in these coordinates. The shape of the recovery is approximately correct, characterized by a rate of return roughly proportional to the distance from the flat-wall correlation.

The following sections discuss the predictions of cases with differing values of a single parameter. Table 4-1 shows the case numbers and figure numbers that constitute each separate-effect study.

Table 4-1

Prediction Runs

Effect	Case	Parameter Value	Figure #'s
δ_{99}/R	070280	0.10	4-2, 4-3
	022680	0.05	4-4, 4-5
	060480	0.02	4-6, 4-7
U_{pw}	112779	26.4 m/s	4-8, 4-9
	070280	14.8 m/s	4-2, 4-3
	011380	7.0 m/s	4-10, 4-11
K	022680	0	4-4, 4-5
	051080	1.25×10^{-6}	4-12, 4-13
Unheated	022680	Base	4-4, 4-5
Starting	113079	$\Delta_2/R(\theta=0) = 0.0$	4-14, 4-15
Length	030280	$\Delta_2/R(\theta=90°) = 0.0$	4-16, 4-17

4.3 Prediction of Cases with Differing Initial Boundary Layer Thickness

Figures 4-2 through 4-7 show the ability of the program to model cases of differing boundary layer thickness. The "predictions" are good, even for the thin boundary layer case where $\delta_{99}/R = 0.02$. The term "prediction" might be misleading, especially in this study, because values of S_{crit} were chosen that would optimize the comparison of calculated and measured Stanton number and skin friction. No adjustment to the model has been made for subsequent studies; therefore, sections 4-4 through 4-6 can, more honestly, be called predictions.

Note that the preplate prediction of Stanton number (Figs. 4-3, 4-5, and 4-7) is progressively lower than the correlation for thinner boundary layer cases. This is probably due to the Reynolds number effect. In Case 060480, where $\delta_{99}/R(\theta=0) = 0.02$ (Figs. 4-6, 4-7), the momentum thickness Reynolds number was 464 at $S = -35$ cm and estimated to be 1724 at the start of curvature, indicating a late-transitional and early turbulent boundary layer. The turbulence model was developed for a fully turbulent boundary layer and apparently underpredicts the preplate data for the thin boundary layer cases. The modeling is expected to improve as the boundary layer thickens downstream. The predicted Re_{δ_2} at the end of the curve for Case 060480 was 3200.

The predicted recovery of the thinner boundary layer cases appears to be slightly too rapid. Case 022680, where $\delta_{99}/R(\theta=0) = 0.05$ (Figs. 4-4, 4-5), shows a faster recovery of skin friction than seen in the measured values and a recovery of Stanton number similar to that seen in the data. Figure 3-4 shows a decrease in Pr_t within the recovery region for this case, however, so that a Stanton number prediction with a Pr_t correction would show too strong a recovery.

4.4 Prediction of Cases with Differing U_{pw}

Figures 4-2, 4-3, and 4-8 through 4-11 show predictions of cases with differing U_{pw}. There seems to be a slight U_{pw} effect that is not modeled. This effect apparently begins at the introduction of curvature. Since the present model is based mainly on data from the asymptotic state, it is not surprising that there are some deficiencies near

the beginning of curvature. One might expect that the strength of the introduction of curvature might scale as

$$\frac{d}{ds}\left(\frac{U_{pw}^2}{R}\right)$$

4.5 Prediction of Cases with Freestream Acceleration

Figures 4-12 and 4-13 show the prediction of the combined effects of strong free-stream acceleration and curvature. The prediction models the -2 slope (Fig. 4-13) quite well in the early region. Apparently, however, the shear stress profile has developed an inflection, and the extrapolation technique is jumping from one δ_{sl} to another quite different one. This is seen both near the end of the curve and in the recovery section. The model proposed in Section 4.1, where δ_{sl} is calculated by integration might correct this problem, and it is expected that the prediction of the acceleration case would be quite good.

4.6 Prediction of Cases with Differing Unheated Starting Lengths

Figures 4-14 and 4-15 show the prediction of the case in which heating begins at the beginning of curvature inside a mature momentum boundary layer. Figures 4-16 and 4-17 show the prediction of a similar case in which heating begins at the start of the recovery region. The figures show an excellent prediction of the two cases.

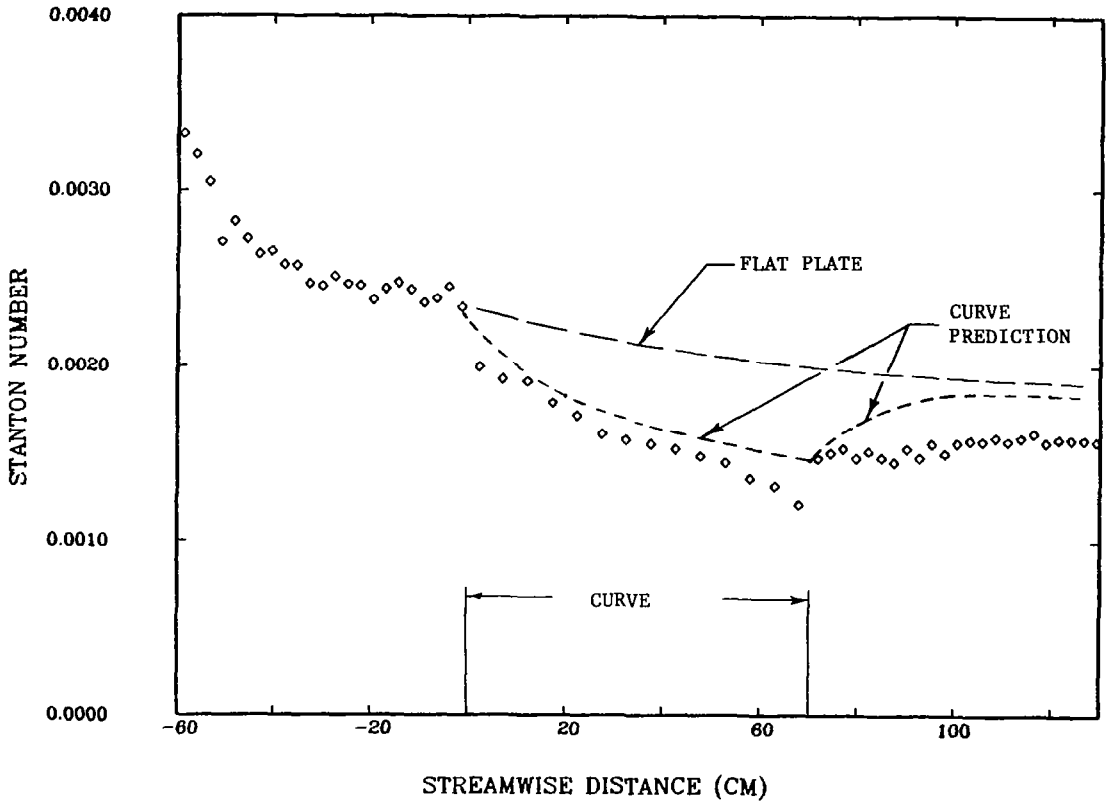

Fig. 4-1. Prediction of the baseline case with the Johnston and Eide model.

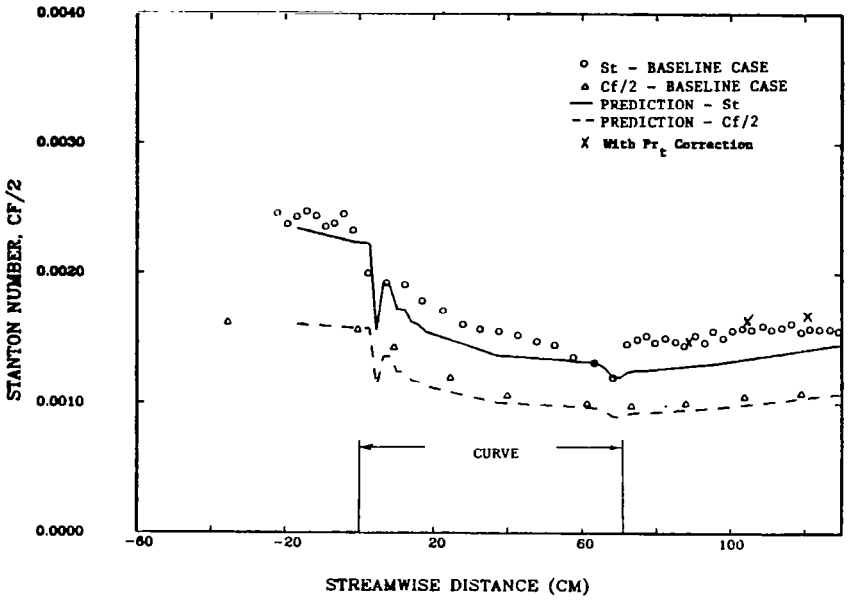

Fig. 4-2. Prediction of the baseline case: Stanton number versus streamwise distance.

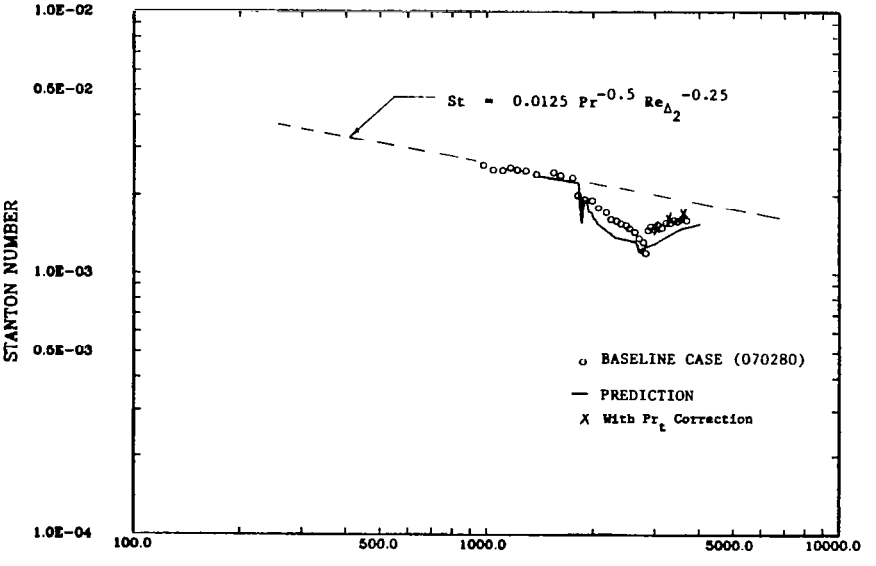

Fig. 4-3. Prediction of the baseline case: Stanton number versus enthalpy thickness Reynolds number.

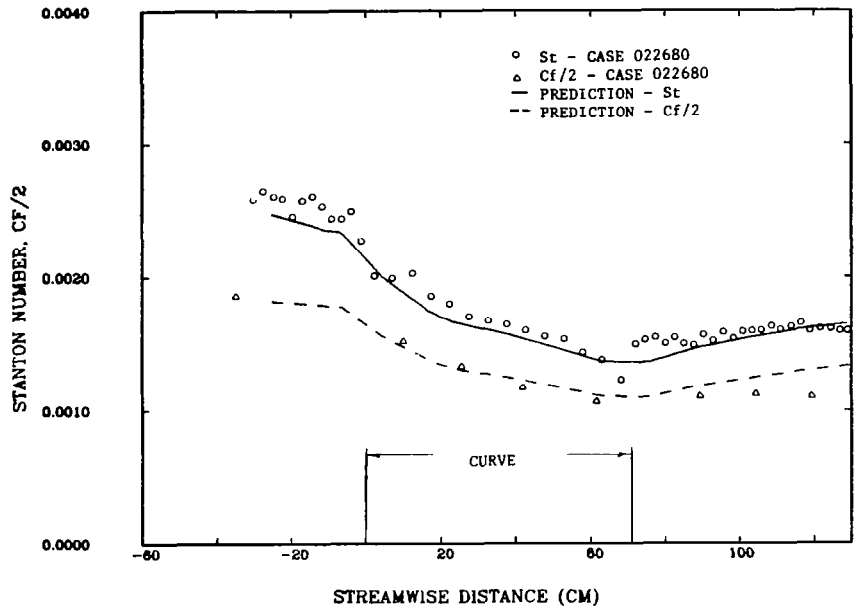

Fig. 4-4. Prediction of Case 022680, $\delta_{99}/R(\theta=0) = 0.05$: Stanton number versus streamwise distance.

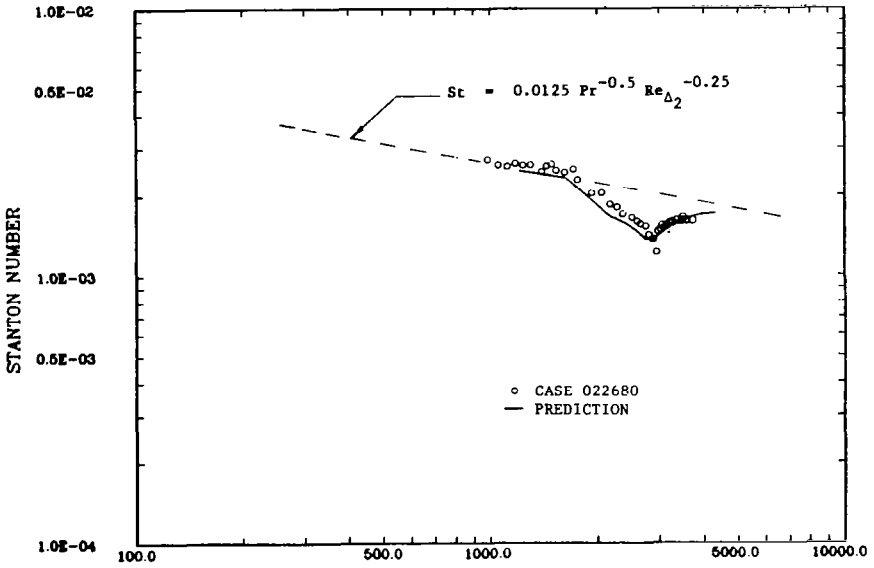

Fig. 4-5. Prediction of Case 022680, $\delta_{99}/R(\theta=0) = 0.05$: Stanton number versus enthalpy thickness Reynolds number.

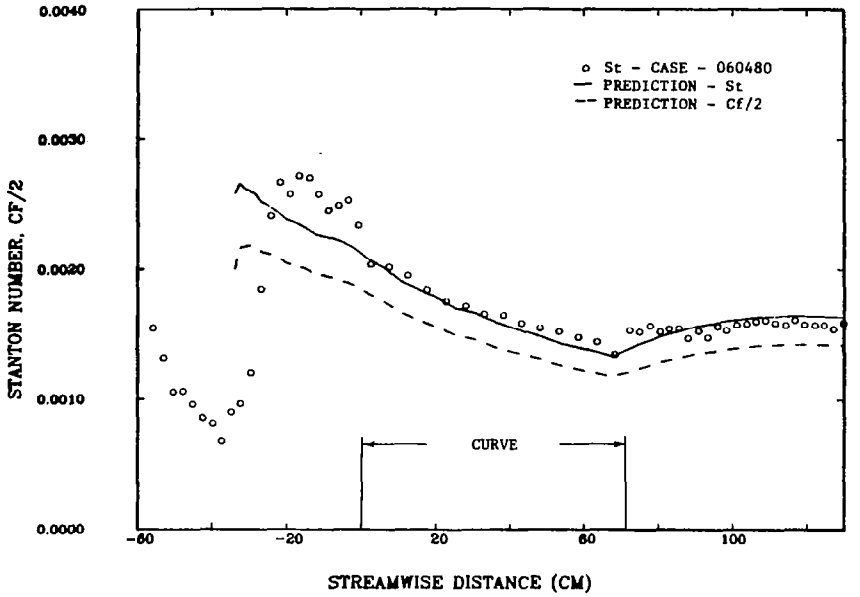

Fig. 4-6. Prediction of Case 060480, $\delta_{99}/R(\theta=0) = 0.02$: Stanton number versus streamwise distance.

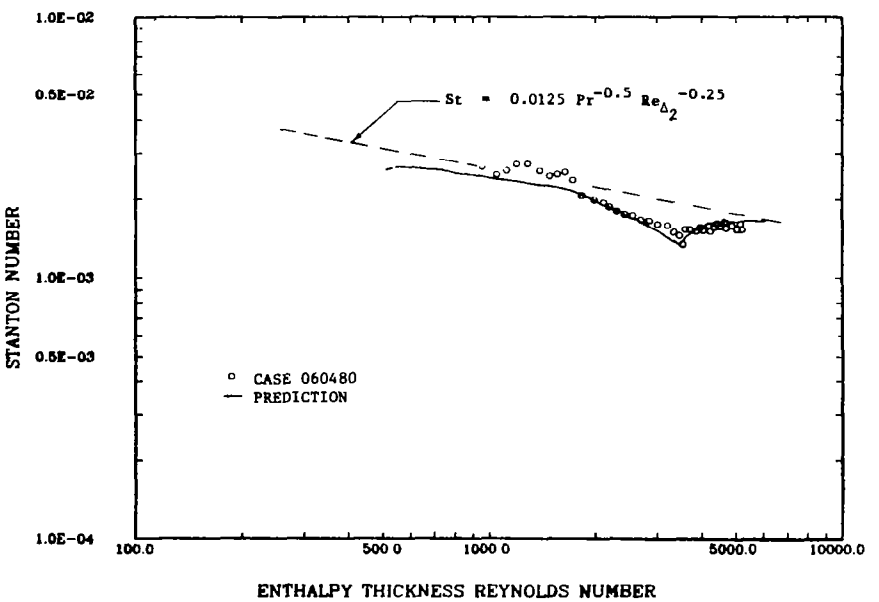

Fig. 4-7. Prediction of Case 060480, $\delta_{99}/R(\theta=0) = 0.02$: Stanton number versus enthalpy thickness Reynolds number.

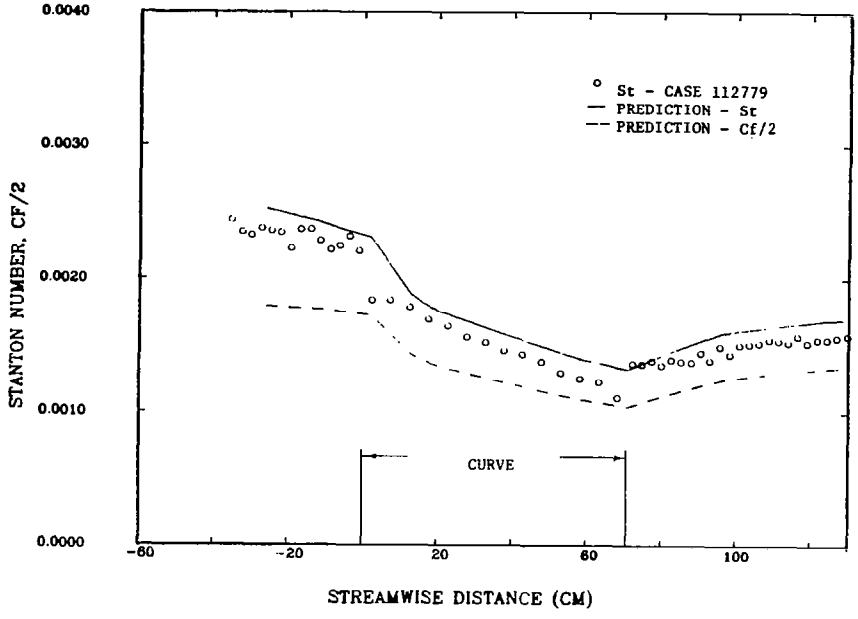

Fig. 4-8. Prediction of Case 112779, U_{pw} = 26 m/s: Stanton number versus streamwise distance.

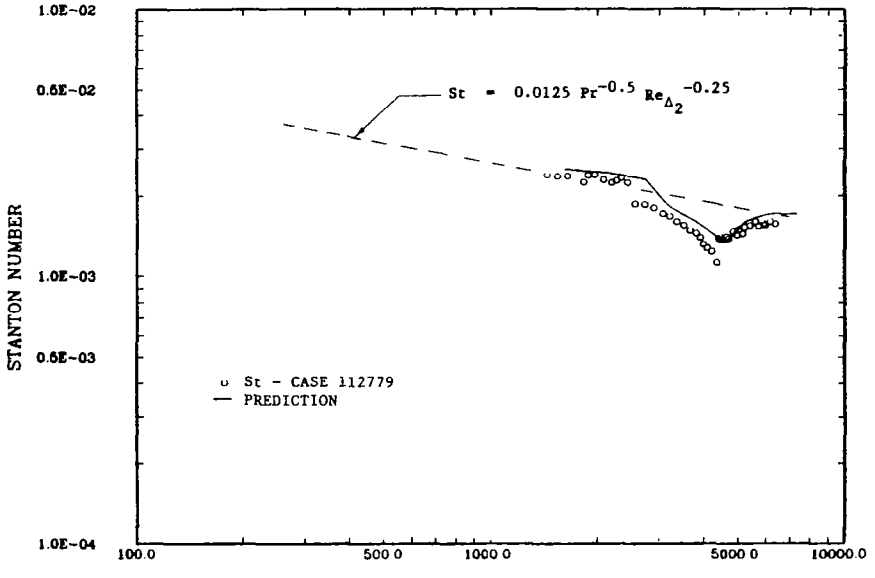

Fig. 4-9. Prediction of Case 112779, U_{pw} = 26 m/s: Stanton number versus enthalpy thickness Reynolds number.

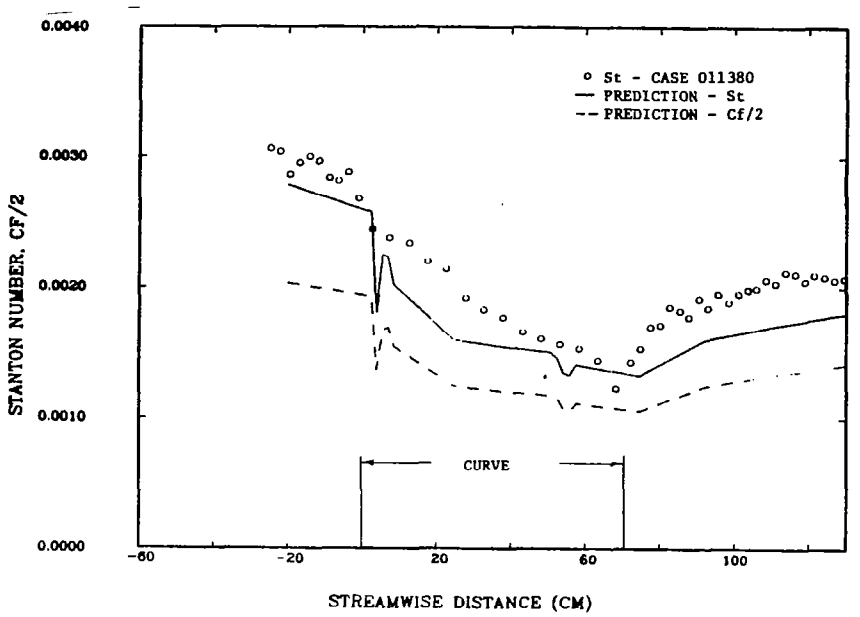

Fig. 4-10. Prediction of Case 011380, U_{pw} = 7 m/s: Stanton number versus streamwise distance.

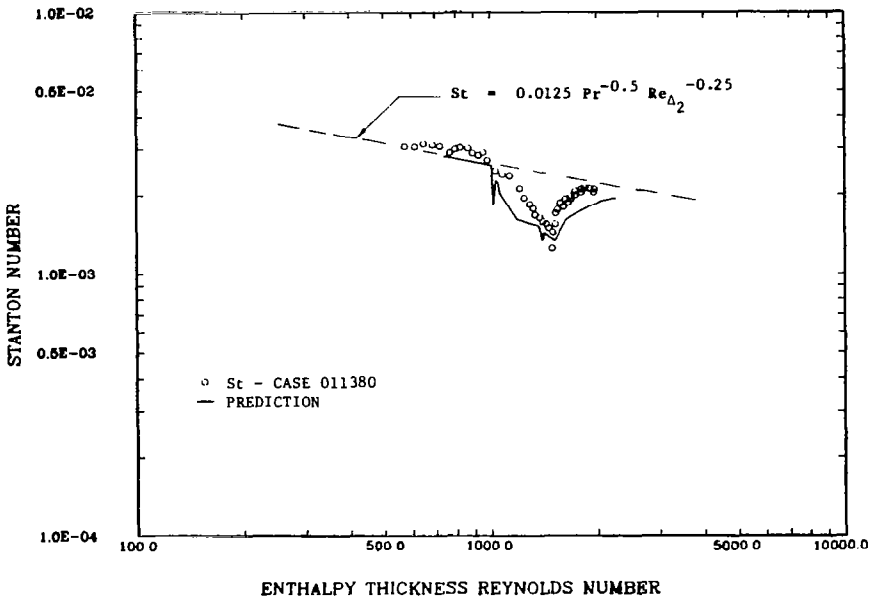

Fig. 4-11. Prediction of Case 011380, U_{pw} = 7 m/s: Stanton number versus enthalpy thickness Reynolds number.

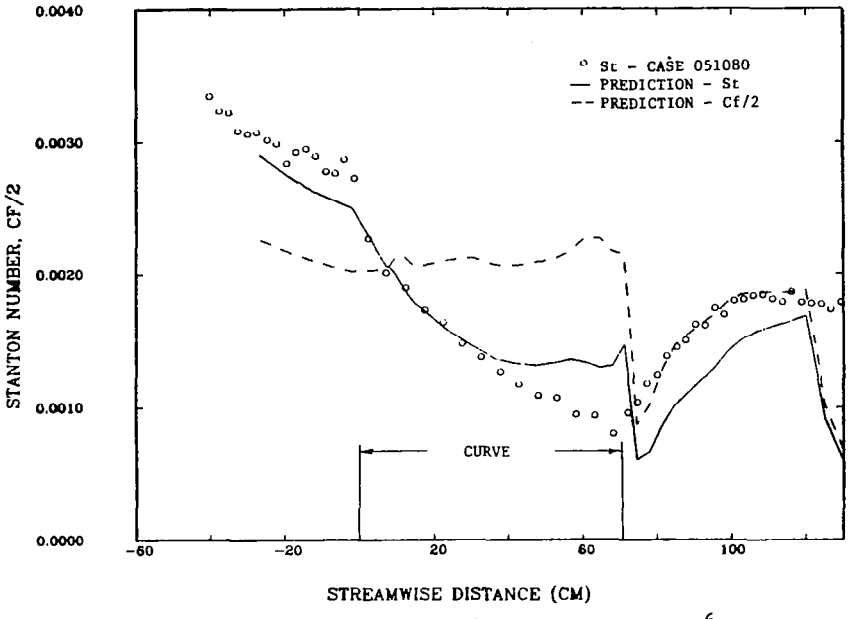

Fig. 4-12. Prediction of Case 051080, $K = 1.25 \times 10^{-6}$: Stanton number versus streamwise distance.

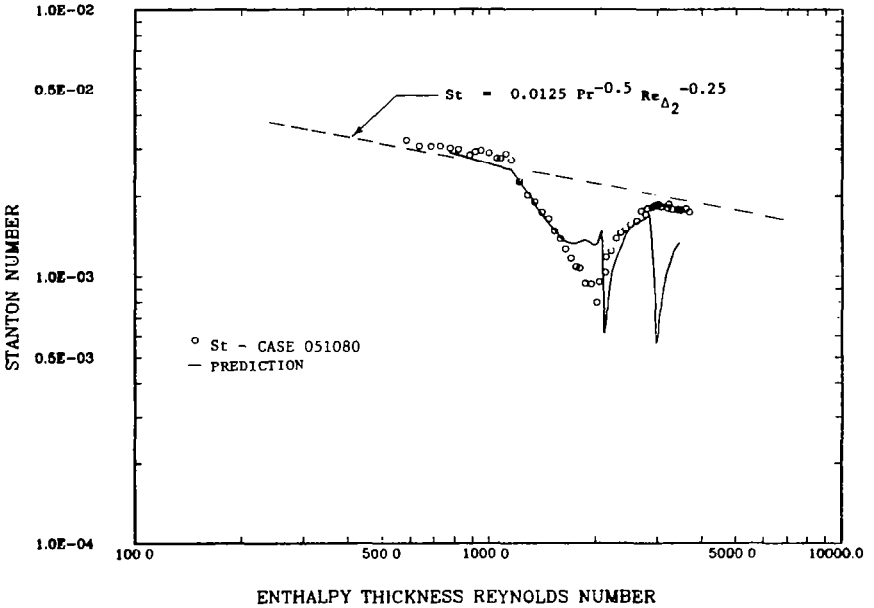

Fig. 4-13. Prediction of Case 051080, $K = 1.25 \times 10^{6}$: Stanton number versus enthalpy thickness Reynolds number.

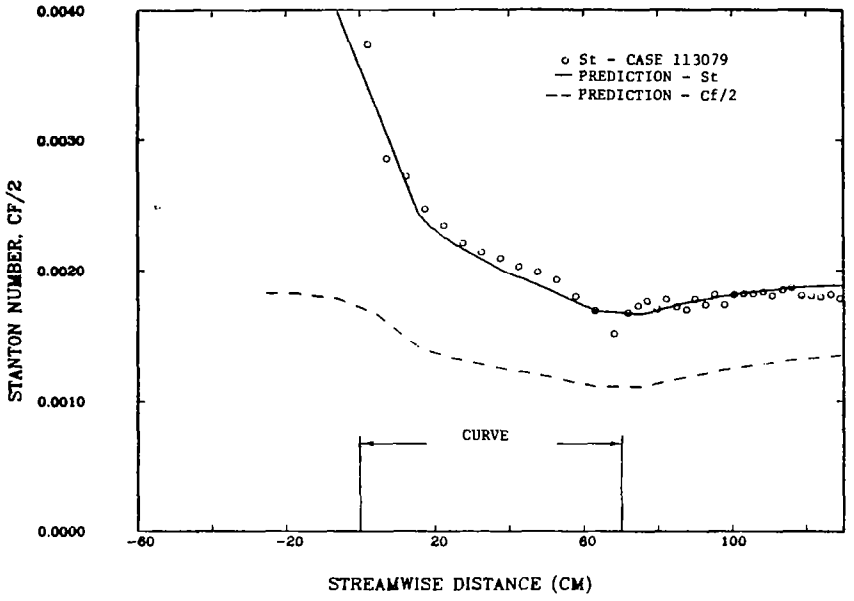

Fig. 4-14. Prediction of Case 113079, $\Delta_2/R(\theta=0) = 0.0$: Stanton number versus streamwise distance.

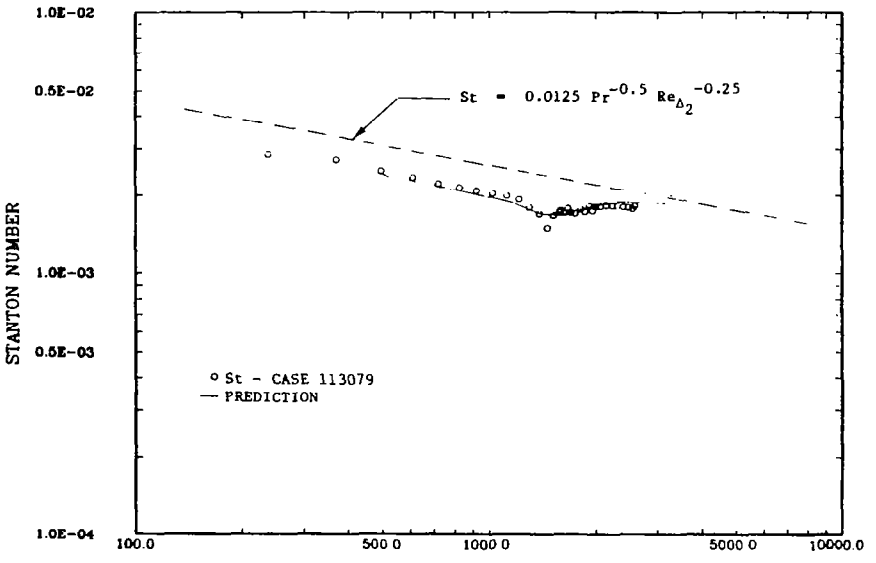

Fig. 4-15. Prediction of Case 113079, $\Delta_2/R(\theta=0) = 0.0$: Stanton number versus enthalpy thickness Reynolds number.

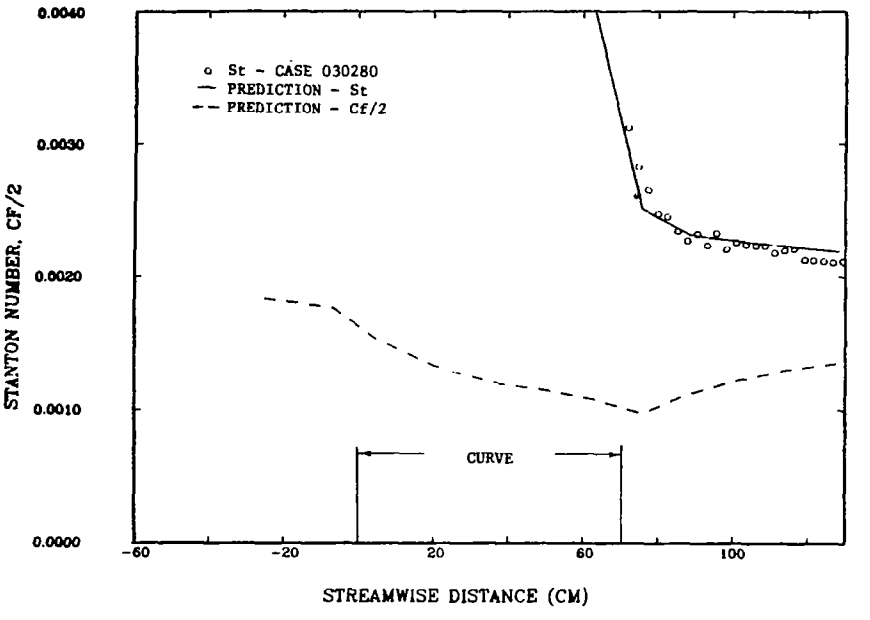

Fig. 4-16. Prediction of Case 030280, $\Delta_2/R(\theta=90°) = 0.0$: Stanton number versus streamwise distance.

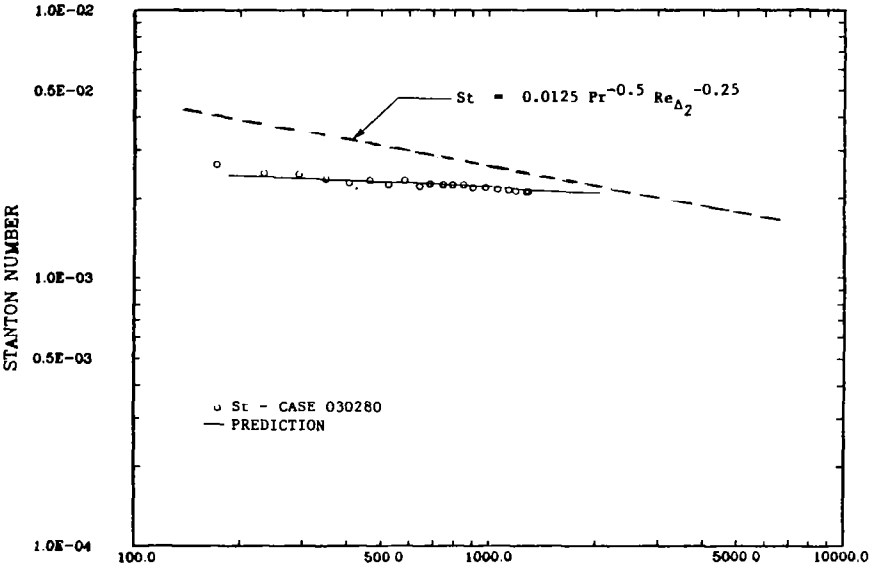

Fig. 4-17. Prediction of Case 030280, $\Delta_2/R(=90°) = 0.0$: Stanton number versus enthalpy thickness Reynolds number.

Chapter 5
CONCLUSIONS AND RECOMMENDATIONS

This study presents results of experiments on the effect of convex curvature on heat transfer through turbulent and transitional boundary layers. For the baseline case, the effect of curvature was separated from other effects such as streamwise accleration, which usually accompanies curvature in practice. Where there were combined effects, they were carefully controlled, i.e., where streamwise acceleration with curvature was to be tested, acceleration was with a constant $K = \nu/U_{pw}^2 \cdot dU_{pw}/ds$.

The results of the 15 cases studied here provide considerable insight into the effects of curvature on turbulent boundary layer heat transfer. They complement the detailed hydrodynamic measurements of the previous investigations, e.g., Gillis and Johnston [35], So and Mellor [16], etc. The studies of separate effects isolated several important parameters and revealed some new characteristics of curved boundary layers (e.g., the -1 slope in Stanton number versus enthalpy thickness Reynolds number coordinates). Also, they checked the robustness of hypotheses, like the "shear layer hypothesis," derived in single-run experiments by subjecting them to a broad range of conditions. Most important to the modeler and, eventually, the designer, these tests provide a broad data base with which to verify future prediction models.

5.1 Conclusions

The main conclusions are as follows:

1. The effect of convex curvature on heat transfer rates is significant for all the cases studied. Reductions of Stanton number of 20-50% below the expected flat-wall values were observed. The effect of convex curvature is seen immediately at the beginning of curvature and continues to grow throughout the curve. The recovery of the heat transfer rate on a downstream flat wall is extremely slow. After 60 cm of recovery length, (15-20 boundary-layer thicknesses), the local Stanton number may still be 15-20% below what would be expected without upstream curvature, at the same enthalpy thickness Reynolds number.

2. The boundary layer eventually reaches an asymptotic curved condition characterized by $St \propto Re_{\Delta_2}^{-1}$. The -1 slope is considered to be significant. It may be indicating that the overall heat transfer from the wall has become conduction-dominated as in a laminar boundary layer or a strongly accelerated boundary layer.

3. Separate effects studies on this one curved surface show that the boundary layer thickness, free-stream velocity, and maturity of the boundary layer affect the response to the introduction of curvature and the rate at which the asymptotic state is approached, but not the eventual asymptotic state characterized by the -1 slope.

4. Studies of combined streamwise acceleration and streamwise curvature effects show that they both can be significant and that they seem to be additive. Convex curvature seems to increase the boundary layer's sensitivity to acceleration, as has previously been observed when acceleration and wall suction were combined.

5. Studies of the effect of convex curvature on laminar and transitional boundary layers show that this stabilizing curvature delays transition from laminar to turbulent. When the curved boundary layer is near-laminar or early-transitional, the effect of the curved region is soon "forgotten," and the recovery data rapidly return to flat-wall expected values. When the curved boundary layer is late-transitional, recovery is slow, similar to that of a mature turbulent boundary layer.

6. Turbulent Prandtl number deduced from the thermal law-of-the-wall or calculated as $St/(C_f/2)$ increases slightly (10-15%) within the curved region and decreases rapidly in the recovery region. At the end of the recovery section, the log-law deduced Pr_t is ~ 0.50 and continuing to decrease.

7. The "shear layer" model proposed by Gillis and Johnston [35] seems to be an effective model with which to view the effect of convex curvature on turbulent boundary layers.

8. The curvature prediction model presented by Gillis and Johnston [35] and modified herein predicts the present heat transfer studies reasonably well, although it must still be considered "developmental."

5.2 Recommendations for Future Work on the Convex Problem

This program has answered several important questions about the curved wall convective heat transfer problem. It dealt with the scaling and sensitivity questions and provided a broad data base to build upon.

An important next step is to study in detail the difference between the effects of curvature on the diffusivity of heat and momentum. This involves taking profiles of the shear stress $\overline{u'v'}$ and the turbulent transport of heat $\overline{v't'}$ to give profiles of Pr_t. Development of a four-wire anemometer probe at Stanford is now nearly complete, and such data should be available soon. Of the four wires, three are for measuring the three components of velocity and the fourth is a temperature sensor. Prediction of the recovery of Stanton number will require development of a turbulent Prandtl model, which, in turn, will require that we know more about the processes than the present data can reveal.

Another important separate effect study not done in the present experiment would be of the effect of radius of curvature. It has been assumed, but not shown, that the appropriate parameter for the strength of curvature is δ_{99}/R. This study has indicated that δ_{99}/R affects only the rate at which the asymptotic state is approached. The questions that remain are: (1) If the radius is changed but $\delta_{99}/R(\theta=0)$ is held constant, does the approach trajectory to the asymptotic state change? (2) Does the nature of the asymptotic state itself change?

Other important questions remain about the curved and recovery regions. These are: If the curved wall were allowed to continue indefinitely (without influence of secondary flow), would the conclusion that the asymptotic state is represented by $St \propto Re_{\Delta_2}^{-1}$ remain true? Or, if the recovery wall were much longer, what would be the continued trajectory of Pr_t versus s (Fig. 3-4)?

Still unanswered are questions about the combined effects of convex curvature and transpiration, or surface roughness. These are key questions to the designer. A hydrodynamically smooth wall may become transitionally rough when it becomes convexly curved and the scale of the boundary layer decreases. It has been shown that convex curvature or wall suction increases sensitivity to streamwise acceleration. How

sensitive to acceleration would a curved boundary layer with wall suction become?

Another important question to gas turbine blade designers is: How does convex curvature influence the jet-freestream interaction for film-cooled blades?* It most likely will be learned that the optimum blowing rate is curvature-dependent.

*Research activity now under way at Stanford.

References

1. Crawford, M. E. and W. M. Kays, "STAN5--A Program for Numerical Computation of Two-dimensional Internal and External Boundary Layer Flows," NASA CR-2742, Dec. 1976.

2. Bradshaw, P., "Effects of Streamline Curvature on Turbulent Flow," AGARDograph No. 169, 1972.

3. Wilcken, H., "Turbulente Grenzschichten an Gewoelbten Flaechen," Berlin, Vol. 1, No. 4, Sept. 1930, translated as NASA TT-F-11, 421, Dec. 1967.

4. Wendt, F., "Turbulente Strömungen zwischen zesi rotierenden honaxialen Zylindren," Ing.-Arch., Vol. 4, p. 577 (1933).

5. Schmidbauer, H., "Behavior of Turbulent Boundary Layers on Curved Convex Walls" (1936), NACA-TM No. 791.

6. Wattendorf, F. L., "A Study of the Effect of Curvature on Fully Developed Turbulent Flow," Proc. Royal Soc., Vol. 148, 1935.

7. Clauser, M., and F. Clauser, "The Effect of Curvature on the Transition from Laminar to Turbulent Boundary Layer," NACA-TN No. 613 (1937).

8. Liepmann, H. W., "Investigations on Laminar Boundary-Layer Stability and Transition on Curved Boundaries," NACA Advance Confidential Report (1943).

9. Kreith, F., "The Influence of Curvature on Heat Transfer to Incompressible Fluids," Trans. ASME, Nov. 1955.

10. Eskinazi, S., and Y. Yeh, "An Investigation of Fully Developed Turbulent Flows in a Curved Channel," J. of Aero Science, Vol. 23, No. 1 (1956).

11. Schneider, W. G., and J. H. T. Wade, "Flow Phenomena and Heat Transfer Effects in a 90° Bend," Canadian Aeronautics and Space Journal, Feb. 1967.

12. Patel, V. C., "The Effects of Curvature on the Turbulent Boundary Layer," Aeronautical Research Council, A.R.C. 30 427, F.M. 3974, Aug. 1968.

13. Thomann, H., "Effect of Streamwise Wall Curvature on Heat Transfer in a Turbulent Boundary Layer," JFM., Vol. 33, Part 2, pp. 283-292 (1968).

14. Bradshaw, P., "The Analogy Between Streamwise Curvature and Buoyancy in Turbulent Shear Flow," JFM, Vol. 36, Part 1, pp. 177-191 (1969).

15. Bradshaw, P., "Review--Complex Turbulent Flows," Transactions of the ASME, June 1975.

16. So, R.M.C., and G. L. Mellor, "An Experimental Investigation of Turbulent Boundary Layers along Curved Surfaces," NASA-CR-1940, April 1972.

17. So, R.M.C., and G. L. Mellor, "Experiment on Turbulent Boundary Layers on a Concave Wall," The Aeronautical Quarterly, Vol. 16, 25, Feb. 1975.

18. So, R.M.C., and G. L. Mellor, "Experiment on Convex Curvature Effects in Turbulent Boundary Layers," JFM, Vol. 60, Part 1, pp. 43-62 (1973).

19. Ellis, L. B., and Joubert, P. N., "Turbulent Shear Flow in a Curved Duct," JFM, Vol. 62, Part 1, pp. 54-84 (1974).

20. Meroney, R. N., and P. Bradshaw, "Turbulent Boundary Layer Growth over a Longitudinally Curved Surface," AIAA Journal, Vol. 13, No. 11, Nov. 1975.

21. Hoffmann, P. H., and P. Bradshaw, "Turbulent Boundary Layers on Surfaces of Mild Longitudinal Curvature," Imperial College, Aero. Rept. 78-04 (1978) (submitted to JFM).

22. Smits, A. J., S.T.B. Young, and P. Bradshaw, "The Effects of Short Regions of High Surface Curvature on Turbulent Boundary Layers," JFM, Vol. 94, Part 2, pp. 209-242, Dec. 1978.

23. Smits, A. J., J. A. Eaton, and P. Bradshaw, "The Response of a Turbulent Boundary Layer to Lateral Divergence," JFM, Vol. 94, Part 2, pp. 243-268, Dec. 1978.

24. Castro, I. R., and P. Bradshaw, "The Turbulence Structure of a Highly Curved Mixing Layer," JFM, Vol. 73, Part 2, pp. 265-304 (1976).

25. Ramaprian, B. R., and B. G. Shivaprasad, "Mean Flow Measurements in Turbulent Boundary Layers along Mildely Curved Surfaces," AIAA Journal, Vol. 15, No. 2 (1977).

26. Ramaprian, B. R., and B. G. Shivaprasad, "Turbulence Measurements in Boundary Layers along Mildly Curved Surfaces," ASME 77-WA/FE-6, Dec. 1977.

27. Ramaprian, B. R., and B. G. Shivaprasad, "Some Effects of Longitudinal Wall Curvature on Turbulent Boundary Layers," presented at First Turbulent Shear Flow Conference, April 1977.

28. Ramaprian, B. R., and B. G. Shivaprasad, "The Structure of Turbulent Boundary Layers along Mildly Curved Surfaces," JFM, Vol. 85, p. 273 (1978).

29. Hunt, I. A., and Joubert, P. N., "Effects of Small Streamline Curvature on Turbulent Duct Flow," JFM, VOl. 91, Part 4, pp. 633-659.

30. Brinich, P. F., and R. W. Graham, "Flow and Heat Transfer in a Curved Channel," NASA TND-8464, May, 1977.

31. So, R.M.C., "The Effects of Streamline Curvature on Reynolds Analogy," ASME 77-WA/FE-17 (1977).

32. Mayle, R. E., M. F. Blair, and F. C. Kopper, "Turbulent Boundary Layer Heat Transfer on Curved Surfaces," J. of Heat Transfer, Vol. 101, No. 3, Aug. 1979.

33. Reynolds, W. C., W. M. Kays, and S. J. Kline, "Heat Transfer in a Turbulent Incompressible Boundary Layer. I. Constant Wall Temperature," NASA Memo 12-1-58A, 1958.

34. Gillis, J. C., and J. P. Johnston, "Experiments on the Turbulent Boundary Layer over Convex Walls and Its Recovery to Flat-Wall Conditions," 2nd Symposium on Turbulent Shear Flows, July 1979.

35. Gillis, J. C., and J. P. Johnston, "Turbulent Boundary Layer on a Convex, Curved Surface," draft of technical report for NASA-Lewis Research Center (Ph.D. thesis of J. C. Gillis, Dept. of Mech. Engrg., Stanford University) (1980). NASA-CR 3391, March 1981.

36. Kays, W. M., and M. E. Crawford, Convective Heat and Mass Transfer, McGraw-Hill Publishing Co. (1980)

37. Simon, T. W., and S. Honami, "Final Evaluation Report: Incompressible Flow Entry Test Cases Having Boundary Layers with Streamwise Wall Curvature (0230)," 1980-81 AFOSR-HTTM-Stanford Conference on Cmplex Turbulent Flows: Comparison of Computation and Experiment, Stanford University, 1980.

38. Kays, W. M., and R. J. Moffat, "The Behavior of Transpired Turbulent Boundary Layers," HMT-20, Thermoscience Division, Department of Mechanical Engineering, Stanford University, April 1975.

39. Irwin, H.P.A.H., and P. A. Smith, "Prediction of the Effect of Streamline Curvature on Turbulence," Physics of Fluids, Vol. 18, No. 6, June 1975.

40. Johnston, J. P., and S. A. Eide, "Turbulent Boundary Layers in Centrifugal Compressor Blades: Prediction of the Effects of Surface Curvature and Rotation," J. of Fluids Engrg., 98(1), 374-381 (1976).

41. Johnston, J. P., and S. A. Eide, "Prediction of the Effects of Longitudinal Wall Curvature and System Rotation on Turbulent Boundary Layers," Report PD-19, Thermosciences Division, Dept. of Mechanical Engrg., Stanford University, Nov. 1974.

42. Gibson, M. M., "An Algebraic Stress and Heat-Flux Model for Turbulent Shear Flow with Streamline Curvature," Int'l. Jour. of Heat and Mass Transfer, Vol. 21, 1609-1617 (1978).

43. Crawford, M. E., W. M. Kays, and R. J. Moffat, "Heat Transfer to a Full-Coverage Film-Cooled Surface with 30° Slant-Hole Injection," NASA Contractors' Report CR-2786, Dec. 1976.

44. Choe, H., W. M. Kays, and R. J. Moffat, "Turbulent Boundary Layer on a Full-Coverage, Film-COoled Surface - An Experimental Heat Transfer Study with Normal Injection," NASA Contractors' Report CR-2642, Jan. 1976.

45. Kim, H. K., R. J. Moffat, and W. M. Kays, "Heat Transfer to a Full-Coverage, Film-Cooled Surface with Compound-Angle (30° and 45°) Hole Injectin," HMT-28, Thermosciences Division, Mech. Engrg. Dept., Stanford University, 1978.

46. McCuen, P., "Heat Transfer with Laminar and Turbulent Flow between Parallel Planes with Constant and Variable Wall Temperature and Heat FLux," Ph.D. thesis, Thermosciences Division, Mech. Engrg. Dept., Stanford University, 1962.

47. Morretti, P. A., "Heat Transfer through an Incompressible Turbulent Boundary Layer with Varying Free-Stream Velocity and Varying Surface Temperature," Ph.D. thesis, Thermosciences Division, Mech. Engrg. Dept., Stanford University, 1965.

48. Kays, W. M., R. J. Moffat, and J. P. Johnston, "Heat Transfer and Hydrodynamic Studies on a Curved Surface with Full-Coverage Film Cooling," Proposal to NASA-Lewis Research Center, June 1976.

49. Moffat, R. J., "Temperature Measurement in Solids," ISA Paper 68-514 (1968).

50. Blackwell, B. F., and R. J. Moffat, "Design and Construction of a Low-Velocity Boundary Layer Temperature Probe," Transactions of the ASME, Journal of Heat Transfer, May 1975.

51. Moffat, R. J., "Gas Temperature Measurement," Temperature--Its Measurement and Control in Science and Industry, Vol. 3, Part 2, 553-571, Reinhold Publishing Corp., New York, N. Y. (1962).

52. Honami, S., "New Definition of Integral thickness on the Curved Surface," Internal Lab. Report, Thermosciences Division, Dept. of Mech. Engrg., Stanford University (1980).

53. Gibson, M. M., "An Algebraic Stress and Heat-Flux Model for Turbulent Shear Flow with Streamline Curvature," Int. Jour. of Heat and Mass Transfer, Vol. 21, 1609-1617 (1978).

54. Launder, B. E., C. H. Priddin, and B. I. Sharma, "The Calculation of Turbulent Boundary Layers on Spinning and Curved Surfaces," ASME J. of Fluids Engrg., March 1977.

55. Mellor, G. L., "Analytic Prediction of the Properties of Stratified Planetary Surface Layers," J. Atmos. Sci., 30, 1061-1069 (1973).

56. So, R. M. C., "A Turbulence Velocity Scale for Curved Shear Flows," J. Fluid Mech., 70, 37-57 (1975).

57. So, R. M. C., "Turbulence Velocity Scales for Swirling Flows," Turbulence in Internal Flows, edited by S. N. B. Murthy, Hemisphere Publishing Corp., Washington/London, 347-369 (1977).

Appendix A
THE UNCERTAINTY ANALYSIS

Processing the data included the calculation of each reduced quantity and the uncertainty of that quantity (output in Appendix G). The uncertainty can be interpreted as the band above or below the stated value within which it is believed the value would lie, with 20:1 odds, or 95% of the time. The uncertainty tells how closely each stated value listed in Appendix G and discussed in the body of this report can be believed. The uncertainty analysis also tells the designer or data-taker how much effort should be given to the measurement of any particular quantity. The uncertainty analysis was brought on-line early in the design phase of this project and used in that capacity to guide the design.

One note: the uncertainty interval applies to any one data point. When many data points are taken over a region where there are no discontinuities, i.e., the preplate, the curved wall, or the recovery wall, the mean of the data is known with more certainty than any one data point; integration or averaging tends to decrease the uncertainty. Though the uncertainty presented is typically 3-5%, the uncertainty of the mean of the data is much smaller.

The uncertainty analysis built into the Stanton number data-reduction program was one that, as a first step, calculated all the sensitivity coefficients,

$$S_{P'} = \frac{\partial St}{\partial P} \delta P'$$

the influence on the Stanton number uncertainty of the uncertainty of a particular parameter, P'. This is done by first rerunning the data-reduction with that parameter changed by, typically, 1%, to get the partial derivative, then multiplying by the uncertainty of P'. After the sensitivity coefficients was calculated, the overall uncertainty was calculated using Kline and McClintock [A-1]:

$$\delta St = \sqrt{\sum_i \left[\frac{\partial St}{\partial P'i} \delta P'i \right]^2}$$

The following table shows the parameters included in the uncertainty analysis and their estimated uncertainty:

Table A-1

Input to the Uncertainty Analysis

Parameter	Uncertainty
Embedded, calibrated thermocouple output	3 μv
Calibration constant for thermocouples in pre- and after-plate	30%
Plate-plate gap heat conductance	10%
Heat flux meter signal	20 μv
Wattmeter reading	0.05 w
Heat flux meter calibration constant	3%
Plate area	0.46 mm^2
Ambient pressure	7.6 mm Hg
Relative humidity	1%
Free-stream temperature	3 μv
Dynamic pressure difference	0.13 mm H_2O
Emissivity	0.02
Wattmeter calibration constant	0.015 w
Plate heater electrical resistance	0.015 Ω

(Table A-1 (cont.)

Plate Heater and delivery line electrical resistance	0.015 Ω
Plate heater and delivery line electrical resistance, including transformer	0.015 Ω
Resistance of the ammeter circuitry	0.005 Ω
Tunnel static pressure	0.13 mm H_2O
Spanwise heat transfer correction	20%
Support section temperature	4 μv
Recovery factor of free-stream thermocouple	0.04
Thermocouple calibration constant	0.10
Saturation pressure of water	0.14 atm
Saturation density of water	0.0016 kg/m^3
Inductance of ammeter circuitry	0.003 Ω
Resistance of voltmeter	100 Ω
Resistance between wattmeter and transformer	0.005 Ω
Preplate-curved section gap conductance	10%
Curved section/afterplate gap conductance	10%

The uncertainty analysis was written into both the profile data-reduction program (listed in App. E) and the Stanton number-reduction program (listed in App. F). The total uncertainty of each quantity is given, along with the reduced quantity in Appendix G. More detailed output giving the maxima and minima of the sensitivity coefficients within the developing region, curved region, or recovery region for each input to the uncertainty analysis is also available. This is the detailed information used in the rig design. An example of this is given on the following page for the baseline case.

References

A-1. Kline, S. J., and F. A. McClintock, "Describing Uncertainties in Single-Sample Experiments," Mechanical Engineering, Jan. 1953.

RUN 070280 *** CURVATURE RIG *** NASA-NAG-3-3 SENSITIVITY COEFFICIENTS (DST/DARG * DELTA ARG)

ARGUMENT	PREPLATE MAX	PREPLATE MIN	TEST SECTION MAX	TEST SECTION MIN	AFTERPLATE MAX	AFTERPLATE MIN
TO(I)	0.26079E-04	0.19330E-04	0.38653E-05	0.00000E 00	0.20279E-04	0.17171E-04
(J= 2 DELTA ARG= 0.00300)	(# 1)	(#22)	(#25)	(#26)	(#61)	(#46)
TTOP(I)	0.00000E 00	0.00000E 00	0.60197E-05	0.42149E-05	0.00000E 00	0.00000E 00
(J= 3 DELTA ARG= 0.00300)	(# 1)	(# 1)	(#25)	(#26)	(#39)	(#39)
TCEN(I)	0.82785E-05	0.00000E 00	0.43886E-04	0.26972E-04	0.44829E-05	0.00000E 00
(J= 4 DELTA ARG= 0.00300)	(#24)	(# 1)	(#25)	(#38)	(#39)	(#40)
TBOT(I)	0.00000E 00	0.00000E 00	0.14686E-04	0.99133E-05	0.00000E 00	0.00000E 00
(J= 5 DELTA ARG= 0.00300)	(# 1)	(# 1)	(#25)	(#37)	(#39)	(#39)
B(I)	0.45173E-05	0.10257E-05	0.00000E 00	0.00000E 00	0.75369E-05	0.16503E-05
(J= 6 DELTA ARG= 0.00039)	(# 1)	(#24)	(#25)	(#25)	(#44)	(#41)
S(I)	0.13696E-03	0.53416E-06	0.17573E-05	0.15367E-06	0.46905E-04	0.46892E-06
(J= 7 DELTA ARG= 0.07700)	(# 1)	(#15)	(#38)	(#32)	(#62)	(#48)
HM(I)	0.10121E-04	0.31961E-05	0.00000E 00	0.00000E 00	0.77771E-05	0.45852E-05
(J= 8 DELTA ARG= 0.02000)	(# 1)	(# 5)	(#25)	(#25)	(#58)	(#55)
Q(I)	0.00000E 00	0.00000E 00	0.76188E-05	0.70733E-05	0.00000E 00	0.00000E 00
(J= 9 DELTA ARG= 0.05000)	(# 1)	(# 1)	(#25)	(#38)	(#39)	(#39)
K(I)	0.13056E-03	0.69306E-04	0.34976E-06	0.28317E-07	0.53652E-04	0.44104E-04
(J=10 DELTA ARG= 0.98160)	(# 1)	(#17)	(#31)	(#37)	(#62)	(#40)
A(I)	0.37771E-05	0.22978E-08	0.42677E-05	0.24642E-05	0.15659E-05	0.15342E-07
(J=11 DELTA ARG= 0.00050)	(# 1)	(#23)	(#25)	(#38)	(#62)	(#47)
PAMB	0.22846E-06	0.16041E-06	0.13699E-06	0.82757E-07	0.11104E-06	0.93708E-07
(J=12 DELTA ARG= 0.30000)	(# 2)	(#24)	(#25)	(#38)	(#56)	(#62)
RHUM	0.36108E-04	0.25454E-04	0.21862E-04	0.13102E-04	0.17679E-04	0.14917E-04
(J=13 DELTA ARG= 1.00000)	(# 2)	(#24)	(#25)	(#38)	(#56)	(#62)
TRECOV	0.13754E-04	0.84155E-05	0.71244E-05	0.43376E-05	0.57944E-05	0.50328E-05
(J=14 DELTA ARG= 0.00300)	(# 1)	(#24)	(#25)	(#38)	(#60)	(#45)
PDYN	0.30459E-05	0.21380E-05	0.18259E-05	0.11031E-05	0.14801E-05	0.12493E-05
(J=15 DELTA ARG= 0.00500)	(# 2)	(#24)	(#25)	(#38)	(#56)	(#62)
EMIS	0.74226E-05	0.72271E-05	0.73668E-05	0.72550E-05	0.74413E-05	0.73016E-05
(J=16 DELTA ARG= 0.02000)	(#22)	(# 4)	(#28)	(#37)	(#41)	(#62)
WCAL	0.00000E 00	0.00000E 00	0.76684E-05	0.71334E-05	0.00000E 00	0.00000E 00
(J=17 DELTA ARG= 0.05000)	(# 1)	(# 1)	(#25)	(#38)	(#39)	(#39)
RO(I)	0.00000E 00	0.00000E 00	0.46238E-05	0.43014E-05	0.00000E 00	0.00000E 00
(J=18 DELTA ARG= 0.01500)	(# 1)	(# 1)	(#25)	(#38)	(#39)	(#39)
RBO(I)	0.00000E 00	0.00000E 00	0.45330E-05	0.42166E-05	0.00000E 00	0.00000E 00
(J=19 DELTA ARG= 0.01500)	(# 1)	(# 1)	(#25)	(#38)	(#39)	(#39)
RLOD(I)	0.00000E 00	0.00000E 00	0.75734E-07	0.70482E-07	0.00000E 00	0.00000E 00
(J=20 DELTA ARG= 0.01500)	(# 1)	(# 1)	(#25)	(#38)	(#39)	(#39)
RA	0.00000E 00	0.00000E 00	0.12569E-05	0.78217E-06	0.00000E 00	0.00000E 00
(J=21 DELTA ARG= 0.00500)	(# 1)	(# 1)	(#25)	(#38)	(#39)	(#39)
PSTAT	0.83559E-08	0.26587E-08	0.41780E-08	0.11394E-08	0.34183E-08	0.15193E-08
(J=22 DELTA ARG= 0.00500)	(# 1)	(# 9)	(#25)	(#38)	(#39)	(#48)
SPAN(I)	0.00000E 00	0.00000E 00	0.00000E 00	0.00000E 00	0.00000E 00	0.00000E 00
(J=23 DELTA ARG= -0.19815)	(# 1)	(# 1)	(#25)	(#25)	(#39)	(#39)
TSUPP10	0.00000E 00	0.00000E 00	0.96736E-06	0.00000E 00	0.00000E 00	0.00000E 00
(J=24 DELTA ARG= 0.00400)	(# 1)	(# 1)	(#25)	(#31)	(#39)	(#39)
RFW	0.10429E-05	0.63785E-06	0.55121E-06	0.32596E-06	0.44075E-06	0.38336E-06
(J=25 DELTA ARG= 0.04000)	(# 1)	(#24)	(#25)	(#38)	(#60)	(#45)
TCAL	0.67102E-06	0.19418E-06	0.16857E-06	0.94995E-07	0.45029E-06	0.20955E-07
(J=26 DELTA ARG= 0.10000)	(# 1)	(#19)	(#25)	(#37)	(#44)	(#43)
PS	0.16621E-07	0.90028E-08	0.11773E-07	0.48477E-08	0.96954E-08	0.55402E-08
(J=27 DELTA ARG= 2.00000)	(# 7)	(#24)	(#25)	(#38)	(#56)	(#52)
RHOS	0.14268E-05	0.99635E-06	0.85607E-06	0.51332E-06	0.69187E-06	0.58347E-06
(J=28 DELTA ARG= 0.00010)	(# 2)	(#24)	(#25)	(#38)	(#56)	(#62)
XA	0.00000E 00	0.00000E 00	0.12196E-07	0.55436E-08	0.00000E 00	0.00000E 00
(J=29 DELTA ARG= 0.00300)	(# 1)	(# 1)	(#35)	(#30)	(#39)	(#39)
RV	0.00000E 00	0.00000E 00	0.55370E-07	0.35375E-07	0.00000E 00	0.00000E 00
(J=30 DELTA ARG=100.00000)	(# 1)	(# 1)	(#25)	(#38)	(#39)	(#39)
RB	0.00000E 00	0.00000E 00	0.12995E-05	0.80771E-06	0.00000E 00	0.00000E 00
(J=31 DELTA ARG= 0.00500)	(# 1)	(# 1)	(#25)	(#38)	(#39)	(#39)
KUP	0.00000E 00	0.00000E 00	0.43539E-06	0.00000E 00	0.00000E 00	0.00000E 00
(J=32 DELTA ARG= 0.00860)	(# 1)	(# 1)	(#25)	(#26)	(#39)	(#39)
KDOWN	0.00000E 00	0.00000E 00	0.20978E-06	0.00000E 00	0.00000E 00	0.00000E 00
(J=33 DELTA ARG= 0.01790)	(# 1)	(# 1)	(#38)	(#25)	(#39)	(#39)

Appendix B

Curved-Wall Integral Parameters and the Momentum and Energy Integral Equations

When there is streamwise curvature, it becomes necessary to alter the definitions of the integral parameters somewhat and, hence, the form for the momentum and energy integral equations. The following curved-wall definitions of the displacement and momentum thickness presented by Honami [52,37] were used in the present study:

Displacement Thickness of Curved-Wall Boundary Layers

$$\delta_1 = \int_o^\infty \frac{(U_p - U)}{U_{pw}} \, dn \qquad (B\text{-}1)$$

Momentum Thickness of Curved-Wall Boundary Layers

$$\delta_2 = \int_o^\infty (1+kn) \frac{U(U_p - U)}{U_{pw}^2} \, dn \qquad (B\text{-}2)$$

Where it is assumed that $U_p = U_{pw}/(1+kn)$, the integral momentum equation becomes [52,37]:

$$\frac{d}{ds}(U_{pw}^2 \delta_2) + \delta_1 U_{pw} \frac{dU_{pw}}{ds} - U_{pw}^2 \, q_1(s) \frac{dk}{ds} = U_\tau^2 \qquad (B\text{-}3)$$

where

$$q_1(s) = \int_o^\infty \frac{nU_p(U_p - U)}{} \, dn + \int_o^\infty \frac{nU(U_p - U)}{U_{pw}^2} \, dn$$

The definition of the curved-wall enthalpy thickness used in the following study was derived by starting with the basic equation:

$$\int_o^{\Delta_2} \rho_\infty U_p (i_w - i_\infty) \, dn = \int_o^\infty \rho U (i - i_\infty) \, dn \qquad (B\text{-}4)$$

After substituting the estimate $U_p = U_{pw}/(1+kn)$ and integrating:

$$\Delta_2 = \frac{1}{k}\left\{e^{\left[k\int_o^\infty \frac{\rho U}{\rho_\infty U_{pw}} \frac{i-i_\infty}{i_w-i_\infty}\, dn\right]} - 1\right\} \qquad \text{(B-5)}$$

The simplest form of the energy integral equation is:

$$\dot{q}_o'' = \frac{d}{ds}\int_o^\infty (\rho U(i-i_\infty)\, dn) \qquad \text{(B-6)}$$

Writing $\dot{q}_o''$ in terms of the Stanton number defined as

$$St = \dot{q}_o''/[\rho_\infty U_{pw}(i_w-i_\infty)]$$

Eqn. (B-6) (assuming constant free-stream enthalpy and density) becomes:

$$St = \frac{d}{ds}\int_o^\infty \frac{\rho U(i-i_\infty)}{\rho_\infty U_{pw}(i_w-i_\infty)}\, dn + \frac{1}{k}\,\ell n(1+k\Delta_2)\left[\frac{1}{i_w-i_\infty}\frac{di_w}{ds} + \frac{1}{U_{pw}}\frac{dU_{pw}}{ds}\right] \qquad \text{(B-7)}$$

Taking the derivative, Eqn. (B-5) becomes

$$\frac{d\Delta_2}{ds} = -\frac{\Delta_2}{k}\frac{dk}{ds} + \frac{1+k\Delta_2}{k}\left\{\frac{dk}{dx}\left(\frac{1}{k}\,\ell n(1+k\Delta_2)\right) + k\frac{d}{ds}\int_o^\infty \frac{\rho U(i-i_\infty)}{\rho_\infty U_{pw}(i_w-i_\infty)}\, dn\right\}$$

Equating the two terms that (B-7) and (B-8) have in common leads to:

$$St = \frac{1}{1+k\Delta_2}\frac{d\Delta_2}{ds} + \left[\frac{\Delta_2}{k(1+k\Delta_2)} - \ell n(1+k\Delta_2)\right]\frac{dk}{ds} + \frac{1}{k}\,\ell n(1+k\Delta_2)\left(\frac{1}{U_{pw}}\frac{dU_{pw}}{ds} + \frac{1}{i_w-i_\infty}\frac{di_w}{ds}\right) \qquad \text{(B-9)}$$

on the flat wall, $k = 0$, and (B-9) reduces to

$$St = \frac{d\Delta_2}{ds} + \Delta_2\left(\frac{1}{U_{pw}}\frac{dU_{pw}}{ds} + \frac{1}{i_w - i_\infty}\frac{di_w}{ds}\right) \qquad \text{(B-10)}$$

Equation (B-9) is the integral energy equation used in the present study. Note that the appropriate equation for high-speed flows would have accounted for changes in i_∞ and ρ_∞.

In the Stanton number data-reduction program, Eqn. (B-9) is integrated over a wall streamwise distance δs to determine the change in enthalpy thickness as:

$$\delta\Delta_2 = (1+k\Delta_2)\ St\ \delta s - \frac{1+k\Delta_2}{k}\,\ell n(1+k\Delta_2)\left(\frac{1}{U_{pw}}\,\delta U_{pw} + \frac{\delta i_w}{i_w - i_\infty}\right) - \left[\frac{\Delta_2}{k} - \frac{1+k\Delta_2}{k^2}\,\ell n(1+k\Delta_2)\right]\delta k$$

Appendix C
Calibration of the Heat Flux Meters

Calibration of the heat flux meters required designing a heater that would asure a precisely known and carefully controlled one-dimensional heat flow through the heat flux meter. This device is shown in Fig. C-1.

The heater consisted of a uniform-power-distribution patch heater that was 15.2 cm wide by 45.7 cm high, backed by a 2.5 cm thick piece of styrofoam. On the outside of the styrofoam was another patch heater, and beyond that another 2.5 cm thick piece of styrofoam. The power to the heating pad sandwiched between the two styrofoam sheets was controlled so that the temperature difference between the two heaters was small (typically less than 0.1°C), preventing any back-loss from the heater adjacent to the copper plates. The input signal to the controller came from an iron-constantan thermopile.

The power supplied to the heater adjacent to the copper plates was adjusted to give a representative heat flux. The input power was regulated AC power controlled with a transformer and was measured with a galvanometric-type precision AC wattmeter. The temperature of the copper plates was controlled to a representative value with the built-in controller on the hot-water circulating system. After one-half hour, the entire assembly reached steady-state, and the average heat flux of the heating pad was equal to the local heat flux near the center of the assembly.

The heating pad covered six copper plate segments. It was found that heat flux meter calibration constants, K, measured with the plate at the two center positions agreed with one another to within less than 2%, and usually less than 1%.

Writing down the energy balance for the i^{th} plate and dividing by the plate area gives:

$$\dot{q}''_i = K_i HF_i + S_{i-1}(T_i - T_{i-1}) + S_{i+1}(T_i - T_{i+1})$$

where

$\dot{q}''_i$ = the measured heating pad power divided by pad area, with small corrections for wattmeter insertion and back-conduction;

HF_i = the output signal of the heat flux meter;

S_{i-1}, S_{i+1} = the gap conductance between the i^{th} plate and the upstream or downstream plate.

When the test plate was in one of the two center positions, there were either two or three guard plates on each side, and the neighboring plates were at nearly the same temperature. Therefore, only a very small correction was needed in the above equation for streamwise conduction. This correction was made using estimated values of S. The only unknown, then, was the desired calibration constant, K_i. The measured calibration constant was then input to the Stanton number data-reduction program along with a correction for temperature, as suggested by the manufacturer,

$$K_i = K_{ref,i}(1 - (T_i - 80°F)/700°F)$$

Once the calibration constant was found, the plate was moved to one side of the heater and the above test was rerun--then to the other side. When on the side of the heater, plate-plate temperature differences were larger and the streamwise conduction terms became significant. The two S-values could then be calculated from the two tests, since there were two equations and two unknowns. The calibration device was designed for very accurate calibration of the heat flux meters but, unfortunately, did not give accurate S-value measurements. The estimated uncertainty on the S-values was 10%. This term is not a large contributor to the overall uncertainty, however.

An uncertainty analysis on the heat flux meter calibration using representative values was performed with the technique of Kline and McClintock [C-1]. It was found that the uncertainty on K was ~ 2.7%. A value of 3% was used in the Stanton number data-reduction program.

References

C-1. Kline, S. J., and F. A. McClintock, "Describing Uncertainties in Single-Sample Experiments," Mechanical Engineering, Jan. 1953.

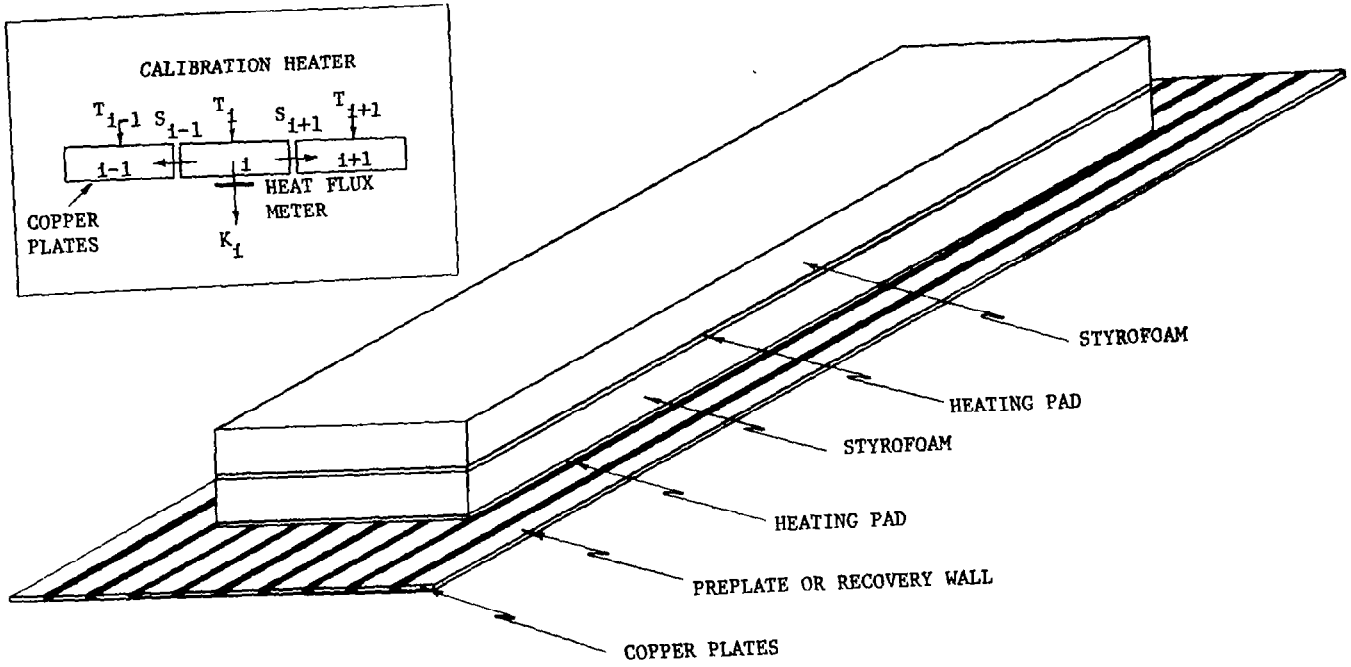

Fig. C-1. Heat flux meter calibration heater.

Appendix D
Simple Model for Ordering the Transitional Boundary Layer Cases

In the study of the effect of maturity of the momentum boundary layer, it was decided to order the cases according to $Re_{\delta_2}(\theta=0)$. Initializing profiles were taken 35 cm upstream of curvature, and, in the case of a fully turbulent boundary layer at this point, standard correlations were used to estimate $Re_{\delta_2}(\theta=0)$. When the boundary layer at $S = -35$ cm was laminar or transitional, the extrapolation became more difficult. The following simple model was used for this extrapolation.

The following correlations were used for the fully laminar or fully turbulent boundary layers:

Turbulent:

$$Re_{\delta_2} = 0.037\ Re_s^{0.8},$$
$$C_f/2 = 0.0295\ Re_s^{-0.2}$$
$$C_f/2 \tilde{=} d\delta 2/ds$$

leading to:

$$d\delta_2/ds = 0.0129\ Re_{\delta_2}^{-0.25}$$

and

$$\delta_2 = 0.037 \left(\frac{\nu}{U_{pw}}\right)^{0.2} s^{0.8}$$

(s is the distance from turbulent boundary layer virtual origin.)

Laminar:

$$Re_{\delta_2} = 0.664\ Re_s^{1/2}$$
$$C_f/2 = 0.664\ Re_s^{-1/2}$$
$$C_f/2 \tilde{=} d\delta_2/ds$$

leading to:

$$d\delta_2/ds = 0.441\ Re_{\delta_2}^{-1.0}$$

and

$$\delta_2 = 0.664\sqrt{\frac{\nu s}{U_{pw}}}$$

(s is distance from laminar boundary layer virtual origin.)

It was also assumed, where needed, that transition was always in the interval

$$400 < Re_{\delta_2} < 800$$

When Re_{δ_2} (s = -35 cm) was less than 400, the average Re_{δ_2} between s = -35 cm and the beginning of transition was estimated as

$$\overline{Re}_{\delta_2} = (Re_{\delta_2}(s = -35\ cm) + 400)/2$$

from which the average $d\delta_2/ds$ was calculated.

$$\overline{\frac{d\delta_2}{ds}} = 0.441\ Re_{\delta_2}^{-1.0}$$

Since $\delta_2(s = -35\ cm)$ and $\delta_2(Re_{\delta_2} = 400)$ are available, the s-distance where $Re_{\delta_2} = 400$ can be estimated as:

$$s(Re_{\delta_2} = 400) = -35\ cm + \Delta\delta_2 \Big/ \overline{\frac{d\delta_2}{ds}}$$

Within the transition region,

$$\overline{Re}_{\delta_2} = (400 + 800)/2$$

and

$$\overline{\frac{d\delta_2}{ds}} = \left(0.441\ Re_{\delta_2}^{-1.0} + 0.0129\ Re_{\delta_2}^{-0.25}\right) \div 2$$

and $s(Re_{\delta_2} = 800)$ is estimated.

The virtual origin of the turbulent boundary layer can be calculated from

$$s(Re_{\delta_2} = 800) \quad \text{and} \quad \delta_2(Re_{\delta_2} = 800)$$

from which $Re_{\delta_2}(\theta=0)$ can be calculated.

Of course, each case is different; some may be transitional at $s = -35$ cm and others at $s = 0$ cm, requiring variations on the above scheme.

Appendix E
Listing of the Profile Program

The following listing is that of the Fortran program used to reduce the velocity and temperature-profile data.

```
      $WATFIV       LIST
      C
      C     VELOCITY & TEMPERATURE DATA REDUCTION PROGRAM
      C     REVISED JULY 1980
      C
 1          DIMENSION NRN(36),AUB(60),ATB(60),ZA(60)
 2          DIMENSION U(60),Y(60),V(60),T(60),Z(60),CF(60)
 3          DIMENSION TU(60),DUR(60),Q(60),QGRAD(60),YM(60)
 4          DATA KCT,NMAX,NZMAX,AUINF,AUB,ATB,ATO,AVISC,U,V,T/3*0,303*0./
 5          DATA Y,Z /120*0./
 6          DATA DEH2,DELT99,VPW,VIST,TO/5*0./
 7          INTEGER ZLIM,REG
 8          ZLIM=60
      C
      C *1*     READ PROFILE INFORMATION
      C
      C         NPORT    PORT NUMBER FOR PROFILE MEASUREMENT
      C         IPT      PRESSURE TRANSDUCER FOR VELOCITY PROFILE
      C                  IPT=1    COMBIST MICROMANOMETER
      C                  IPT=2    PRESSURE TRANSDUCER
      C         ITC      THERMOCOUPLE PROBE FOR TEMPERATURE PROFILE
      C                  ITC=0    NO ACCOMPANYING TEMPERATURE PROFILE
      C                  ITC=1    GOOSE NECK THERMOCOUPLE PROBE(6.5 MIL OFFSET)
      C                  ITC=2    ELBOW  THERMOCOUPLE PROBE (21.5 MIL OFFSET)
      C                  ITC=3    BLACKWELL PROBE  (5.0 MIL OFFSET)
      C         MODE     TYPE OF DATA REDUCTION REQUIRED
      C                  MODE=0   COMPUTATION OF INTEGRAL PARAMETERS,U+,Y+,XVO
      C                  MODE=1   COMPUTATION OF INTEGRAL PARAMETERS ONLY
      C         REG      FLOW REGIME - FOR CALCULATION OF CF/2 AND XVO
      C                  REG=0    TURBULENT
      C                  REG=1    LAMINAR
      C
 9          READ (5,10) NPORT,IPT,ITC,MODE,REG
10       10 FORMAT (5I5)
      C     PGM RETURNS HERE  ***  TO TERMINATE PGM, READ BLANK CARD
11          IF (NPORT.EQ.0.AND.MODE.EQ.0) GO TO 670
      C
      C *2*     READ RUN NUMBER AND RUN INFO. , A FORMAT  COL 1-72
      C
12          READ (5,50) (NRN(I), I=1,36)
13       50 FORMAT (36A2)
      C
      C *3*     READ TUNNEL CONDITIONS FOR VELOCITY PROFILE
      C
      C         TRECOV   MAINSTREAM TEMPERATURE, I-C TC (MV)
      C         PSTAT    WALL STATIC PRESSURE (INCHES H2O)
      C         PAMB     AMBIENT PRESSURE (INCHES HG CORRECTED TO 32 DEG F)
      C         RH       AMBIENT RELATIVE HUMIDITY (PERCENT)
      C         X        PROFILE MEASUREMENT LOCATION FROM START OF CURVATURE-IN
      C         RAD      RECIPROCAL OF RADIUS OF CURVATURE (1/INCHES)
14          READ (5,100) TRECOV,PSTAT,PAMB,RH,X,RAD
15       100 FORMAT (6F10.0)
      C     PITOT TUBE O.D.=0.028 INCH
16          OD=0.028
17          OFFSET=0.014
      C
      C *4*     READ VELOCITY PROFILE DATA
      C
      C         Y        MICROMETER READING (INCHES)
      C         U        TRANSDUCER READING ( INCHES OF WATER)
      C         READ BLANK CARD AS LAST PROFILE POINT
      C
18          DO 200 I=1,50
19          READ (5,150) Y(I),U(I)
20       150 FORMAT(2F10.0)
21          NMAX=I-1
22          IF (U(I).LE.0.) GO TO 250
23       200 CONTINUE
24       250 CONTINUE
      C
      C *5*     READ LIMITS FOR COMPUTING SHEAR STRESS FROM CLAUSER PLOT
      C
```

```
C        YPLO    LOWER LIMIT OF LOG REGION
C                SUGGESTED VALUE 75 FOR HI REDEL2 FLOWS
C                                22 FOR VERY LOW REDEL2 FLOWS
C                                40 FOR CURVE OR RECOVERY
C        YPHI    UPPER LIMIT OF LOG REGION
C                SUGGESTED VALUE 125 TO 200 FOR HI REDEL2 FLOWS
C                                62 FOR VERY LOW REDEL2 FLOWS
C                                90 FOR CURVE OR RECOVERY
C
25        READ (5,150) YPLO,YPHI
26        IF (ITC.EQ.0) GO TO 370
C *6*    READ TUNNEL CONDITIONS FOR TEMPERATURE PROFILE
27        READ(5,901) PAM,PSTA,PDN,RL,TO,STANT
C
C        PAM     AMBIENT PRESSURE (INCHES HG CORRECTED TO 32 DEG F)
C        PSTA    WALL STATIC PRESSURE (INCHES H2O)
C        PCN     MAINSTREAM TOT PRES-WALL STATIC PRES (IN H2O)
C        RL      AMBIENT RELATIVE HUMIDITY (PERCENT)
C        TO      PLATE TEMPERATURE, I-C TC (MV)
C        STANT   LOCAL STANTON NUMBER
28      901 FORMAT(7F10.0)
C
C *7*    READ TEMPERATURE PROFILE DATA
C        Z       MICROMETER READING (INCHES)
C        T       THERMOCOUPLE READING (MV)
C        READ BLANK CARD AS LAST PROFILE POINT
C
29        DO 360 I=1,50
30        READ (5,151) Z(I),T(I)
31      151 FORMAT (2F10.0)
32        NZMAX=I-1
33        IF (T(I).LE.0.) GO TO 370
34      360 CONTINUE
35      370 CONTINUE
C
C       WRITE ALL RAW DATA
36        WRITE (6,5) (NRN(I), I=1,36)
37        5 FORMAT (1H1,/9X,'CURVATURE PROJECT  *** NASA-NAG-3-3  *** CONVEX
          1TEST SECTION'/10X,'VELOCITY AND TEMPERATURE PROFILE RAW DATA',/10X
          2,36A2)
38        WRITE (6, 6) NPORT,IPT,ITC,MODE,REG
39        6 FORMAT (/10X,'NPORT=',I3,'  IPT=',I3,'  ITC=',I3,'  MODE=',I3,
          7'   REG=',I3)
40        WRITE (6,8)
41        8 FORMAT (/10X,'NPORT',5X,'IPT(PRESSURE)',4X,'ITC(THERMOCOUPLE)  MOD
          1E',14X,'REGIME'/10X,'1=BOTTOM  1=COMBIST MICRO  0=NO TEMP PROFILE
          5 0=INTEGRAL,+,XVO'
          2,2X,'0=TURBULENT'/10X,'4=CENTER  2=TRANSDUCER     1=GOOSE NECK'
          3,7X,'1=INTEGRAL ONLY',3X,'1=LAMINAR'/10X,'7=TOP',22X,'2=ELBOW',
          4/37X,'3=BLACKWELL PROBE')
42        WRITE (6,7)RAD
43        7 FORMAT (/10X,'INVERSE RADIUS OF CURVATURE',F6.4,'(1/INCHES)')
44        WRITE (6,12)
45        12 FORMAT (/10X,'VELOCITY PROFILE RAW DATA')
46        WRITE (6,15) TRECOV,PSTAT,PAMB,RH,X
47        15 FORMAT (/10X,'TRECOV(MV)=',F6.3,'  PSTAT(IN.H2O)=',F6.3,
          1 '  PAMB(IN.HG,32F)=',F6.2,'  RH(PCT)=',F4.0,'  X(IN.)=',F7.2)
48        IF (IPT.EQ.1) WRITE (6,20)
49        IF (IPT.EQ.2) WRITE (6,21)
50        21 FORMAT (10X,'Y(IN).,U(INCHES OF WATER) :')
51        20 FORMAT (10X,'Y(IN.), U(INCHES OF COMBIST FLUID-S.G.=.8154 :')
52        WRITE (6,25) (Y(I),U(I), I=1,NMAX)
53        25 FORMAT ( 9X,F6.4,F8.3,4X,F6.4,F8.3,4X,F6.4,F8.3,4X,F6.4,F8.3,4X
          1 ,F6.4,F8.3)
54        IF (ITC.NE.0) WRITE (6,30)
55        30 FORMAT (/10X,'TEMPERATURE PROFILE RAW DATA')
56        IF (ITC.NE.0) WRITE (6,35) PAM,PSTA,PDN,RL,TO
57        35 FORMAT (/10X,'PAM(IN.HG,32F)=',F6.2,'  PST-WALL(IN.H2O)=',F6.3,
          1 '  PDN(IN.H2O)=',F6.3,'  RL(PCT)=',F4.0,'  TWALL(MV)=',F6.3)
58        IF (ITC.NE.0) WRITE (6,40)
59        40 FORMAT (10X,'Z(IN.), T(MV):        ')
60        IF (ITC.NE.0) WRITE (6,25) (Z(I),T(I), I=1,NZMAX)
```

```
      C
   61       IF(IPT.EQ.1)  CALIB=0.8154
   62       TRECOV=TC(TRECOV)
   63       IF(IPT.EQ.2) CALIB=1.0
      C     PDYN=DYNAMIC PRESSURE IN INCHES OF H2O
   64       PDYN=U(NMAX)*CALIB
   65       CALL TUNNEL(PDYN,RAD,Y(NMAX),PSTAT,PAMB,TRECOV,RH,UINF,TINF,VISC,C
           1P,RHOG,RM,P,PR)
   66       UPW=UINF*(1.0+RAD*Y(NMAX))
      C
      C      CORRECTION TO MICROMETER READING
      C      APPLY YOUNG & MAAS CORRECTION FOR PROBE
      C      SHEAR ERROR
      C      FIND DYNAMIC PRESSURE
   67       DO 120 I=1,NMAX
      C      INTERPOLATE TO FIND TOTAL PRESSURE
   68       A=1+RAD*Y(I)
   69   120 Q(I)=U(I)-PDYN*(1.0-1.0/(A*A))
      C      FIND GRADIENT OF DYNAMIC PRESSURE,
      C      YOUNG AND MAAS PARAMETER
   70       QGRAD(1)=Q(2)/Y(2)
   71       N1=NMAX-1
   72       DO 123 I=2,N1
   73   123 QGRAD(I)=(Q(I+1)-Q(I-1))/(Y(I+1)-Y(I-1))
   74       QGRAD(NMAX)=QGRAD(N1)
   75       DO 128 I=1,NMAX
   76       YM(I)=OD*QGRAD(I)/Q(I)
   77       IF (YM(I).GT.0.1) GO TO 124
   78       DELTA=OD*1.80*YM(I)
   79       GO TO 128
   80   124 DELTA=0.18*OD
   81   126 TU(I)=TINF
   82   128 Y(I)=Y(I)+DELTA+OFFSET
   83       IF (ITC.NE.0) GO TO 894
   84       DO 892 I=1,NMAX
   85       Z(I)=0.
   86   892 TU(I)=TINF
   87       NZMAX=0
   88       GO TO 312
   89   894 IF (ITC.EQ.1) OFFS=0.0065
   90       IF (ITC.EQ.2)  OFFS=0.0215
   91       IF (ITC .EQ. 3) OFFS=.0055
   92       DO 380 I=1,NZMAX
   93       Z(I)=Z(I)+OFFS
   94       IF (NPORT.EQ.1) ZA(I)=Z(I)
   95   380 T(I)=TTC(T(I))
   96       TO=TC(TO)
   97       TINFF=T(NZMAX)
   98       IF (NPORT.EQ.1) ZLIM=NZMAX
   99       IF (MODE.EQ.2) GO TO 312
  100       IF (Y(1).GE.Z(1)) GO TO 301
  101       DO 309 I=1,NMAX
  102       NT=I
  103       IF (Y(I).GE.Z(1)) GO TO 300
  104   309 TU(I)=TO+(T(1)-TO)*Y(I)/Z(1)
  105   300 KC=NT
  106       GO TO 302
  107   301 KC=1
  108   302 NC=1
  109       DO 303 I=KC,NMAX
  110       IF (Y(I).GE.Z(NZMAX)) GO TO 307
  111       DO 304 K=NC,NZMAX
  112       IF (.NOT.Z(K).GT.Y(I)) GO TO 304
  113       J=K-1
  114       TU(I)=(T(J+1)-T(J))*(Y(I)-Z(J))/(Z(J+1)-Z(J))+T(J)
  115       JJ=K
  116       GO TO 308
  117   304 CONTINUE
  118   307 TU(I)=T(NZMAX)
  119       GO TO 303
  120   308 NC=JJ
  121   303 CONTINUE
```

```
122     312 CONTINUE
      C     X LOCATION UNCERTAINTY, INCHES
123         DX=0.1
      C     TEMPERATURE UNCERTAINTY, DEG F
124         DT=0.12
      C     DYNAMIC, STATIC PRESSURE UNCERTAINTY, SLANT TUBE MANO., IN. H2O
125         DPMAN=0.010
      C     DYNAMIC PRESSURE UNCERTAINTY, PM-5,97 TRANSDUCERS, PCT/100.
126         DPTR=0.5/100.
      C     AMBIENT PRESSURE UNCERTAINTY, IN. HG
127         DPAMB=0.10
128         GC=32.1739
129         PUNITS=2116.21/33.932/12.
130         C=2.*GC*PUNITS*RM*CALIB/P
131         DO 275 I=1,NMAX
      C     VELOCITY UNCERTAINTY, RATIO
132         DUR(I)=0.5*SQRT((DT/(TINF+459.69))**2+DPTR**2+(DPAMB/PAMB)**2)
133         U(I)=C*(TU(I)+459.69)*U(I)-UPW*UPW*RAD*Y(I)*(2.0+RAD*Y(I))/((1.0+R
           1AD*Y(I))**2.)
134         U(I)=SQRT(U(I))
135     275 CONTINUE
136         DUINFR=DUR(NMAX)
137         WRITE (6,45)
138      45 FORMAT (/10X,'Y LOC (IN.), VELOCITY UNCERTAINTY RATIO, PCT :')
139         WRITE (6,25) (Y(I),DUR(I)*100. , I=1,NMAX)
140         CF2=1.
141         IF (MODE.EQ.0) CALL STRESS (NMAX,REG,U,Y,UPW,VISC,CF2,DUR,YPLO,
           2YPHI,CF)
142     890 CALL DEL99 (1,NMAX,U,UPW,RAD,T,Y,TO,DEL)
143         CALL DEL12 (NMAX,RAD,UPW,U,Y,TU,DE1,DE2,DUR,DDE2R)
144         H=DE1/DE2
145         REM=UPW*DE2/(VISC*12.)
146         DREMR=SQRT(DUINFR**2+DDE2R**2)*100.
147         XVO=0.
148         DXVO=0.
149         REX=1.
150         DREXR=0.
151         DEH2=0.
152         DDEH2=0.
153         IF (MODE.NE.0) GO TO 310
154         IF(REG.EQ.1) GO TO 891
155         XVO=DE2*((UPW/VISC)**0.2)/(12.*0.037)
156         XVO=(XVO**1.25)*12.
157         DXVO=XVO*SQRT((1.25*DDE2R)**2+(0.25*DUINFR)**2)
158         GO TO 893
159     891 XVO=(DE2*DE2*UPW)/(5.292*VISC)
160         DXVO=XVO*SQRT((2.0*DDE2R)**2+(DUINFR)**2)
161     893 DXVOR=DXVO/XVO
162         XVO=X-XVO
163         IF (REG.EQ.0) REX=(REM/0.037)**1.25
164         IF (REG.EQ.1) REX=(REM/0.664)**2
165         DREXR=SQRT(DUINFR**2+(DX/XVO)**2+(DXVOR)**2)*100.
166     310 WRITE (6,305) REX,DREXR,REM,DREMR,XVO,DXVO
167     305 FORMAT (/10X,'REX=',E12.5,5X,'UNCERTAINTY IN REX (PCT) =',F6.3,//,
           110X,'REM=',F6.0,5X,'UNCERTAINTY IN REM (PCT) =',F6.3,//10X,
           2 'XVO (IN.) =',F6.1,5X,'UNCERTAINTY IN XVO (IN.) =',F6.3)
168         IF (ITC.EQ.0) GO TO 600
      C
      C     *****   TEMPERATURE REDUCTION SECTION   *****
      C
169         UISC=VISC
170         DUINFR=DPMAN/PDN
171         CALL DEL99 (2,NZMAX,U,UPW,RAD,T,Z,TO,DELT99)
      C     NO PROVISION IS MADE TO MAKE SLIGHT ADJUSTMENT IN VELOCITY
      C     PROFILE IF PDN.NE.PDYN
172         PDN=PDYN
173         CALL TUNNEL (PDN,RAD,Z(NZMAX),PSTA,PAM,TINFF,RL,VINF,TINF,VIST,CP,
           1RHOG,RM,P,PR)
174         VPW=VINF*(1.0+RAD*Z(NZMAX))
175         IF ( Z(1).GE.Y(1)) GO TO 401
176         DO 399 I=1,NZMAX
177         NT=I
```

```
178         IF (Z(I).GE.Y(1)) GO TO 400
179         V(I)=U(1)*Z(I)/Y(1)
180       399 CONTINUE
181       400 KC=NT
182           GO TO 402
183       401 KC=1
184       402 NC=1
185           DO 403 I=KC,NZMAX
186           IF (Z(I).GE.Y(NMAX)) GO TO 407
187             DO 404 K=NC,NMAX
188           IF (.NOT.Y(K).GT.Z(I)) GO TO 404
189           J=K-1
190           V(I)=U(J)+(U(J+1)-U(J))*(Z(I)-Y(J))/(Y(J+1)-Y(J))
191           JJ=K
192           GO TO 408
193       404 CONTINUE
194       407 V(I)=UPW/(1.0+RAD*Z(I))
195           DUR(I)=DUINFR
196           GO TO 403
197       408 NC=JJ
198           IF (NZMAX.GT.NMAX) DUR(I)=DUINFR
199       403 CONTINUE
          C   OBTAIN STATIC TEMPERATURE PROFILES
          C   RECOVERY FACTOR FOR TC WIRE NORMAL TO FLOW
200           RTC=0.68
201           DO 987 I=1,NZMAX
202       987 T(I)=T(I)-RTC*V(I)*V(I)/(2.*32.2*778.26*CP)
203           DELT=TO-TINF
204           CALL DELH2 (NZMAX,RAD,UPW,V,T,Z,TO,CP,DEH2,DUR,DSUMHR)
205           REH=VPW*DEH2/VIST/12.
206           DREHR=SQRT(DUINFR**2+DSUMHR**2)*100.
207           DDEH2=DEH2*DSUMHR
208           WRITE (6,595) REH,DREHR
209       595 FORMAT (/10X,'REH=',F6.0,5X,'UNCERTAINTY IN REH (PCT) =',F6.3)
          C
          C
          C
210       600 WRITE (6,605) (NRN(I), I=1,36)
211       605 FORMAT(1H1,/9X,36A2)
212           XVOCM=XVO*2.54
213           DE2CM=DE2*2.54
214           DEH2CM=DEH2*2.54
215           UPWMS=UPW*0.3048
216           DELCM=DEL*2.54
217           DELTCM=DELT99*2.54
218           VISCSI=VISC*0.0929
219           RHOGM=RHOG*16.02
220           DE1CM=DE1*2.54
221           VPWMS=VPW*0.3048
222           VISTSI=VIST*0.0929
223           XCM=X*2.54
224           TINFC=5.*(TINF-32.)/9.
225           TOC=5.*(TO-32.)/9.
226           IF (ITC.NE.0) WRITE (6,610) REX,REM,REH,XVOCM,DE2CM,DEH2CM,
              1 UPWMS,DELCM,DELTCM,VISCSI,DE1CM,VPWMS,NPORT,H,VISTSI,XCM,
              2 CF2,TINFC,RHOGM,TOC
227       610 FORMAT (/10X,'REX  =',E12.5,7X,'REM  =',F12.0,24X,'REH    =',F12.0
              1/10X,'XVO  =',F12.2,' CM    DEL2 =',F12.3,' CM',21X,'DEH2   =',F12
              2.3,' CM ',/10X,'UPW  =',F12.2,' M/S   DEL99=',F12.3,' CM',21X,'DEL
              3T99 =',F12.3,' CM ',/10X,'VISC =',E12.5,' M2/S  DEL1 =',F12.3,' CM
              4',21X,'UPW    =',F12.2,' M/S ',/10X,'PORT =',9X,I3,7X,'H    =',F12
              5.3,24X,'VISC   =',E12.5,' M2/S ',/10X,'XLOC =',F12.2,' CM    CF/2
              6=',E12.5,24X,'TINF   =',F12.2,' DEG C',/10X,'DENS =',F12.2,' KG/M3
              7',43X,'TPLATE =',F12.2,' DEG C')
228           IF (ITC.NE.0 .AND. STANT.NE.0.0) WRITE (6,611) STANT
229       611 FORMAT (77X,'STANTON=',E12.5)
230           IF (ITC.EQ.0) WRITE (6,615) REX,REM,XVOCM,DE2CM,UPWMS,DELCM,
              1 VISCSI,DE1CM,NPORT,H,XCM,CF2,RHOGM
231       615 FORMAT (/10X,'REX  =',E12.5,7X,'REM  =',F12.0,                //10
              1X,'XVO  =',F12.2,' CM    DEL2 =',F12.3,' CM ',
              2       /10X,'UPW =',F12.2,'  M/S   DEL99=',F12.3,' CM ',
              3             /10X,'VISC =',E12.5,' M2/S  DEL1 =',F12.3,' CM ',
```

```
     4                        /10X,'PORT =',9X,I3,7X,'H    =',F12.3,
     5                  /10X,'XLOC =',F12.2,' CM    CF/2 =',E12.5,
     6/10X,'DENS =',F12.2,' KG/M3')
232       IF (ITC.NE.0 .AND.STANT.EQ.0.0) WRITE (6,620)
233   620 FORMAT (/10X,'Y(CM)  Y/DEL  U(M/S)  U/UP     Y+     U+',6X,
     1'CF/2   T(DEG C)       Y(CM)      Y+  U(M/S) T(DEG C)  TBAR 1-TBAR
     2')
234       IF (ITC.NE.0 .AND.STANT.NE.0.0) WRITE (6,621)
235   621 FORMAT (/10X,'Y(CM)  Y/DEL  U(M/S)  U/UP     Y+     U+',6X,
     1'CF/2   T(DEG C)       Y(CM)      Y+  U(M/S) T(DEG C)  TBAR  T+
     1   PRT')
236       IF (ITC.EQ.0) WRITE (6,625)
237   625 FORMAT(/10X,'Y(CM)  Y/DEL  U(M/S) U/UP     Y+       U+     CF/2'/)
238       F1=UPW*SQRT(CF2)/VISC/12.
239       F2=1./SQRT(CF2)/UPW
240       MIN=NMAX
241       IF (NZMAX.LT.NMAX) MIN=NZMAX
242       MAX=NMAX
243       IF (NZMAX.GT.NMAX) MAX=NZMAX
244       KK=0
245       DO 660 I=1,MAX
246       KK=KK+1
247       IF (KK.NE.6) GO TO 602
248       KK=1
249       WRITE (6,601)
250   601 FORMAT (10X)
251   602 CONTINUE
252       YCM=Y(I)*2.54
253       ZCM=Z(I)*2.54
254       UMS=U(I)*0.3048
255       UMST=V(I)*0.3048
256       TK=5.*(T(I)-32.)/9.
257       YBAR=Y(I)/DEL
258       UBAR=U(I)*(1.0+RAD*Y(I))/UPW
259       YPL=Y(I)*F1
260       ZPL=Z(I)*F1
261       UPL=U(I)*F2
262       IF (ITC.EQ.0) WRITE (6,645) YCM,YBAR,UMS,UBAR,YPL,UPL,CF(I)
263       IF (ITC.EQ.0) GO TO 660
264       TBAR=(TO-T(I))/DELT
265       IF (STANT.EQ.0.0) GO TO 603
266       IF (I .GT. NZMAX) GO TO 603
267       TPLUS=((SQRT(CF2))/STANT)*TBAR
268       PRT=((TPLUS-13.2*PR)*0.41)/(ALOG(ZPL/13.2))
269   603 CONTINUE
270       TM1=1.-TBAR
271       IF (I.LE.NMAX) TKK=5.*(TU(I)-32.)/9.
272       IF (I.GT.MIN) GO TO 640
273       IF (STANT.EQ.0.0) WRITE (6,630) YCM,YBAR,UMS,UBAR,YPL,UPL,CF(I),TK
     2K,ZCM,ZPL,UMST,TK,TBAR,TM1
274       IF (STANT.NE.0.0) WRITE (6,630) YCM,YBAR,UMS,UBAR,YPL,UPL,CF(I),TK
     2K,ZCM,ZPL,UMST,TK,TBAR,TPLUS,PRT
275   630 FORMAT (8X,F7.3,F7.3,F7.2,F8.3,F7.1,F8.2,F10.6,F8.2, 5X,F8.4,F8.2,
     2F7.2,F9.2,2F7.3,1F9.3)
276       GO TO 660
277   640 IF (NMAX.GT.NZMAX) WRITE (6,645) YCM,YBAR,UMS,UBAR,YPL,UPL,CF(I),T
     2KK
278   645 FORMAT (8X,F7.3,F7.3,F7.2,F8.3,F7.1,F8.2,F10.6,F8.2)
279       IF (NZMAX.GT.NMAX .AND. STANT.EQ.0.0) WRITE (6,650) ZCM,ZPL,UMST,T
     1K,TBAR,TM1
280       IF (NZMAX.GT.NMAX .AND. STANT.NE.0.0) WRITE (6,650) ZCM,ZPL,UMST,T
     1K,TBAR,TPLUS,PRT
281   650 FORMAT (74X,F9.4,F8.2,F7.2,F9.2,2F7.3,1F9.3)
282   660 CONTINUE
283       GO TO 1
284   670 CONTINUE
285       WRITE (6,680)
286   680 FORMAT (1H1)
C
287         RETURN
288       END
```

```
289         FUNCTION TC(T)
      C     FUNCTION CONVERTS TEMP FROM IRON-CONSTANTAN MV TO DEG F
      C     FREE-STREAM THERMOCOUPLE CALIBRATED 3-80
290         TC=32.350+35.300*T-.405*T*T
291         RETURN
292         END




293         FUNCTION  TTC(T)
      CC     THIS FUNCTION CONVERTS TEMP FROM CHROMEL-CONSTANTAN MV TO DEG F.
      C     BLACKWELL THERMOCOUPLE PROBE CALIBRATION 3-80
294         TTC=32.478+31.028*T-.59000*T*T
295         RETURN
296         END



297         SUBROUTINE TUNNEL (PDYN,RAD,YMAX,PSTAT,PAMB,TRECOV,RHUM,UINF,TINF,
           1 VISC,CP,RHOG,RM,P,PR)
      C        RHOG       FREE STREAM DENSITY
      C        VISC       FREE STREAM KINEMATIC VISCOSITY
      C        CP         FREE STREAM SPECIFIC HEAT
      C        PR         FREE STREAM PRANDTL NUMBER
      C        W          FREE STREAM ABSOLUTE HUMIDITY
      C
      C
      C        THIS ROUTINE COMPUTES THE WIND TUNNEL FLOW CONDITIONS
      C
      C        UINF       FREE STREAM VELOCITY
      C        TINF       FREE STREAM STATIC TEMPERATURE
      C
      C     SATURATION DATA FROM K AND K 1969 STEAM TABLES
298         DIMENSION TEMP(10),PSAT(10),RHOSAT(10)
299         DATA TEMP/     40.,     50.,     60.,     70.,     80.,
           1      90.,    100.,    110.,    120.,    130.0/
300         DATA PSAT/     17.519,   25.636,   36.907,   52.301,   73.051,
           1      100.627,  136.843,  183.787,  244.008,  320.400/
301         DATA RHOSAT/   .0004090, .0005868, .0008286, .0011525, .0015803,
           1      .0021381, .0028571, .0037722, .0049261, .0063625/
302         REAL NU,MFA,MFV,MWA,MWV,JF
303         TAMB=TRECOV
304         DO 10 N=1,9
305         IF(TEMP(N).GT.TAMB) GO TO 20
306      10 CONTINUE
307      20 T = TEMP(N)
308         EPS = T - TAMB
309         VAPH = PSAT(N)
310         VAPL = PSAT(N-1)
311         VEPS = VAPH - VAPL
312         RHOH = RHOSAT(N)
313         RHOL = RHOSAT(N-1)
314         REPS = RHOH - RHOL
315         RHOG = RHOL + (10.0 - EPS)*REPS/10.
316         RA=1545.32/28.970
317         PG = VAPL + (10.0 - EPS)*VEPS/10.0
318         PUNITS=2116.21/33.932/12.
319         P=PAMB*2116.21/29.9213 + PSTAT*PUNITS
320         RHUM=RHUM/100.
321         PVAP = RHUM*PG
322         PA = P - PVAP
323         RHOA = PA/(RA*(TAMB + 459.67))
324         RHOV = RHUM*RHOG
325         W=RHOV/RHOA
326         RHOM = RHOA + RHOV
327         MWA = 28.970
328         MWV = 18.016
329         MFV = RHOV/RHOM
```

```
330         MFA = 1.0 - MFV
331         RM = 1545.32*(MFA/MWA + MFV/MWV)
332         CP = MFA*0.240 + MFV*0.445
333         GC=32.1739
334         JF=778.26
335         RCF=0.7**0.33333
336         RHOG=(P/RM+PDYN*PUNITS*RCF/(CP*JF))/(TRECOV+459.67)
337         UINF=SQRT(2.*GC*PDYN*PUNITS/RHOG)/(1.0+RAD*YMAX)
      C      OBTAIN STATIC TEMPERATURE
      C      USING UINF FOR RECOVERY CORRECTION
      C      UINF IS APPROX FREESTREAM VELOCITY AT FREESTREAM THERMOCOUPLE
      C      RECOVERY FACTOR FOR TC WIRE PARALLEL TO FLOW
338         RTC=0.86
339         TINF=TRECOV-RTC*UINF*UINF/(2.*GC*JF*CP)
340         VISC=(11.+0.0175*TINF)/(1.E06*RHOG)*(1.-.7*W)
341         PR=.710*(530./(TINF+459.67))**(.1)*(1.+.9*W)
      C     NOTE FOR HIGH VELOCITY THIS ROUTINE SHOULD BE ITERATED
342         RETURN
343         END



344         SUBROUTINE STRESS(NMAX,REG,U,Y,UINF,VISC,CF2,DUR,YPLO,YPHI,PSUMCF)
      C
      C        FRICTION COEFFICIENT FOUND BY SEARCHING DATA
      C        FOR ALL POINTS SATISFYING FLAT PLATE LAW-OF-THE-WALL
      C        BETWEEN THE RANGES OF YPLUS OF 75 AND 125
      C        FOR THE CASE OF LOW RE  USE THE INTERVAL OF YP  BETWEEN 22 AND
      C        62. FOR CURVED AND RECOVERY REGIONS USE THE INTERVAL OF YP
      C        BETWEEN 40 AND 90
      C        AN AVERAGE CF2 IS OBTAINED FOR THESE YPLUS VALUES
      C        FOR LAMINAR BOUNDARY LAYER USE THE INTERVAL OF YP BETWEEN 0 AND
      C        20.
      C
345         DIMENSION U(1),Y(1),DUR(1),PSUMCF(60),YPLUS(60),YLIST(60)
346         INTEGER REG
      C
      C * * * * * *   NOTE: HIGH RE FOR UINF=   55-112 FT/SEC
      C * * * * * *   NOTE: LOW RE FOR UINF .LT. 50 FT/SEC
      C
347         SUMCF=0.
348         NUMCF=0
349         FYPO=0.
350         DCFR=0.
351         EPS=5.E-3
352         J=0
353         YP=YPLO
354         DUINFR=DUR(NMAX)
      C     UNCERTAINTY IN Y POSITION, IN.
355         DY=0.002
356         IF (REG.EQ.0) GO TO 602
357         DO 601 I=1,NMAX
358         PSUMCF(I)=12.0*U(I)*VISC/(UINF*UINF*Y(I))
359       601 YPLUS(I)=SQRT(PSUMCF(I))*UINF*Y(I)/(VISC*12.0)
360       602 DO 800 I=1,NMAX
361         PUY=U(I)*Y(I)/(12.*VISC)
      C     UNCERTAINTY IN Y+, RATIO
362         DYPR=0.10
363         IF (REG .NE. 0 ) GO TO 603
364         KONT=0
365       600 KONT=KONT+1
366         FYP=YP*(ALOG(YP)/0.41+5.)-PUY
367         IF (YP.GT.YPHI) EPS=5.E-2
368         IF (ABS(FYP-FYPO).LT.EPS) GO TO 700
369         EPS=5.E-3
370         FDERV=(ALOG(YP)+1.)/0.41+5.
371         YP=YP-FYP/FDERV
372         IF (KONT.LE.200) GO TO 600
373         WRITE (6,910) Y(I)
374       910 FORMAT (10X,'FAILURE TO CONVERGE FOR CF2',10X,'Y=',F8.3)
```

```
375         RETURN
376     700 CONTINUE
377         YPLUS(I)=YP
378         PSUMCF(I)=(VISC*YP*12./(Y(I)*UINF))**2
379     800 CONTINUE
380     603 CONTINUE
381         DO 825 I=1,NMAX
382         IF (YPLUS(I).LT.YPLO) GO TO 825
383         IF (YPLUS(I).GT.YPHI) GO TO 850
384         SUMCF=SUMCF+PSUMCF(I)
385         DCFR=SQRT(DCFR**2+4.*(DY/Y(I))**2+4.*DUINFR**2+4.*DYPR**2)
386         NUMCF=NUMCF+1
387     825 CONTINUE
388     850 CF2=SUMCF/FLOAT(NUMCF)
389         DCFR=DCFR/FLOAT(NUMCF)*100.
390         WRITE (6,900) CF2,DCFR
391     900 FORMAT (/10X,'CF/2=',E12.5,5X,'UNCERTAINTY IN CF/2 (PCT) =',F6.2)
392         RETURN
393         END
```

```
394         SUBROUTINE DEL99 (M,K1,U,UPW,RAD,T,Y,TPL,DE)
        C   SUBROUTINE WRITTEN BY MARCOS PIMENTA
395         DIMENSION U(1),T(1),Y(1),Z(60)
396         ZB=.99
397         DO 101 K=1,K1
398         IF(M.EQ.1)Z(K)=U(K)*(1.0+RAD*Y(K))/UPW
399         IF(M.EQ.2)Z(K)=(TPL-T(K))/(TPL-T(K1))
400       101 CONTINUE
401         DO 10 K=1,K1
402         IF(Z(K).GE.ZB)GO TO 2
403        10 CONTINUE
404         2  D=Y(K-2)**2*Y(K-1)+Y(K)**2*Y(K-2)+Y(K-1)**2*Y(K)-Y(K)**2*Y(K-1)-Y(
           1K-1)**2*Y(K-2)-Y(K-2)**2*Y(K)
405         F1=((Z(K-1)-Z(K-2))*(Y(K)-Y(K-2))-(Z(K)-Z(K-2))*(Y(K-1)-Y(K-2)))/D
406         F2=((Z(K)-Z(K-2))*(Y(K-1)**2-Y(K-2)**2)-(Z(K-1)-Z(K-2))*(Y(K)**2-Y
           1(K-2)**2))/D
407         F3=(Y(K-2)**2*Y(K-1)*Z(K)+Y(K)**2*Y(K-2)*Z(K-1)+Y(K-1)**2*Y(K)*Z(K
           1-2)-Y(K)**2*Y(K-1)*Z(K-2)-Y(K-1)**2*Y(K-2)*Z(K)-Y(K-2)**2*Y(K)*Z(K
           2-1))/D
408         DE=Y(K-1)
409         DO 3 I=1,10
410         DE=DE+(ZB-F1*DE**2-F2*DE-F3)/(2.*F1*DE+F2)
411         ERR=(ZB-F1*DE**2-F2*DE-F3)/(2.*F1*DE+F2)
412         IF(ERR.LE.1.E-03)GO TO 4
413        3  CONTINUE
414        4  CONTINUE
415         RETURN
416         END
```

```
      SUBROUTINE DEL12 (K1,RAD,UPW,U,Y,T,DE1T,DE2T,DUR,DDE2R)
      DIMENSION U(1),Y(1),T(1),DUR(1),F(60),G(60)
      DIMENSION FF(60),GG(60)
C     DUR, UNCERTAINTY IN VELOCITY, RATIO
C     DY, UNCERTAINTY IN Y LOCATION, IN.
      DY=0.002
      DO 10 I=1,K1
      F(I)=U(I)/(T(I)+459.69)
      FF(I)=1.-U(I)/UPW
      GG(I)=U(I)*FF(I)/UPW
   10 G(I)=F(I)*U(I)
      F01=F(1)*0.5
      G01=G(1)*0.5
      DY01=Y(1)
      SUM1=F01*DY01
      SUMP=DY01/(1.0+RAD*Y(1))
      SUM2=G01*DY01*(1.0+RAD*Y(1))
      DSUM1=(0.5*FF(1)*DY)**2
      DSUM2=(0.5*GG(1)*DY)**2
      KLIM=K1-1
      DO 20 I=2,KLIM
      DY12=Y(I)-Y(I-1)
      F12=0.5*(F(I)+F(I-1))
      G12=0.5*(G(I)+G(I-1))
      SUM1=SUM1+F12*DY12
      YM=0.5*(Y(I)+Y(I-1))
      SUMP=SUMP+DY12/(1.0+RAD*YM)
      SUM2=SUM2+G12*DY12*(1.0+RAD*YM)
      DF1=1.414*DUR(I)*U(I)/UPW
      DG1=DF1*(1.-2.*U(I)/UPW  )
      DSUM1=DSUM1+(0.5*(Y(I+1)-Y(I-1))*DF1)**2 + (0.5*(FF(I-1)-
     1 FF(I+1))*DY)**2
      DSUM2=DSUM2+(0.5*(Y(I+1)-Y(I-1))*DG1)**2 + (0.5*(GG(I-1)-
     1 GG(I+1))*DY)**2
   20 DY01=DY12
      DYN=Y(K1)-Y(K1-1)
      SUM1=SUM1+0.5*(F(K1)+F(K1-1))*DYN
      YM=0.5*(Y(K1)+Y(K1-1))
      SUMP=SUMP+DYN/(1.0+RAD*YM)
      SUM2=SUM2+0.5*(G(K1)+G(K1-1))*DYN*(1.0+RAD*YM)
      DFN=1.414*DUR(K1)
      DGN=DFN*(1.-2.)
      DSUM1=DSUM1+(0.5*DYN*DFN)**2 + (0.5*(FF(K1)+FF(K1-1))*DY)**2
      DSUM2=DSUM2+(0.5*DYN*DGN)**2 + (0.5*(GG(K1)+GG(K1-1))*DY)**2
      DSUM1=SQRT(DSUM1)
      DSUM2=SQRT(DSUM2)
      DE1T=SUMP-SUM1*(T(K1)+459.69)/UPW
      DE2T=SUMP-DE1T-SUM2*(T(K1)+459.69)/(UPW*UPW)
      DDE2R=DSUM2/DE2T
      WRITE (6,30) DE1T,DSUM1
   30 FORMAT(/10X,'DE1 (IN.) =',F7.4,5X,'UNCERT IN DE1 (IN.) =',F7.4)
      WRITE (6,40) DE2T,DSUM2
   40 FORMAT(/10X,'DE2 (IN.) =',F7.4,5X,'UNCERT IN DE2 (IN.) =',F7.4)
      RETURN
      END
```

```
468         SUBROUTINE DELH2 (K1,RAD,UPW,U,T,Y,TPL,CP1,SUMH,DUR,DSUMHR)
      C     CAUTION  THIS ROUTINE COMPUTES ENTHALPY THICKNESS BASED
      C     UPON STAGNATION ENTHALPY PROFILES.  THIS PRESUMES
      C     THAT THE TEMPERATURE PROFILES ARE STATIC TEMPERATURE.
469         DIMENSION U(1),T(1),Y(1),DUR(1),Z(60),DZ(60),ZZ(60)
      C     DUR, UNCERTAINTY IN VELOCITY, RATIO
      C     DT, UNCERTAINTY IN TEMPERATURE, DEG F
470         DT=0.25
      C     DY, UNCERTAINTY IN Y POSITION, IN.
471         DY=0.002
472         DO 10 I=1,K1
473         TB=(T(I)-T(K1))/(TPL-T(K1))
474         DZ(I)=U(I)*TB/U(K1)*1.414*SQRT(DUR(I)**2+(DT/(TPL-T(K1)))**2)
475         ZZ(I)=U(I)*TB/U(K1)
476         Z(I)=CP1*(T(I)-T(K1))+(U(I)**2-(UPW/(1.0+RAD*Y(I)))**2)/
           1 (2.*32.174*778.)
477       10 Z(I)=U(I)*Z(I)/(T(I)+459.69)
478         ZW=CP1*(TPL-T(K1))-UPW**2/(2.*32.174*778.)
479         Z01=Z(1)*0.5
480         DY01=Y(1)
481         SUMH=Z01*DY01
482         DSUMH=(0.5*ZZ(1)*DY)**2
483         KLIM=K1-1
484         DO 20 I=2,KLIM
485         DY12=Y(I)-Y(I-1)
486         C=(((Z(I-1)-Z(I))/(Y(I-1)-Y(I)))-((Z(I)-Z(I+1))/(Y(I)-Y(I+1))))/
           1(Y(I-1)-Y(I+1))
487         B=((Z(I)-Z(I+1))/(Y(I)-Y(I+1)))-C*(Y(I)+Y(I+1))
488         A=Z(I-1)-B*Y(I-1)-C*Y(I-1)*Y(I-1)
489         SUMH=SUMH+A*(Y(I+1)-Y(I-1))/2.+.125*B*((Y(I+1)+Y(I))**2-(Y(I-1)+
           1Y(I))**2)+0.0417*C*((Y(I+1)+Y(I))**3-(Y(I-1)+Y(I))**3)
490         DSUMH=DSUMH+(0.5*(Y(I+1)-Y(I-1))*DZ(I))**2 + (0.5*(ZZ(I-1)-ZZ(I+1)
           1 )*DY)**2
491       20 DY01=DY12
492         DYN=Y(K1)-Y(K1-1)
493         SUMH=SUMH+(Z(K1)+Z(K1-1))*DYN*0.5
494         DSUMH=DSUMH+(0.5*DZ(K1))**2 + (0.5*(ZZ(K1)+ZZ(K1-1))*DY)**2
495         DSUMH=SQRT(DSUMH)
496         SUMH=SUMH*(T(K1)+459.69)/(UPW*ZW)
497         DSUMHR=DSUMH/SUMH
498         IF(RAD .LT. 0.001) GO TO 25
499         SUMH=SUMH*RAD
500         SUMH=(1.0/RAD)*(EXP(SUMH)-1.0)
501       25 WRITE (6,30) SUMH,DSUMH
502       30 FORMAT(/10X,'DEH2 (IN.)=',F7.4,5X,'UNCERT IN DEH2 (IN.)=',F7.4)
503         RETURN
504         END
```

Appendix F

Listing of the Stanton Program

The following listing is that of the Fortran program used to reduce the wall-measured heat flux data.

```
      $WATFIV
      C
      C     STANTON NUMBER DATA REDUCTION PROGRAM
      C     CURVATURE RIG  NASA-NAG-3-3
      C     THIS PROGRAM CALCULATES STANTON NUMBERS AND ENTHALPY THICK.
      C     REVISED JULY 1980
      C     PRESENT VERSION ALSO CALCULATES SENSITIVITY COEFFICIENTS FOR
      C     STANTON NUMBER AND UNCERTAINTY IN STANTON NUMBER
      C
 1          REAL K
 2          INTEGER PLATE0, PLATE1, D2LOC, PLATE2
 3          COMMON ARG(63),ARG0
 4          DIMENSION SCT(62,40,3)
 5          DIMENSION SMAXDR(40),SMINDR(40),SMAXTS(40),SMINTS(40),
           1 SMAXRR(40),SMINRR(40)
 6          DIMENSION ST(62),PD(62),UNCERT(33),DST(62),
           1 USTREL(62),DELQC(62),DDELQC(62)
 7          DIMENSION DESC(64),XCM(62)
 8          COMMON/ BLK1 /PAMB,PSTAT,TRECOV,RHUM,PDYN,TAMB
 9          COMMON/ BLK2 /UINF,TINF,TADIAB,RHOINF,VISC,PR,CP,W
10          COMMON/ BLK3 /T00,TO(63),HM(62),Q(38),TEND(38),
           1 TFRAME(38),QDOT(62),DQDOT(62),QW(38),
           2 DKK(62),DSS(63),NTAG(63),NTAG0,REENP(62),STP(62)
11          COMMON/ BLK4/OST(62),USTABS(62),REEN(62),DREEN(62),D2(62),DD2(62)
           1 ,PCOEFF(62),X(62)
12          COMMON/ BLK5 /SENCO(62,39),VMAX,VMIN,NA,NB
13          DIMENSION TTOP(38),TCEN(38),TBOT(38),REX(62),
           1 NRN(4),KOMMNT(40),TSUPP(12),B(64),NUM(63),UB(63)
14          DIMENSION TTOPMV(39),TCENMV(39),TBOTMV(39),TSUPMV(12),
           1 TOMV(64),POST(62),PXCM(62)
15          CALL STARTG('GENIL*',0.)
16          DATA X/ 25.17,26.20,27.23,28.25,29.28,30.31,31.34,32.37,33.39,
           1        34.42,35.45,36.48,37.51,38.53,39.56,40.59,41.62,42.64,
           2        43.67,44.70,45.73,46.76,47.78,48.81,50.25,52.18,54.18,
           3        56.17,58.17,60.16,62.16,64.15,66.15,68.15,70.14,72.14,
           4        74.13,76.13,77.64,78.67,79.70,80.73,81.75,82.78,83.81,
           5        84.84,85.86,86.89,87.92,88.95,89.98,91.00,92.03,93.06,
           6        94.09,95.12,96.14,97.17,98.20,99.23,100.26,101.28/
      C
17          B0=0.01
18          DATA B/       .0157,   .0123,   .0113,   .0065,   .0139,
           1     .0120,   .0147,   .0144,   .0080,   .0097,   .0105,
           1     .0113,   .0102,
           2              .00909,  .01026,  .00962,  .01530,  .01028,
           3     .00585,  .00907,  .00704,  .00808,  .00437,  .00382,
           4       14*0.0,
           5     .00752,  .00866,  .00631,  .01165,  .00838,  .02904,
           6     .01560,  .00843,  .01218,  .00971,  .01562,  .01238,
           7     .00801,  .01207,  .00818,  .01077,  .01384,  .01067,
           8     .01231,  .00833,  .00788,  .01455,  .01579,  .00776, .01,0.0/
19          IRUN=0
      C
      C        CHANGE ORIGIN OF X FROM START OF COPPER PLATES
      C        TO START OF CURVATURE
      C
20          UB0=.05*B0
21          DO 130 I=1,62
22          UB(I)=.05*B(I)
23        130 X(I) = X(I) - 49.3125
24          UB(63)=.05*B(63)
      C
25          DO 120 I=1,24
26        120 NUM(I) = I + 24
27          DO 121 I=25,38
28        121 NUM(I) = I - 24
29          DO 122 I=39,63
30        122 NUM(I) = I - 38
      C
      C *1*     READ RUN NUMBER AND CONTROL PARAMETER
      C
      C         NRN      8 DIGIT RUN NUMBER
      C         IOUT     PARAMETER TO TERMINATE PROGRAM
```

```
C                IOUT=0 TO READ DATA SET
C                IOUT NE 0 TO TERMINATE PROGRAM
C                JOUT  UNCERTAINTY OUTPUT INDEX
C                      JOUT=0  OUTPUTS ALL UNCERTAINTIES WITH BASIC
C                              OUTPUT INFORMATION (INPUT DATA, CONVERTED
C                              DATA, STANTON NUMBERS, ETC.)
C                              PLUS MAXIMUM AND MINIMUM SENSITIVITY
C                              COEFFICIENTS FOR EACH VARIABLE OR PARAMETER
C                      JOUT=1  OUTPUTS ONLY RAW AND CONVERTED INPUT DATA
C                      JOUT=2  OUTPUTS ONLY MAXIMUM AND MINIMUM SENSITIVITY
C                              COEFFICIENTS FOR EACH VARIABLE OR PARAMETER
C                      JOUT=3  OUTPUTS SENSITIVITY COEFFICIENTS AT ALL
C                              STATIONS PLUS MAXIMUMS AND MINIMUMS
C                      JOUT=4  OUTPUTS UNCERTAINTIES WITH BASIC OUTPUT
C                              PLUS SENSITIVITY COEFFICIENTS AT ALL STATIONS
C                              PLUS MAXIMUMS AND MINIMUMS
C                         ***  NOTE  ***
C                              JOUT=3 AND JOUT=4 YIELD LARGE AMOUNTS OF
C                              OUTPUT.  FOR SOME CONTROL OF OUTPUT SIZE
C                              MODIFY SIZE OF MAIN UNCERTAINTY LOOP FIRST.
C
31     200 READ (5,1000) (NRN(I),I=1,4),IOUT,JOUT
32    1000 FORMAT(4A2,I2,I3)
33         IF (IOUT.NE.0) GO TO 210
C
C *2*    READ DATA RUN DESCRIPTION, A FORMAT  COL 1-80
C
34         READ (5,1010) (KOMMNT(I), I=1,35)
35    1010 FORMAT (35A2)
C
C *3*    READ TEST CONDITIONS
C
C        TAMB    AMBIENT TEMPERATURE (DEG F)
C        PAMB    AMBIENT PRESSURE (INCHES HG CORRECTED TO 32 DEG F)
C        RHUM    RELATIVE HUMIDITY (PERCENT)
C
36         READ (5,1020) TAMB,PAMB,RHUM
37    1020 FORMAT (7F10.0,I3)
38         PLATE2=0
C
C *4*    READ TUNNEL CONDITIONS
C
C        TRECMV  TUNNEL AIR RECOVERY TEMPERATURE (I-C TC, MV)
C        PDYN    TUNNEL AIR VELOCITY DYNAMIC PRESSURE (INCHES H2O)
C        PSTAT   TUNNEL GAGE STATIC PRESSURE (INCHES H2O)
C        XVO     VIRTUAL ORIGIN, TBL, FROM PGM PROFILE (INCHES)
C        DXVO    UNCERTAINTY IN XVO, FROM PGM PROFILE (INCHES)
C        D2INIT  ENTHALPY THICKNESS, FROM PGM PROFILE (INCHES)
C        DD2INT  UNCERTAINTY IN D2LOC, FROM PGM PROFILE (INCHES)
C        D2LOC   LOCATION OF PROFILE MEASUREMENTS (PLATE #)
C
39         READ (5,1020) TRECMV,PDYN,PSTAT,XVO,DXVO,D2INIT,DD2INT,D2LOC
C
C *5*    READ DEVELOPMENT SECTION CONDITIONS
C
C        PLATE1     PLATE # WHERE DATA BEGINS
C        PLATE2     PLATE # WHERE HEATING BEGINS
C        TOMV(I)    PLATE TEMPERATURE (MV)
C        HM(I)      HEAT FLUX METER SIGNAL (MV)
C        PCOEFF(I) PRESSURE COEFFICIENT
40         READ (5,1030) PLATE1,PLATE2
41    1030 FORMAT (2I3)
42         PLATE0 = PLATE1 - 1
43         READ (5,1031) TOMV0
44         READ (5,1031) (TOMV(I), HM(I), PCOEFF(I), I=PLATE1,24)
45    1031 FORMAT(3F10.0)
46    1032 FORMAT(F10.0)
C
C *6*    READ TEST SECTION CONDITIONS
C
C        TTOPMV(I)  PLATE TOP TEMPERATURE (MV)
C        TCENMV(I)  PLATE CENTER TEMPERATURE (MV)
```

```
C        TBOTMV(I)  PLATE BOTTOM TEMPERATURE (MV)
C        QW(I)      PLATE POWER (WATTS)
C        PCOEFF(I)  PRESSURE COEFFICIENT
47        READ (5,1040) (TBOTMV(I),TCENMV(I),TTOPMV(I),QW(I),
         1 PCOEFF(I), I=25,38)
48     1040 FORMAT (5F10.0)
C
C *7*    READ RECOVERY SECTION CONDITIONS
C
C        TOMV(I)   PLATE TEMPERATURE (I-C TC, MV)
C        HM(I)   HEAT FLUX METER SIGNAL (MV)
C       PCOEFF(I)   PRESSURE COEFFICIENT
49        READ (5,1031) (TOMV(I),HM(I),PCOEFF(I),I=39,62)
50        READ (5,1032) TOMV(63)
C
C *8*    READ SUPPORT TEMPERATURES
C
C        TSUPMV(I) TEST SECTION SUPPORT TEMPERATURE (I-C TC, MV)
C
51        READ (5,1050) (TSUPMV(I), I=1,12)
52     1050 FORMAT (6F10.0)
C
C *******   WRITE OUT ALL RAW DATA  *******
C
53        IF(JOUT.EQ.3.OR.JOUT.EQ.2) GO TO 252
54        WRITE(6,3000)
55        WRITE(6,2000) (NRN(I), I=1,4)
56     2000 FORMAT (10X,'RUN ',4A2,' *** CURVATURE RIG *** NASA-NAG-3-3',
         1 5X,'INPUT DATA'/)
57        WRITE(6,2010) (KOMMNT(I), I=1,35)
58     2010 FORMAT (10X,35A2/)
C
59        WRITE(6,2020) TAMB,PAMB,RHUM
60     2020 FORMAT(10X,'AMB TEMP =',F6.1,' F',5X,'AMB PRESS =',F6.2,' IN HG',
         1 5X,'REL HUM =',F5.1,' %',/)
61        WRITE(6,2030) PSTAT,PDYN,TRECMV,D2INIT,D2LOC,DD2INT,XVO,DXVO
62     2030 FORMAT (10X,'STAT PRESS =',F5.2,' IN H2O  DYN PRESS =',F6.3,
         1 ' IN H2O  RECOV TEMP =',F6.3,' MV'//10X,'ENTHALPY THICKNESS ='
         2 ,F7.4,' IN  AT PLATE #',I3,4X,'UNCERTAINTY =',F8.5,' IN',//,
         3 10X,'VIRTUAL ORIGIN:  X =',F6.1,'  IN',4X,'UNCERTAINTY =',
         4 F5.2,' IN',/)
C
63        WRITE(6,2040)
64     2040 FORMAT(/,10X,'PLATE',6X,'TPLATE',6X,'HM',8X,'CP',/,22X,'(MV)',6X,
         1 '(MV)',/)
65        I = 24
66        WRITE(6,2050) PLATE0, I, TOMV0
67        WRITE(6,2050) (I,NUM(I),TOMV(I),HM(I), PCOEFF(I), I=PLATE1,24)
68     2050 FORMAT(10X,I2,I4,2F11.3,F10.3)
C
69        WRITE(6,2060)
70     2060 FORMAT (/,10X,'PLATE',7X,'TTOP      TCEN      TBOT',6X,'QDOT',
         1 8X,'CP'/22X,'(MV)      (MV)      (MV)     (WATTS)',/)
71        WRITE(6,2070) (I,NUM(I),TTOPMV(I),TCENMV(I),TBOTMV(I),QW(I),
         1  PCOEFF(I), I=25,38)
72     2070 FORMAT (10X,I2,I4,1X,3F10.3,3X,F7.2,F10.3)
C
73        WRITE(6,3000)
74        WRITE(6,2000) (NRN(I), I=1,4)
75        WRITE(6,2010) (KOMMNT(I), I=1,35)
C
76        WRITE(6,2040)
77        WRITE(6,2050) (I,NUM(I),TOMV(I),HM(I), PCOEFF(I), I=39,62)
78        I = 63
79        WRITE(6,2050) I, NUM(I), TOMV(I)
80        WRITE(6,2080) (TSUPMV(I), I=1,12)
81     2080 FORMAT (///,10X,'SUPPORT TEMPERATURES  (MV)',///,24X,
         1 'TOP     CEN     BOT',//,10X,'UPSTREAM  ',3F8.3,/,10X,
         2 'DOWNSTREAM',3F8.3,//,24X,'UP      CEN     DOWN',//,
         3 10X,'TOP       ',3F8.3,/,10X,'BOTTOM    ',3F8.3)
82     252   CONTINUE
C
```

```
C *******  PERTURBATION BLOCK *******
C
C      INPUTS VARIED INDIVIDUALLY BY 1%
C
C       PERTURBATION LOOP INDICES:
C
C               J    MAIN PERTURBATION LOOP
C               JT   SUBSIDIARY LOOP TO ALLOW CALCULATION OF PARTIAL
C                    DERIVATIVES WITH RESPECT TO T(I+1) AND T(I-1)
C                    AS WELL AS T(I)
C               JS   SUBSIDIARY LOOP FOR S(I+1) AND S(I)
C
C               NTAG(I) MARKS ARGUMENT IN SUBISIDIARY LOOPS,
C               DISTINGUISHING AMONG I, I+1, AND I-1 FOR LATER USE
C               IN COMPUTING SENSITIVITY COEFFICIENTS.
 83       DATA DESC/ 'TO(I',')   ','TTOP','(I) ','TCEN','(I) ',
     1             'TBOT','(I) ','B(I)',',    ','S(I)','    ',
     2             'HM(I',')   ','Q(I)',',    ','K(I)','    ',
     3             'A(I)',',    ','PAMB',',    ','RHUM','    ',
     4             'TREC','OV  ','PDYN',',    ','EMIS',',    ',
     5             'WCAL',',    ','RO(I',')   ','RBO(','I)  ',
     6             'RLOD','(I) ','RA  ',',    ','PSTA','T   ',
     7             'SPAN','(I) ','TSUP','P10 ','RFW ',',    ',
     8             'TCAL',',    ','PS  ',',    ','RHOS',',    ',
     9             'XA  ',',    ','RV  ',',    ','RB  ',',    ',
     1             'KUP ',',    ','KDOW','N   '/
 84       DATA UNCERT/400.0,4*0.003, 0.003, 0.01, 0.020, 0.05, 0.02,
     1         0.0005, 0.30, 1.00, 0.003, 0.00500, 0.02, 0.05,3*.015,
     2            0.005, 0.005, 20., 0.004, 0.04, 0.1, 2.0, 0.0001,
     3            0.003, 100.0, .005, 0.0086, 0.01790/
 85       JS=1;  JSC=1;  JT=1
 88       ARG0=100.0
 89       DO 160 I=PLATE1,63
 90       ARG(I)=100.0
 91  160  CONTINUE
 92       DO 500 J=1,33
 93       JCOUNT=J
 94       DO 141 JS=1,2
 95       JSC=JS
 96       NT=2; MT=62
 98       TOMV(64)=0.0
 99       TTOPMV(39)=0.0;  TCENMV(39)=0.0;  TBOTMV(39)=0.0
102       DO 142 JT=1,3
103       IF(J.GT.6) GO TO 245
104       IF(J.EQ.1) GO TO 280
105       JTC=JT
106       IF(JT.EQ.3) MT=63
107       IF(NT.NE.0) GO TO 225
108       IF(J.EQ.2) CALL CHANGE(0,JTC,TOMV0,TOMV(1))
109       IF(J.EQ.6) CALL CHANGE(0,JTC,B0,B(1))
110       NT=3
111  225  CONTINUE
112       DO 143 I=NT,MT,3
113       ICOUNT=I
114       IF(I.LE.38.AND.I.GE.25) GO TO 220
115       IF(J.EQ.2) CALL CHANGE(ICOUNT,JTC,TOMV(I),TOMV(I+1))
116  226  IF(J.EQ.3.AND.JT.EQ.1) GO TO 223
117       GO TO 224
118  223  TOMV(24)=ARG(24)
119       TOMV(63)=ARG(63)
120       TOMV0=ARG0
121       IF(I.EQ.40.OR.I.EQ.39) GO TO 224
122       IF(I.GT.2) TOMV(I-2)=ARG(I-2)
123  224  IF(J.EQ.6) CALL CHANGE(ICOUNT,JTC,B(I),B(I+1))
124       GO TO 221
125  220  IF(J.EQ.3) CALL CHANGE(ICOUNT,JTC,TTOPMV(I),TTOPMV(I+1))
126       IF(J.EQ.4.AND.JT.EQ.1.AND.I.GT.26) TTOPMV(I-2)=ARG(I-2)
127       IF(J.EQ.4.AND.JT.EQ.1) TTOPMV(25)=ARG(25)
128       IF(J.EQ.4) CALL CHANGE(ICOUNT,JTC,TCENMV(I),TCENMV(I+1))
129       IF(J.EQ.5.AND.JT.EQ.1.AND.I.GT.26) TCENMV(I-2)=ARG(I-2)
130       IF(J.EQ.5.AND.JT.EQ.1) TCENMV(25)=ARG(25)
131       IF(J.EQ.5) CALL CHANGE(ICOUNT,JTC,TBOTMV(I),TBOTMV(I+1))
```

```
132         IF(J.NE.6) GO TO 221
133         IF(JT.EQ.1.AND.I.GT.26) TBOTMV(I-2)=ARG(I-2)
134         IF(JT.EQ.1) TBOTMV(25)=ARG(25)
135         ARG(I)=0.0
136         IF(I.EQ.0) GO TO 228
137   221   NTAG(I)=0
138   228   NTAG0=0
139         IF(I.EQ.63) GO TO 222
140         NTAG(I+1)=-1
141         IF(I.EQ.1) GO TO 143
142   222   NTAG(I-1)=1
143   143   CONTINUE
144   245   IF(J.EQ.7) B0=ARG0
145         DO 144 I=1,63
146         ICOUNT=I
147         IF(J.EQ.7.AND.JS.EQ.1) B(I)=ARG(I)
148         IF(I.GE.25.AND.I.LE.38) GO TO 247
149         IF(I.GT.62) GO TO 144
150         IF(J.EQ.8) CALL CHAN(ICOUNT,HM(I))
151         IF(J.EQ.9) HM(I)=ARG(I)
152         GO TO 144
153   247   IF(J.EQ.9) CALL CHAN(ICOUNT,QW(I))
154         IF(J.EQ.10) QW(I)=ARG(I)
155   144   CONTINUE
156         IF(J.EQ.12) CALL CHAN(1,PAMB)
157         IF(J.EQ.13) CALL CHANGE(1,4,RHUM,PAMB)
158         IF(J.EQ.14) CALL CHANGE(1,4,TRECMV,RHUM)
159         IF(J.EQ.15) CALL CHANGE(1,4,PDYN,TRECMV)
160         IF(J.EQ.16) PDYN=ARG(1)
161         IF(J.EQ.22) CALL CHAN(1,PSTAT)
162         IF (J.EQ.23) PSTAT=ARG(1)
163         IF (J.NE.23 .AND. J.NE.24) GO TO 145
164         DO 146 I=25,38
165         ICOUNT=I
166         IF (J.EQ.23) CALL CHAN(ICOUNT,DELQC(I))
167         IF (J.EQ.24) DELQC(I)=ARG(I)
168       146 CONTINUE
169       145 CONTINUE
170         IF(J.EQ.24) CALL CHAN(1,TSUPMV(10))
171         IF(J.EQ.25) TSUPMV(10)= ARG(1)
172   280   CONTINUE
      C
      C *******  DATA CONVERSION BLOCK  *******
      C
173         IF(J.GT.1) GO TO 250
      C       AVOIDS CONVERTING PRESSURE AND HUMIDITY MORE THAN ONCE
174         RHUM = RHUM / 100.
      C       CONVERT ALL PRESSURES TO LBF/SQFT
175         PDYN = PDYN * 5.195
176         PSTAT = PSTAT * 5.195
177         PAMB = PAMB * 70.726
178   250   CONTINUE
      C        CONVERT ALL TEMPERATURES FROM MV TO DEG F
179         IF(J.EQ.7.AND.JS.EQ.2) GO TO 253
180         TRECOV=TC(JCOUNT,TRECMV,0.0,TAMB)
181         TC0=TC(JCOUNT,TOMV0,B0,TAMB)
182         DO 100 I=1,12
183         TSUPP(I)=TC(JCOUNT,TSUPMV(I),0.0,TAMB)
184       100 CONTINUE
185         DO 101 I=PLATE1,24
186         TO(I)=TC(JCOUNT,TOMV(I),B(I),TAMB)
187       101 CONTINUE
188         DO 102 I=25,38
189         TTOP(I)=TC(JCOUNT,TTOPMV(I),B(I),TAMB)
190         TCEN(I)=TC(JCOUNT,TCENMV(I),B(I),TAMB)
191         TBOT(I)=TC(JCOUNT,TBOTMV(I),B(I),TAMB)
192       102 CONTINUE
193         DO 103 I=39,63
194         TO(I)=TC(JCOUNT,TOMV(I),B(I),TAMB)
195       103 CONTINUE
196   253   CONTINUE
      C
```

```
C     COMPUTE THE TEMPERATURES IN THE FRAME NEAR THE ENDS OF THE PLATES
C     BY A QUADRATIC FIT TO THE TEMPS. MEASURED IN THE PLATE SUPPORTS.
C     ALSO COMPUTE AVERAGES OF END AND OVERALL TEMPS. OF THE PLATES.
C
197       A2 = ((TSUPP(7)+TSUPP(10)-TSUPP(8)-TSUPP(11))/5. - (TSUPP(8)+
         1 TSUPP(11)-TSUPP(9)-TSUPP(12))/6.)/22.
198       A1 = (TSUPP(8)+TSUPP(11)-TSUPP(7)-TSUPP(10))/10. - A2 * 9.
199       A0 = (TSUPP(7)+TSUPP(10))/2. - A1 * 2. - A2 * 4.
C
200       DO 104 I=25,38
201       TFRAME(I) = A0 + A1 * (I-24) + A2 * (I-24)*(I-24)
202       TO(I) = TCEN(I)
203       TEND(I) = (TTOP(I) + TBOT(I)) /2.
204     104 CONTINUE
C
205       TUP   = (TSUPP(1) + TSUPP(2) + TSUPP(3)) /3.
206       TDOWN = (TSUPP(4) + TSUPP(5) + TSUPP(6)) /3.
C
C        COMPUTE WIND TUNNEL FLOW CONDITIONS
207       CALL TUNNEL (JCOUNT)
C
C        COMPUTE NET ENERGY TRANSFER FROM DEVELOPMENT
C        REGION, TEST SECTION AND RECOVERY REGION
208       CALL POWER (JSC,JCOUNT,TINF,TUP,TDOWN,PLATE1)
C     CORRECTION FOR SPANWISE HEAT FLOW AND UPDATE PLATE CENTER TEMP
209       DO 106 I=1,62
210       DDELQC(I)=0.0
211     106 CONTINUE
212       DO 109 I=25,38
213       TFC=0.0221*(TBOT(I)-TCEN(I))-0.0127*(TCEN(I)-TTOP(I))
214       TFB=-0.142*(TCEN(I)-TTOP(I))-4.06*TFC
215       TO(I)=TBOT(I)+5.56*TFB-30.9*TFC
216       DELQC(I)=414.0*TFC
217       DDELQC(I)=0.10*DELQC(I)
218       QDOT(I)=QDOT(I)+DELQC(I)
219     109 CONTINUE
C
C *******  WRITE ALL CONVERTED DATA  *******
C
220       IF(J.GT.1) GO TO 251
221       IF(JOUT.EQ.3.OR.JOUT.EQ.2) GO TO 251
222       WRITE(6,3000)
223       WRITE(6,2140) (NRN(I), I=1,4)
224       WRITE(6,2010) (KOMMNT(I), I=1,35)
225       WRITE(6,2100)
226    2100 FORMAT(/,10X,'PLATE',6X,'TPLATE',5X,'HM',8X,'QFLUX',/,
         1 22X,'(F)',6X,'(MV)    (BTU/HR/SQFT)',/)
227       I = PLATE0 + 24
228       WRITE(6,2110) PLATE0, I, TO0
229       WRITE(6,2110) (I,NUM(I),TO(I),HM(I),QDOT(I),I=PLATE1,24)
230    2110 FORMAT (10X,I2,I4,F10.2,F10.3,F11.2)
C
231       WRITE(6,2120)
232    2120 FORMAT (/,10X,'PLATE',6X, 'TPLATE',5X,'QDOT',6X,'QFLUX',
         1  6X,'TFRAME',/,22X,'(F)',5X,'(WATTS)  (BTU/HR/SQFT)   (F)',/)
233       WRITE(6,2130) (I,NUM(I),TO(I),Q(I),QDOT(I),TFRAME(I), I=25,38)
234    2130 FORMAT(10X,I2,I4,2F10.2,F11.2,F12.2)
C
235       WRITE(6,3000)
236       WRITE(6,2140) (NRN(I), I=1,4)
237    2140 FORMAT (10X,'RUN ',4A2,' *** CURVATURE RIG *** NASA-NAG-3-3 ',
         1 5X,'CONVERTED DATA'/)
238       WRITE(6,2010) (KOMMNT(I), I=1,35)
C
239       WRITE(6,2100)
240       WRITE(6,2110) (I,NUM(I),TO(I),HM(I),QDOT(I),I=39,62)
241       I = 63
242       WRITE(6,2110) I, NUM(I), TO(I)
243       WRITE(6,2150) (TSUPP(I), I=1,12)
244    2150 FORMAT (///,10X,'SUPPORT TEMPERATURES  (DEG F)',///,24X,
         1 'TOP     CEN     BOT',//,10X,'UPSTREAM  ',3F8.2,/,10X,
         2 'DOWNSTREAM',3F8.2,//,24X,'UP      CEN     DOWN',//,
```

```
     3 10X,'TOP       ',3F8.2,/,10X,'BOTTOM    ',3F8.2)
245  251  CONTINUE
     C
     C *******  COMPUTE STANTON NUMBER  *******
     C
     C     X REYNOLDS NUMBER BASED ON VIRTUAL ORIGIN TBL
246        FACT=UINF/(VISC*12.)
247        DREX=FACT*DXVO
248        DO 110 I=1,62
249   110  REX(I)=FACT*(X(I)-XVO)*(1.0-PCOEFF(I))**0.5
     C     COMPUTE STANTON NUMBERS
250        DENOM=RHOINF*UINF*CP*3600.
251        DO 111 I=1,62
252        ST(I)=QDOT(I)/(DENOM*(TO(I)-TADIAB)*(1.0-PCOEFF(I))**0.5)
253   111  CONTINUE
     C ******  COMPUTE UNCERTAINTY IN STANTON NUMBER  ******
     C
     C
     C       OST(I) ORIGINAL (UNPERTURBED) STANTON NUMBER
     C       DST(I) CHANGE IN STANTON NUMBER DUE TO PERTURBATON
     C       DARG   CHANGE IN VARIABLE OR PARAMETER DUE TO PERTURBATION
     C       PD(I)  PARTIAL DERIVATIVE  DST/DARG
     C       SENCO(I,J)  SENSITIVITY COEFFICIENT  PD(I)*ABSOLUTE UNCERTAINTY
     C                   IN VARIABLE OR PARAMETER
     C
254        IF(J.EQ.1) GO TO 284
255        DO 180 I=1,62
256        DST(I)=OST(I)-ST(I)
257        IF(J.GE.12.AND.J.LE.16) GO TO 290
258        IF(J.GE.21.AND.J.LE.25 .AND. J.NE.23) GO TO 290
259        IF(J.GE.27) GO TO 290
260        IF(J.GE.33) GO TO 290
261        GO TO 281
     C       FOR VARIABLES OR PARAMETERS APPLYING TO ALL PLATES,
     C       DARG IS MADE THE SAME AT EACH PLATE
262  290   DO 181 IARG=1,62
263  181   ARG(IARG)=ARG(1)
264  281   CONTINUE
265        DARG=ARG(I)*0.01
266        IF(J.GT.7) GO TO 282
267        IF(NTAG(I).EQ.1) DARG=ARG(I+1)*0.01
268        IF(NTAG(I).EQ.-1) DARG=ARG(I-1)*0.01
     C       FOR J=6, B(25)-B(28) ALL EQUAL ZERO
     C       FOR J=28, THE THERMOCOUPLE CALIBRATION EQUATION RESULT IS
     C       PERTURBED BY 0.05F RATHER THAN 1% TO SIMPLIFY DETERMINATION OF ARG
     C       FOR J=34, XB(I)=0.0
269  282   IF(J.EQ.6.AND.I.LE.38.AND.I.GE.25) DARG=0.0001
270        IF(J.EQ.8.AND.I.LE.38.AND.I.GE.25) DARG=0.0001
271         IF(J.EQ.6.AND.JT.EQ.1.AND.I.EQ.39) DARG=0.0001
272         IF(J.EQ.6.AND.JT.EQ.2.AND.I.EQ.24) DARG=0.0001
273         IF(J.EQ.26) DARG=0.05
274         IF (ABS(DARG) .LT. 1.0E-8) DARG=1.0E-8
275         PD(I)=DST(I)/DARG
     C       UNCERTAINTIES IN K(I) AND S(I) CALCULATED IN SUBROUTINE POWER
     C       USING RELATIVE (PERCENT) UNCERTAINTIES
276        UNCERT(10)=DKK(I)
277        UNCERT(7)=DSS(I)
278        UNCERT(6)=UB(I)
279        UNCERT(23)=DDELQC(I)
280        IF (I .GE. 38) UNCERT(23)=DDELQC(38)
281        PDU=PD(I)*UNCERT(J)
     C       COMPUTE SENSITIVITY COEFFICIENTS
282        SENCO(I,J)=ABS(PDU)
283  445   CONTINUE
     C       DETERMINE ARRAYS IN SUBSIDIARY LOOPS
284        IF(J.GT.6) GO TO 283
285        SCT(I,J,JT)=SENCO(I,J)
286  283   IF(J.NE.7) GO TO 180
287        SCT(I,J,JS)=SENCO(I,J)
288  180   CONTINUE
289        NT=NT-1
290        MT=MT-1
```

```
291         IF(J.GT.6) GO TO 292
292   142   CONTINUE
293   292   IF(J.NE.7) GO TO 291
294   141   CONTINUE
295   291   CONTINUE
296         GO TO 500
297   284   DO 185 I=1,62
298   185   OST(I)=ST(I)
299         NT=2
300         MT=62
301   500   CONTINUE
302         SCT(24,2,1)=SQRT(SENCO(24,3)*SENCO(24,3)+SENCO(24,4)*SENCO(24,4)
          1 +SENCO(24,5)*SENCO(24,5))
303         SCT(39,2,1)=SQRT(SENCO(39,3)*SENCO(39,3)+SENCO(39,4)*SENCO(39,4)
          1 +SENCO(39,5)*SENCO(39,5))
304         DO 182 J=2,6
305         DO 182 I=1,62
306   182   SENCO(I,J)=(SCT(I,J,1)*SCT(I,J,1)+SCT(I,J,2)*SCT(I,J,2)
          1 +SCT(I,J,3)*SCT(I,J,3))**0.5
307         DO 183 I=1,62
308   183   SENCO(I,J)=(SCT(I,J,1)*SCT(I,J,1)+SCT(I,J,2)*SCT(I,J,2))**0.5
309         DO 171 I=1,62
310         SUM=0.0
311         DO 170 J=2,33
312   170   SUM=SUM+SENCO(I,J)*SENCO(I,J)
313         USTABS(I)=SUM**0.5
314   171   USTREL(I)=USTABS(I)/ST(I)*100.0
      C
      C        COMPUTE DEL2 AND REDEL2 BASED ON ACTUAL ST-DATA
315         CALL ENTHAL (FACT,D2INIT,DD2INT,D2LOC)
316         DO 172 I=1,62
317         REENP(I)=0.0
318         STP(I)=0.0
319         IF (I .LT. D2LOC) GO TO 172
320         NP=I-D2LOC+1
321         REENP(NP)=REEN(I)
322         STP(NP)=OST(I)
323     172 CONTINUE
      C
      C *******  WRITE STANTON NUMBER DATA  *******
      C
324         IF(JOUT.LE.3.AND.JOUT.GE.1) GO TO 285
325         WRITE(6,3000)
326         WRITE(6,2200) (NRN(I), I=1,4)
327    2200 FORMAT (10X,'RUN ',4A2,' *** CURVATURE RIG *** NASA-NAG-3-3 ',
          1 5X,'STANTON NUMBER DATA'/)
328         TADBC=5.*(TADIAB-32.)/9.
329         TINFC=5.*(TINF-32.)/9.
330         UINFMS=UINF*0.3048
331         XVOCM=XVO*2.54
332         RHOKM3=RHOINF*16.02
333         VISCI=VISC*0.0929
334         CPJKGK=CP*4184.
335         WRITE(6,2210) TADBC,UINFMS,TINFC,RHOKM3,VISCI,XVOCM,CPJKGK,PR
336    2210 FORMAT(10X,'TADB=',F6.2,' DEG C    UREF=',F12.2,' M/S     TINF=',
          1 F6.2,' DEG C'/10X,'RHO=',F7.3,' KG/M3    VISC=',E12.5,' M2/S',
          2 4X,'XVO=',F7.1,' CM'/10X,'CP=',F8.0,' J/KGK    PR=',F14.3/)
337         WRITE(6,2220)  (KOMMNT(I),I=1,35)
338    2220 FORMAT(10X,35A2/)
339         WRITE(6,2230)
340    2230 FORMAT(10X,'PLATE',3X,'X',3X,'UPW',5X,'K',5X,6X,'REXVO',7X,'TO',6X
          1 ,'STANTON NO',6X,'REENTH', 7X,'DST',9X,'DST(%)',7X,'DREEN',/
          2 16X,'(CM) ',' (M/S)',27X,'DEG C',/)
341         DO 113 I=1,62
342         POST(I)=OST(I)
343         XCM(I)=X(I)*2.54
344         PXCM(I)=XCM(I)
345         IF (I .EQ. 25) WRITE(6,4000)
346         IF (I .EQ. 39) WRITE(6,4100)
347    4000 FORMAT(/10X,'CURVE BEGINS'/)
348    4100 FORMAT(/10X,'RECOVERY BEGINS'/)
349         IF (I.EQ.39) WRITE(6,3000)
```

```
350         IF (I .GT. 1) XCML=X(I-1)*2.54
351         ULOC=UINFMS*(1.0-PCOEFF(I))**0.5
352         TEMPC=5.*(TO(I)-32.)/9.
353         IF (I .GT. 1) ACC=(100.*(VISCI/(2.0*ULOC))*
           1 ((PCOEFF(I-1)-PCOEFF(I))/(XCM(I)-XCML)))/(1.0-PCOEFF(I))
354         IF (I .EQ.1) ACC=0.0
355         IF (I .GE. D2LOC) GO TO 114
356         IF (I .GE. PLATE2) GO TO 115
357         WRITE (6,2245) I,XCM(I),ULOC,ACC,REX(I),TEMPC
358    2245 FORMAT(10X,I3,F7.1,F7.2,1X,E10.3,1X,E12.5,F7.2)
359         GO TO 113
360     115 WRITE(6,2240) I,XCM(I),ULOC,ACC,REX(I),TEMPC,OST(I),USTABS(I),USTR
           2EL(I)
361    2240 FORMAT(10X,I3,F7.1,F7.2,1X,E10.3,1X,E12.5,F7.2,2X,E12.5,16X,E9.3,
           1 3X,F9.3)
362         GO TO 113
363     114   WRITE(6,2250) I,XCM(I),ULOC,ACC,REX(I),TEMPC,OST(I),REEN(I),USTABS
           1 (I),USTREL(I),DREEN(I)
364    2250 FORMAT(10X,I3,F7.1,F7.2,1X,E10.3,1X,E12.5,F7.2,2(2X,E12.5),2X,
           1 E9.3,3X,F9.3,4X,F7.0)
365     113 CONTINUE
366         WRITE(6,2260) DREX
367    2260 FORMAT (/12X,'UNCERTAINTY IN REX=',F6.0)
       C
368    285   CONTINUE
       C
       C ***** ADDITIONAL UNCERTAINTY INFORMATION *****
       C
       C       COMPUTE AND WRITE OUT MAXIMUM AND MINIMUM SENSITIVITY
       C       COEFFICIENTS FOR EACH VARIABLE OR PARAMETER
       C
369         IF(JOUT.EQ.1) GO TO 293
370         WRITE(6,3000)
371         WRITE(6,2340)(NRN(I),I=1,4)
372    2340  FORMAT(10X,'RUN',4A2,' *** CURVATURE RIG *** NASA-NAG-3-3 ',
           1 5X,'SENSITIVITY COEFFICIENTS (DST/DARG * DELTA ARG)'//,
           2 50X,'PREPLATE',16X,'TEST SECTION',15X,'AFTERPLATE'//5X,
           8' ARGUMENT        ',25X,
           9 'MAX          MIN          MAX          MIN',10X,
           1 'MAX          MIN'//)
373         DO 184 J=2,33
374         JCOUNT=J
375         SMAXDR(J)=25.0;SMINDR(J)=25.0;SMAXTS(J)=25.0;SMINTS(J)=25.0
379         SMAXRR(J)=25.0;SMINRR(J)=25.0
381         CALL MAXMIN(1,24,JCOUNT)
382         SMAXDR(J)=VMAX; SMINDR(J)=VMIN; N1=NA; N2=NB
386         CALL MAXMIN(25,38,JCOUNT)
387         SMAXTS(J)=VMAX; SMINTS(J)=VMIN; N3=NA; N4=NB
391         CALL MAXMIN(39,62,JCOUNT)
392         SMAXRR(J)=VMAX; SMINRR(J)=VMIN; N5=NA; N6=NB
396         JDESC1=2*J-3; JDESC2=2*J-2
398         WRITE(6,2300)DESC(JDESC1),DESC(JDESC2),SMAXDR(J),SMINDR(J),
           1 SMAXTS(J),SMINTS(J),SMAXRR(J),SMINRR(J)
399    2300  FORMAT(6X,2A4,26X,E13.5,5E13.5)
400         WRITE(6,2310)J,UNCERT(J),N1,N2,N3,N4,N5,N6
401    2310  FORMAT(6X,'( J=',I2,'  DELTA ARG=',F9.5,' )', 8X,'(#',I2,')',
           1 5( 8X,'(#',I2,')'))
402    184   CONTINUE
403         WRITE(6,3000)
404    293   CONTINUE
       C
       C       WRITE OUT ALL SENSITIVITY COEFFICIENTS
       C
405         IF(JOUT.LT.3) GO TO 286
406         WRITE(6,3000)
407         WRITE(6,2350)(NRN(I),I=1,4)
408         DO 190 J=2,33
409         WRITE(6,3000)
410         JDESC1=2*J-3;  JDESC2=2*J-2
412         WRITE(6,2351) DESC(JDESC1),DESC(JDESC2)
413         DO 190 I=1,62
414    190   WRITE(6,2352) I,SENCO(I,J),ST(I)
```

```
 2350  FORMAT(10X,'RUN',4A2,' *** CURVATURE RIG *** NASA-NAG-3-3
     1      SENSITIVITY COEFFICIENTS'/)
 2351  FORMAT(10X,'PLATE     SENSITIVITY (DST/D',2A4,')     STANTON
     1 NUMBER')
 2352  FORMAT(12X,I2,11X,E12.6,12X,E12.6)
  286  CONTINUE
       NUMP1=62-PLATE1
       IF (PLATE2.GT.PLATE1) NUMP1=62-PLATE2
       IF (PLATE2 .LT. PLATE1) GO TO 287
       DO 288 I=PLATE2,62
       NOFF=I-PLATE2+1
       POST(NOFF)=OST(I)
       PXCM(NOFF)=XCM(I)
  288 CONTINUE
  287 CONTINUE
       NUMP2=62-D2LOC
       IF (IRUN .EQ. 1) CALL PICTRG(0.0)
       CALL SETSMG(23,0.0)
       CALL SETSMG(24,0.0)
       CALL SUBJEG(-60.,0.0,130.0,0.0040)
       CALL SETSMG(130,0.01)
       CALL SETSMG(131,0.01)
       CALL SETSMG(132,1.0)
       CALL CSETG('DUPLEX*')
       CALL GRAPHG('*',0,NUMP1,PXCM,POST,3,'STREAMWISE DISTANCE (CM)*',
     1'STANTON NUMBER*','STANTON NUMBER VERSUS STREAMWISE DISTANCE*')
       CALL PICTRG(0.0)
       CALL SETSMG(23,1.0)
       CALL SETSMG(24,1.0)
       CALL CSETG('DUPLEX*')
       CALL SUBJEG(200.,0.0005,5000.,0.005)
       CALL SETSMG(133,2.0)
       CALL SETSMG(134,2.0)
       CALL GRAPHG('*',0,NUMP2,REENP,STP,3,'ENTHALPY THICKNESS REYNOLDS N
     2UMBER*','STANTON NUMBER*','STANTON NUMBER VERSUS ENTHALPY THICKNES
     3S REYNOLDS NUMBER*')
       IRUN=1
       GO TO 200
  210 CONTINUE
 3000 FORMAT (1H1)
       CALL EXITG
       RETURN
       END
```

```
       FUNCTION TC(J,EMF,B,TAMB)
C         FUNCTION CONVERTS TEMP FROM IRON-CONSTANTAN MV TO DEG F
       T = 32.350 + 35.300 * EMF - 0.405 * EMF * EMF
       IF(J.EQ.26) T=T+0.05
       TC = T + B * (T - TAMB)
       RETURN
       END
```

```
      SUBROUTINE TUNNEL (J)
C
C        THIS ROUTINE COMPUTES THE WIND TUNNEL  FLOW CONDITIONS
C
C        UINF       FREE STREAM VELOCITY (FT/SEC)
C        TINF       FREE STREAM STATIC TEMPERATURE (DEG F)
C        RHOINF     FREE STREAM DENSITY (LBM/FT3)
C        VISC       FREE STREAM KINEMATIC VISCOSITY (FT2/SEC)
C        CP         FREE STREAM SPECIFIC HEAT (BTU/LBM/DEG R)
C        PR         FREE STREAM PRANDTL NUMBER
C        W          FREE STREAM ABSOLUTE HUMIDITY (LBM H2O/LBM DRY AIR)
C
      COMMON/ BLK1 /PAMB,PSTAT,TRECOV,RHUM,PDYN,TAMB
      COMMON/ BLK2 /UINF,TINF,TADIAB,RHOINF,VISC,PR,CP,W
      COMMON ARG(63),ARG0
C
C     SATURATION DATA FROM K AND K 1969 STEAM TABLES
      DIMENSION TEMP(10),PSAT(10),RHOSAT(10)
      REAL MFA,MFV,MWA,MWV,JF
      DATA TEMP/     40.,     50.0,     60.0,     70.0,     80.0,
     1     90.0,     100.0,    110.0,    120.0,     130.0/
      DATA PSAT/     17.519,   25.636,   36.907,   52.301,   73.051,
     1     100.627,  136.843,  183.787,  244.008,  320.400/
      DATA RHOSAT/   .0004090, .0005868, .0008286, .0011525, .0015803,
     1     .0021381, .0028571, .0037722, .0049261, .0063625/
      DO 10 N=1,9
      IF(TEMP(N).GT.TAMB) GO TO 20
   10 CONTINUE
   20 DT = (TAMB - TEMP(N-1))/10.
      PS = PSAT(N-1) + DT*(PSAT(N) - PSAT(N-1))
      RHOS = RHOSAT(N-1) + DT*(RHOSAT(N) - RHOSAT(N-1))
      IF(J.EQ.27) CALL CHAN(1,PS)
      IF(J.EQ.28) CALL CHAN(1,RHOS)
      RA=1545.32/28.970
      P = PAMB + PSTAT
      RHOV = RHUM*RHOS
      PVAP = RHUM*PS
      PA = P - PVAP
      RHOA = PA/(RA*(TAMB + 459.67))
      W=RHOV/RHOA
      RHOM = RHOA + RHOV
      MWA = 28.970
      MWV = 18.016
      MFV = RHOV/RHOM
      MFA = 1.0 - MFV
      RM = 1545.32*(MFA/MWA + MFV/MWV)
      CP = MFA*0.240 + MFV*0.445
      GC=32.1739
      JF=778.26
C     RFW: RECOVERY FACTOR FOR WIRE
C          RFW=0.68    WIRE NORMAL TO FLOW
C          RFW=0.86    WIRE PARALLEL TO FLOW
      RFW=0.86
      IF(J.EQ.25) CALL CHAN(1,RFW)
      TINF=(TRECOV+459.67)/(1. + RFW*PDYN*RM/(JF*CP*P)) - 459.67
      RHOINF=P/RM/(TINF+459.67)
      UINF=SQRT(2.*GC*PDYN/RHOINF)
      VISC=(11.+0.0175*TINF)/(1.E06*RHOINF)*(1.-.7*W)
      PR=.710*(530./(TINF+459.67))**(.1)*(1.+.9*W)
C     CONVERT TO ADIABATIC WALL TEMPERATURE
      RCF=PR**0.33333
      TADIAB=TINF+RCF*UINF*UINF/(2.*GC*JF*CP)
      RETURN
      END
```

```
503         SUBROUTINE POWER (JSC,J,TINF,TUP,TDOWN,PLATE1)
      C
      C        THIS ROUTINE :
      C
      C             (1) CORRECTS THE INDICATED PLATE POWER READING FOR
      C                 WATTMETER CALIBRATION AND CIRCUIT INSERTION LOSSES
      C             (2) COMPUTES NET ENERGY LOST FROM PLATES BY FORCED
      C                 CONVECTION HEAT TRANSFER
      C             (3) COMPUTES HEAT FLUX FROM RECOVERY REGION PLATES
      C
504         COMMON/ BLK3 /TOO,TO(63),HM(62),Q(38),TEND(38),
           1 TFRAME(38),QDOT(62),DQDOT(62),QW(38),
           2 DKK(62),DSS(63),NTAG(63),NTAGO,REENP(62),STP(62)
505         COMMON ARG(63),ARGO
506         INTEGER PLATE1
507         REAL KL,KR,KBP,K,KUP,KDOWN
508         DIMENSION RO(14),RBO(14),RLOD(14)
509         DIMENSION RL(14),K(62),S(64),SS(63),
           1 A(62),AA(62),QR(62)
      C     HEAT FLUX METER CALIBRATION CONSTANTS #  1-24 (BTU/HR/SQFT)/MV
510         DATA K/    40.07,   32.59,   30.42,   32.79,   13.97,   35.72,
           1           31.88,   29.86,   31.58,   35.70,   34.36,   34.47,
           2           31.58,   41.04,   28.65,   30.51,   27.39,   32.62,
           3           29.46,   31.15,   27.47,   32.11,   34.37,   35.80,
      C     END LOSS CONSTANTS FOR TEST SECTION (PLATES 25-38)  (BTU/HR/F)
           4         .244,    .293,    .256,    .224,    .241,    .283,    .227,
           5         .227,    .227,    .230,    .225,    .196,    .296,    .244,
      C     HEAT FLUX METER CALIBRATION CONSTANTS # 39-62 (BTU/HR/SQFT)/MV
           6           33.46,   33.05,   35.21,   33.64,   33.53,   31.92,
           7           25.16,   33.10,   27.15,   30.71,   30.42,   31.39,
           8           33.01,   33.91,   31.47,   29.60,   22.66,   31.41,
           9           32.34,   38.41,   32.70,   22.08,   36.58,   32.72/
      C
      C       COMPUTE UNCERTAINTIES IN K(I)
      C
511         IF(J.GT.1) GO TO 132
512         DO 130 I=1,62
513         DKK(I)=0.01
514         IF(I.LE.24) DKK(I)=0.03*K(I)
515         IF(I.GE.39) DKK(I)=0.03*K(I)
516   130   CONTINUE
517   132   CONTINUE
518         DO 131 I=1,62
519         ICOUNT=I
520         IF(J.EQ.10) CALL CHAN(ICOUNT,K(I))
521         IF(J.EQ.11) K(I)=ARG(I)
522   131   CONTINUE
      C
523         DATA  A /  24*0.15706, 0.2320, 13*0.2495, 24*0.1290/
524         IF(J.NE.11) GO TO 220
525         DO 120 I=1,62
526         ICOUNT=I
527         AA(I)=A(I)
528         CALL CHAN(ICOUNT,A(I))
529   120   CONTINUE
530   220   IF(J.NE.12) GO TO 222
531         DO 121 I=1,62
532   121   A(I)=AA(I)
533   222   CONTINUE
      C        AXIAL CONDUCTION LOSS CONSTANTS  (BTU/HR/F)
534         DATA  S  /  24*0.7,  0.847,  13*1.08,
           1   .545,  .654,  .689,  .696,  .690,  .710,  .720,  .664,  .624,
           2   .761,  .697,  .777,  .730,  .718,  .730,  .744,  .724,  .746,
           3   .775,  .693,  .755,  .677,  .772,  .770,  .776,   .00/
535         DO 142 I=1,63
536         IF(J.EQ.8) S(I)=SS(I)
537         IF(JSC.NE.1) GO TO 142
      C
      C       COMPUTE UNCERTAINTIES IN S(I)
      C
538         DSS(I)=0.10*S(I)
539         SS(I)=S(I)
```

```
  142   CONTINUE
        IF(J.NE.7) GO TO 241
        NS=2;MS=62
        IF(JSC.EQ.1) GO TO 240
        NS=1;MS=63
  240   DO 140 I=NS,MS,2
        ICOUNT=I
        CALL CHANGE(ICOUNT,JSC,S(I),S(I+1))
        NTAG(I)=0
        IF(I.NE.1) GO TO 249
        NTAG0=1
        GO TO 140
  249   NTAG(I-1)=1
  140   CONTINUE
  241   CONTINUE
C          WATTMETER CIRCUIT RESISTANCES
        DATA RO  / 8.18,   8.03,   8.19,   8.12,   8.03,   8.11,   8.09,
       1           8.11,   8.25,   8.04,   8.07,   8.17,   7.98,   7.97/
        DATA RBO / 8.08,   7.92,   8.08,   8.01,   7.92,   7.99,   7.96,
       1           7.97,   8.08,   7.93,   7.96,   8.08,   7.88,   7.88/
        DATA RLOD/ 7.89,   7.84,   7.83,   7.86,   7.84,   7.84,   7.85,
       1           7.84,   7.87,   7.83,   7.87,   7.88,   7.87,   7.86/
        DATA RA,XA,RV,RB/  0.080,  0.063,  7569.0,  0.1780/
        DATA KUP, KDOWN /  0.086,  0.179/
        DO 150 I= 1,14
        ICOUNT=I
        IF(J.EQ.18) CALL CHAN(ICOUNT,RO(I))
        IF(J.EQ.19) CALL CHANGE(ICOUNT,4,RBO(I),RO(I))
        IF(J.EQ.20) CALL CHANGE(ICOUNT,4,RLOD(I),RBO(I))
        IF(J.EQ.21) RLOD(I)=ARG(I)
  150   CONTINUE
        IF(J.EQ.21) CALL CHAN(1,RA)
        IF(J.EQ.22) RA=0.064
        IF(J.LT.29) GO TO 250
        IF(J.EQ.29) CALL CHAN(1,XA)
        IF(J.EQ.30) CALL CHANGE(1,4,RV,XA)
        IF(J.EQ.31) CALL CHANGE(1,4,RB,RV)
        IF(J.EQ.32) CALL CHANGE(1,4,KUP,RB)
        IF(J.EQ.33) CALL CHANGE(1,4,KDOWN,KUP)
  250   CONTINUE
        IF(J.EQ.34) KDOWN=0.179
C
C          THIS BLOCK CORRECTS INDICATED WATTMETER READING USING
C          WATTMETER CALIBRATION EQUATION
        DO 10 I=25,38
        JWC= I-24
        ICOUNT=I
        QP=QW(I)/75.
        QCOR=QP*(0.0728*QP-0.0427*QP*QP-0.0292)
        QCOR=0.99*QW(I)+QCOR*75.0
        IF (QW(I) .LT. 5.0) GO TO 11
        QCOR=QCOR+(0.00833/QP)*SIN(QP*40.55)
   11   IF(J.EQ.17) CALL CHAN(ICOUNT,QCOR)
C
C          THIS BLOCK CORRECTS FOR WATTMETER INSERTION LOSSES
        SUMRO=RO(JWC)
        SUMRBO=RBO(JWC)
        ZROSQ=SUMRO*SUMRO+(XA*XA)
        ZRBOSQ=SUMRBO*SUMRBO
        RL(JWC) = RLOD(JWC) - RB
        ZVALSQ=(RV+RA+RLOD(JWC))*(RV+RA+RLOD(JWC))+XA*XA
        Q(I)=QCOR*(ZROSQ/ZRBOSQ)*(ZVALSQ/RV/RV)
       1  *(RL(JWC)/(RA+RLOD(JWC)))
   10   CONTINUE
C
C          THIS BLOCK CORRECTS POWER DELIVERED TO PLATES IN
C          TEST SECTION FOR CONDUCTION AND RADIATION LOSSES
        SF=1.
        EMIS=0.05
        IF(J.EQ.16) CALL CHAN(1,EMIS)
        TAR=(TINF+460.)/100.
        DO 109 I=25,38
```

```
601         TOR=(TO(I)+460.)/100.
602         QCOND = K(I)*(TEND(I)-TFRAME(I)) + S(I)*(TO(I)-TO(I-1))
           1 + S(I+1)*(TO(I)-TO(I+1))
603         IF (I .EQ. 25) QCOND = QCOND + KUP*(TO(I) - TUP)
604         IF (I .EQ. 38) QCOND = QCOND + KDOWN*(TO(I) - TDOWN)
605         QRAD=A(I)*SF*EMIS*.1714*(TOR*TOR*TOR*TOR-TAR*TAR*TAR*TAR)
      C
      C     ENERGY BALANCE IS APPLIED TO PLATE
606         QDOT(I) = (Q(I)*3.4129 - QCOND - QRAD)/A(I)
607       109 CONTINUE
      C
      C        THIS BLOCK COMPUTES HEAT FLUX FROM DEVELOPMENT REGION PLATES
608         SF=1.0
609         EMIS=0.05
610         IF(J.EQ.16) CALL CHAN(1,EMIS)
611         TAR=(TINF+460.)/100.
      C
612         DO 200 I=PLATE1,24
613         TOR=(TO(I)+460.)/100.
614         QR(I) = SF*EMIS*.1714*(TOR*TOR*TOR*TOR-TAR*TAR*TAR*TAR)
615         IF(I.GT.1) GO TO 195
616         QDOT(1) = K(1)*HM(1)*(1.+(80.-TO(1))/700.) - QR(1)
           1 - (S(1)*(TO(1)-TO0) + S(2)*(TO(1)-TO(2)))/A(I)
617         GO TO 200
618       195 QDOT(I)=K(I)*HM(I)*(1.+(80.-TO(I))/700.) - QR(I)
           1 - (S(I)*(TO(I)-TO(I-1)) + S(I+1)*(TO(I)-TO(I+1)))/A(I)
619       200   CONTINUE
      C
      C        THIS BLOCK COMPUTES HEAT FLUX FROM RECOVERY REGION PLATES
620         DO 201 I=39,62
621         TOR=(TO(I)+460.)/100.
622         QR(I) = SF*EMIS*.1714*(TOR*TOR*TOR*TOR-TAR*TAR*TAR*TAR)
623       201 QDOT(I)=K(I)*HM(I)*(1.+(80.-TO(I))/700.) - QR(I)
           1 - (S(I)*(TO(I)-TO(I-1)) + S(I+1)*(TO(I)-TO(I+1)))/A(I)
      C
      C
624         RETURN
625         END


626         SUBROUTINE ENTHAL (FACT,D2INIT,DD2INT,D2LOC)
      C
      C     COMPUTE ENTHALPY THICKNESS BASED ON CONTROL
      C        VOLUME FOR ENERGY ADDITION
      C
627         INTEGER D2LOC
628         COMMON/ BLK2 /UINF,TINF,TADIAB,RHOINF,VISC,PR,CP,W
629         COMMON/ BLK3 /TO0,TO(63),HM(62),Q(38),TEND(38),
           1 TFRAME(38),QDOT(62),DQDOT(62),QW(38),
           2 DKK(62),DSS(63),NTAG(63),NTAG0,REENP(62),STP(62)
630         COMMON/ BLK4 /ST(62),DST(62),REEN(62),DREEN(62),D2(62),DD2(62),
           1 PCOEFF(62),X(62)
631         DIMENSION DX(62)
632         DATA DX/ 24*1.028,1.856,13*1.996,24*1.028/
      C     ASSUMES D2 AT BEGINNING OF PLATE # D2LOC
633         DDX = 0.005
634         D2(D2LOC) = D2INIT+ST(D2LOC)*DX(D2LOC)/2.
635         REEN(D2LOC)=FACT*D2(D2LOC)*(1.0-PCOEFF(D2LOC))**0.5
636         DD2(D2LOC) = DD2INT
637         DREEN(D2LOC)=FACT*DD2(D2LOC)*(1.0-PCOEFF(D2LOC))**0.5
638         I2 = D2LOC + 1
      C
639         DO 100 I=I2,62
640         IF (I .LE. 24 .OR. I .GE. 39) GO TO 20
641         D2(I) = D2(I-1) + ST(I-1)*(1.0+.0564*D2(I-1))*DX(I-1)/2.
           1 + ST(I)*(1.0+.0564*D2(I-1))*DX(I)/2.
           2 +(0.5*((1.0+.0564*D2(I-1))/.0564)*(ALOG(1.0+
           3.0564*D2(I-1)))/(1.0-PCOEFF(I)))*(PCOEFF(I)
           4 -PCOEFF(I-1))-2.*((1.0+.0564*D2(I-1))/.0564)*
           5(ALOG(1.0+.0564*D2(I-1)))*(TO(I)-TO(I-1))/(TO(I)+TO(I-1)-2.*TINF)
642         IF (I .EQ.25) D2(I)=D2(I)-((D2(I)/0.0564)-((1.0
           1+.0564*D2(I))/.003186*(ALOG(1.0+0.0564*D2(I)))))*.0564
```

```
643         GO TO 10
644      20 CONTINUE
645         D2(I) = D2(I-1) + ST(I-1)*DX(I-1)/2. + ST(I)*DX(I)/2.
           1 +(0.5*D2(I-1)/(1.0-PCOEFF(I)))*(PCOEFF(I)
           2 -PCOEFF(I-1))-2.*D2(I-1)*(TO(I)-TO(I-1))/(TO(I)+TO(I-1)-2.*TINF)
646         IF (I .EQ.39) D2(I)=D2(I)+((D2(I)/0.0564)-((1.0
           1+.0564*D2(I))/.003186*(ALOG(1.0+0.0564*D2(I)))))*.0564
647      10 CONTINUE
648         DD2(I) = SQRT( DD2(I-1)**2 + (ST(I-1)*DDX/2.)**2
           1 + (DX(I-1)*DST(I-1)/2.)**2 + (ST(I)*DDX/2.)**2 +
           2 (DX(I)*DST(I)/2.)**2 )
649         REEN(I) = FACT * D2(I)*(1.0-PCOEFF(I))**0.5
650         DREEN(I) = FACT * DD2(I) *(1.0-PCOEFF(I))**0.5
651     100 CONTINUE
652         RETURN
653         END
      C
      C
```

```
654         SUBROUTINE CHAN(N,XX)
      C
      C       SUBROUTINE CHAN FIRST STORES THE VALUE OF XX AS A
      C       MEMBER OF THE DUMMY ARRAY ARG AND THEN INCREASES
      C       XX BY ONE PERCENT.
      C
655         COMMON ARG(63),ARG0
656         IF(N.NE.0) GO TO 10
657         ARG0=XX
658         GO TO 20
659   10    ARG(N)=XX
660   20    XX=XX+XX*0.01
661         RETURN
662         END
      C
      C
```

```
663         SUBROUTINE CHANGE(N,M,XX,YY)
      C
      C       SUBROUTINE RESTORES THE VALUE OF YY, THE PREVIOUSLY
      C       PERTURBED INPUT, TO ITS ORIGINAL VALUE, THEN STORES
      C       XX IN THE ARRAY ARG, THEN INCREASES XX BY ONE PERCENT.
      C
664         COMMON ARG(63),ARG0
665         IF(M.EQ.1.OR.N.GE.63) GO TO 10
666         YY=ARG(N+1)
667         IF(M.LT.4) GO TO 10
668         IF(N.EQ.0) YY=ARG0
669         IF(N.NE.0) YY=ARG(N)
670   10    IF(N.NE.0) ARG(N)=XX
671         IF(N.EQ.0) ARG0=XX
672         XX=XX+XX*0.01
673         RETURN
674         END
      C
      C
```

```
675         SUBROUTINE MAXMIN(N,M,JCOUNT)
      C
      C       SUBROUTINE MAXMIN FINDS THE MAXIMUM AND MINIMUM VALUES
      C       IN THE COMMONED ARRAY OVER THE RANGE OF I FROM N TO M
      C       AND MARKS THE I-LOCATIONS OF THE MAXIMUM AND MINIMUM
      C
676         COMMON/ BLK5 /SENCO(62,39),VMAX,VMIN,NA,NB
677         VMAX=0.0
678         VMIN=10.0
679         DO 810 I=N,M
680         IF(SENCO(I,JCOUNT).LE.VMAX) GO TO 820
681         VMAX=SENCO(I,JCOUNT)
682         NA=I
683         GO TO 810
684   820   IF(SENCO(I,JCOUNT).LT.VMIN) GO TO 840
685         GO TO 810
686   840   VMIN=SENCO(I,JCOUNT)
687         NB=I
688   810   CONTINUE
689         IF(VMAX.EQ.0.0) NA=NB
690         RETURN
691         END
```

Appendix G
The Reduced Data

The following pages show lists and plots of the reduced data of the 15 cases shown in Table 3-1. Stanton number data and starting profile data are presented for each case. Additional velocity and temperature profile data are listed according to the following cases:

Case #	s-distance in cm of profile data, in addition to the s = -35 cm starting profiles.
100779	10.0 (θ = 13°)
	41.0 (θ = 52°)
	61.0 (θ = 78°)
	119.0
070280	0.0
	10.03 (θ = 13°)
	25.5 (θ = 32°)
	40.5 (θ = 51°)
	61.3 (θ = 77°)
	72.3
	88.2
	104.0
	119.1
022680 (Profiles are 030180)	10.0 (θ = 13°)
	25.0 (θ = 32°)
	41.0 (θ = 52°)
	61.5 (θ = 78°)
	89.0
	104.0
	119.0
060480	9.9 (θ = 12.6°), velocity only
	25.0 (θ = 32°), velocity only
051080	40.8 (θ = 52.5°), velocity only

100779 STARTING PROFILES; ENERGY BALANCE -DEL99/R(THETA=0)=0.10 S=-35 CM

REX	= 0.17857E 07	REM	= 3712.			REH	= 796.				
XVO	= -217.41 CM	DEL2	= 0.379 CM			DEH2	= 0.082 CM				
UPW	= 15.11 M/S	DEL99	= 3.334 CM			DELT99	= 1.461 CM				
VISC	= 0.15434E-04 M2/S	DEL1	= 0.531 CM			UPW	= 15.15 M/S				
PORT	= 4	H	= 1.399			VISC	= 0.15540E-04 M2/S				
XLOC	= -35.05 CM	CF/2	= 0.16090E-02			TINF	= 25.81 DEG C				
DENS	= 1.18 KG/M3					TPLATE	= 40.52 DEG C				

Y(CM)	Y/DEL	U(M/S)	U/UP	Y+	U+	CF/2	T(DEG C)	Y(CM)	Y+	U(M/S)	T(DEG C)	TBAR	1-TBAR
0.048	0.015	6.57	0.435	19.0	10.84	0.001324	31.74	0.0140	5.49	1.90	35.21	0.361	0.639
0.074	0.022	7.87	0.521	29.0	12.98	0.001562	30.72	0.0394	15.46	5.35	32.18	0.567	0.433
0.099	0.030	8.44	0.559	38.9	13.92	0.001607	30.11	0.0648	25.44	7.41	30.92	0.652	0.348
0.150	0.045	9.07	0.600	58.9	14.95	0.001611	29.27	0.1156	45.39	8.64	29.69	0.736	0.264
0.201	0.060	9.50	0.628	78.9	15.66	0.001611	28.75	0.1664	65.35	9.20	29.03	0.781	0.219
0.249	0.075	9.82	0.650	97.8	16.20	0.001613	28.40	0.2172	85.30	9.61	28.58	0.812	0.188
0.323	0.097	10.18	0.673	127.0	16.79	0.001604	27.94	0.2934	115.23	10.03	28.07	0.846	0.154
0.373	0.112	10.40	0.688	146.4	17.16	0.001608	27.72	0.3442	135.18	10.27	27.80	0.865	0.135
0.448	0.134	10.68	0.707	175.8	17.61	0.001610	27.43	0.4204	165.11	10.58	27.49	0.886	0.114
0.549	0.165	10.99	0.727	215.5	18.12	0.001612	27.12	0.5220	205.02	10.90	27.15	0.909	0.091
0.675	0.202	11.38	0.753	265.1	18.77	0.001634	26.83	0.6490	254.91	11.30	26.83	0.930	0.070
0.801	0.240	11.69	0.773	314.6	19.28	0.001647	26.60	0.7760	304.79	11.63	26.59	0.947	0.053
1.004	0.301	12.11	0.801	394.3	19.98	0.001668	26.34	0.9792	384.60	12.06	26.31	0.966	0.034
1.207	0.362	12.50	0.827	473.9	20.62	0.001696	26.18	1.1824	464.42	12.46	26.14	0.977	0.023
1.486	0.446	12.97	0.858	583.5	21.39	0.001731	26.04	1.4618	574.16	12.93	25.99	0.987	0.013
1.739	0.522	13.35	0.883	683.2	22.02	0.001764	25.98	1.7158	673.93	13.32	25.93	0.992	0.008
2.247	0.674	14.01	0.927	882.5	23.12	0.001826	25.92	2.2238	873.46	13.98	25.86	0.997	0.003
2.754	0.826	14.55	0.963	1081.9	24.00	0.001875	25.90	2.7318	1073.00	14.52	25.83	0.998	0.002
3.389	1.016	14.99	0.992	1331.1	24.73	0.001901	25.90						
4.151	1.245	15.15	1.002	1630.4	24.98	0.001863	25.90						

100779 PROFILE;ENERGY BALANCE-DEL99/R(THETA=0)=0.10 S=10.0CM THETA=13DEG

REX = 0.23369E 07 REM = 4604. REH = 1669.
XVO = -232.34 CM DEL2 = 0.478 CM DEH2 = 0.173 CM
UPW = 14.98 M/S DEL99= 4.190 CM DELT99 = 2.637 CM
VISC = 0.15549E-04 M2/S DEL1 = 0.678 CM UPW = 14.98 M/S
PORT = 4 H = 1.420 VISC = 0.15549E-04 M2/S
XLOC = 10.16 CM CF/2 = 0.14291E-02 TINF = 25.86 DEG C
DENS = 1.17 KG/M3 TPLATE = 41.21 DEG C

Y(CM)	Y/DEL	U(M/S)	U/UP	Y+	U+	CF/2	T(DEG C)	Y(CM)	Y+	U(M/S)	T(DEG C)	TBAR	1-TBAR
0.048	0.012	5.85	0.391	17.6	10.33	0.001115	33.31	0.0140	5.09	1.69	36.66	0.296	0.704
0.074	0.018	7.16	0.478	26.9	12.63	0.001357	32.26	0.0394	14.34	4.76	33.76	0.485	0.515
0.099	0.024	7.68	0.514	36.1	13.57	0.001397	31.64	0.0648	23.60	6.69	32.46	0.570	0.430
0.150	0.036	8.34	0.559	54.6	14.73	0.001424	30.80	0.1156	42.10	7.90	31.22	0.651	0.349
0.201	0.048	8.78	0.589	73.1	15.50	0.001434	30.25	0.1664	60.61	8.48	30.56	0.694	0.306
0.251	0.060	9.11	0.611	91.4	16.08	0.001439	29.84	0.2172	79.11	8.89	30.06	0.726	0.274
0.325	0.077	9.54	0.642	118.3	16.85	0.001460	29.36	0.2934	106.87	9.36	29.50	0.763	0.237
0.373	0.089	9.76	0.657	135.8	17.23	0.001466	29.11	0.3442	125.38	9.63	29.22	0.781	0.219
0.447	0.107	10.02	0.675	163.0	17.69	0.001468	28.78	0.4204	153.14	9.93	28.85	0.805	0.195
0.548	0.131	10.28	0.695	199.6	18.15	0.001462	28.42	0.5220	190.15	10.22	28.46	0.831	0.169
0.674	0.161	10.59	0.717	245.6	18.69	0.001466	28.06	0.6490	236.42	10.53	28.09	0.855	0.145
0.801	0.191	10.80	0.734	291.7	19.07	0.001460	27.77	0.7760	282.68	10.76	27.78	0.875	0.125
1.003	0.239	11.18	0.762	365.5	19.73	0.001473	27.41	0.9792	356.71	11.13	27.40	0.899	0.101
1.206	0.288	11.46	0.785	439.4	20.24	0.001480	27.11	1.1824	430.73	11.43	27.09	0.920	0.080
1.485	0.354	11.82	0.815	541.1	20.87	0.001495	26.77	1.4618	532.52	11.79	26.75	0.942	0.058
1.739	0.415	12.09	0.838	633.5	21.35	0.001506	26.54	1.7158	625.05	12.07	26.50	0.958	0.042
2.247	0.536	12.59	0.882	818.4	22.23	0.001536	26.24	2.2238	810.11	12.57	26.19	0.978	0.022
2.754	0.657	12.97	0.918	1003.4	22.90	0.001554	26.06	2.7318	995.17	12.95	26.01	0.990	0.010
3.389	0.809	13.33	0.957	1234.6	23.54	0.001568	25.97	3.3668	1226.50	13.32	25.91	0.997	0.003
4.151	0.991	13.57	0.989	1512.0	23.95	0.001555	25.94	4.1288	1504.09	13.56	25.88	0.999	0.001
4.913	1.172	13.51	1.000	1789.6	23.86	0.001495	25.94						

100779 PROFILE;ENERGY BALANCE-DEL99/R(THETA=0)=0.10 S=41CM THETA=52DEG

REX	= 0.28112E 07	REM	= 5337.	REH	= 2267.				
XVO	= -251.93 CM	DEL2	= 0.556 CM	DEH2	= 0.236 CM				
UPW	= 14.93 M/S	DEL99	= 4.514 CM	DELT99	= 3.254 CM				
VISC	= 0.15549E-04 M2/S	DEL1	= 0.844 CM	UPW	= 14.93 M/S				
PORT	= 4	H	= 1.518	VISC	= 0.15545E-04 M2/S				
XLOC	= 40.89 CM	CF/2	= 0.10540E-02	TINF	= 25.81 DEG C				
DENS	= 1.18 KG/M3			TPLATE	= 41.23 DEG C				

Y(CM)	Y/DEL	U(M/S)	U/UP	Y+	U+	CF/2	T(DEG C)	Y(CM)	Y+	U(M/S)	T(DEG C)	TBAR	1-TBAR
0.048	0.011	4.57	0.307	15.1	9.43	0.000748	34.59	0.0140	4.35	1.32	37.26	0.257	0.743
0.074	0.016	5.72	0.384	23.0	11.81	0.000939	33.61	0.0394	12.27	3.72	35.01	0.403	0.597
0.099	0.022	6.27	0.421	30.9	12.95	0.000998	33.04	0.0648	20.19	5.31	33.80	0.482	0.518
0.150	0.033	6.95	0.467	46.7	14.34	0.001049	32.22	0.1156	36.02	6.49	32.65	0.556	0.444
0.201	0.044	7.30	0.491	62.6	15.07	0.001051	31.69	0.1664	51.85	7.06	31.99	0.599	0.401
0.252	0.056	7.61	0.513	78.4	15.70	0.001062	31.27	0.2172	67.69	7.40	31.51	0.630	0.370
0.327	0.072	8.05	0.543	101.9	16.61	0.001092	30.75	0.2934	91.44	7.86	30.93	0.668	0.332
0.377	0.083	8.28	0.559	117.4	17.09	0.001106	30.46	0.3442	107.27	8.13	30.63	0.688	0.312
0.452	0.100	8.66	0.586	140.7	17.88	0.001143	30.05	0.4204	131.02	8.51	30.18	0.717	0.283
0.552	0.122	9.09	0.616	171.9	18.75	0.001183	29.57	0.5220	162.69	8.96	29.67	0.749	0.251
0.677	0.150	9.57	0.650	210.9	19.74	0.001234	29.04	0.6490	202.27	9.46	29.11	0.786	0.214
0.802	0.178	9.92	0.676	250.1	20.46	0.001263	28.63	0.7760	241.85	9.84	28.67	0.815	0.185
1.005	0.223	10.42	0.714	313.1	21.50	0.001311	28.05	0.9792	305.18	10.36	28.07	0.853	0.147
1.207	0.267	10.83	0.745	376.2	22.34	0.001347	27.60	1.1824	368.52	10.78	27.60	0.884	0.116
1.486	0.329	11.28	0.781	463.1	23.28	0.001386	27.17	1.4618	455.60	11.24	27.16	0.913	0.087
1.739	0.385	11.59	0.806	542.1	23.91	0.001405	26.89	1.7158	534.77	11.56	26.86	0.932	0.068
2.247	0.498	12.13	0.853	700.3	25.02	0.001445	26.46	2.2238	693.10	12.10	26.42	0.960	0.040
2.754	0.610	12.55	0.892	858.5	25.89	0.001475	26.21	2.7318	851.43	12.53	26.16	0.977	0.023
3.389	0.751	13.01	0.937	1056.3	26.84	0.001510	26.02	3.3668	1049.34	12.99	25.96	0.990	0.010
4.151	0.920	13.37	0.978	1293.7	27.59	0.001527	25.92	4.1288	1286.84	13.36	25.86	0.997	0.003
4.912	1.088	13.41	0.997	1531.0	27.68	0.001487	25.89	4.8908	1524.34	13.41	25.83	0.999	0.001
5.674	1.257	13.26	1.000	1768.5	27.36	0.001417	25.89						

100779 PROFILE;ENERGY BALANCE-DEL99/R(THETA=0)=0.10 S=61CM THETA=78DEG

REX	= 0.28542E 07	REM	= 5402.	REH	= 2601.				
XVO	= -231.97 CM	DEL2	= 0.555 CM	DEH2	= 0.267 CM				
UPW	= 15.12 M/S	DEL99	= 4.504 CM	DELT99	= 3.544 CM				
VISC	= 0.15536E-04 M2/S	DEL1	= 0.845 CM	UPW	= 15.12 M/S				
PORT	= 4	H	= 1.522	VISC	= 0.15534E-04 M2/S				
XLOC	= 61.39 CM	CF/2	= 0.10601E-02	TINF	= 25.84 DEG C				
DENS	= 1.18 KG/M3			TPLATE	= 40.78 DEG C				

Y(CM)	Y/DEL	U(M/S)	U/UP	Y+	U+	CF/2	T(DEG C)	Y(CM)	Y+	U(M/S)	T(DEG C)	TBAR	1-TBAR
0.048	0.011	4.94	0.327	15.3	10.03	0.000827	34.97	0.0140	4.43	1.43	37.56	0.215	0.785
0.074	0.016	5.94	0.394	23.4	12.08	0.000976	33.97	0.0394	12.47	4.02	35.38	0.362	0.638
0.099	0.022	6.51	0.432	31.4	13.23	0.001036	33.34	0.0648	20.52	5.59	34.22	0.439	0.561
0.150	0.033	7.07	0.469	47.5	14.36	0.001053	32.52	0.0902	28.56	6.31	33.48	0.489	0.511
0.201	0.045	7.44	0.495	63.6	15.13	0.001060	32.01	0.1410	44.66	6.97	32.60	0.548	0.452
0.252	0.056	7.75	0.515	79.7	15.74	0.001067	31.60	0.1918	60.75	7.38	32.07	0.583	0.417
0.326	0.072	8.15	0.543	103.1	16.57	0.001090	31.10	0.2426	76.84	7.69	31.64	0.612	0.388
0.375	0.083	8.35	0.557	118.7	16.98	0.001097	30.82	0.3188	100.98	8.12	31.12	0.646	0.354
0.451	0.100	8.66	0.579	142.8	17.59	0.001114	30.43	0.3696	117.07	8.33	30.82	0.667	0.333
0.551	0.122	9.08	0.608	174.6	18.45	0.001153	29.97	0.4458	141.21	8.64	30.43	0.693	0.307
0.677	0.150	9.51	0.639	214.5	19.33	0.001191	29.45	0.5474	173.39	9.06	29.96	0.724	0.276
0.803	0.178	9.93	0.668	254.4	20.17	0.001234	28.97	0.6744	213.62	9.50	29.43	0.760	0.240
1.005	0.223	10.49	0.709	318.4	21.31	0.001293	28.33	0.8014	253.86	9.92	28.94	0.792	0.208
1.207	0.268	10.95	0.744	382.5	22.24	0.001339	27.82	1.0046	318.22	10.49	28.30	0.836	0.164
1.486	0.330	11.45	0.782	470.7	23.26	0.001387	27.28	1.2078	382.59	10.95	27.78	0.871	0.129
1.739	0.386	11.78	0.809	550.9	23.94	0.001412	26.96	1.4872	471.10	11.45	27.24	0.907	0.093
2.247	0.499	12.31	0.855	711.7	25.00	0.001447	26.54	1.7412	551.56	11.78	26.91	0.929	0.071
2.754	0.612	12.72	0.893	872.5	25.84	0.001473	26.26	2.2492	712.49	12.31	26.49	0.957	0.043
3.389	0.752	13.16	0.936	1073.6	26.75	0.001505	26.10	2.7572	873.41	12.72	26.21	0.976	0.024
4.151	0.922	13.54	0.978	1314.9	27.50	0.001521	25.99	3.3922	1074.56	13.16	26.04	0.987	0.013
4.912	1.091	13.60	0.998	1556.1	27.64	0.001486	25.94	4.1542	1315.95	13.54	25.92	0.995	0.005
5.674	1.260	13.43	1.000	1797.5	27.28	0.001413	25.92	4.9162	1557.33	13.60	25.88	0.998	0.002
								5.6782	1798.71	13.42	25.86	0.999	0.001

100779 PROFILE FOR ENERGY BALANCE -DEL99/R(THETA=0)=0.10 S=119 CM

REX = 0.33816E 07	REM = 6187.			REH = 3655.					
XVO = -227.16 CM	DEL2 = 0.633 CM			DEH2 = 0.374 CM					
UPW = 15.20 M/S	DEL99= 4.922 CM			DELT99 = 4.209 CM					
VISC = 0.15548E-04 M2/S	DEL1 = 0.975 CM			UPW = 15.19 M/S					
PORT = 4	H = 1.540			VISC = 0.15549E-04 M2/S					
XLOC = 118.87 CM	CF/2 = 0.10737E-02			TINF = 25.90 DEG C					
DENS = 1.17 KG/M3				TPLATE = 41.06 DEG C					

Y(CM)	Y/DEL	U(M/S)	U/UP	Y+	U+	CF/2	T(DEG C)
0.048	0.010	4.90	0.322	15.5	9.84	0.000808	34.66
0.074	0.015	6.08	0.400	23.6	12.21	0.001004	33.80
0.099	0.020	6.59	0.434	31.8	13.24	0.001047	33.32
0.150	0.030	7.18	0.473	48.0	14.42	0.001071	32.67
0.201	0.041	7.56	0.497	64.3	15.18	0.001077	32.22
0.249	0.051	7.81	0.514	79.9	15.68	0.001073	31.91
0.324	0.066	8.13	0.535	103.9	16.32	0.001074	31.54
0.374	0.076	8.33	0.549	119.8	16.74	0.001081	31.34
0.449	0.091	8.61	0.567	143.7	17.29	0.001093	31.06
0.549	0.112	8.90	0.586	175.9	17.88	0.001103	30.73
0.676	0.137	9.23	0.607	216.5	18.53	0.001118	30.37
0.803	0.163	9.59	0.631	257.0	19.26	0.001149	30.02
1.005	0.204	10.10	0.665	321.9	20.29	0.001197	29.50
1.208	0.245	10.59	0.697	386.8	21.27	0.001250	29.05
1.487	0.302	11.23	0.739	476.2	22.55	0.001326	28.45
1.740	0.354	11.76	0.774	557.3	23.62	0.001392	27.97
2.248	0.457	12.68	0.835	719.8	25.47	0.001512	27.18
2.755	0.560	13.41	0.882	882.2	26.92	0.001603	26.65
3.390	0.689	14.05	0.924	1085.4	28.21	0.001675	26.34
4.151	0.843	14.64	0.963	1329.3	29.39	0.001734	26.16
4.659	0.947	14.93	0.983	1491.9	30.00	0.001760	26.10
5.167	1.050	15.12	0.995	1654.5	30.36	0.001765	26.06
5.928	1.204	15.19	0.999	1898.4	30.50	0.001735	26.03
6.386	1.297	15.20	1.000	2044.8	30.53	0.001714	26.01

Y(CM)	Y+	U(M/S)	T(DEG C)	TBAR	1-TBAR
0.0140	4.47	1.41	36.98	0.269	0.731
0.0394	12.61	3.99	35.03	0.398	0.602
0.0648	20.74	5.66	33.96	0.468	0.532
0.1156	37.01	6.78	33.00	0.532	0.468
0.1664	53.28	7.30	32.49	0.566	0.434
0.2172	69.54	7.64	32.07	0.593	0.407
0.2934	93.94	8.00	31.65	0.621	0.379
0.3442	110.21	8.21	31.43	0.635	0.365
0.4204	134.61	8.51	31.14	0.655	0.345
0.5220	167.15	8.82	30.78	0.678	0.322
0.6490	207.81	9.16	30.41	0.702	0.298
0.7760	248.48	9.51	30.06	0.726	0.274
0.9792	313.55	10.04	29.52	0.761	0.239
1.1824	378.62	10.53	29.07	0.791	0.209
1.4618	468.09	11.17	28.45	0.832	0.168
1.7158	549.43	11.71	27.96	0.864	0.136
2.2238	712.10	12.64	27.15	0.918	0.082
2.7318	874.77	13.37	26.61	0.954	0.046
3.2398	1037.45	13.90	26.33	0.972	0.028
3.7478	1200.12	14.32	26.16	0.983	0.017
4.2558	1362.79	14.70	26.08	0.989	0.011
4.7638	1525.46	14.97	26.01	0.993	0.007
5.2718	1688.14	15.13	25.97	0.995	0.005
5.7798	1850.81	15.17	25.96	0.996	0.004
6.2878	2013.48	15.20	25.94	0.998	0.002
6.7958	2176.16	15.20	25.92	0.999	0.001

RUN 100779 *** CURVATURE RIG *** NASA-NAG-3-3 STANTON NUMBER DATA

TADB= 25.92 DEG C UREF= 15.15 M/S TINF= 25.82 DEG C
RHO= 1.176 KG/M3 VISC= 0.15542E-04 M2/S XVO= -217.4 CM
CP= 1014. J/KGK PR= 0.716

STANTON RUN FOR ENERGY BALANCE - DEL99/R (THETA =0) =0.10

PLATE	X (CM)	UPW (M/S)	K	REXVO	TO DEG C	STANTON NO	REENTH	DST	DST(%)	DREEN
1	-61.3	15.10	0.000E 00	0.15167E 07	38.21	0.31118E-02		0.195E-03	6.260	
2	-58.7	15.10	0.000E 00	0.15421E 07	39.49	0.33498E-02		0.113E-03	3.371	
3	-56.1	15.10	0.000E 00	0.15675E 07	39.78	0.32371E-02		0.106E-03	3.266	
4	-53.5	15.11	0.200E-07	0.15935E 07	39.99	0.30737E-02		0.103E-03	3.356	
5	-50.9	15.11	0.000E 00	0.16189E 07	39.29	0.26873E-02		0.847E-04	3.152	
6	-48.3	15.11	0.000E 00	0.16443E 07	40.19	0.28643E-02		0.963E-04	3.362	
7	-45.7	15.12	0.197E-07	0.16706E 07	40.36	0.27465E-02		0.906E-04	3.300	
8	-43.0	15.12	0.000E 00	0.16960E 07	40.35	0.26607E-02		0.871E-04	3.274	
9	-40.4	15.12	0.000E 00	0.17212E 07	40.45	0.26873E-02		0.883E-04	3.286	
10	-37.8	15.12	0.000E 00	0.17467E 07	40.47	0.26052E-02		0.855E-04	3.282	
11	-35.2	15.12	0.197E-07	0.17730E 07	40.56	0.25941E-02	0.82879E 03	0.857E-04	3.302	5.
12	-32.6	15.12	0.000E 00	0.17985E 07	40.52	0.24934E-02	0.89593E 03	0.823E-04	3.299	5.
13	-30.0	15.12	0.000E 00	0.18239E 07	40.44	0.24843E-02	0.96362E 03	0.815E-04	3.280	5.
14	-27.4	15.13	0.199E-07	0.18501E 07	40.52	0.25203E-02	0.10221E 04	0.831E-04	3.297	6.
15	-24.8	15.11	-0.593E-07	0.18727E 07	40.56	0.24926E-02	0.10819E 04	0.821E-04	3.294	6.
16	-22.2	15.09	-0.595E-07	0.18953E 07	40.59	0.24906E-02	0.11444E 04	0.833E-04	3.346	6.
17	-19.5	15.06	-0.598E-07	0.19178E 07	40.12	0.23591E-02	0.12423E 04	0.763E-04	3.233	6.
18	-16.9	15.04	-0.607E-07	0.19399E 07	40.41	0.24878E-02	0.12790E 04	0.825E-04	3.316	6.
19	-14.3	15.02	-0.604E-07	0.19622E 07	40.57	0.25139E-02	0.13281E 04	0.835E-04	3.323	6.
20	-11.7	14.99	-0.810E-07	0.19835E 07	40.41	0.24570E-02	0.14051E 04	0.808E-04	3.287	7.
21	-9.1	14.96	-0.815E-07	0.20046E 07	40.36	0.23788E-02	0.14705E 04	0.778E-04	3.271	7.
22	-6.5	15.03	0.201E-06	0.20402E 07	40.58	0.23743E-02	0.15081E 04	0.788E-04	3.318	7.
23	-3.9	15.11	0.200E-06	0.20757E 07	40.68	0.24233E-02	0.15594E 04	0.800E-04	3.302	7.
24	-1.3	15.18	0.195E-06	0.21116E 07	40.72	0.22922E-02	0.16145E 04	0.767E-04	3.348	7.
CURVE BEGINS										
25	2.4	15.25	0.124E-06	0.21570E 07	40.67	0.19840E-02	0.16965E 04	0.990E-04	4.980	8.
26	7.3	15.28	0.408E-07	0.22094E 07	40.73	0.19496E-02	0.17844E 04	0.913E-04	4.672	8.
27	12.4	15.19	-0.120E-06	0.22460E 07	40.86	0.19474E-02	0.18659E 04	0.914E-04	4.685	9.
28	17.4	15.10	-0.123E-06	0.22817E 07	40.88	0.18443E-02	0.19578E 04	0.867E-04	4.693	9.
29	22.5	15.11	0.102E-07	0.23322E 07	40.90	0.17725E-02	0.20447E 04	0.836E-04	4.710	10.
30	27.6	15.15	0.508E-07	0.23873E 07	41.01	0.16667E-02	0.21144E 04	0.804E-04	4.812	10.
31	32.6	15.17	0.302E-07	0.24405E 07	41.03	0.16375E-02	0.21943E 04	0.795E-04	4.845	11.
32	37.7	15.14	-0.407E-07	0.24848E 07	40.88	0.16206E-02	0.22960E 04	0.779E-04	4.796	11.
33	42.8	15.15	0.101E-07	0.25356E 07	40.94	0.15824E-02	0.23676E 04	0.775E-04	4.886	11.
34	47.8	15.13	-0.203E-07	0.25825E 07	40.83	0.15251E-02	0.24609E 04	0.744E-04	4.870	12.
35	52.9	15.11	-0.307E-07	0.26277E 07	40.98	0.15081E-02	0.25124E 04	0.742E-04	4.912	12.
36	58.0	15.16	0.705E-07	0.26865E 07	41.20	0.14604E-02	0.25491E 04	0.738E-04	5.042	12.
37	63.0	15.30	0.177E-06	0.27603E 07	40.97	0.13818E-02	0.26590E 04	0.689E-04	4.974	13.
38	68.1	15.30	0.979E-08	0.28117E 07	41.00	0.12597E-02	0.27201E 04	0.645E-04	5.113	13.
RECOVERY BEGINS										
39	72.0	15.15	-0.281E-06	0.28200E 07	40.93	0.14782E-02	0.27790E 04	0.513E-04	3.472	13.
40	74.6	15.00	-0.383E-06	0.28183E 07	40.82	0.15313E-02	0.28380E 04	0.524E-04	3.420	13.
41	77.2	15.02	0.603E-07	0.28479E 07	41.14	0.15716E-02	0.28169E 04	0.555E-04	3.534	13.
42	79.8	15.05	0.799E-07	0.28790E 07	41.22	0.15109E-02	0.28407E 04	0.532E-04	3.523	13.
43	82.4	15.08	0.602E-07	0.29085E 07	41.21	0.15469E-02	0.28818E 04	0.539E-04	3.482	13.
44	85.0	15.10	0.594E-07	0.29384E 07	41.24	0.15300E-02	0.29145E 04	0.543E-04	3.547	13.
45	87.6	15.11	0.198E-07	0.29653E 07	41.26	0.15004E-02	0.29489E 04	0.529E-04	3.529	13.
46	90.2	15.12	0.394E-07	0.29937E 07	41.11	0.15646E-02	0.30164E 04	0.539E-04	3.443	13.
47	92.8	15.14	0.397E-07	0.30219E 07	41.04	0.15298E-02	0.30704E 04	0.534E-04	3.492	13.
48	95.4	15.15	0.196E-07	0.30489E 07	40.98	0.16084E-02	0.31218E 04	0.558E-04	3.470	13.
49	98.1	15.15	0.000E 00	0.30744E 07	41.02	0.15502E-02	0.31550E 04	0.544E-04	3.506	13.
50	100.7	15.15	0.000E 00	0.30999E 07	41.12	0.16048E-02	0.31742E 04	0.569E-04	3.548	13.
51	103.3	15.15	0.000E 00	0.31254E 07	40.99	0.16204E-02	0.32410E 04	0.557E-04	3.438	13.
52	105.9	15.15	0.000E 00	0.31507E 07	41.11	0.16166E-02	0.32568E 04	0.569E-04	3.522	13.
53	108.5	15.15	0.000E 00	0.31762E 07	41.05	0.16344E-02	0.33110E 04	0.565E-04	3.460	13.
54	111.1	15.15	0.000E 00	0.32017E 07	41.09	0.16099E-02	0.33436E 04	0.572E-04	3.556	13.
55	113.7	15.15	0.000E 00	0.32272E 07	40.80	0.16242E-02	0.34495E 04	0.551E-04	3.392	13.
56	116.4	15.15	0.000E 00	0.32527E 07	41.05	0.16664E-02	0.34334E 04	0.589E-04	3.535	13.
57	118.9	15.15	0.000E 00	0.32779E 07	41.06	0.16154E-02	0.34738E 04	0.572E-04	3.541	13.
58	121.6	15.15	0.000E 00	0.33034E 07	40.83	0.16176E-02	0.35678E 04	0.562E-04	3.474	14.
59	124.2	15.15	0.000E 00	0.33289E 07	40.77	0.16323E-02	0.36242E 04	0.577E-04	3.536	14.
60	126.8	15.15	0.000E 00	0.33544E 07	40.43	0.16051E-02	0.37475E 04	0.544E-04	3.391	14.
61	129.4	15.15	0.000E 00	0.33799E 07	40.73	0.16266E-02	0.37117E 04	0.600E-04	3.689	14.
62	132.0	15.15	0.000E 00	0.34051E 07	40.37	0.14045E-02	0.38423E 04	0.742E-04	5.284	14.

UNCERTAINTY IN REX=27203.

070280 DEL99/R(THETA=0)=0.10 PROFILES AT STATION 5 S=-35.05CM

REX	= 0.17262E 07	REM	= 3613.	REH	= 941.
XVO	= -213.75 CM	DEL2	= 0.374 CM	DEH2	= 0.098 CM
UPW	= 14.76 M/S	DEL99	= 3.173 CM	DELT99	= 1.740 CM
VISC	= 0.15283E-04 M2/S	DEL1	= 0.527 CM	UPW	= 14.81 M/S
PORT	= 4	H	= 1.410	VISC	= 0.15401E-04 M2/S
XLOC	= -35.05 CM	CF/2	= 0.16097E-02	TINF	= 24.09 DEG C
DENS	= 1.18 KG/M3			TPLATE	= 40.50 DEG C
				STANTON	= 0.25600E-02

Y(CM)	Y/DEL	U(M/S)	U/UP	Y+	U+	CF/2	T(DEG C)
0.048	0.015	6.55	0.443	18.7	11.05	0.001376	31.18
0.053	0.017	6.80	0.461	20.7	11.48	0.001417	30.83
0.074	0.023	7.73	0.524	28.6	13.05	0.001583	29.78
0.099	0.031	8.30	0.562	38.4	14.02	0.001633	28.99
0.150	0.047	8.91	0.603	58.1	15.04	0.001633	28.01
0.201	0.063	9.29	0.629	77.8	15.69	0.001622	27.40
0.248	0.078	9.58	0.649	96.2	16.17	0.001615	27.00
0.323	0.102	9.92	0.672	125.3	16.74	0.001603	26.49
0.373	0.118	10.14	0.687	144.5	17.13	0.001609	26.25
0.448	0.141	10.41	0.705	173.5	17.57	0.001608	25.94
0.548	0.173	10.72	0.726	212.5	18.09	0.001613	25.60
0.675	0.213	11.04	0.748	261.5	18.64	0.001619	25.28
0.801	0.253	11.36	0.769	310.5	19.17	0.001636	25.04
1.004	0.316	11.77	0.797	389.0	19.87	0.001657	24.76
1.207	0.380	12.13	0.822	467.6	20.48	0.001680	24.58
1.486	0.468	12.62	0.855	575.8	21.31	0.001724	24.44
1.739	0.548	13.03	0.882	674.1	21.99	0.001766	24.35
2.247	0.708	13.75	0.931	870.9	23.21	0.001845	24.27
2.754	0.868	14.31	0.969	1067.5	24.16	0.001905	24.23
3.389	1.068	14.72	0.997	1313.4	24.84	0.001923	24.21
4.151	1.308	14.77	1.001	1608.7	24.94	0.001862	24.20

Y(CM)	Y+	U(M/S)	T(DEG C)	TBAR	T+	PRT
0.0165	6.40	2.24	35.62	0.297	4.658	2.711
0.0190	7.38	2.58	35.19	0.323	5.067	3.090
0.0216	8.37	2.92	34.65	0.356	5.583	3.475
0.0241	9.35	3.27	34.14	0.387	6.069	4.018
0.0267	10.34	3.61	33.73	0.413	6.465	4.999
0.0292	11.32	3.95	33.31	0.438	6.861	6.902
0.0317	12.31	4.30	32.95	0.460	7.212	13.049
0.0368	14.27	4.99	32.27	0.501	7.854	-8.346
0.0419	16.24	5.67	31.73	0.534	8.376	-2.116
0.0470	18.21	6.36	31.26	0.563	8.822	-0.796
0.0622	24.12	7.20	30.21	0.627	9.821	0.255
0.0825	31.99	7.93	29.41	0.676	10.592	0.530
0.1181	45.77	8.53	28 47	0.733	11.487	0.673
0.1689	65.46	9.05	27.69	0.780	12.230	0.713
0.2197	85.15	9.41	27.19	0.811	12.711	0.718
0.2959	114.68	9.79	26.62	0.846	13.255	0.722
0.3467	134.37	10.02	26.33	0.864	13.535	0.722
0.4229	163.90	10.32	26.00	0.884	13.847	0.716
0.5245	203.28	10.64	25.62	0.906	14.206	0.714
0.6515	252.50	10.98	25.28	0.927	14.534	0.707
0.7785	301.72	11.30	25.03	0.942	14.769	0.697
0.9817	380.47	11.72	24.74	0.960	15.052	0.684
1.1849	459.23	12.09	24.54	0.972	15.241	0.669
1.4389	557.67	12.54	24.40	0.981	15.369	0.649
1.6929	656.11	12.95	24.30	0.987	15.466	0.632
2.2009	852.99	13.68	24.22	0.992	15.550	0.600
2.7089	1049.87	14.26	24.16	0.996	15.602	0.577
3.3439	1295.97	14.69	24.14	0.997	15.621	0.552
4.1059	1591.29	14.77	24.12	0.998	15.638	0.530
4.8679	1886.61	14.76	24.11	0.999	15.653	0.513
5.0889	1972.26	14.76	24.11	0.999	15.653	0.508

070280 DEL99/R(THETA=0)=0.10 PROFILES AT STATION 6 S=0.0

REX = 0.22368E 07 REM = 4445.
XVO = -235.20 CM DEL2 = 0.467 CM
UPW = 14.54 M/S DEL99= 4.256 CM
VISC = 0.15284E-04 M2/S DEL1 = 0.666 CM
PORT = 4 H = 1.426
XLOC = 0.00 CM CF/2 = 0.15497E-02
DENS = 1.18 KG/M3

REH = 1756.
DEH2 = 0.185 CM
DELT99 = 2.824 CM
UPW = 14.58 M/S
VISC = 0.15381E-04 M2/S
TINF = 23.86 DEG C
TPLATE = 40.61 DEG C
STANTON= 0.23000E-02

Y(CM)	Y/DEL	U(M/S)	U/UP	Y+	U+	CF/2	T(DEG C)
0.089	0.021	7.31	0.503	33.3	12.77	0.001402	30.22
0.135	0.032	8.18	0.563	50.4	14.29	0.001501	29.25
0.180	0.042	8.65	0.595	67.6	15.12	0.001522	28.66
0.261	0.061	9.23	0.635	97.6	16.14	0.001544	28.03
0.321	0.075	9.52	0.655	120.2	16.64	0.001543	27.63
0.396	0.093	9.84	0.677	148.2	17.20	0.001552	27.25
0.483	0.114	10.15	0.699	180.9	17.75	0.001560	26.89
0.599	0.141	10.48	0.721	224.3	18.31	0.001565	26.50
0.738	0.173	10.84	0.746	276.2	18.95	0.001585	26.10
0.917	0.216	11.18	0.769	343.4	19.54	0.001593	25.70
1.133	0.266	11.54	0.794	424.1	20.17	0.001609	25.31
1.399	0.329	11.95	0.822	523.8	20.88	0.001634	24.94
1.726	0.406	12.36	0.850	646.3	21.59	0.001659	24.61
2.135	0.502	12.82	0.882	799.3	22.40	0.001696	24.35
2.635	0.619	13.31	0.916	986.6	23.26	0.001739	24.17
3.255	0.765	13.80	0.949	1218.5	24.12	0.001781	24.05
4.022	0.945	14.25	0.980	1505.6	24.90	0.001811	24.00
4.489	1.055	14.54	1.000	1680.4	25.41	0.001839	23.99
4.961	1.166	14.54	1.000	1857.3	25.41	0.001805	23.98

Y(CM)	Y+	U(M/S)	T(DEG C)	TBAR	T+	PRT
0.0140	5.23	1.15	37.04	0.213	3.644	2.570
0.0165	6.18	1.36	36.51	0.245	4.193	2.839
0.0190	7.13	1.56	36.00	0.275	4.710	3.154
0.0216	8.08	1.77	35.53	0.304	5.196	3.553
0.0241	9.03	1.98	34.99	0.336	5.747	3.999
0.0267	9.98	2.19	34.53	0.363	6.217	4.742
0.0292	10.94	2.40	34.18	0.384	6.575	6.255
0.0317	11.89	2.61	33.81	0.406	6.949	9.768
0.0343	12.84	2.82	33.35	0.434	7.421	29.813
0.0394	14.74	3.23	32.69	0.473	8.090	-5.039
0.0444	16.64	3.65	32.23	0.500	8.564	-1.560
0.0597	22.35	4.90	31.25	0.559	9.565	0.093
0.0800	29.95	6.57	30.44	0.607	10.391	0.473
0.1156	43.27	7.81	29.50	0.663	11.350	0.657
0.1664	62.29	8.50	28.76	0.708	12.110	0.704
0.2172	81.30	8.92	28.31	0.735	12.574	0.706
0.2934	109.83	9.39	27.77	0.767	13.122	0.711
0.3442	128.85	9.62	27.46	0.785	13.437	0.718
0.4204	157.38	9.93	27.10	0.806	13.803	0.721
0.5220	195.42	10.26	26.70	0.831	14.219	0.726
0.6490	242.96	10.61	26.30	0.854	14.619	0.728
0.7760	290.51	10.92	25.96	0.875	14.969	0.733
0.9792	366.58	11.29	25.52	0.901	15.420	0.737
1.1824	442.66	11.62	25.18	0.921	15.772	0.738
1.4364	537.75	11.99	24.85	0.941	16.107	0.737
1.6904	632.84	12.31	24.59	0.957	16.376	0.734
2.1984	823.03	12.88	24.25	0.977	16.714	0.721
2.7064	1013.21	13.37	24.09	0.987	16.885	0.703
3.3414	1250.95	13.85	23.97	0.994	17.006	0.681
4.1034	1536.22	14.30	23.93	0.996	17.044	0.655
4.8654	1821.50	14.54	23.91	0.997	17.063	0.634
6.1354	2296.97	14.54	23.90	0.998	17.079	0.607
7.4054	2772.43	14.54	23.88	0.999	17.096	0.587
8.6754	3247.89	14.54	23.88	0.999	17.096	0.570

070280 DEL99/R(THETA=0)=0.10 PROFILES AT STATION 7 S=10.03CM THETA=13DEG

REX = 0.23539E 07 REM = 4630.
XVO = -236.27 CM DEL2 = 0.485 CM
UPW = 14.61 M/S DEL99= 4.074 CM
VISC = 0.15284E-04 M2/S DEL1 = 0.699 CM
PORT = 4 H = 1.443
XLOC = 10.03 CM CF/2 = 0.14282E-02
DENS = 1.18 KG/M3

REH = 1827.
DEH2 = 0.192 CM
DELT99 = 2.857 CM
UPW = 14.65 M/S
VISC = 0.15399E-04 M2/S
TINF = 24.07 DEG C
TPLATE = 40.61 DEG C
STANTON= 0.20000E-02

Y(CM)	Y/DEL	U(M/S)	U/UP	Y+	U+	CF/2	T(DEG C)
0.048	0.012	5.57	0.382	17.5	10.09	0.001075	33.12
0.053	0.013	5.90	0.405	19.3	10.69	0.001143	32.80
0.074	0.018	6.85	0.470	26.6	12.42	0.001321	31.77
0.099	0.024	7.34	0.504	35.8	13.30	0.001353	30.94
0.150	0.037	7.97	0.547	54.2	14.43	0.001378	29.85
0.201	0.049	8.40	0.577	72.5	15.21	0.001390	29.15
0.251	0.062	8.76	0.603	90.5	15.87	0.001409	28.66
0.324	0.080	9.12	0.629	117.2	16.51	0.001412	28.09
0.373	0.092	9.36	0.646	134.9	16.96	0.001428	27.81
0.448	0.110	9.61	0.664	161.7	17.41	0.001429	27.44
0.548	0.135	9.88	0.685	197.9	17.90	0.001429	27.04
0.674	0.165	10.16	0.706	243.4	18.40	0.001427	26.65
0.801	0.197	10.36	0.722	289.1	18.77	0.001421	26.31
1.003	0.246	10.71	0.749	362.4	19.40	0.001431	25.89
1.206	0.296	11.01	0.774	435.7	19.94	0.001443	25.55
1.485	0.365	11.36	0.803	536.5	20.58	0.001460	25.17
1.739	0.427	11.68	0.830	628.1	21.16	0.001483	24.91
2.247	0.551	12.18	0.875	811.5	22.06	0.001517	24.55
2.754	0.676	12.64	0.918	994.8	22.89	0.001555	24.35
3.389	0.832	13.04	0.960	1224.0	23.63	0.001580	24.21
4.150	1.019	13.27	0.992	1499.0	24.04	0.001568	24.15
4.912	1.206	13.18	1.001	1774.1	23.87	0.001499	24.15
5.674	1.393	12.98	1.001	2049.3	23.51	0.001419	24.15

Y(CM)	Y+	U(M/S)	T(DEG C)	TBAR	T+	PRT
0.0140	5.05	1.61	37.85	0.167	3.157	2.681
0.0165	5.96	1.90	37.17	0.208	3.931	2.845
0.0190	6.88	2.19	36.62	0.241	4.563	3.073
0.0216	7.80	2.49	36.13	0.271	5.123	3.367
0.0241	8.71	2.78	35.68	0.298	5.630	3.768
0.0267	9.63	3.07	35.30	0.321	6.065	4.399
0.0292	10.55	3.36	34.92	0.344	6.501	5.388
0.0343	12.38	3.95	34.30	0.382	7.210	14.373
0.0394	14.22	4.54	33.79	0.412	7.793	-9.113
0.0444	16.05	5.12	33.36	0.439	8.287	-2.429
0.0597	21.56	6.19	32.40	0.497	9.385	-0.051
0.0800	28.90	6.97	31.47	0.553	10.449	0.524
0.1156	41.74	7.54	30.45	0.614	11.605	0.769
0.1664	60.09	8.11	29.53	0.670	12.655	0.868
0.2172	78.43	8.52	28.94	0.706	13.339	0.895
0.2934	105.95	8.97	28.26	0.747	14.115	0.919
0.3442	124.30	9.21	27.93	0.767	14.486	0.921
0.4204	151.82	9.52	27.53	0.791	14.950	0.924
0.5220	188.52	9.81	27.09	0.818	15.451	0.926
0.6490	234.38	10.10	26.68	0.842	15.916	0.922
0.7760	280.25	10.32	26.32	0.864	16.325	0.923
0.9792	353.64	10.67	25.90	0.890	16.810	0.918
1.1824	427.03	10.97	25.54	0.911	17.221	0.917
1.4364	518.76	11.30	25.18	0.933	17.632	0.914
1.6904	610.50	11.62	24.90	0.950	17.951	0.909
2.1984	793.97	12.13	24.52	0.973	18.383	0.894
2.7064	977.44	12.59	24.31	0.986	18.630	0.875
3.3414	1206.78	13.01	24.16	0.995	18.801	0.849
4.1034	1481.99	13.26	24.09	0.999	18.878	0.819
4.8654	1757.19	13.18	24.09	0.999	18.878	0.791

070280 DEL99/R(THETA=0)=0.10 PROFILES AT STATION 8 S=25.5CM THETA=32DEG

REX = 0.26062E 07 REM = 5024.
XVO = -247.05 CM DEL2 = 0.525 CM
UPW = 14.62 M/S DEL99= 4.212 CM
VISC = 0.15284E-04 M2/S DEL1 = 0.779 CM
PORT = 4 H = 1.483
XLOC = 25.40 CM CF/2 = 0.12072E-02
DENS = 1.18 KG/M3

REH = 2198.
DEH2 = 0.231 CM
DELT99 = 3.333 CM
UPW = 14.67 M/S
VISC = 0.15401E-04 M2/S
TINF = 24.10 DEG C
TPLATE = 40.50 DEG C
STANTON= 0.16900E-02

Y(CM)	Y/DEL	U(M/S)	U/UP	Y+	U+	CF/2	T(DEG C)
0.048	0.011	5.13	0.351	16.1	10.11	0.000938	33.87
0.053	0.013	5.45	0.373	17.8	10.73	0.001001	33.56
0.074	0.018	6.31	0.432	24.5	12.41	0.001146	32.55
0.099	0.024	6.77	0.464	33.0	13.33	0.001178	31.74
0.150	0.036	7.36	0.505	49.8	14.50	0.001202	30.71
0.201	0.048	7.78	0.534	66.7	15.31	0.001215	30.04
0.251	0.060	8.01	0.551	83.3	15.77	0.001204	29.56
0.326	0.077	8.43	0.580	108.3	16.58	0.001228	28.95
0.375	0.089	8.64	0.596	124.7	17.01	0.001238	28.61
0.450	0.107	8.98	0.620	149.6	17.68	0.001265	28.17
0.550	0.131	9.34	0.647	182.8	18.39	0.001290	27.68
0.676	0.160	9.74	0.676	224.6	19.17	0.001322	27.17
0.802	0.190	10.06	0.700	266.5	19.80	0.001345	26.74
1.004	0.238	10.47	0.732	333.7	20.62	0.001373	26.22
1.206	0.286	10.78	0.757	401.0	21.22	0.001388	25.85
1.486	0.353	11.18	0.790	493.7	22.00	0.001415	25.43
1.739	0.413	11.48	0.816	578.0	22.61	0.001436	25.15
2.247	0.533	11.99	0.861	746.8	23.61	0.001472	24.74
2.755	0.654	12.44	0.903	915.5	24.48	0.001508	24.49
3.389	0.805	12.90	0.949	1126.4	25.39	0.001546	24.32
4.150	0.985	13.22	0.988	1379.5	26.03	0.001554	24.23
5.420	1.287	13.06	1.001	1801.6	25.71	0.001444	24.17

Y(CM)	Y+	U(M/S)	T(DEG C)	TBAR	T+	PRT
0.0140	4.64	1.48	38.04	0.150	3.085	2.496
0.0165	5.49	1.75	37.59	0.177	3.638	2.713
0.0190	6.33	2.02	37.14	0.205	4.212	2.921
0.0216	7.18	2.29	36.66	0.234	4.806	3.122
0.0241	8.02	2.56	36.25	0.259	5.321	3.394
0.0267	8.86	2.83	35.90	0.280	5.758	3.798
0.0292	9.71	3.10	35.56	0.301	6.195	4.339
0.0343	11.40	3.64	35.05	0.332	6.833	7.296
0.0394	13.09	4.18	34.52	0.364	7.491	91.910
0.0444	14.77	4.72	34.11	0.390	8.011	-5.225
0.0597	19.84	5.72	33.16	0.447	9.192	-0.255
0.0800	26.59	6.42	32.25	0.503	10.336	0.521
0.1156	38.41	6.96	31.27	0.562	11.562	0.812
0.1664	55.30	7.50	30.42	0.614	12.631	0.911
0.2172	72.18	7.85	29.83	0.651	13.378	0.949
0.2934	97.51	8.25	29.16	0.691	14.207	0.976
0.3442	114.39	8.51	28.79	0.714	14.673	0.992
0.4204	139.72	8.85	28.29	0.744	15.303	1.018
0.5220	173.49	9.24	27.77	0.776	15.953	1.036
0.6490	215.70	9.65	27.23	0.809	16.625	1.054
0.7760	257.91	9.99	26.78	0.836	17.196	1.069
0.9792	325.45	10.42	26.23	0.870	17.891	1.080
1.1824	392.98	10.74	25.85	0.893	18.361	1.077
1.4364	477.40	11.11	25.44	0.918	18.874	1.077
1.6904	561.83	11.42	25.15	0.936	19.243	1.071
2.1984	730.67	11.94	24.72	0.962	19.779	1.055
2.7064	899.51	12.39	24.45	0.978	20.110	1.036
3.3414	1110.57	12.86	24.27	0.989	20.340	1.008
4.1034	1363.83	13.20	24.17	0.995	20.466	0.974
4.8654	1617.10	13.13	24.12	0.998	20.527	0.945
6.1354	2039.21	12.87	24.11	0.999	20.544	0.903
7.4054	2461.31	12.56	24.11	0.999	20.541	0.870

070280 DEL99/R(THETA=0)=0.10 PROFILES AT STATION 9 S=40.5CM THETA=51DEG

REX = 0.28145E 07 REM = 5342. REH = 2459.
XVO = -254.92 CM DEL2 = 0.561 CM DEH2 = 0.258 CM
UPW = 14.66 M/S DEL99= 4.422 CM DELT99 = 3.675 CM
VISC = 0.15383E-04 M2/S DEL1 = 0.855 CM UPW = 14.66 M/S
PORT = 4 H = 1.525 VISC = 0.15392E-04 M2/S
XLOC = 40.39 CM CF/2 = 0.10712E-02 TINF = 24.00 DEG C
DENS = 1.18 KG/M3 TPLATE = 40.67 DEG C
STANTON= 0.15890E-02

Y(CM)	Y/DEL	U(M/S)	U/UP	Y+	U+	CF/2	T(DEG C)
0.048	0.011	4.66	0.318	15.1	9.72	0.000798	34.36
0.074	0.017	5.72	0.391	23.0	11.92	0.000969	33.09
0.099	0.022	6.23	0.426	30.9	12.99	0.001020	32.33
0.150	0.034	6.82	0.466	46.8	14.20	0.001049	31.33
0.201	0.045	7.23	0.496	62.6	15.07	0.001069	30.66
0.252	0.057	7.52	0.515	78.5	15.66	0.001073	30.16
0.327	0.074	7.93	0.545	101.9	16.53	0.001100	29.53
0.376	0.085	8.17	0.562	117.3	17.02	0.001116	29.19
0.451	0.102	8.50	0.586	140.7	17.72	0.001144	28.74
0.551	0.125	8.91	0.615	172.0	18.56	0.001182	28.21
0.677	0.153	9.35	0.647	211.1	19.48	0.001225	27.61
0.802	0.181	9.70	0.674	250.3	20.22	0.001257	27.10
1.005	0.227	10.18	0.710	313.4	21.21	0.001300	26.49
1.207	0.273	10.55	0.739	376.5	21.99	0.001331	26.02
1.460	0.330	10.95	0.771	455.5	22.83	0.001364	25.58
1.714	0.388	11.27	0.798	534.6	23.48	0.001387	25.27
2.221	0.502	11.82	0.846	693.0	24.64	0.001432	24.80
2.729	0.617	12.26	0.887	851.3	25.54	0.001466	24.51
3.364	0.761	12.73	0.933	1049.3	26.52	0.001505	24.31
4.125	0.933	13.15	0.979	1286.9	27.41	0.001535	24.16
4.887	1.105	13.20	0.998	1524.4	27.51	0.001495	24.10
6.157	1.392	12.90	1.000	1920.6	26.89	0.001374	24.07

Y(CM)	Y+	U(M/S)	T(DEG C)	TBAR	T+	PRT
0.0140	4.36	1.35	38.24	0.145	2.997	2.386
0.0165	5.15	1.59	37.85	0.169	3.483	2.598
0.0190	5.94	1.84	37.45	0.193	3.970	2.813
0.0216	6.73	2.08	36.93	0.224	4.614	2.944
0.0241	7.53	2.33	36.62	0.243	5.004	3.242
0.0267	8.32	2.57	36.25	0.265	5.454	3.546
0.0292	9.11	2.82	36.00	0.280	5.767	4.070
0.0343	10.70	3.31	35.46	0.312	6.434	5.873
0.0394	12.28	3.80	34.98	0.341	7.023	13.771
0.0444	13.87	4.29	34.58	0.365	7.515	-16.089
0.0597	18.62	5.13	33.68	0.419	8.638	-0.963
0.0800	24.96	5.85	32.81	0.471	9.705	0.166
0.1156	36.05	6.42	31.90	0.526	10.833	0.566
0.1664	51.90	6.95	31.03	0.578	11.904	0.736
0.2172	67.74	7.32	30.45	0.613	12.619	0.795
0.2934	91.51	7.75	29.76	0.654	13.476	0.853
0.3442	107.36	8.02	29.37	0.677	13.954	0.882
0.4204	131.13	8.37	28.89	0.707	14.554	0.912
0.5220	162.83	8.79	28.32	0.741	15.254	0.948
0.6490	202.44	9.25	27.71	0.778	16.016	0.987
0.7760	242.06	9.63	27.15	0.811	16.698	1.022
0.9792	305.45	10.12	26.52	0.849	17.483	1.049
1.1824	368.83	10.51	26.03	0.878	18.087	1.064
1.4364	448.07	10.92	25.57	0.906	18.653	1.071
1.6904	527.30	11.24	25.24	0.925	19.058	1.069
2.1984	685.77	11.80	24.77	0.954	19.646	1.059
2.7064	844.24	12.24	24.47	0.972	20.013	1.042
3.3414	1042.32	12.71	24.26	0.985	20.279	1.017
4.1034	1280.02	13.14	24.11	0.994	20.465	0.988
4.8654	1517.72	13.20	24.04	0.998	20.546	0.959
6.1354	1913.89	12.91	24.01	0.999	20.584	0.918
7.4054	2310.06	12.59	24.01	0.999	20.580	0.884

070280 DEL99/R(THETA=0)=0.10 PROFILES AT STATION 10 S=61.3CM THETA=77DEG

REX = 0.30167E 07 REM = 5647.
XVO = -254.38 CM DEL2 = 0.591 CM
UPW = 14.71 M/S DEL99= 4.620 CM
VISC = 0.15384E-04 M2/S DEL1 = 0.918 CM
PORT = 4 H = 1.553
XLOC = 61.21 CM CF/2 = 0.10041E-02
DENS = 1.18 KG/M3

REH = 2886.
DEH2 = 0.302 CM
DELT99 = 3.975 CM
UPW = 14.71 M/S
VISC = 0.15392E-04 M2/S
TINF = 24.00 DEG C
TPLATE = 40.55 DEG C
STANTON= 0.13600E-02

Y(CM)	Y/DEL	U(M/S)	U/UP	Y+	U+	CF/2	T(DEG C)
0.048	0.010	4.43	0.301	14.6	9.50	0.000729	34.93
0.074	0.016	5.49	0.374	22.3	11.78	0.000900	33.61
0.099	0.021	6.06	0.413	30.0	13.01	0.000968	32.85
0.150	0.032	6.66	0.454	45.4	14.29	0.001003	31.90
0.201	0.043	7.00	0.478	60.8	15.02	0.001004	31.25
0.251	0.054	7.26	0.496	76.0	15.58	0.001006	30.78
0.326	0.070	7.61	0.521	98.6	16.33	0.001019	30.19
0.375	0.081	7.83	0.537	113.7	16.80	0.001031	29.86
0.451	0.098	8.13	0.558	136.6	17.44	0.001051	29.42
0.551	0.119	8.52	0.587	167.0	18.29	0.001087	28.90
0.677	0.147	8.94	0.617	205.1	19.18	0.001125	28.31
0.803	0.174	9.33	0.646	243.3	20.03	0.001167	27.79
1.005	0.218	9.89	0.688	304.6	21.22	0.001228	27.05
1.208	0.261	10.36	0.723	365.8	22.22	0.001279	26.45
1.461	0.316	10.80	0.758	442.4	23.18	0.001323	25.86
1.714	0.371	11.14	0.786	519.1	23.90	0.001350	25.46
2.222	0.481	11.70	0.835	672.9	25.10	0.001396	24.93
2.729	0.591	12.17	0.878	826.7	26.12	0.001438	24.66
3.364	0.728	12.61	0.921	1018.9	27.06	0.001470	24.39
4.126	0.893	13.07	0.970	1249.6	28.04	0.001508	24.21
4.887	1.058	13.23	0.997	1480.2	28.38	0.001492	24.13
6.157	1.333	12.94	1.000	1864.8	27.78	0.001373	24.10
7.427	1.608	12.63	1.000	2249.5	27.10	0.001269	24.08

Y(CM)	Y+	U(M/S)	T(DEG C)	TBAR	T+	PRT
0.0140	4.23	1.28	38.41	0.129	3.012	2.319
0.0165	5.00	1.51	38.00	0.154	3.588	2.475
0.0190	5.77	1.74	37.66	0.175	4.076	2.661
0.0216	6.54	1.98	37.36	0.193	4.498	2.889
0.0241	7.31	2.21	37.04	0.212	4.942	3.124
0.0267	8.08	2.44	36.79	0.227	5.298	3.463
0.0292	8.85	2.67	36.54	0.243	5.654	3.886
0.0343	10.39	3.14	36.03	0.273	6.368	5.265
0.0394	11.93	3.60	35.59	0.300	6.993	9.902
0.0444	13.46	4.07	35.17	0.325	7.575	-38.763
0.0597	18.08	4.90	34.22	0.383	8.919	-0.687
0.0800	24.23	5.63	33.32	0.437	10.177	0.493
0.1156	35.01	6.26	32.43	0.491	11.438	0.837
0.1664	50.39	6.77	31.63	0.539	12.566	0.955
0.2172	65.78	7.08	31.05	0.574	13.380	1.004
0.2934	88.86	7.46	30.41	0.613	14.285	1.040
0.3442	104.25	7.69	30.04	0.635	14.807	1.064
0.4204	127.33	8.00	29.57	0.664	15.465	1.089
0.5220	158.10	8.41	29.02	0.697	16.239	1.122
0.6490	196.57	8.85	28.40	0.734	17.104	1.163
0.7760	235.04	9.25	27.87	0.766	17.858	1.198
0.9792	296.59	9.82	27.10	0.813	18.933	1.250
1.1824	358.14	10.30	26.47	0.851	19.826	1.289
1.4364	435.08	10.76	25.87	0.887	20.676	1.317
1.6904	512.01	11.10	25.44	0.913	21.274	1.326
2.1984	665.88	11.67	24.90	0.946	22.035	1.316
2.7064	819.76	12.15	24.62	0.963	22.430	1.289
3.3414	1012.10	12.59	24.34	0.980	22.825	1.264
4.1034	1242.91	13.05	24.16	0.991	23.083	1.230
4.8654	1473.72	13.22	24.07	0.996	23.200	1.196
6.1354	1858.40	12.95	24.04	0.998	23.242	1.143
7.4054	2243.08	12.63	24.03	0.998	23.262	1.103
8.6754	2627.76	12.33	24.01	0.999	23.281	1.072

070280 DEL99/R(THETA=0)=0.10 PROFILES AT STATION 11 S=72.3CM

REX	= 0.30495E 07	REM	= 5696.	REH	= 2930.
XVO	= -252.37 CM	DEL2	= 0.607 CM	DEH2	= 0.312 CM
UPW	= 14.45 M/S	DEL99	= 4.689 CM	DELT99	= 3.972 CM
VISC	= 0.15384E-04 M2/S	DEL1	= 0.947 CM	UPW	= 14.45 M/S
PORT	= 4	H	= 1.561	VISC	= 0.15395E-04 M2/S
XLOC	= 72.39 CM	CF/2	= 0.99139E-03	TINF	= 24.03 DEG C
DENS	= 1.18 KG/M3			TPLATE	= 41.08 DEG C
				STANTON	= 0.15600E-02

Y(CM)	Y/DEL	U(M/S)	U/UP	Y+	U+	CF/2	T(DEG C)
0.048	0.010	4.53	0.314	14.3	9.95	0.000783	34.92
0.074	0.016	5.49	0.381	21.8	12.08	0.000934	33.83
0.099	0.021	6.00	0.416	29.3	13.18	0.000985	33.17
0.150	0.032	6.54	0.454	44.3	14.37	0.001006	32.27
0.201	0.043	6.82	0.474	59.4	14.99	0.000995	31.66
0.249	0.053	7.03	0.489	73.8	15.46	0.000988	31.21
0.325	0.069	7.34	0.511	96.0	16.13	0.000991	30.61
0.375	0.080	7.53	0.526	110.7	16.56	0.001000	30.27
0.451	0.096	7.79	0.545	133.5	17.13	0.001011	29.81
0.551	0.118	8.23	0.577	163.0	18.10	0.001060	29.31
0.677	0.144	8.59	0.604	200.1	18.89	0.001087	28.73
0.804	0.171	8.98	0.633	237.7	19.75	0.001129	28.23
1.006	0.215	9.59	0.678	297.4	21.08	0.001204	27.49
1.208	0.258	10.09	0.717	357.1	22.19	0.001266	26.84
1.461	0.312	10.53	0.753	431.9	23.15	0.001310	26.20
1.714	0.366	10.88	0.782	506.7	23.91	0.001341	25.70
2.222	0.474	11.42	0.829	656.8	25.10	0.001386	25.07
2.729	0.582	11.89	0.873	806.9	26.14	0.001429	24.71
3.364	0.717	12.28	0.913	994.5	26.99	0.001452	24.44
4.126	0.880	12.76	0.964	1219.7	28.05	0.001496	24.24
4.887	1.042	12.99	0.997	1444.8	28.56	0.001496	24.13
6.157	1.313	12.71	1.000	1820.2	27.95	0.001378	24.10
7.427	1.584	12.41	1.001	2195.7	27.28	0.001273	24.10

Y(CM)	Y+	U(M/S)	T(DEG C)	TBAR	T+	PRT
0.0140	4.13	1.31	38.79	0.134	2.706	2.378
0.0165	4.88	1.55	38.22	0.167	3.376	2.502
0.0190	5.63	1.78	37.80	0.192	3.880	2.679
0.0216	6.38	2.02	37.41	0.215	4.347	2.878
0.0241	7.13	2.26	37.11	0.233	4.702	3.161
0.0267	7.89	2.50	36.76	0.253	5.114	3.448
0.0292	8.64	2.73	36.46	0.271	5.469	3.843
0.0317	9.39	2.97	36.17	0.288	5.807	4.377
0.0343	10.14	3.21	35.95	0.301	6.070	5.245
0.0394	11.64	3.69	35.52	0.326	6.577	9.351
0.0444	13.14	4.16	35.12	0.349	7.048	222.009
0.0597	17.65	4.96	34.30	0.398	8.029	-2.002
0.0800	23.65	5.62	33.61	0.438	8.841	-0.425
0.1156	34.17	6.17	32.76	0.488	9.844	0.172
0.1664	49.19	6.63	32.01	0.532	10.735	0.402
0.2172	64.21	6.89	31.47	0.564	11.381	0.501
0.2934	86.74	7.21	30.82	0.602	12.141	0.587
0.3442	101.75	7.41	30.45	0.623	12.580	0.629
0.4204	124.28	7.69	29.95	0.653	13.171	0.681
0.5220	154.32	8.10	29.42	0.684	13.802	0.726
0.6490	191.87	8.51	28.82	0.719	14.510	0.776
0.7760	229.42	8.90	28.31	0.749	15.124	0.815
0.9792	289.49	9.51	27.54	0.794	16.027	0.874
1.1824	349.57	10.03	26.88	0.833	16.817	0.922
1.4364	424.66	10.49	26.21	0.872	17.608	0.964
1.6904	499.76	10.85	25.69	0.903	18.226	0.991
2.1984	649.95	11.39	25.05	0.940	18.981	1.003
2.7064	800.14	11.87	24.67	0.963	19.429	0.997
3.3414	987.88	12.26	24.39	0.979	19.761	0.980
4.1034	1213.16	12.74	24.19	0.991	19.997	0.957
4.8654	1438.45	12.98	24.07	0.998	20.134	0.934
6.1354	1813.93	12.72	24.04	0.999	20.170	0.893
7.4054	2189.40	12.41	24.05	0.999	20.167	0.860

070280 DEL99/R(THETA=0)=0.10 PROFILES AT STATION 12 S=88.2CM

REX	= 0.32702E 07	REM	= 6024.	REH	= 3236.
XVO	= -257.00 CM	DEL2	= 0.636 CM	DEH2	= 0.342 CM
UPW	= 14.58 M/S	DEL99	= 4.834 CM	DELT99	= 4.298 CM
VISC	= 0.15383E-04 M2/S	DEL1	= 0.990 CM	UPW	= 14.58 M/S
PORT	= 4	H	= 1.557	VISC	= 0.15394E-04 M2/S
XLOC	= 88.14 CM	CF/2	= 0.10083E-02	TINF	= 24.01 DEG C
DENS	= 1.18 KG/M3			TPLATE	= 41.58 DEG C
				STANTON	= 0.14900E-02

Y(CM)	Y/DEL	U(M/S)	U/UP	Y+	U+	CF/2	T(DEG C)
0.048	0.010	4.86	0.333	14.6	10.49	0.000863	35.04
0.074	0.015	5.78	0.397	22.2	12.50	0.001000	33.69
0.099	0.021	6.21	0.426	29.8	13.42	0.001026	32.91
0.150	0.031	6.70	0.460	45.1	14.49	0.001032	32.04
0.201	0.042	6.98	0.479	60.4	15.09	0.001018	31.48
0.249	0.051	7.19	0.493	74.9	15.54	0.001009	31.10
0.324	0.067	7.48	0.513	97.4	16.16	0.001007	30.60
0.374	0.077	7.65	0.525	112.6	16.52	0.001008	30.32
0.450	0.093	7.92	0.543	135.3	17.11	0.001023	29.96
0.551	0.114	8.23	0.565	165.7	17.78	0.001041	29.53
0.677	0.140	8.63	0.592	203.8	18.64	0.001076	29.00
0.804	0.166	9.03	0.620	241.9	19.52	0.001121	28.53
1.006	0.208	9.66	0.663	302.8	20.88	0.001199	27.81
1.209	0.250	10.21	0.700	363.6	22.06	0.001269	27.17
1.462	0.302	10.82	0.743	439.8	23.38	0.001351	26.47
1.715	0.355	11.35	0.779	515.9	24.52	0.001421	25.92
2.222	0.460	12.14	0.833	668.5	26.24	0.001520	25.17
2.730	0.565	12.76	0.876	821.2	27.58	0.001595	24.77
3.364	0.696	13.39	0.918	1012.2	28.92	0.001667	24.49
4.126	0.854	14.03	0.962	1241.3	30.31	0.001744	24.31
4.887	1.011	14.45	0.992	1470.4	31.23	0.001783	24.18
6.157	1.274	14.58	1.000	1852.5	31.51	0.001736	24.13

Y(CM)	Y+	U(M/S)	T(DEG C)	TBAR	T+	PRT
0.0178	5.35	1.79	38.49	0.176	3.744	2.588
0.0203	6.11	2.04	38.11	0.197	4.203	2.793
0.0229	6.88	2.30	37.72	0.220	4.680	2.997
0.0254	7.64	2.55	37.37	0.239	5.101	3.259
0.0279	8.41	2.81	37.06	0.257	5.484	3.600
0.0305	9.17	3.06	36.71	0.277	5.906	3.985
0.0330	9.93	3.32	36.42	0.293	6.252	4.609
0.0381	11.46	3.83	35.92	0.322	6.867	7.496
0.0432	12.99	4.34	35.47	0.348	7.406	52.517
0.0483	14.52	4.85	35.04	0.372	7.927	-6.536
0.0635	19.11	5.41	34.10	0.425	9.066	-0.422
0.0838	25.22	5.95	33.26	0.474	10.091	0.409
0.1194	35.92	6.41	32.43	0.521	11.100	0.677
0.1702	51.20	6.82	31.75	0.559	11.916	0.747
0.2210	66.49	7.07	31.27	0.587	12.500	0.774
0.2972	89.41	7.38	30.74	0.617	13.143	0.792
0.3480	104.70	7.56	30.44	0.634	13.514	0.805
0.4242	127.62	7.83	30.05	0.656	13.983	0.820
0.5258	158.19	8.15	29.61	0.681	14.511	0.836
0.6528	196.40	8.55	29.07	0.712	15.177	0.870
0.7798	234.61	8.96	28.60	0.739	15.747	0.898
0.9830	295.75	9.59	27.85	0.781	16.652	0.950
1.1862	356.88	10.15	27.20	0.818	17.441	0.994
1.4402	433.30	10.77	26.48	0.859	18.311	1.041
1.6942	509.72	11.31	25.91	0.892	19.004	1.073
2.2022	662.56	12.11	25.14	0.936	19.938	1.098
2.7102	815.40	12.74	24.73	0.959	20.437	1.093
3.3452	1006.45	13.37	24.43	0.976	20.800	1.074
4.1072	1235.71	14.01	24.24	0.987	21.024	1.046
4.8692	1464.97	14.44	24.11	0.994	21.187	1.022
6.1392	1847.07	14.58	24.06	0.997	21.248	0.979
7.4092	2229.18	14.58	24.04	0.998	21.268	0.945
8.6792	2611.28	14.58	24.03	0.999	21.288	0.918

070280 DEL99/R(THETA=0)=0.10 STATION 13 S=104.0CM

REX = 0.34015E 07 REM = 6216.
XVO = -255.20 CM DEL2 = 0.657 CM
UPW = 14.56 M/S DEL99= 4.977 CM
VISC = 0.15383E-04 M2/S DEL1 = 1.019 CM
PORT = 4 H = 1.552
XLOC = 104.14 CM CF/2 = 0.10523E-02
DENS = 1.18 KG/M3

REH = 3539.
DEH2 = 0.374 CM
DELT99 = 4.567 CM
UPW = 14.56 M/S
VISC = 0.15394E-04 M2/S
TINF = 24.01 DEG C
TPLATE = 41.28 DEG C
STANTON= 0.16200E-02

Y(CM)	Y/DEL	U(M/S)	U/UP	Y+	U+	CF/2	T(DEG C)
0.048	0.010	4.90	0.336	14.8	10.37	0.000877	34.67
0.074	0.015	5.86	0.402	22.6	12.40	0.001023	33.40
0.099	0.020	6.28	0.431	30.4	13.29	0.001047	32.68
0.150	0.030	6.80	0.467	46.0	14.39	0.001059	31.83
0.201	0.040	7.13	0.490	61.6	15.10	0.001058	31.30
0.249	0.050	7.34	0.504	76.3	15.53	0.001048	30.93
0.323	0.065	7.62	0.523	99.3	16.13	0.001043	30.47
0.373	0.075	7.78	0.535	114.7	16.48	0.001043	30.24
0.449	0.090	8.02	0.551	137.9	16.99	0.001049	29.90
0.550	0.110	8.33	0.572	168.8	17.64	0.001066	29.51
0.676	0.136	8.65	0.594	207.6	18.32	0.001084	29.04
0.803	0.161	8.99	0.617	246.6	19.03	0.001113	28.63
1.006	0.202	9.51	0.653	308.8	20.13	0.001168	28.02
1.208	0.243	10.00	0.687	371.0	21.18	0.001226	27.46
1.462	0.294	10.59	0.727	448.9	22.42	0.001302	26.81
1.715	0.345	11.13	0.764	526.6	23.56	0.001375	26.24
2.222	0.447	12.01	0.825	682.4	25.42	0.001493	25.36
2.730	0.548	12.67	0.870	838.2	26.81	0.001576	24.89
3.364	0.676	13.32	0.915	1033.0	28.21	0.001657	24.57
4.126	0.829	13.94	0.957	1266.9	29.51	0.001727	24.36
4.887	0.982	14.38	0.988	1500.7	30.45	0.001770	24.23
6.157	1.237	14.57	1.000	1890.7	30.84	0.001736	24.13

Y(CM)	Y+	U(M/S)	T(DEG C)	TBAR	T+	PRT
0.0165	5.07	1.67	38.16	0.181	3.616	2.498
0.0190	5.85	1.93	37.82	0.201	4.018	2.735
0.0216	6.63	2.19	37.44	0.223	4.456	2.971
0.0241	7.41	2.44	37.09	0.243	4.859	3.257
0.0267	8.19	2.70	36.76	0.262	5.244	3.609
0.0292	8.97	2.96	36.41	0.282	5.647	4.031
0.0317	9.75	3.21	36.16	0.297	5.941	4.742
0.0343	10.53	3.47	35.87	0.313	6.272	5.757
0.0368	11.31	3.73	35.60	0.329	6.585	7.588
0.0419	12.87	4.24	35.16	0.355	7.101	37.853
0.0470	14.43	4.76	34.74	0.379	7.581	-8.595
0.0622	19.11	5.42	33.83	0.431	8.633	-0.901
0.0825	25.35	6.00	33.05	0.476	9.540	0.059
0.1181	36.27	6.47	32.24	0.524	10.486	0.422
0.1689	51.87	6.92	31.56	0.563	11.267	0.546
0.2197	67.46	7.21	31.11	0.589	11.788	0.589
0.2959	90.86	7.52	30.58	0.619	12.404	0.629
0.3467	106.46	7.70	30.34	0.633	12.684	0.636
0.4229	129.86	7.94	29.99	0.654	13.095	0.654
0.5245	161.06	8.26	29.58	0.677	13.563	0.675
0.6515	200.05	8.59	29.10	0.705	14.125	0.706
0.7785	239.05	8.92	28.68	0.730	14.612	0.731
0.9817	301.44	9.45	28.06	0.765	15.327	0.771
1.1849	363.84	9.95	27.49	0.798	15.986	0.808
1.4389	441.83	10.54	26.82	0.837	16.760	0.854
1.6929	519.82	11.08	26.24	0.871	17.441	0.892
2.2009	675.81	11.97	25.34	0.923	18.484	0.942
2.7089	831.80	12.64	24.84	0.952	19.056	0.951
3.3439	1026.78	13.30	24.51	0.971	19.440	0.941
4.1059	1260.76	13.92	24.29	0.983	19.692	0.921
4.8679	1494.74	14.37	24.16	0.991	19.849	0.902
6.1379	1884.70	14.57	24.06	0.997	19.964	0.869
7.4079	2274.67	14.56	24.04	0.998	19.983	0.839
8.6779	2664.63	14.56	24.03	0.999	20.002	0.815

070280 DEL99/R(THETA=0)=0.10 PROFILES AT STATION 14 S=119.1CM

REX = 0.35033E 07 REM = 6365.
XVO = -250.60 CM DEL2 = 0.672 CM
UPW = 14.58 M/S DEL99= 5.086 CM
VISC = 0.15383E-04 M2/S DEL1 = 1.035 CM
PORT = 4 H = 1.541
XLOC = 119.13 CM CF/2 = 0.10829E-02
DENS = 1.18 KG/M3

REH = 3746.
DEH2 = 0.396 CM
DELT99 = 4.664 CM
UPW = 14.58 M/S
VISC = 0.15394E-04 M2/S
TINF = 24.01 DEG C
TPLATE = 41.26 DEG C
STANTON= 0.17100E-02

Y(CM)	Y/DEL	U(M/S)	U/UP	Y+	U+	CF/2	T(DEG C)
0.048	0.010	5.03	0.345	15.1	10.48	0.000914	34.57
0.074	0.015	6.04	0.414	23.0	12.59	0.001074	33.30
0.099	0.019	6.48	0.445	30.9	13.51	0.001103	32.58
0.150	0.029	6.99	0.479	46.8	14.56	0.001107	31.73
0.201	0.039	7.28	0.500	62.6	15.18	0.001094	31.21
0.249	0.049	7.51	0.515	77.5	15.66	0.001089	30.85
0.323	0.064	7.79	0.534	100.7	16.23	0.001081	30.39
0.373	0.073	7.95	0.545	116.2	16.57	0.001080	30.17
0.448	0.088	8.16	0.560	139.8	17.00	0.001078	29.86
0.549	0.108	8.44	0.579	171.3	17.59	0.001087	29.46
0.676	0.133	8.75	0.601	210.8	18.25	0.001104	29.04
0.802	0.158	9.08	0.623	250.1	18.94	0.001132	28.67
1.005	0.198	9.51	0.653	313.4	19.83	0.001166	28.14
1.208	0.237	9.96	0.684	376.6	20.77	0.001215	27.64
1.462	0.287	10.47	0.719	455.7	21.84	0.001274	27.03
1.715	0.337	11.00	0.755	534.8	22.93	0.001344	26.51
2.222	0.437	11.89	0.816	692.9	24.79	0.001464	25.63
2.730	0.537	12.60	0.865	851.1	26.27	0.001558	25.00
3.364	0.661	13.28	0.911	1049.0	27.68	0.001643	24.60
4.126	0.811	13.91	0.954	1286.4	29.00	0.001717	24.37
4.887	0.961	14.35	0.985	1523.9	29.92	0.001760	24.24
6.157	1.211	14.58	1.000	1919.9	30.40	0.001736	24.13

Y(CM)	Y+	U(M/S)	T(DEG C)	TBAR	T+	PRT
0.0140	4.36	1.45	38.59	0.155	2.984	2.390
0.0165	5.15	1.72	38.07	0.185	3.563	2.561
0.0190	5.94	1.98	37.67	0.208	4.003	2.795
0.0216	6.73	2.24	37.23	0.234	4.495	3.014
0.0241	7.52	2.51	36.90	0.253	4.865	3.341
0.0267	8.32	2.77	36.55	0.273	5.253	3.721
0.0292	9.11	3.04	36.27	0.290	5.571	4.281
0.0317	9.90	3.30	35.90	0.311	5.977	4.943
0.0343	10.69	3.56	35.68	0.323	6.225	6.266
0.0394	12.28	4.09	35.16	0.354	6.810	14.887
0.0444	13.86	4.62	34.79	0.375	7.219	-18.734
0.0597	18.61	5.48	33.90	0.427	8.214	-1.470
0.0800	24.95	6.15	33.02	0.478	9.194	-0.162
0.1156	36.03	6.64	32.17	0.527	10.140	0.283
0.1664	51.87	7.08	31.50	0.566	10.891	0.433
0.2172	67.71	7.36	31.05	0.592	11.393	0.488
0.2934	91.47	7.68	30.53	0.622	11.967	0.534
0.3442	107.31	7.85	30.26	0.638	12.272	0.553
0.4204	131.07	8.08	29.95	0.655	12.614	0.566
0.5220	162.75	8.36	29.53	0.680	13.082	0.593
0.6490	202.35	8.69	29.10	0.705	13.569	0.619
0.7760	241.95	9.01	28.71	0.728	14.002	0.642
0.9792	305.30	9.46	28.17	0.759	14.599	0.673
1.1824	368.66	9.91	27.67	0.788	15.160	0.704
1.4364	447.86	10.42	27.05	0.824	15.850	0.745
1.6904	527.06	10.95	26.51	0.855	16.450	0.779
2.1984	685.45	11.85	25.61	0.907	17.453	0.831
2.7064	843.85	12.57	24.96	0.945	18.185	0.862
3.3414	1041.84	13.25	24.54	0.969	18.645	0.863
4.1034	1279.43	13.89	24.31	0.982	18.906	0.848
4.8654	1517.02	14.34	24.18	0.990	19.056	0.830
6.1354	1913.01	14.58	24.06	0.997	19.186	0.802
7.4054	2308.99	14.58	24.04	0.998	19.204	0.775
8.6754	2704.98	14.58	24.03	0.999	19.223	0.753
9.9377	3098.59	14.58	24.03	0.999	19.223	0.734

RUN 070280 *** CURVATURE RIG *** NASA-NAG-3-3 STANTON NUMBER DATA

TADB= 23.98 DEG C UREF= 14.76 M/S TINF= 23.88 DEG C
RHO= 1.189 KG/M3 VISC= 0.15282E-04 M2/S XVO= -213.9 CM
CP= 1014. J/KGK PR= 0.717

STANTON RUN DEL99/R(THETA=0)=0.10

PLATE	X (CM)	UPW (M/S)	K	REXVO	TO DEG C	STANTON NO	REENTH	DST	DST(%)	DREEN
1	-61.3	14.76	0.000E 00	0.14737E 07	37.61	0.31359E-02		0.195E-03	6.222	
2	-58.7	14.76	0.000E 00	0.14990E 07	39.15	0.33214E-02		0.115E-03	3.452	
3	-56.1	14.76	0.000E 00	0.15242E 07	39.50	0.32034E-02		0.107E-03	3.337	
4	-53.5	14.76	0.000E 00	0.15493E 07	39.77	0.30439E-02		0.104E-03	3.428	
5	-50.9	14.76	0.000E 00	0.15746E 07	38.97	0.27050E-02		0.870E-04	3.215	
6	-48.3	14.76	0.000E 00	0.15998E 07	40.02	0.28242E-02		0.970E-04	3.434	
7	-45.7	14.76	0.000E 00	0.16251E 07	40.19	0.27219E-02		0.916E-04	3.364	
8	-43.0	14.76	0.000E 00	0.16504E 07	40.19	0.26335E-02		0.880E-04	3.342	
9	-40.4	14.76	0.000E 00	0.16754E 07	40.30	0.26488E-02		0.883E-04	3.353	
10	-37.8	14.76	0.000E 00	0.17007E 07	40.33	0.25728E-02		0.861E-04	3.347	
11	-35.2	14.82	0.156E-06	0.17328E 07	40.41	0.25706E-02	0.98104E 03	0.865E-04	3.367	7.
12	-32.6	14.82	0.000E 00	0.17582E 07	40.37	0.24664E-02	0.10475E 04	0.829E-04	3.363	8.
13	-30.0	14.81	-0.392E-07	0.17818E 07	40.30	0.24529E-02	0.11144E 04	0.820E-04	3.342	8.
14	-27.4	14.79	-0.397E-07	0.18051E 07	40.39	0.25060E-02	0.11705E 04	0.842E-04	3.362	8.
15	-24.8	14.78	-0.394E-07	0.18286E 07	40.45	0.24639E-02	0.12293E 04	0.827E-04	3.357	8.
16	-22.2	14.76	-0.396E-07	0.18521E 07	40.48	0.24550E-02	0.12893E 04	0.839E-04	3.417	8.
17	-19.5	14.76	0.000E 00	0.18774E 07	39.92	0.23740E-02	0.13943E 04	0.780E-04	3.286	8.
18	-16.9	14.76	0.000E 00	0.19024E 07	40.28	0.24366E-02	0.14240E 04	0.825E-04	3.385	8.
19	-14.3	14.76	-0.198E-07	0.19267E 07	40.44	0.24718E-02	0.14721E 04	0.836E-04	3.381	8.
20	-11.7	14.68	-0.201E-06	0.19422E 07	40.26	0.24325E-02	0.15477E 04	0.814E-04	3.348	9.
21	-9.1	14.62	-0.184E-06	0.19583E 07	40.21	0.23580E-02	0.16140E 04	0.787E-04	3.338	9.
22	-6.5	14.56	-0.165E-06	0.19752E 07	40.45	0.23813E-02	0.16493E 04	0.805E-04	3.380	9.
23	-3.9	14.54	-0.418E-07	0.19978E 07	40.53	0.24475E-02	0.17019E 04	0.822E-04	3.360	9.
24	-1.3	14.65	0.284E-06	0.20373E 07	40.59	0.23314E-02	0.17549E 04	0.787E-04	3.377	9.
CURVE BEGINS										
25	2.4	14.88	0.442E-06	0.21058E 07	40.76	0.19910E-02	0.18139E 04	0.544E-04	2.733	9.
26	7.3	14.88	0.000E 00	0.21535E 07	40.73	0.19212E-02	0.19108E 04	0.432E-04	2.250	9.
27	12.4	14.76	-0.163E-06	0.21856E 07	40.79	0.19110E-02	0.19986E 04	0.424E-04	2.221	9.
28	17.4	14.71	-0.724E-07	0.22265E 07	40.79	0.17877E-02	0.20894E 04	0.415E-04	2.324	10.
29	22.5	14.73	0.205E-07	0.22777E 07	40.71	0.17117E-02	0.21847E 04	0.409E-04	2.391	10.
30	27.6	14.76	0.512E-07	0.23323E 07	40.71	0.16087E-02	0.22658E 04	0.400E-04	2.484	10.
31	32.6	14.79	0.304E-07	0.23849E 07	40.70	0.15732E-02	0.23466E 04	0.397E-04	2.525	10.
32	37.7	14.78	-0.102E-07	0.24326E 07	40.72	0.15498E-02	0.24207E 04	0.395E-04	2.548	10.
33	42.8	14.76	-0.204E-07	0.24793E 07	40.72	0.15223E-02	0.24964E 04	0.394E-04	2.590	10.
34	47.8	14.73	-0.513E-07	0.25220E 07	40.76	0.14824E-02	0.25633E 04	0.390E-04	2.633	10.
35	52.9	14.72	-0.103E-07	0.25694E 07	40.80	0.14450E-02	0.26295E 04	0.386E-04	2.671	10.
36	58.0	14.74	0.307E-07	0.26223E 07	40.71	0.13540E-02	0.27126E 04	0.380E-04	2.810	10.
37	63.0	14.88	0.190E-06	0.26964E 07	40.67	0.13137E-02	0.27851E 04	0.375E-04	2.853	11.
38	68.1	14.88	0.000E 00	0.27459E 07	40.72	0.12030E-02	0.28398E 04	0.353E-04	2.933	11.
RECOVERY BEGINS										
39	72.0	14.64	-0.457E-06	0.27376E 07	40.93	0.14699E-02	0.28478E 04	0.522E-04	3.553	10.
40	74.6	14.58	-0.164E-06	0.27514E 07	40.84	0.14993E-02	0.29006E 04	0.518E-04	3.456	10.
41	77.2	14.56	-0.412E-07	0.27735E 07	41.21	0.15249E-02	0.28747E 04	0.547E-04	3.586	11.
42	79.8	14.62	0.143E-06	0.28085E 07	41.28	0.14743E-02	0.29011E 04	0.525E-04	3.560	11.
43	82.4	14.66	0.122E-06	0.28420E 07	41.25	0.15109E-02	0.29441E 04	0.530E-04	3.508	11.
44	85.0	14.68	0.603E-07	0.28714E 07	41.31	0.14760E-02	0.29710E 04	0.530E-04	3.591	11.
45	87.6	14.72	0.998E-07	0.29039E 07	41.32	0.14487E-02	0.30051E 04	0.517E-04	3.572	11.
46	90.2	14.68	-0.101E-06	0.29217E 07	41.15	0.15259E-02	0.30719E 04	0.532E-04	3.483	11.
47	92.8	14.75	0.180E-06	0.29600E 07	41.06	0.14749E-02	0.31262E 04	0.520E-04	3.525	11.
48	95.4	14.76	0.396E-07	0.29882E 07	41.02	0.15548E-02	0.31715E 04	0.547E-04	3.516	11.
49	98.1	14.76	0.000E 00	0.30135E 07	41.04	0.14983E-02	0.32068E 04	0.530E-04	3.537	11.
50	100.7	14.76	0.000E 00	0.30387E 07	41.16	0.15560E-02	0.32231E 04	0.558E-04	3.585	11.
51	103.3	14.76	0.000E 00	0.30640E 07	41.03	0.15720E-02	0.32861E 04	0.547E-04	3.480	11.
52	105.9	14.76	0.000E 00	0.30890E 07	41.16	0.15661E-02	0.33026E 04	0.557E-04	3.558	11.
53	108.5	14.76	0.000E 00	0.31143E 07	41.07	0.15911E-02	0.33578E 04	0.556E-04	3.492	11.
54	111.1	14.76	0.000E 00	0.31396E 07	41.13	0.15686E-02	0.33860E 04	0.563E-04	3.589	11.
55	113.7	14.76	0.000E 00	0.31649E 07	40.84	0.15875E-02	0.34836E 04	0.544E-04	3.429	11.
56	116.4	14.76	0.000E 00	0.31901E 07	41.11	0.16138E-02	0.34687E 04	0.577E-04	3.578	11.
57	118.9	14.76	0.000E 00	0.32152E 07	41.10	0.15596E-02	0.35111E 04	0.558E-04	3.576	11.
58	121.6	14.76	0.000E 00	0.32404E 07	40.83	0.15808E-02	0.36061E 04	0.554E-04	3.505	11.
59	124.2	14.76	0.000E 00	0.32657E 07	40.77	0.15800E-02	0.36595E 04	0.567E-04	3.590	11.
60	126.8	14.76	0.000E 00	0.32910E 07	40.36	0.15779E-02	0.37888E 04	0.538E-04	3.412	11.
61	129.4	14.78	0.394E-07	0.33196E 07	40.74	0.15691E-02	0.37423E 04	0.591E-04	3.766	12.
62	132.0	14.78	0.000E 00	0.33446E 07	40.22	0.13621E-02	0.38962E 04	0.765E-04	5.613	12.

UNCERTAINTY IN REX=27041.

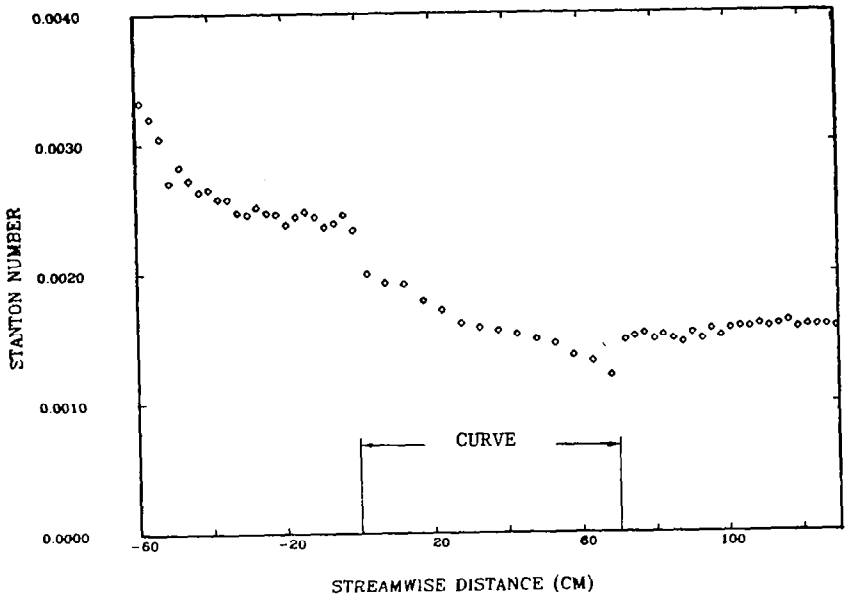

Fig. G-1. Case 070280: Stanton number versus streamwise distance.

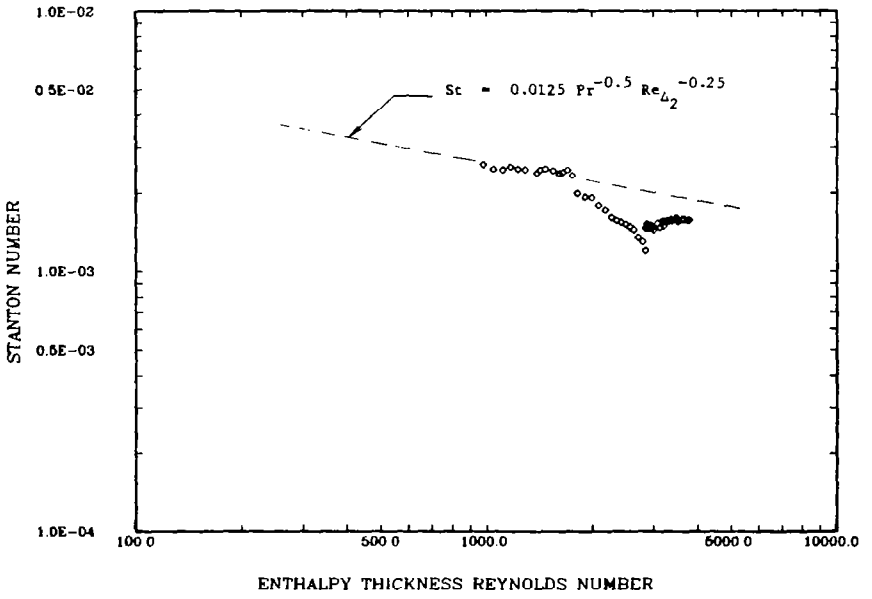

Fig. G-2. Case 070280: Stanton number versus enthalpy thickness Reynolds number.

022680 STARTING PROFILES DEL99/R(THETA=0)=0.05 S=-35 CM

REX	= 0.79165E 06	REM	= 1937.	REH	= 957.
XVO	= -118.56 CM	DEL2	= 0.204 CM	DEH2	= 0.101 CM
UPW	= 14.48 M/S	DEL99	= 1.779 CM	DELT99	= 1.337 CM
VISC	= 0.15276E-04 M2/S	DEL1	= 0.322 CM	UPW	= 14.47 M/S
PORT	= 4	H	= 1.578	VISC	= 0.15226E-04 M2/S
XLOC	= -35.05 CM	CF/2	= 0.17785E-02	TINF	= 22.60 DEG C
DENS	= 1.19 KG/M3			TPLATE	= 37.24 DEG C

Y(CM)	Y/DEL	U(M/S)	U/UP	Y+	U+	CF/2	T(DEG C)
0.084	0.047	7.27	0.502	33.6	11.90	0.001425	28.56
0.125	0.070	8.64	0.597	49.8	14.15	0.001700	27.28
0.163	0.091	9.16	0.632	65.0	14.99	0.001740	26.57
0.201	0.113	9.54	0.658	80.3	15.61	0.001762	26.15
0.266	0.150	10.00	0.691	106.4	16.38	0.001777	25.56
0.317	0.178	10.33	0.713	126.8	16.91	0.001797	25.20
0.379	0.213	10.64	0.735	151.7	17.43	0.001811	24.85
0.454	0.255	11.01	0.760	181.7	18.02	0.001837	24.49
0.550	0.309	11.39	0.787	219.8	18.65	0.001866	24.13
0.668	0.376	11.84	0.817	267.2	19.38	0.001907	23.77
0.815	0.458	12.33	0.852	325.9	20.19	0.001961	23.45
0.995	0.559	12.89	0.890	397.6	21.11	0.002030	23.15
1.217	0.684	13.46	0.929	486.6	22.04	0.002097	22.92
1.490	0.838	14.00	0.967	595.8	22.93	0.002157	22.77
1.830	1.029	14.37	0.992	731.5	23.53	0.002165	22.72
2.246	1.263	14.47	0.999	898.0	23.69	0.002103	22.69

Y(CM)	Y+	U(M/S)	T(DEG C)	TBAR	1-TBAR
0.0140	5.59	1.21	35.99	0.086	0.914
0.0165	6.60	1.43	35.87	0.094	0.906
0.0190	7.62	1.65	35.76	0.101	0.899
0.0216	8.63	1.87	35.65	0.109	0.891
0.0241	9.65	2.09	35.51	0.118	0.882
0.0267	10.66	2.31	35.40	0.126	0.874
0.0292	11.68	2.53	35.27	0.135	0.865
0.0317	12.69	2.75	35.11	0.146	0.854
0.0368	14.72	3.19	34.67	0.176	0.824
0.0419	16.76	3.63	33.31	0.268	0.732
0.0571	22.85	4.95	30.53	0.459	0.541
0.0775	30.97	6.71	28.78	0.578	0.422
0.1130	45.19	8.25	27.47	0.668	0.332
0.1638	65.50	9.17	26.53	0.732	0.268
0.2299	91.90	9.74	25.79	0.782	0.218
0.3162	126.43	10.32	25.17	0.825	0.175
0.4178	167.05	10.83	24.60	0.864	0.136
0.5321	212.74	11.32	24.14	0.895	0.105
0.7099	283.83	11.98	23.59	0.932	0.068
0.9639	385.38	12.80	23.13	0.964	0.036
1.2179	486.92	13.46	22.86	0.982	0.018
1.4719	588.47	13.97	22.71	0.993	0.007
1.9799	791.57	14.41	22.62	0.999	0.001

030180 STATION 5 DEL99/R(THETA=0)=0.05 S=-35 CM

REX = 0.76698E 06 REM = 1888.
XVO = -116.27 CM DEL2 = 0.200 CM
UPW = 14.43 M/S DEL99= 1.747 CM
VISC = 0.15281E-04 M2/S DEL1 = 0.294 CM
PORT = 4 H = 1.472
XLOC = -35.05 CM CF/2 = 0.18528E-02
DENS = 1.19 KG/M3

REH = 900.
DEH2 = 0.095 CM
DELT99 = 1.263 CM
UPW = 14.44 M/S
VISC = 0.15275E-04 M2/S
TINF = 23.14 DEG C
TPLATE = 37.24 DEG C
STANTON= 0.25000E-02

Y(CM)	Y/DEL	U(M/S)	U/UP	Y+	U+	CF/2	T(DEG C)
0.048	0.028	7.45	0.517	19.7	12.00	0.001787	29.43
0.074	0.042	8.38	0.581	30.0	13.49	0.001900	28.22
0.099	0.057	8.82	0.611	40.3	14.19	0.001893	27.55
0.150	0.086	9.39	0.650	61.0	15.11	0.001871	26.77
0.201	0.115	9.78	0.677	81.6	15.74	0.001853	26.25
0.249	0.143	10.11	0.701	101.3	16.28	0.001855	25.87
0.324	0.186	10.49	0.727	131.7	16.89	0.001850	25.41
0.374	0.214	10.76	0.746	152.1	17.33	0.001867	25.15
0.449	0.257	11.10	0.769	182.4	17.88	0.001886	24.82
0.550	0.315	11.49	0.796	223.4	18.50	0.001908	24.49
0.676	0.387	11.95	0.828	274.7	19.24	0.001948	24.14
0.802	0.459	12.36	0.856	326.1	19.89	0.001989	23.88
1.005	0.575	12.96	0.898	408.3	20.87	0.002060	23.60
1.207	0.691	13.47	0.933	490.6	21.68	0.002119	23.42
1.485	0.850	14.00	0.970	603.7	22.54	0.002173	23.30
1.738	0.995	14.28	0.989	706.5	22.99	0.002179	23.26
2.246	1.286	14.44	1.001	913.0	23.24	0.002109	23.23

Y(CM)	Y+	U(M/S)	T(DEG C)	TBAR	T+	PRT
0.0140	5.68	2.15	33.83	0.242	4.173	2.565
0.0165	6.71	2.54	33.30	0.280	4.815	2.809
0.0190	7.74	2.94	32.74	0.319	5.498	3.039
0.0216	8.78	3.33	32.26	0.353	6.084	3.382
0.0241	9.81	3.72	31.83	0.384	6.612	3.919
0.0267	10.84	4.11	31.44	0.411	7.082	4.932
0.0292	11.87	4.50	31.07	0.438	7.533	7.420
0.0317	12.91	4.89	30.77	0.459	7.907	28.056
0.0343	13.94	5.28	30.51	0.478	8.222	-9.262
0.0368	14.97	5.68	30.28	0.494	8.498	-3.104
0.0394	16.00	6.07	30.07	0.508	8.755	-1.482
0.0444	18.07	6.85	29.69	0.536	9.230	-0.288
0.0495	20.13	7.50	29.33	0.561	9.666	0.209
0.0546	22.20	7.68	29.02	0.583	10.041	0.465
0.0597	24.26	7.87	28.73	0.604	10.396	0.637
0.0648	26.33	8.05	28.52	0.619	10.653	0.714
0.0775	31.49	8.44	28.07	0.651	11.208	0.829
0.0902	36.65	8.66	27.69	0.677	11.663	0.888
0.1029	41.81	8.86	27.45	0.695	11.960	0.892
0.1156	46.98	9.00	27.21	0.712	12.258	0.907
0.1283	52.14	9.14	27.04	0.723	12.457	0.897
0.1410	57.30	9.29	26.85	0.737	12.695	0.906
0.1664	67.62	9.51	26.54	0.759	13.073	0.909
0.1918	77.95	9.71	26.29	0.777	13.371	0.905
0.2172	88.27	9.89	26.07	0.793	13.650	0.906
0.2680	108.92	10.21	25.71	0.818	14.089	0.901
0.3188	129.57	10.46	25.40	0.840	14.468	0.901
0.3696	150.22	10.74	25.13	0.859	14.788	0.900
0.4204	170.87	10.97	24.89	0.876	15.088	0.903
0.4712	191.52	11.19	24.69	0.890	15.328	0.901
0.5220	212.17	11.38	24.53	0.902	15.529	0.897
0.6490	263.79	11.85	24.15	0.929	15.991	0.895
0.7760	315.41	12.27	23.87	0.949	16.334	0.889
1.0300	418.65	13.03	23.50	0.975	16.780	0.869
1.2840	521.90	13.61	23.30	0.989	17.026	0.845
1.5380	625.14	14.06	23.22	0.995	17.131	0.816
2.0460	831.63	14.38	23.16	0.999	17.194	0.766

030180 STATION 7 DEL99/R(THETA=0)=0.05 S=10 CM THETA=13 DEG

REX	= 0.12721E 07	REM	= 2830.	REH	= 1774.		
XVO	= -125.13 CM	DEL2	= 0.301 CM	DEH2	= 0.188 CM		
UPW	= 14.40 M/S	DEL99	= 2.484 CM	DELT99	= 2.183 CM		
VISC	= 0.15312E-04 M2/S	DEL1	= 0.451 CM	UPW	= 14.38 M/S		
PORT	= 4	H	= 1.499	VISC	= 0.15260E-04 M2/S		
XLOC	= 10.16 CM	CF/2	= 0.15174E-02	TINF	= 23.04 DEG C		
DENS	= 1.19 KG/M3			TPLATE	= 37.64 DEG C		
				STANTON	= 0.19740E-02		

Y(CM)	Y/DEL	U(M/S)	U/UP	Y+	U+	CF/2	T(DEG C)
0.048	0.019	6.05	0.421	17.7	10.79	0.001271	31.10
0.074	0.030	7.10	0.494	27.0	12.66	0.001444	29.94
0.099	0.040	7.57	0.527	36.3	13.50	0.001469	29.14
0.150	0.060	8.26	0.576	54.9	14.73	0.001511	28.29
0.201	0.081	8.71	0.607	73.5	15.52	0.001524	27.73
0.251	0.101	9.06	0.633	92.0	16.15	0.001537	27.26
0.325	0.131	9.47	0.663	119.1	16.89	0.001554	26.69
0.374	0.151	9.73	0.681	136.9	17.35	0.001573	26.42
0.448	0.181	10.01	0.702	164.3	17.86	0.001581	26.13
0.549	0.221	10.36	0.728	201.1	18.47	0.001598	25.81
0.675	0.272	10.72	0.756	247.3	19.12	0.001617	25.43
0.801	0.323	11.03	0.780	293.6	19.67	0.001636	25.11
1.004	0.404	11.49	0.816	367.8	20.49	0.001671	24.65
1.207	0.486	11.93	0.851	442.1	21.27	0.001715	24.25
1.486	0.598	12.43	0.892	544.2	22.16	0.001765	23.85
1.739	0.700	12.83	0.925	637.0	22.87	0.001806	23.61
2.246	0.904	13.38	0.976	822.8	23.86	0.001849	23.27
2.753	1.109	13.54	0.998	1008.5	24.15	0.001814	23.15
3.388	1.364	13.40	1.000	1241.1	23.89	0.001707	23.12

Y(CM)	Y+	U(M/S)	T(DEG C)	TBAR	T+	PRT
0.0140	5.12	1.75	34.81	0.194	3.819	2.436
0.0216	7.91	2.70	33.54	0.281	5.541	3.129
0.0368	13.49	4.61	31.81	0.399	7.877	-29.711
0.0571	20.93	6.42	30.54	0.486	9.597	0.131
0.0927	33.96	7.45	29.23	0.576	11.364	0.830
0.1435	52.56	8.18	28.34	0.637	12.567	0.925
0.2095	76.75	8.77	27.61	0.687	13.554	0.956
0.2959	108.38	9.31	26.82	0.741	14.631	1.009
0.3975	145.60	9.82	26.26	0.779	15.380	1.013
0.5118	187.46	10.23	25.89	0.805	15.889	0.995
0.6896	252.58	10.76	25.35	0.842	16.618	0.996
0.9436	345.62	11.35	24.72	0.885	17.460	1.006
1.1976	438.65	11.91	24.21	0.920	18.149	1.018
1.4516	531.68	12.37	23.84	0.946	18.661	1.022
1.9596	717.75	13.07	23.34	0.980	19.331	1.014
2.4676	903.81	13.45	23.11	0.996	19.645	0.989
3.1026	1136.39	13.46	23.06	0.999	19.712	0.944

030180 STATION 8 DEL99/R(THETA=0)=0.050 S=25 CM THETA=32 DEG

REX	= 0.13989E 07	REM	= 3054.	REH	= 2269.
XVO	= -124.64 CM	DEL2	= 0.328 CM	DEH2	= 0.243 CM
UPW	= 14.28 M/S	DEL99	= 2.593 CM	DELT99	= 2.470 CM
VISC	= 0.15319E-04 M2/S	DEL1	= 0.509 CM	UPW	= 14.26 M/S
PORT	= 4	H	= 1.555	VISC	= 0.15259E-04 M2/S
XLOC	= 25.40 CM	CF/2	= 0.13303E-02	TINF	= 23.03 DEG C
DENS	= 1.19 KG/M3			TPLATE	= 37.09 DEG C
				STANTON	= 0.16100E-02

Y(CM)	Y/DEL	U(M/S)	U/UP	Y+	U+	CF/2	T(DEG C)
0.048	0.019	5.17	0.363	16.4	9.93	0.000996	31.57
0.074	0.028	6.34	0.445	25.1	12.17	0.001213	30.41
0.099	0.038	6.96	0.489	33.7	13.37	0.001295	29.85
0.150	0.058	7.57	0.532	51.0	14.53	0.001322	29.05
0.201	0.077	7.98	0.561	68.3	15.31	0.001332	28.51
0.252	0.097	8.28	0.583	85.5	15.90	0.001338	28.07
0.326	0.126	8.71	0.614	111.0	16.73	0.001364	27.54
0.376	0.145	8.97	0.634	127.8	17.23	0.001385	27.26
0.451	0.174	9.33	0.660	153.4	17.90	0.001416	26.87
0.551	0.213	9.78	0.693	187.4	18.78	0.001467	26.41
0.677	0.261	10.25	0.728	230.1	19.68	0.001517	25.93
0.802	0.309	10.64	0.758	272.8	20.42	0.001557	25.55
1.005	0.387	11.15	0.798	341.6	21.40	0.001609	25.01
1.207	0.466	11.59	0.833	410.5	22.24	0.001655	24.58
1.486	0.573	12.12	0.877	505.3	23.27	0.001715	24.19
1.739	0.671	12.51	0.910	591.5	24.01	0.001755	23.92
2.247	0.866	13.16	0.967	764.0	25.26	0.001824	23.44
2.754	1.062	13.40	0.996	936.4	25.73	0.001809	23.18
3.389	1.307	13.29	1.000	1152.3	25.50	0.001709	23.10

Y(CM)	Y+	U(M/S)	T(DEG C)	TBAR	T+	PRT
0.0140	4.75	1.49	34.76	0.166	3.750	2.287
0.0165	5.61	1.77	34.42	0.190	4.313	2.464
0.0190	6.48	2.04	34.00	0.220	4.980	2.575
0.0216	7.34	2.31	33.65	0.245	5.544	2.730
0.0241	8.21	2.58	33.35	0.266	6.032	2.948
0.0267	9.07	2.85	33.12	0.282	6.392	3.341
0.0317	10.80	3.40	32.66	0.315	7.139	4.716
0.0368	12.52	3.94	32.28	0.342	7.758	13.207
0.0521	17.71	5.34	31.33	0.410	9.285	-0.231
0.0724	24.62	6.28	30.43	0.474	10.737	0.846
0.1079	36.71	7.07	29.64	0.530	12.010	1.026
0.1587	53.98	7.64	28.91	0.582	13.181	1.086
0.2248	76.44	8.12	28.25	0.629	14.250	1.120
0.3111	105.81	8.63	27.60	0.675	15.295	1.151
0.4127	140.36	9.15	27.03	0.716	16.212	1.173
0.5270	179.23	9.67	26.47	0.755	17.104	1.203
0.7048	239.69	10.34	25.79	0.804	18.209	1.239
0.9588	326.07	11.03	25.07	0.855	19.369	1.268
1.2128	412.44	11.60	24.53	0.893	20.240	1.285
1.4668	498.82	12.08	24.16	0.919	20.824	1.284
1.9748	671.57	12.81	23.62	0.958	21.701	1.278
2.4828	844.32	13.27	23.17	0.990	22.418	1.279
3.1178	1060.26	13.34	23.04	0.999	22.629	1.232

030180 STATION 9 DEL99/R(THETA=0)=0.05 S=41 CM THETA=52 DEG

REX =	0.15577E 07	REM =	3328.	REH =	2359.
XVO =	-126.95 CM	DEL2 =	0.359 CM	DEH2 =	0.254 CM
UPW =	14.23 M/S	DEL99=	2.729 CM	DELT99 =	2.604 CM
VISC =	0.15329E-04 M2/S	DEL1 =	0.574 CM	UPW =	14.21 M/S
PORT =	4	H =	1.600	VISC =	0.15285E-04 M2/S
XLOC =	40.89 CM	CF/2 =	0.11691E-02	TINF =	23.32 DEG C
DENS =	1.19 KG/M3			TPLATE =	37.28 DEG C
				STANTON=	0.15670E-02

Y(CM)	Y/DEL	U(M/S)	U/UP	Y+	U+	CF/2	T(DEG C)
0.048	0.018	4.65	0.327	15.3	9.56	0.000842	31.93
0.074	0.027	5.67	0.399	23.4	11.65	0.001013	31.03
0.099	0.036	6.29	0.443	31.5	12.93	0.001099	30.40
0.150	0.055	6.96	0.491	47.6	14.31	0.001153	29.61
0.201	0.074	7.37	0.520	63.7	15.15	0.001172	29.09
0.252	0.092	7.68	0.543	79.8	15.78	0.001182	28.68
0.327	0.120	8.12	0.575	103.8	16.68	0.001214	28.17
0.377	0.138	8.37	0.593	119.7	17.21	0.001235	27.88
0.452	0.165	8.77	0.623	143.3	18.04	0.001282	27.51
0.552	0.202	9.19	0.654	175.0	18.90	0.001325	27.06
0.678	0.248	9.69	0.691	215.1	19.92	0.001384	26.56
0.803	0.294	10.16	0.727	255.0	20.89	0.001447	26.13
1.005	0.368	10.76	0.773	319.0	22.11	0.001522	25.52
1.208	0.442	11.27	0.813	383.2	23.16	0.001587	25.04
1.486	0.544	11.82	0.858	471.6	24.29	0.001652	24.56
1.740	0.637	12.22	0.892	552.0	25.11	0.001695	24.26
2.247	0.823	12.90	0.952	713.0	26.52	0.001773	23.78
2.754	1.009	13.29	0.991	873.8	27.32	0.001796	23.51
3.389	1.242	13.24	1.001	1075.3	27.22	0.001712	23.40

Y(CM)	Y+	U(M/S)	T(DEG C)	TBAR	T+	PRT
0.0190	6.05	1.83	34.26	0.217	4.728	2.480
0.0343	10.88	3.30	32.68	0.330	7.196	4.785
0.0546	17.33	4.90	31.59	0.408	8.902	-0.827
0.0902	28.61	6.07	30.54	0.483	10.536	0.575
0.1410	44.73	6.84	29.69	0.544	11.872	0.813
0.2070	65.69	7.41	29.01	0.593	12.933	0.890
0.2934	93.09	7.92	28.34	0.640	13.970	0.949
0.3950	125.33	8.47	27.76	0.682	14.884	0.990
0.5093	161.60	9.02	27.21	0.722	15.748	1.031
0.6871	218.02	9.72	26.49	0.773	16.869	1.084
0.9411	298.62	10.57	25.64	0.834	18.197	1.150
1.1951	379.23	11.24	25.02	0.879	19.170	1.187
1.4491	459.83	11.74	24.56	0.911	19.888	1.205
1.9571	621.03	12.51	23.95	0.955	20.841	1.213
2.4651	782.23	13.07	23.55	0.984	21.460	1.206
3.1001	983.73	13.26	23.34	0.999	21.795	1.174

030180 STATION 10 DEL99/R(THETA=0)=0.05 S=61.5 CM THETA=78 DEG

REX	= 0.17932E 07	REM	= 3725.	REH	= 2730.				
XVO	= -131.49 CM	DEL2	= 0.401 CM	DEH2	= 0.293 CM				
UPW	= 14.24 M/S	DEL99	= 2.924 CM	DELT99	= 2.935 CM				
VISC	= 0.15323E-04 M2/S	DEL1	= 0.656 CM	UPW	= 14.22 M/S				
PORT	= 4	H	= 1.636	VISC	= 0.15284E-04 M2/S				
XLOC	= 61.47 CM	CF/2	= 0.10724E-02	TINF	= 23.31 DEG C				
DENS	= 1.19 KG/M3			TPLATE	= 37.37 DEG C				
				STANTON	= 0.13610E-02				

Y(CM)	Y/DEL	U(M/S)	U/UP	Y+	U+	CF/2	T(DEG C)	Y(CM)	Y+	U(M/S)	T(DEG C)	TBAR	T+	PRT
0.048	0.017	4.27	0.300	14.7	9.15	0.000730	32.49	0.0140	4.25	1.23	35.37	0.143	3.433	2.178
0.074	0.025	5.36	0.377	22.4	11.49	0.000920	31.56	0.0190	5.80	1.68	34.65	0.193	4.655	2.390
0.099	0.034	6.01	0.423	30.2	12.90	0.001017	30.86	0.0241	7.34	2.13	34.05	0.236	5.688	2.631
0.150	0.051	6.65	0.469	45.6	14.26	0.001065	30.14	0.0394	11.98	3.47	32.90	0.318	7.654	7.606
0.201	0.069	7.02	0.495	61.1	15.05	0.001075	29.61	0.0597	18.17	4.75	31.97	0.384	9.244	-0.265
0.252	0.086	7.28	0.514	76.6	15.62	0.001077	29.23	0.0952	28.99	5.91	30.91	0.460	11.059	0.838
0.326	0.111	7.66	0.542	99.2	16.43	0.001098	28.76	0.1460	44.45	6.60	30.17	0.512	12.326	0.971
0.376	0.129	7.88	0.558	114.5	16.90	0.001110	28.49	0.2121	64.54	7.08	29.48	0.562	13.512	1.049
0.452	0.154	8.23	0.584	137.5	17.65	0.001144	28.12	0.2984	90.83	7.52	28.89	0.603	14.507	1.075
0.552	0.189	8.65	0.615	167.9	18.55	0.001189	27.69	0.4000	121.75	7.99	28.34	0.642	15.449	1.107
0.678	0.232	9.11	0.649	206.3	19.54	0.001239	27.19	0.5143	156.53	8.49	27.81	0.680	16.365	1.146
0.804	0.275	9.57	0.684	244.6	20.52	0.001299	26.75	0.6921	210.64	9.16	27.11	0.730	17.561	1.200
1.006	0.344	10.18	0.731	306.2	21.83	0.001377	26.08	0.9461	287.94	10.00	26.23	0.792	19.067	1.279
1.208	0.413	10.78	0.777	367.7	23.11	0.001462	25.46	1.2001	365.24	10.75	25.44	0.848	20.409	1.353
1.487	0.508	11.42	0.829	452.4	24.49	0.001551	24.88	1.4541	442.54	11.35	24.89	0.888	21.362	1.390
1.740	0.595	11.89	0.867	529.5	25.49	0.001612	24.51	1.9621	597.13	12.21	24.13	0.942	22.656	1.420
2.247	0.768	12.62	0.931	683.9	27.07	0.001702	23.96	2.4701	751.73	12.85	23.73	0.970	23.335	1.408
2.754	0.942	13.15	0.980	838.2	28.20	0.001759	23.64	3.1051	944.98	13.21	23.39	0.994	23.926	1.390
3.389	1.159	13.25	1.001	1031.4	28.42	0.001712	23.43	4.1211	1254.18	13.05	23.32	0.999	24.036	1.313

030180 STATION 12 DEL99/R(THETA=0)=0.05 S=89 CM

REX	=	0.21356E 07	REM	=	4284.	REH	= 3386.
XVO	=	-138.65 CM	DEL2	=	0.456 CM	DEH2	= 0.360 CM
UPW	=	14.36 M/S	DEL99	=	3.174 CM	DELT99	= 3.109 CM
VISC	=	0.15281E-04 M2/S	DEL1	=	0.743 CM	UPW	= 14.37 M/S
PORT	=	4	H	=	1.629	VISC	= 0.15276E-04 M2/S
XLOC	=	88.65 CM	CF/2	=	0.11089E-02	TINF	= 23.21 DEG C
DENS	=	1.19 KG/M3				TPLATE	= 38.10 DEG C
						STANTON	= 0.14910E-02

Y(CM)	Y/DEL	U(M/S)	U/UP	Y+	U+	CF/2	T(DEG C)
0.048	0.015	5.01	0.349	15.1	10.47	0.000933	32.78
0.074	0.023	5.94	0.414	23.1	12.43	0.001076	31.76
0.099	0.031	6.46	0.450	31.0	13.50	0.001127	31.17
0.150	0.047	6.93	0.483	46.9	14.49	0.001123	30.47
0.200	0.063	7.23	0.503	62.5	15.12	0.001113	30.05
0.249	0.079	7.40	0.515	78.0	15.48	0.001090	29.72
0.325	0.102	7.76	0.541	101.6	16.23	0.001104	29.32
0.374	0.118	7.92	0.552	116.9	16.57	0.001104	29.11
0.449	0.142	8.18	0.570	140.6	17.11	0.001115	28.81
0.551	0.173	8.51	0.593	172.3	17.80	0.001136	28.44
0.677	0.213	8.92	0.621	211.8	18.65	0.001173	27.96
0.804	0.253	9.31	0.648	251.5	19.47	0.001216	27.54
1.007	0.317	9.96	0.694	314.9	20.83	0.001301	26.89
1.209	0.381	10.57	0.736	378.3	22.10	0.001388	26.31
1.488	0.469	11.34	0.790	465.4	23.73	0.001506	25.57
1.741	0.549	11.98	0.835	544.7	25.06	0.001607	25.02
2.248	0.708	13.06	0.909	703.3	27.31	0.001778	24.17
2.755	0.868	13.83	0.963	861.9	28.92	0.001892	23.69
3.389	1.068	14.33	0.998	1060.3	29.96	0.001937	23.41
4.151	1.308	14.37	1.001	1298.7	30.05	0.001872	23.30

Y(CM)	Y+	U(M/S)	T(DEG C)	TBAR	T+	PRT
0.0165	5.17	1.71	35.60	0.168	3.749	2.492
0.0190	5.96	1.97	35.26	0.191	4.272	2.670
0.0216	6.75	2.23	34.94	0.213	4.748	2.878
0.0267	8.34	2.76	34.40	0.249	5.559	3.479
0.0317	9.93	3.29	33.89	0.283	6.324	4.510
0.0470	14.70	4.86	32.83	0.354	7.907	-5.876
0.0673	21.06	5.70	31.90	0.416	9.300	-0.132
0.1029	32.18	6.49	31.07	0.473	10.553	0.507
0.1537	48.08	6.95	30.41	0.517	11.542	0.663
0.2197	68.74	7.30	29.88	0.552	12.339	0.718
0.3061	95.76	7.67	29.38	0.586	13.090	0.753
0.4077	127.55	8.04	28.94	0.615	13.744	0.776
0.5220	163.31	8.42	28.52	0.644	14.376	0.803
0.6998	218.94	8.99	27.85	0.688	15.373	0.865
0.9538	298.41	9.79	27.01	0.745	16.642	0.946
1.2078	377.88	10.56	26.27	0.794	17.743	1.014
1.4618	457.34	11.27	25.59	0.841	18.773	1.078
1.9698	616.28	12.47	24.47	0.915	20.446	1.173
2.4778	775.22	13.41	23.81	0.960	21.436	1.206
3.1128	973.89	14.11	23.38	0.989	22.082	1.204
4.1288	1291.77	14.37	23.23	0.999	22.306	1.150

030180 STATION 13 DEL99/R(THETA=0)=0.05 S=104 CM

REX	= 0.23164E 07	REM	= 4571.	REH	= 3804.
XVO	= -143.41 CM	DEL2	= 0.488 CM	DEH2	= 0.405 CM
UPW	= 14.33 M/S	DEL99	= 3.299 CM	DELT99	= 3.398 CM
VISC	= 0.15281E-04 M2/S	DEL1	= 0.791 CM	UPW	= 14.34 M/S
PORT	= 4	H	= 1.623	VISC	= 0.15274E-04 M2/S
XLOC	= 103.63 CM	CF/2	= 0.11177E-02	TINF	= 23.20 DEG C
DENS	= 1.19 KG/M3			TPLATE	= 37.86 DEG C
				STANTON	= 0.16300E-02

Y(CM)	Y/DEL	U(M/S)	U/UP	Y+	U+	CF/2	T(DEG C)
0.048	0.015	5.05	0.352	15.2	10.54	0.000949	32.56
0.074	0.022	5.98	0.417	23.1	12.48	0.001091	31.59
0.099	0.030	6.39	0.446	31.1	13.34	0.001111	31.00
0.150	0.045	6.93	0.484	47.0	14.46	0.001127	30.36
0.201	0.061	7.23	0.504	62.9	15.09	0.001116	29.93
0.249	0.075	7.46	0.520	78.0	15.56	0.001110	29.64
0.324	0.098	7.73	0.540	101.5	16.14	0.001103	29.28
0.374	0.113	7.92	0.553	117.1	16.54	0.001108	29.07
0.449	0.136	8.16	0.569	140.8	17.03	0.001113	28.76
0.550	0.167	8.48	0.592	172.5	17.71	0.001134	28.38
0.676	0.205	8.85	0.617	212.0	18.47	0.001162	27.99
0.803	0.243	9.17	0.640	251.8	19.14	0.001189	27.64
1.006	0.305	9.75	0.680	315.3	20.34	0.001258	27.09
1.209	0.366	10.27	0.716	378.8	21.43	0.001324	26.55
1.488	0.451	10.95	0.764	466.3	22.86	0.001421	25.96
1.741	0.528	11.58	0.808	545.8	24.17	0.001518	25.40
2.248	0.681	12.72	0.888	704.8	26.55	0.001704	24.45
2.755	0.835	13.62	0.950	863.7	28.42	0.001848	23.86
3.389	1.027	14.24	0.994	1062.4	29.73	0.001924	23.50
4.151	1.258	14.34	1.001	1301.2	29.93	0.001873	23.28

Y(CM)	Y+	U(M/S)	T(DEG C)	TBAR	T+	PRT
0.0140	4.38	1.46	35.51	0.160	3.289	2.290
0.0165	5.18	1.72	35.18	0.183	3.754	2.494
0.0190	5.97	1.99	34.83	0.207	4.243	2.692
0.0241	7.56	2.52	34.32	0.242	4.955	3.311
0.0292	9.16	3.05	33.82	0.275	5.645	4.266
0.0444	13.93	4.64	32.74	0.349	7.166	-17.307
0.0648	20.30	5.65	31.79	0.414	8.489	-0.916
0.1003	31.45	6.40	30.96	0.471	9.658	0.098
0.1511	47.38	6.94	30.33	0.514	10.536	0.348
0.2172	68.08	7.31	29.78	0.551	11.302	0.463
0.3035	95.15	7.66	29.34	0.581	11.912	0.511
0.4051	127.00	8.02	28.92	0.609	12.500	0.552
0.5194	162.83	8.38	28.45	0.641	13.157	0.605
0.6972	218.57	8.90	27.90	0.679	13.928	0.654
0.9512	298.19	9.59	27.20	0.727	14.906	0.718
1.2052	377.81	10.26	26.52	0.773	15.864	0.784
1.4592	457.44	10.88	25.98	0.810	16.618	0.829
1.9672	616.68	12.09	24.86	0.886	18.177	0.931
2.4752	775.93	13.12	24.02	0.943	19.351	0.996
3.1102	974.99	13.97	23.51	0.978	20.069	1.012
4.1262	1293.48	14.33	23.21	0.999	20.485	0.987

030180 STATION 14 DEL99/R(THETA=0)=0.05 S=119 CM

REX = 0.25633E 07 REM = 4957.
XVO = -154.22 CM DEL2 = 0.528 CM
UPW = 14.34 M/S DEL99= 3.504 CM
VISC = 0.15281E-04 M2/S DEL1 = 0.856 CM
PORT = 4 H = 1.620
XLOC = 118.87 CM CF/2 = 0.10967E-02
DENS = 1.19 KG/M3

REH = 4261.
DEH2 = 0.454 CM
DELT99 = 3.575 CM
UPW = 14.35 M/S
VISC = 0.15283E-04 M2/S
TINF = 23.29 DEG C
TPLATE = 37.94 DEG C
STANTON= 0.16540E-02

Y(CM)	Y/DEL	U(M/S)	U/UP	Y+	U+	CF/2	T(DEG C)
0.048	0.014	4.69	0.327	15.0	9.88	0.000840	32.61
0.074	0.021	5.80	0.404	22.9	12.20	0.001034	31.71
0.099	0.028	6.32	0.441	30.8	13.31	0.001089	31.12
0.150	0.043	6.87	0.479	46.6	14.46	0.001108	30.41
0.201	0.057	7.14	0.498	62.4	15.03	0.001090	30.04
0.250	0.071	7.40	0.516	77.7	15.58	0.001092	29.77
0.324	0.092	7.71	0.537	100.6	16.23	0.001094	29.44
0.374	0.107	7.87	0.549	116.2	16.57	0.001093	29.24
0.449	0.128	8.13	0.567	139.5	17.12	0.001105	28.95
0.550	0.157	8.41	0.586	170.8	17.71	0.001115	28.62
0.676	0.193	8.75	0.610	210.1	18.43	0.001138	28.25
0.803	0.229	9.06	0.632	249.5	19.07	0.001162	27.93
1.006	0.287	9.55	0.666	312.6	20.11	0.001212	27.42
1.208	0.345	10.06	0.702	375.6	21.19	0.001276	26.92
1.487	0.424	10.69	0.745	462.3	22.50	0.001357	26.36
1.741	0.497	11.24	0.783	541.2	23.66	0.001435	25.89
2.248	0.642	12.31	0.858	698.9	25.92	0.001603	24.99
2.756	0.786	13.28	0.926	856.5	27.96	0.001764	24.27
3.389	0.967	14.11	0.984	1053.5	29.71	0.001889	23.72
4.151	1.185	14.34	1.000	1290.1	30.19	0.001870	23.38
4.913	1.402	14.35	1.001	1527.0	30.22	0.001814	23.38

Y(CM)	Y+	U(M/S)	T(DEG C)	TBAR	T+	PRT
0.0140	4.34	1.36	35.56	0.162	3.253	2.286
0.0165	5.13	1.60	35.19	0.187	3.751	2.474
0.0190	5.92	1.85	34.86	0.210	4.207	2.682
0.0241	7.50	2.34	34.30	0.248	4.968	3.252
0.0292	9.08	2.83	33.83	0.281	5.621	4.196
0.0444	13.82	4.31	32.77	0.353	7.064	-21.434
0.0648	20.13	5.40	31.90	0.412	8.248	-1.168
0.1003	31.19	6.33	31.08	0.468	9.369	-0.039
0.1511	46.98	6.87	30.38	0.516	10.337	0.286
0.2172	67.50	7.23	29.91	0.548	10.976	0.383
0.3035	94.35	7.62	29.50	0.576	11.529	0.433
0.4051	125.93	7.98	29.08	0.604	12.104	0.482
0.5194	161.46	8.33	28.68	0.632	12.657	0.525
0.6972	216.72	8.80	28.16	0.668	13.366	0.574
0.9512	295.68	9.42	27.53	0.711	14.233	0.631
1.2052	374.63	10.06	26.89	0.754	15.101	0.692
1.4592	453.58	10.62	26.37	0.790	15.816	0.738
1.9672	611.49	11.72	25.42	0.855	17.114	0.819
2.4752	769.39	12.75	24.55	0.914	18.305	0.893
3.1102	966.77	13.75	23.79	0.966	19.342	0.944
4.1262	1282.58	14.33	23.31	0.999	19.997	0.945

RUN 022680 *** CURVATURE RIG *** NASA-NAG-3-3 STANTON NUMBER DATA

TADB= 23.25 DEG C UREF= 14.48 M/S TINF= 23.16 DEG C
RHO= 1.189 KG/M3 VISC= 0.15271E-04 M2/S XVO= -118.6 CM
CP= 1013. J/KGK PR= 0.716

STANTON RUN DEL99/R(THETA=0)=0.05

PLATE	X (CM)	UPW (M/S)	K	REXVO	TO DEG C	STANTON NO	REENTH	DST	DST(%)	DREEN
1	-61.3	14.42	0.000E 00	0.54106E 06	34.90	0.34250E-02		0.204E-03	5.954	
2	-58.7	14.43	0.204E-07	0.56605E 06	36.19	0.36114E-02		0.125E-03	3.449	
3	-56.1	14.44	0.203E-07	0.59107E 06	36.50	0.34785E-02		0.116E-03	3.340	
4	-53.5	14.44	0.205E-07	0.61587E 06	36.73	0.33063E-02		0.113E-03	3.422	
5	-50.9	14.45	0.203E-07	0.64093E 06	36.06	0.28660E-02		0.928E-04	3.237	
6	-48.3	14.46	0.202E-07	0.66602E 06	36.95	0.30478E-02		0.105E-03	3.434	
7	-45.7	14.46	0.202E-07	0.69114E 06	37.14	0.29101E-02		0.982E-04	3.375	
8	-43.0	14.47	0.202E-07	0.71627E 06	37.13	0.28185E-02		0.943E-04	3.346	
9	-40.4	14.48	0.204E-07	0.74120E 06	37.24	0.28212E-02		0.948E-04	3.362	
10	-37.8	14.48	0.000E 00	0.76600E 06	37.26	0.27294E-02		0.916E-04	3.355	
11	-35.2	14.48	0.000E 00	0.79081E 06	37.36	0.27167E-02	0.98729E 03	0.916E-04	3.372	10.
12	-32.6	14.48	0.000E 00	0.81561E 06	37.34	0.26043E-02	0.10551E 04	0.878E-04	3.372	10.
13	-30.0	14.48	0.000E 00	0.84042E 06	37.28	0.25722E-02	0.11230E 04	0.864E-04	3.360	10.
14	-27.4	14.48	0.000E 00	0.86498E 06	37.33	0.26308E-02	0.11841E 04	0.887E-04	3.370	10.
15	-24.8	14.47	-0.202E-07	0.88934E 06	37.40	0.25902E-02	0.12427E 04	0.874E-04	3.373	10.
16	-22.2	14.46	-0.202E-07	0.91368E 06	37.41	0.25792E-02	0.13057E 04	0.884E-04	3.426	10.
17	-19.5	14.46	-0.202E-07	0.93799E 06	36.93	0.24481E-02	0.14122E 04	0.810E-04	3.308	10.
18	-16.9	14.44	-0.410E-07	0.96155E 06	37.25	0.25701E-02	0.14423E 04	0.872E-04	3.392	10.
19	-14.3	14.44	-0.203E-07	0.98579E 06	37.40	0.25923E-02	0.14909E 04	0.881E-04	3.398	11.
20	-11.7	14.46	0.607E-07	0.10120E 07	37.25	0.25204E-02	0.15694E 04	0.848E-04	3.366	11.
21	-9.1	14.48	0.605E-07	0.10384E 07	37.21	0.24339E-02	0.16359E 04	0.815E-04	3.348	11.
22	-6.5	14.50	0.602E-07	0.10648E 07	37.43	0.24310E-02	0.16705E 04	0.825E-04	3.396	11.
23	-3.9	14.52	0.404E-07	0.10905E 07	37.53	0.24920E-02	0.17198E 04	0.840E-04	3.372	11.
24	-1.3	14.54	0.598E-07	0.11170E 07	37.61	0.22690E-02	0.17687E 04	0.806E-04	3.553	11.
CURVE BEGINS										
25	2.4	14.55	0.284E-07	0.11529E 07	36.88	0.20080E-02	0.19358E 04	0.104E-03	5.152	11.
26	7.3	14.54	-0.106E-07	0.11991E 07	36.91	0.19862E-02	0.20253E 04	0.965E-04	4.848	12.
27	12.4	14.41	-0.200E-06	0.12356E 07	37.33	0.20273E-02	0.20619E 04	0.101E-03	4.961	12.
28	17.4	14.36	-0.749E-07	0.12788E 07	37.15	0.18426E-02	0.21804E 04	0.908E-04	4.920	13.
29	22.5	14.37	0.212E-07	0.13279E 07	37.09	0.17941E-02	0.22769E 04	0.891E-04	4.957	13.
30	27.6	14.40	0.424E-07	0.13782E 07	37.11	0.16980E-02	0.23570E 04	0.861E-04	5.058	13.
31	32.6	14.44	0.628E-07	0.14305E 07	37.15	0.16715E-02	0.24327E 04	0.850E-04	5.075	14.
32	37.7	14.46	0.210E-07	0.14797E 07	37.24	0.16383E-02	0.24959E 04	0.845E-04	5.146	14.
33	42.8	14.48	0.311E-07	0.15301E 07	37.16	0.16049E-02	0.25881E 04	0.824E-04	5.122	14.
34	47.8	14.41	-0.105E-06	0.15704E 07	37.23	0.15533E-02	0.26511E 04	0.816E-04	5.239	15.
35	52.9	14.40	-0.106E-07	0.16173E 07	37.17	0.15338E-02	0.27380E 04	0.798E-04	5.195	15.
36	58.0	14.45	0.731E-07	0.16710E 07	37.23	0.14325E-02	0.27967E 04	0.773E-04	5.384	15.
37	63.0	14.57	0.164E-06	0.17326E 07	37.14	0.13782E-02	0.28835E 04	0.754E-04	5.462	15.
38	68.1	14.59	0.405E-07	0.17846E 07	37.17	0.12272E-02	0.29411E 04	0.682E-04	5.544	16.
RECOVERY BEGINS										
39	72.0	14.55	-0.813E-07	0.18159E 07	37.74	0.14991E-02	0.28677E 04	0.550E-04	3.666	16.
40	74.6	14.51	-0.120E-06	0.18353E 07	37.72	0.15259E-02	0.29095E 04	0.537E-04	3.521	16.
41	77.2	14.46	-0.142E-06	0.18537E 07	38.08	0.15421E-02	0.28760E 04	0.563E-04	3.651	16.
42	79.8	14.41	-0.143E-06	0.18718E 07	38.16	0.14979E-02	0.28990E 04	0.542E-04	3.620	16.
43	82.4	14.36	-0.146E-06	0.18896E 07	38.13	0.15478E-02	0.29416E 04	0.552E-04	3.567	16.
44	85.0	14.40	0.123E-06	0.19200E 07	38.19	0.15105E-02	0.29674E 04	0.553E-04	3.664	16.
45	87.6	14.44	0.102E-06	0.19496E 07	38.17	0.14910E-02	0.30075E 04	0.540E-04	3.625	16.
46	90.2	14.47	0.101E-06	0.19792E 07	38.02	0.15678E-02	0.30772E 04	0.554E-04	3.533	16.
47	92.8	14.51	0.101E-06	0.20088E 07	37.96	0.15205E-02	0.31282E 04	0.545E-04	3.584	16.
48	95.4	14.52	0.400E-07	0.20357E 07	37.92	0.15921E-02	0.31741E 04	0.569E-04	3.576	16.
49	98.1	14.54	0.398E-07	0.20626E 07	37.93	0.15431E-02	0.32118E 04	0.555E-04	3.597	16.
50	100.7	14.54	0.000E 00	0.20875E 07	38.03	0.15841E-02	0.32275E 04	0.579E-04	3.654	16.
51	103.3	14.54	0.000E 00	0.21124E 07	37.90	0.15937E-02	0.32968E 04	0.566E-04	3.554	16.
52	105.9	14.54	0.000E 00	0.21371E 07	37.92	0.15893E-02	0.33322E 04	0.572E-04	3.598	16.
53	108.5	14.54	0.000E 00	0.21620E 07	37.92	0.16319E-02	0.33716E 04	0.583E-04	3.571	16.
54	111.1	14.54	0.000E 00	0.21869E 07	37.97	0.16019E-02	0.33992E 04	0.585E-04	3.650	16.
55	113.7	14.54	0.000E 00	0.22118E 07	37.71	0.16279E-02	0.34998E 04	0.568E-04	3.491	16.
56	116.4	14.54	0.199E-07	0.22378E 07	37.95	0.16569E-02	0.34832E 04	0.602E-04	3.633	16.
57	118.9	14.54	0.000E 00	0.22625E 07	37.98	0.15950E-02	0.35183E 04	0.582E-04	3.647	16.
58	121.6	14.54	0.000E 00	0.22874E 07	37.75	0.16106E-02	0.36120E 04	0.575E-04	3.570	16.
59	124.2	14.54	0.000E 00	0.23123E 07	37.71	0.16125E-02	0.36630E 04	0.589E-04	3.650	16.
60	126.8	14.54	0.000E 00	0.23372E 07	37.36	0.15992E-02	0.37911E 04	0.558E-04	3.489	16.
61	129.4	14.54	0.000E 00	0.23621E 07	37.64	0.15995E-02	0.37561E 04	0.612E-04	3.828	16.
62	132.0	14.54	0.000E 00	0.23868E 07	37.20	0.19120E-02	0.39179E 04	0.652E-04	3.412	16.

UNCERTAINTY IN REX=12523.

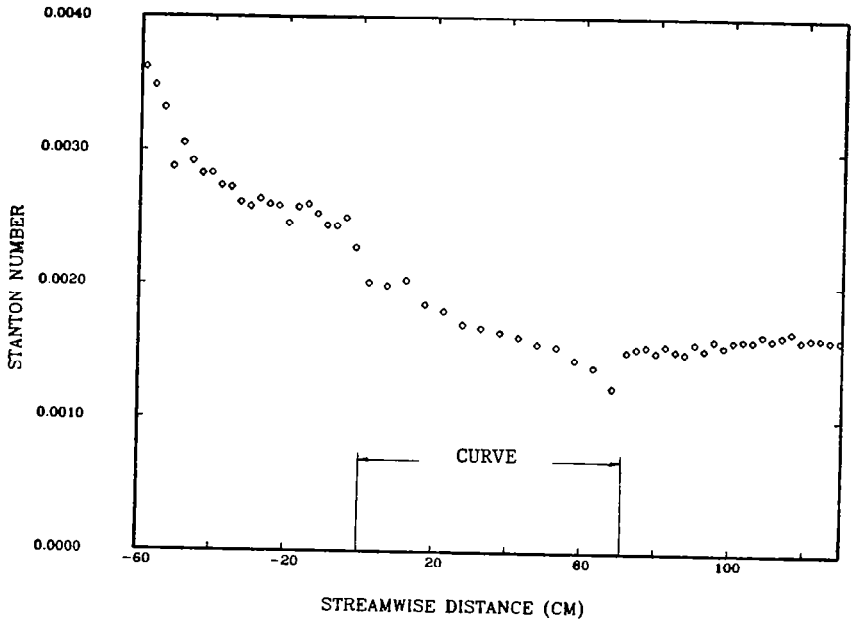

Fig. G-3. Case 022680: Stanton number versus streamwise distance.

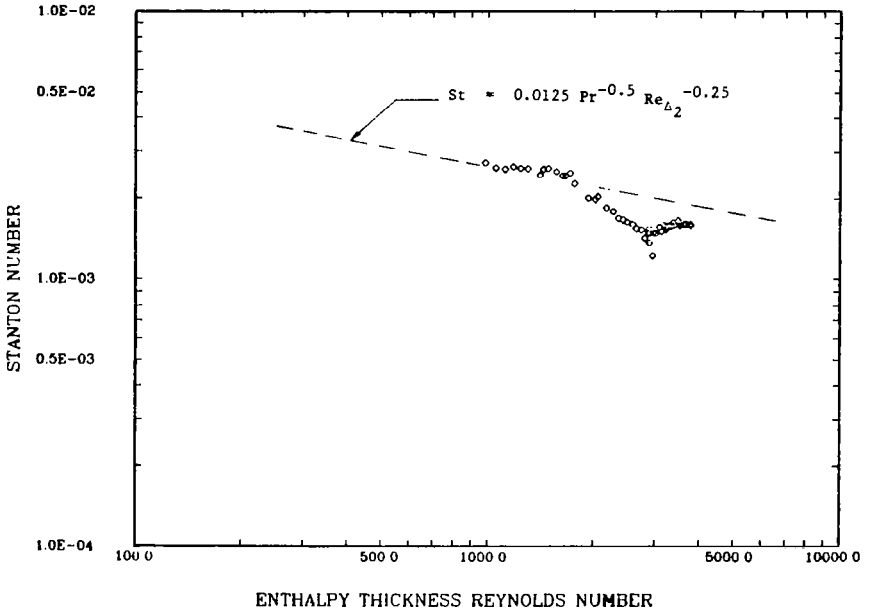

Fig. G-4. Case 022680: Stanton number versus enthalpy thickness Reynolds number.

060480 STARTING PROFILES DEL99/R(THETA=0)=0.02 S=-35 CM

REX = 0.13279E 06	REM = 464.	REH = 442.
XVO = -43.46 CM	DEL2 = 0.029 CM	DEH2 = 0.028 CM
UPW = 24.25 M/S	DEL99= 0.228 CM	DELT99 = 0.226 CM
VISC = 0.15346E-04 M2/S	DEL1 = 0.081 CM	UPW = 24.26 M/S
PORT = 4	H = 2.759	VISC = 0.15382E-04 M2/S
XLOC = -35.05 CM	CF/2 = 0.24844E-02	TINF = 24.26 DEG C
DENS = 1.19 KG/M3		TPLATE = 41.39 DEG C

Y(CM)	Y/DEL	U(M/S)	U/UP	Y+	U+	CF/2	T(DEG C)	Y(CM)	Y+	U(M/S)	T(DEG C)	TBAR	1-TBAR
0.048	0.212	8.69	0.358	38.1	7.19	0.000819	34.38	0.0140	11.00	2.51	38.44	0.172	0.828
0.059	0.256	10.13	0.418	46.1	8.38	0.000997	33.40	0.0241	19.00	4.34	37.27	0.240	0.760
0.069	0.301	11.75	0.485	54.1	9.72	0.001221	32.49	0.0343	27.00	6.16	35.78	0.327	0.673
0.089	0.390	14.98	0.618	70.1	12.39	0.001716	30.70	0.0546	43.00	9.57	33.72	0.448	0.552
0.109	0.479	17.47	0.720	86.1	14.45	0.002114	29.09	0.0749	59.00	12.74	31.88	0.555	0.445
0.130	0.568	19.72	0.813	102.1	16.32	0.002494	27.62	0.0952	75.01	15.74	30.07	0.661	0.339
0.160	0.701	21.94	0.905	126.1	18.15	0.002845	26.13	0.1257	99.01	19.29	27.72	0.798	0.202
0.180	0.790	22.86	0.943	142.1	18.92	0.002969	25.43	0.1460	115.01	20.91	26.52	0.868	0.132
0.211	0.924	23.70	0.978	166.1	19.61	0.003044	24.89	0.1765	139.01	22.68	25.33	0.938	0.062
0.243	1.066	24.16	0.996	191.7	19.99	0.003042	24.67	0.2172	171.01	23.79	24.59	0.980	0.020
0.290	1.272	24.27	1.001	228.7	20.08	0.002941	24.54	0.2680	211.02	24.21	24.37	0.993	0.007
0.340	1.491	24.27	1.001	268.1	20.09	0.002836	24.51	0.3188	251.02	24.27	24.31	0.997	0.003
0.417	1.824	24.27	1.001	328.1	20.09	0.002709	24.51	0.3950	311.03	24.27	24.31	0.997	0.003

060480 VELOCITY PROFILE DEL99/R(THETA=0)=0.02 S=25 CM THETA=32 DEG

REX = 0.91519E 06 REM = 2175.

XVO = -32.04 CM DEL2 = 0.136 CM
UPW = 24.57 M/S DEL99= 1.049 CM
VISC = 0.15351E-04 M2/S DEL1 = 0.216 CM
PORT = 4 H = 1.587
XLOC = 25.15 CM CF/2 = 0.14919E-02
DENS = 1.19 KG/M3

Y(CM)	Y/DEL	U(M/S)	U/UP	Y+	U+	CF/2
0.048	0.046	12.27	0.500	29.9	12.93	0.001425
0.059	0.056	12.81	0.522	36.2	13.50	0.001446
0.069	0.065	13.28	0.542	42.5	14.00	0.001466
0.089	0.085	13.91	0.567	55.0	14.66	0.001472
0.109	0.104	14.42	0.589	67.6	15.20	0.001479
0.130	0.124	14.84	0.606	80.1	15.64	0.001483
0.160	0.153	15.43	0.630	99.0	16.26	0.001501
0.180	0.172	15.76	0.644	111.5	16.61	0.001510
0.211	0.201	16.28	0.666	130.4	17.15	0.001535
0.252	0.240	16.91	0.692	155.5	17.83	0.001571
0.302	0.288	17.64	0.723	186.9	18.59	0.001617
0.353	0.336	18.30	0.751	218.1	19.29	0.001664
0.427	0.407	19.23	0.790	264.2	20.27	0.001737
0.502	0.478	20.06	0.826	310.3	21.14	0.001804
0.628	0.598	21.31	0.880	387.9	22.46	0.001912
0.727	0.693	22.17	0.917	449.4	23.36	0.001987
0.928	0.885	23.41	0.973	573.7	24.67	0.002079
1.053	1.003	23.77	0.990	650.8	25.05	0.002082
1.179	1.123	23.89	0.998	728.5	25.18	0.002052
1.432	1.365	23.80	1.000	885.3	25.08	0.001960
1.813	1.728	23.62	1.000	1120.7	24.89	0.001844
2.194	2.091	23.43	1.000	1356.2	24.69	0.001751

060480 VELOCITY PROFILE DEL99/R(THETA=0)=0.02 S=9.92 CM THETA=12.6 DEG

REX = 0.66220E 06 REM = 1679.

XVO = -31.33 CM DEL2 = 0.105 CM
UPW = 24.63 M/S DEL99= 0.892 CM
VISC = 0.15335E-04 M2/S DEL1 = 0.164 CM
PORT = 4 H = 1.565
XLOC = 9.91 CM CF/2 = 0.17973E-02
DENS = 1.19 KG/M3

Y(CM)	Y/DEL	U(M/S)	U/UP	Y+	U+	CF/2
0.048	0.054	13.66	0.555	32.9	13.08	0.001699
0.059	0.066	14.55	0.592	39.8	13.94	0.001787
0.069	0.077	14.90	0.606	46.8	14.27	0.001774
0.089	0.100	15.53	0.632	60.6	14.87	0.001769
0.109	0.123	16.02	0.652	74.4	15.34	0.001763
0.130	0.145	16.49	0.672	88.3	15.79	0.001771
0.160	0.180	17.10	0.697	109.0	16.38	0.001786
0.180	0.202	17.51	0.714	122.8	16.77	0.001804
0.211	0.237	18.04	0.736	143.6	17.28	0.001828
0.252	0.282	18.69	0.763	171.3	17.90	0.001861
0.302	0.339	19.40	0.793	205.6	18.58	0.001903
0.351	0.393	20.04	0.820	238.7	19.19	0.001945
0.425	0.477	20.84	0.854	289.5	19.96	0.001994
0.500	0.561	21.56	0.885	340.4	20.65	0.002042
0.626	0.702	22.58	0.930	426.0	21.63	0.002110
0.725	0.813	23.27	0.960	493.5	22.29	0.002156
0.926	1.039	23.96	0.993	630.6	22.95	0.002157
1.052	1.179	24.02	0.998	715.9	23.01	0.002111
1.305	1.464	23.93	1.000	888.6	22.92	0.002007
1.559	1.748	23.80	1.000	1061.5	22.80	0.001918

RUN 060480 *** CURVATURE RIG *** NASA-NAG-3-3 STANTON NUMBER DATA

TADB= 24.04 DEG C UREF= 24.45 M/S TINF= 23.78 DEG C
RHO= 1.187 KG/M3 VISC= 0.15339E-04 M2/S XVO= -38.9 CM
CP= 1011. J/KGK PR= 0.715

STANTON RUN DEL99/R(THETA=0)=0.02

PLATE	X (CM)	UPW (M/S)	K	REXVO	TO DEG C	STANTON NO	REENTH	DST	DST(%)	DREEN
1	-61.3	24.45	0.000E 00	-0.35806E 06	36.32	0.25628E-02		0.134E-03	5.226	
2	-58.7	24.45	0.000E 00	-0.31636E 06	38.88	0.19140E-02		0.682E-04	3.563	
3	-56.1	24.45	0.000E 00	-0.27465E 06	39.81	0.15632E-02		0.532E-04	3.401	
4	-53.5	24.45	0.000E 00	-0.23334E 06	40.36	0.13266E-02		0.460E-04	3.467	
5	-50.9	24.34	-0.109E-06	-0.19077E 06	40.06	0.10637E-02		0.351E-04	3.299	
6	-48.3	24.34	0.000E 00	-0.14925E 06	40.95	0.10735E-02		0.378E-04	3.525	
7	-45.7	24.34	0.000E 00	-0.10773E 06	41.26	0.96556E-03		0.335E-04	3.473	
8	-43.0	24.34	0.000E 00	-0.66211E 05	41.43	0.86694E-03		0.302E-04	3.486	
9	-40.4	24.36	0.123E-07	-0.25106E 05	41.58	0.82784E-03		0.289E-04	3.487	
10	-37.8	24.36	0.000E 00	0.16435E 05	41.80	0.69035E-03		0.256E-04	3.715	
11	-35.2	24.36	0.000E 00	0.57976E 05	41.40	0.91659E-03	0.46264E 03	0.317E-04	3.460	12.
12	-32.6	24.36	0.000E 00	0.99517E 05	41.07	0.97264E-03	0.51045E 03	0.343E-04	3.525	12.
13	-30.0	24.36	0.000E 00	0.14106E 06	40.36	0.12136E-02	0.57733E 03	0.424E-04	3.497	12.
14	-27.4	24.36	0.000E 00	0.18220E 06	39.19	0.18518E-02	0.68302E 03	0.621E-04	3.353	12.
15	-24.8	24.33	-0.243E-07	0.22351E 06	38.21	0.24166E-02	0.81645E 03	0.794E-04	3.286	12.
16	-22.2	24.33	0.000E 00	0.26501E 06	37.78	0.26667E-02	0.94611E 03	0.890E-04	3.336	13.
17	-19.5	24.32	-0.122E-07	0.30635E 06	36.96	0.25858E-02	0.11119E 04	0.839E-04	3.245	13.
18	-16.9	24.30	-0.247E-07	0.34708E 06	37.45	0.27164E-02	0.11812E 04	0.904E-04	3.329	13.
19	-14.3	24.30	0.000E 00	0.38852E 06	37.73	0.27028E-02	0.12691E 04	0.900E-04	3.329	13.
20	-11.7	24.28	-0.122E-07	0.42973E 06	37.62	0.25733E-02	0.13880E 04	0.851E-04	3.305	14.
21	-9.1	24.27	-0.123E-07	0.47091E 06	37.60	0.24508E-02	0.14945E 04	0.808E-04	3.296	14.
22	-6.5	24.10	-0.175E-06	0.50865E 06	37.91	0.24921E-02	0.15624E 04	0.828E-04	3.322	14.
23	-3.9	24.05	-0.509E-07	0.54822E 06	38.11	0.25246E-02	0.16437E 04	0.836E-04	3.311	14.
24	-1.3	24.22	0.173E-06	0.59348E 06	38.27	0.23459E-02	0.17255E 04	0.779E-04	3.320	15.
CURVE BEGINS										
25	2.4	25.06	0.550E-06	0.67375E 06	38.48	0.20339E-02	0.18285E 04	0.451E-04	2.216	15.
26	7.3	24.95	-0.542E-07	0.75059E 06	38.53	0.20045E-02	0.19823E 04	0.366E-04	1.825	15.
27	12.4	24.67	-0.136E-06	0.82397E 06	38.72	0.19443E-02	0.21188E 04	0.355E-04	1.827	15.
28	17.4	24.58	-0.489E-07	0.90171E 06	38.72	0.18066E-02	0.22720E 04	0.341E-04	1.889	15.
29	22.5	24.54	-0.183E-07	0.98164E 06	38.66	0.17601E-02	0.24267E 04	0.338E-04	1.918	15.
30	27.6	24.55	0.613E-08	0.10630E 07	38.70	0.17189E-02	0.25616E 04	0.332E-04	1.933	16.
31	32.6	24.55	0.000E 00	0.11443E 07	38.68	0.16651E-02	0.27021E 04	0.329E-04	1.975	16.
32	37.7	24.58	0.122E-07	0.12265E 07	38.61	0.16561E-02	0.28504E 04	0.328E-04	1.983	16.
33	42.8	24.49	-0.430E-07	0.13033E 07	38.52	0.16003E-02	0.30008E 04	0.325E-04	2.033	16.
34	47.8	24.49	0.000E 00	0.13844E 07	38.55	0.15624E-02	0.31235E 04	0.322E-04	2.059	16.
35	52.9	24.48	-0.619E-08	0.14644E 07	38.71	0.15362E-02	0.32151E 04	0.317E-04	2.063	16.
36	58.0	24.66	0.903E-07	0.15570E 07	38.65	0.14963E-02	0.33522E 04	0.312E-04	2.088	16.
37	63.0	24.87	0.100E-06	0.16519E 07	38.76	0.14518E-02	0.34495E 04	0.305E-04	2.102	17.
38	68.1	25.00	0.636E-07	0.17434E 07	38.91	0.13552E-02	0.35316E 04	0.285E-04	2.100	17.
RECOVERY BEGINS										
39	72.0	24.18	-0.566E-06	0.17471E 07	39.02	0.15313E-02	0.35918E 04	0.520E-04	3.399	16.
40	74.6	24.04	-0.152E-06	0.17773E 07	38.88	0.15210E-02	0.36859E 04	0.506E-04	3.325	16.
41	77.2	24.04	0.000E 00	0.18183E 07	39.40	0.15547E-02	0.36259E 04	0.536E-04	3.450	16.
42	79.8	24.10	0.626E-07	0.18641E 07	39.42	0.15233E-02	0.36839E 04	0.517E-04	3.392	16.
43	82.4	24.18	0.876E-07	0.19117E 07	39.39	0.15460E-02	0.37540E 04	0.523E-04	3.383	17.
44	85.0	24.28	0.980E-07	0.19609E 07	39.35	0.15416E-02	0.38280E 04	0.524E-04	3.399	17.
45	87.6	24.37	0.848E-07	0.20094E 07	39.42	0.14995E-02	0.38733E 04	0.512E-04	3.416	17.
46	90.2	24.45	0.839E-07	0.20582E 07	39.26	0.15531E-02	0.39772E 04	0.523E-04	3.367	17.
47	92.8	24.48	0.241E-07	0.21016E 07	39.12	0.15069E-02	0.40757E 04	0.510E-04	3.382	17.
48	95.4	24.66	0.175E-06	0.21593E 07	39.09	0.15880E-02	0.41503E 04	0.537E-04	3.382	17.
49	98.1	24.63	-0.352E-07	0.21981E 07	39.08	0.15262E-02	0.42182E 04	0.516E-04	3.379	17.
50	100.7	24.63	0.000E 00	0.22401E 07	39.26	0.15881E-02	0.42339E 04	0.545E-04	3.432	17.
51	103.3	24.64	0.117E-07	0.22832E 07	39.10	0.15863E-02	0.43439E 04	0.532E-04	3.351	17.
52	105.9	24.64	0.000E 00	0.23249E 07	39.23	0.16040E-02	0.43729E 04	0.547E-04	3.409	18.
53	108.5	24.65	0.117E-07	0.23680E 07	39.16	0.16084E-02	0.44616E 04	0.542E-04	3.370	18.
54	111.1	24.65	0.000E 00	0.24101E 07	39.22	0.15861E-02	0.45123E 04	0.546E-04	3.444	18.
55	113.7	24.65	0.000E 00	0.24521E 07	38.82	0.15800E-02	0.46946E 04	0.523E-04	3.312	18.
56	116.4	24.64	-0.117E-07	0.24929E 07	39.18	0.16377E-02	0.46535E 04	0.562E-04	3.432	18.
57	118.9	24.64	0.000E 00	0.25346E 07	39.18	0.15731E-02	0.47194E 04	0.540E-04	3.431	18.
58	121.6	24.64	0.000E 00	0.25766E 07	38.86	0.15736E-02	0.48849E 04	0.530E-04	3.367	18.
59	124.2	24.63	-0.117E-07	0.26173E 07	38.82	0.15704E-02	0.49651E 04	0.544E-04	3.462	18.
60	126.8	24.60	-0.236E-07	0.26567E 07	38.28	0.15498E-02	0.52091E 04	0.510E-04	3.294	18.
61	129.4	24.58	-0.236E-07	0.26960E 07	38.78	0.15932E-02	0.51012E 04	0.564E-04	3.542	18.
62	132.0	24.58	0.000E 00	0.27375E 07	38.42	0.14239E-02	0.52875E 04	0.636E-04	4.465	18.

UNCERTAINTY IN REX= 5102.

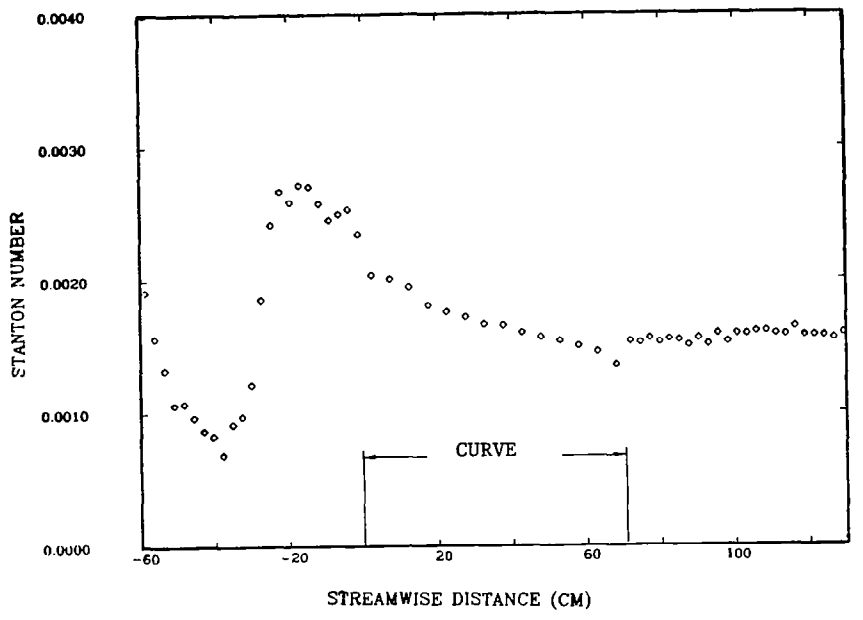

Fig. G-5. Case 060480: Stanton number versus streamwise distance.

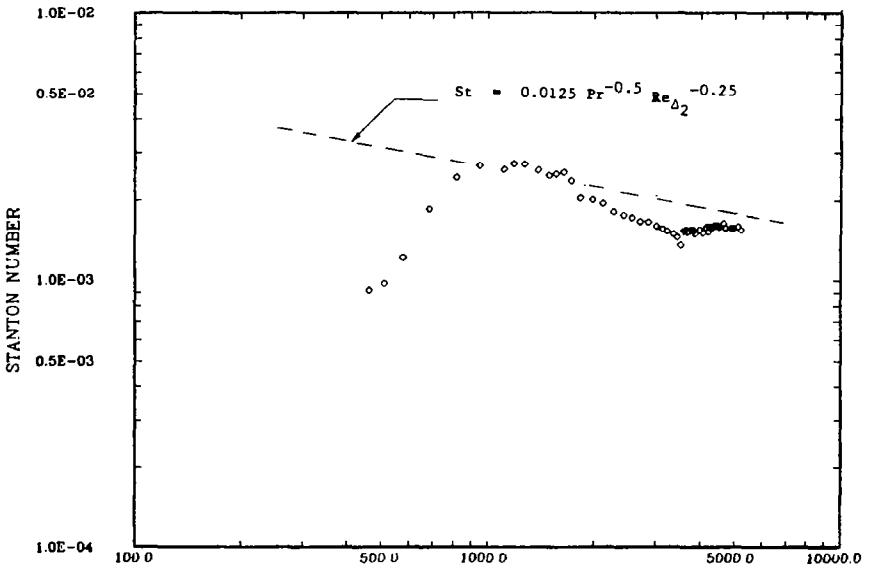

Fig. G-6. Case 060480: Stanton number versus enthalpy thickness Reynolds number.

112779 STARTING PROFILE AT X=-35 CM UPW=26 M/S

REX =	0.18543E 07	REM =	3826.	REH =	1069.
XVO =	-142.53 CM	DEL2 =	0.222 CM	DEH2 =	0.062 CM
UPW =	26.37 M/S	DEL99=	1.899 CM	DELT99 =	1.066 CM
VISC =	0.15284E-04 M2/S	DEL1 =	0.321 CM	UPW =	26.38 M/S
PORT =	4	H =	1.448	VISC =	0.15295E-04 M2/S
XLOC =	-35.05 CM	CF/2 =	0.15451E-02	TINF =	23.80 DEG C
DENS =	1.19 KG/M3			TPLATE =	38.29 DEG C

Y(CM)	Y/DEL	U(M/S)	U/UP	Y+	U+	CF/2	T(DEG C)	Y(CM)	Y+	U(M/S)	T(DEG C)	TBAR	1-TBAR
0.048	0.025	14.07	0.534	32.8	13.58	0.001558	28.76	0.0140	9.47	4.07	31.70	0.455	0.545
0.074	0.039	15.24	0.578	50.0	14.71	0.001575	28.05	0.0394	26.70	11.46	29.01	0.640	0.360
0.099	0.052	15.95	0.605	67.2	15.39	0.001567	27.60	0.0648	43.92	14.83	28.13	0.701	0.299
0.150	0.079	16.89	0.640	101.7	16.29	0.001548	26.93	0.1156	78.37	16.25	27.23	0.764	0.236
0.201	0.106	17.58	0.667	136.1	16.96	0.001542	26.47	0.1664	112.82	17.11	26.65	0.804	0.196
0.249	0.131	18.19	0.690	169.0	17.55	0.001550	26.15	0.2172	147.27	17.79	26.24	0.832	0.168
0.324	0.170	18.89	0.716	219.4	18.23	0.001557	25.75	0.2934	198.95	18.61	25.77	0.864	0.136
0.373	0.197	19.31	0.732	253.2	18.63	0.001565	25.54	0.3442	233.40	19.07	25.54	0.880	0.120
0.449	0.236	19.90	0.755	304.2	19.20	0.001582	25.27	0.4204	285.07	19.68	25.22	0.902	0.098
0.549	0.289	20.59	0.781	372.6	19.86	0.001605	24.98	0.5220	353.97	20.40	24.90	0.924	0.076
0.676	0.356	21.40	0.812	458.3	20.65	0.001643	24.71	0.6490	440.10	21.23	24.60	0.945	0.055
0.802	0.422	22.12	0.839	543.9	21.35	0.001681	24.52	0.7760	526.22	21.98	24.39	0.959	0.041
1.005	0.529	23.16	0.878	681.2	22.35	0.001740	24.29	0.9792	664.02	23.03	24.13	0.977	0.023
1.207	0.636	24.07	0.913	818.6	23.22	0.001795	24.17	1.1824	801.82	23.96	23.99	0.987	0.013
1.486	0.782	25.16	0.954	1007.5	24.27	0.001864	24.11	1.4618	991.29	25.06	23.90	0.993	0.007
1.738	0.915	25.82	0.979	1178.9	24.91	0.001894	24.10	1.7158	1163.54	25.76	23.88	0.995	0.005
2.246	1.182	26.36	1.000	1522.9	25.43	0.001871	24.10						
2.754	1.450	26.39	1.001	1867.4	25.46	0.001804	24.10						

RUN 112779 *** CURVATURE RIG *** NASA-NAG-3-3 STANTON NUMBER DATA

TADB= 24.04 DEG C UREF= 26.36 M/S TINF= 23.74 DEG C
RHO= 1.191 KG/M3 VISC= 0.15291E-04 M2/S XVO= -142.5 CM
CP= 1011. J/KGK PR= 0.714

STANTON RUN DEL99/R(THETA=0)=0.05 UPW=26M/S

PLATE	X (CM)	UPW (M/S)	K	REXVO	TO DEG C	STANTON NO	REENTH	DST	DST(%)	DREEN
1	-61.3	26.36	0.000E 00	0.13992E 07	35.44	0.32494E-02		0.150E-03	4.626	
2	-58.7	26.36	0.000E 00	0.14443E 07	36.90	0.31507E-02		0.105E-03	3.335	
3	-56.1	26.36	0.000E 00	0.14894E 07	37.20	0.30643E-02		0.997E-04	3.255	
4	-53.5	26.36	0.000E 00	0.15341E 07	37.49	0.29104E-02		0.971E-04	3.337	
5	-50.9	26.36	0.000E 00	0.15792E 07	36.41	0.26170E-02		0.823E-04	3.145	
6	-48.3	26.31	-0.446E-07	0.16210E 07	37.73	0.27368E-02		0.912E-04	3.333	
7	-45.7	26.32	0.111E-07	0.16669E 07	37.98	0.26015E-02		0.852E-04	3.273	
8	-43.0	26.35	0.222E-07	0.17136E 07	37.95	0.25339E-02		0.823E-04	3.247	
9	-40.4	26.36	0.112E-07	0.17592E 07	38.12	0.25321E-02		0.827E-04	3.265	
10	-37.8	26.36	0.000E 00	0.18043E 07	38.15	0.24490E-02		0.796E-04	3.252	
11	-35.2	26.36	0.000E 00	0.18494E 07	38.29	0.24392E-02	0.11232E 04	0.798E-04	3.272	9.
12	-32.6	26.36	0.000E 00	0.18944E 07	38.23	0.23466E-02	0.12358E 04	0.766E-04	3.264	9.
13	-30.0	26.33	-0.222E-07	0.19376E 07	38.13	0.23209E-02	0.13487E 04	0.752E-04	3.242	9.
14	-27.4	26.28	-0.452E-07	0.19782E 07	38.31	0.23766E-02	0.14382E 04	0.777E-04	3.270	10.
15	-24.8	26.23	-0.450E-07	0.20191E 07	38.34	0.23588E-02	0.15405E 04	0.769E-04	3.261	10.
16	-22.2	26.21	-0.113E-07	0.20630E 07	38.35	0.23405E-02	0.16448E 04	0.776E-04	3.314	10.
17	-19.5	26.24	0.225E-07	0.21099E 07	37.59	0.22202E-02	0.18355E 04	0.710E-04	3.199	11.
18	-16.9	26.27	0.226E-07	0.21566E 07	38.06	0.23594E-02	0.18765E 04	0.774E-04	3.282	11.
19	-14.3	26.29	0.223E-07	0.22037E 07	38.31	0.23674E-02	0.19500E 04	0.777E-04	3.284	11.
20	-11.7	26.32	0.223E-07	0.22510E 07	38.14	0.22813E-02	0.20781E 04	0.744E-04	3.262	11.
21	-9.1	26.36	0.333E-07	0.22995E 07	38.03	0.22166E-02	0.21949E 04	0.718E-04	3.241	12.
22	-6.5	26.40	0.331E-07	0.23481E 07	38.31	0.22433E-02	0.22527E 04	0.735E-04	3.276	12.
23	-3.9	26.44	0.333E-07	0.23964E 07	38.42	0.23124E-02	0.23386E 04	0.754E-04	3.262	12.
24	-1.3	26.48	0.328E-07	0.24452E 07	38.47	0.22042E-02	0.24331E 04	0.721E-04	3.271	12.
CURVE BEGINS										
25	2.4	28.61	0.105E-05	0.27105E 07	38.54	0.18363E-02	0.25608E 04	0.861E-04	4.680	14.
26	7.3	28.90	0.108E-06	0.28306E 07	38.61	0.18402E-02	0.27194E 04	0.839E-04	4.549	15.
27	12.4	28.83	-0.262E-07	0.29193E 07	38.67	0.17861E-02	0.28835E 04	0.822E-04	4.593	16.
28	17.4	28.78	-0.176E-07	0.30096E 07	38.63	0.16921E-02	0.30565E 04	0.774E-04	4.564	17.
29	22.5	28.73	-0.176E-07	0.31000E 07	38.76	0.16480E-02	0.31902E 04	0.762E-04	4.616	18.
30	27.6	28.74	0.443E-08	0.31963E 07	38.85	0.15595E-02	0.33238E 04	0.731E-04	4.675	19.
31	32.6	28.76	0.440E-08	0.32932E 07	38.74	0.15252E-02	0.34958E 04	0.711E-04	4.653	19.
32	37.7	28.76	0.000E 00	0.33882E 07	38.75	0.14639E-02	0.36363E 04	0.688E-04	4.693	20.
33	42.8	28.65	-0.400E-07	0.34705E 07	38.80	0.14413E-02	0.37634E 04	0.682E-04	4.721	20.
34	47.8	28.52	-0.451E-07	0.35506E 07	38.96	0.13853E-02	0.38576E 04	0.668E-04	4.813	21.
35	52.9	28.46	-0.228E-07	0.36371E 07	38.97	0.12985E-02	0.39842E 04	0.637E-04	4.893	21.
36	58.0	28.52	0.225E-07	0.37396E 07	39.14	0.12563E-02	0.40595E 04	0.628E-04	4.984	21.
37	63.0	28.69	0.623E-07	0.38568E 07	39.03	0.12257E-02	0.42065E 04	0.624E-04	5.078	22.
38	68.1	28.77	0.264E-07	0.39621E 07	39.02	0.11160E-02	0.43232E 04	0.576E-04	5.149	22.
RECOVERY BEGINS										
39	72.0	28.51	-0.125E-06	0.39985E 07	39.07	0.13656E-02	0.43900E 04	0.457E-04	3.345	22.
40	74.6	28.51	0.000E 00	0.40473E 07	38.92	0.13606E-02	0.44997E 04	0.444E-04	3.267	23.
41	77.2	28.51	0.000E 00	0.40961E 07	39.43	0.13882E-02	0.44189E 04	0.470E-04	3.387	23.
42	79.8	28.51	0.000E 00	0.41448E 07	39.46	0.13559E-02	0.44760E 04	0.454E-04	3.346	23.
43	82.4	28.51	0.000E 00	0.41932E 07	39.39	0.14018E-02	0.45644E 04	0.464E-04	3.311	23.
44	85.0	28.51	0.000E 00	0.42419E 07	39.45	0.13810E-02	0.46138E 04	0.466E-04	3.373	23.
45	87.6	28.51	0.000E 00	0.42907E 07	39.42	0.13769E-02	0.46912E 04	0.462E-04	3.356	23.
46	90.2	28.51	0.000E 00	0.43395E 07	39.16	0.14515E-02	0.48365E 04	0.479E-04	3.300	23.
47	92.8	28.51	0.000E 00	0.43876E 07	39.04	0.13996E-02	0.49456E 04	0.466E-04	3.330	23.
48	95.4	28.51	0.000E 00	0.44366E 07	38.94	0.14982E-02	0.50479E 04	0.498E-04	3.322	23.
49	98.1	28.51	0.000E 00	0.44854E 07	38.90	0.14329E-02	0.51309E 04	0.475E-04	3.318	23.
50	100.7	28.51	0.000E 00	0.45341E 07	39.10	0.15139E-02	0.51378E 04	0.511E-04	3.375	23.
51	103.3	28.51	0.000E 00	0.45829E 07	38.91	0.15181E-02	0.52741E 04	0.499E-04	3.286	23.
52	105.9	28.51	0.000E 00	0.46312E 07	39.09	0.15203E-02	0.52856E 04	0.510E-04	3.357	23.
53	108.5	28.51	0.000E 00	0.46800E 07	38.97	0.15480E-02	0.54023E 04	0.510E-04	3.297	23.
54	111.1	28.51	0.000E 00	0.47288E 07	39.05	0.15373E-02	0.54488E 04	0.520E-04	3.382	23.
55	113.7	28.51	0.000E 00	0.47776E 07	38.63	0.15263E-02	0.56760E 04	0.495E-04	3.242	23.
56	116.4	28.51	0.000E 00	0.48264E 07	39.01	0.15798E-02	0.56073E 04	0.533E-04	3.371	24.
57	118.9	28.51	0.000E 00	0.48747E 07	38.98	0.15268E-02	0.56938E 04	0.514E-04	3.370	24.
58	121.6	28.51	0.000E 00	0.49234E 07	38.60	0.15464E-02	0.59148E 04	0.511E-04	3.301	24.
59	124.2	28.51	0.000E 00	0.49722E 07	38.53	0.15454E-02	0.60155E 04	0.524E-04	3.394	24.
60	126.8	28.51	0.000E 00	0.50210E 07	37.92	0.15609E-02	0.63461E 04	0.502E-04	3.216	24.
61	129.4	28.51	0.000E 00	0.50698E 07	38.55	0.15749E-02	0.61475E 04	0.545E-04	3.458	24.
62	132.0	28.51	0.000E 00	0.51186E 07	38.30	0.13638E-02	0.63204E 04	0.609E-04	4.462	24.

UNCERTAINTY IN REX=34371.

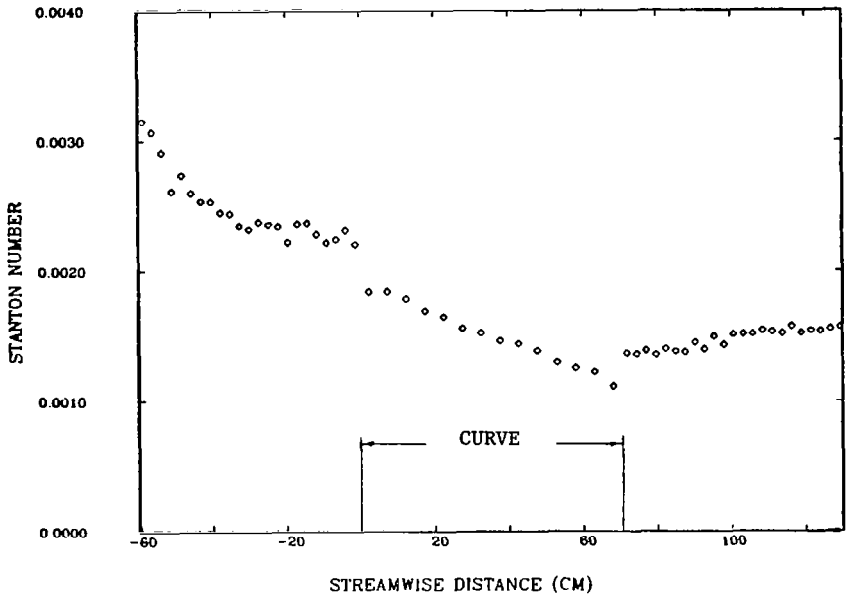

Fig. G-7. Case 112779: Stanton number versus streamwise distance.

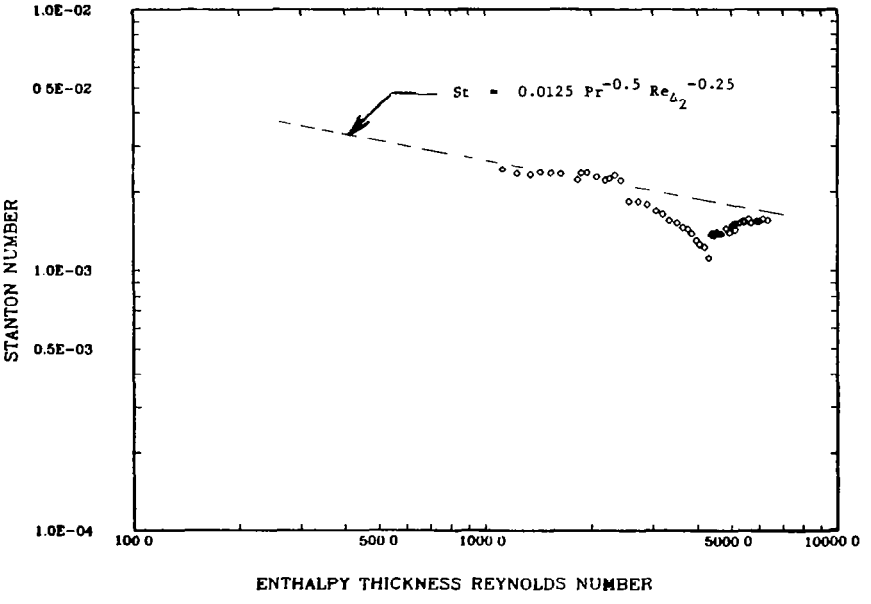

Fig. G-8. Case 112779: Stanton number versus enthalpy thickness Reynolds number.

011380 STARTING PROFILES DEL99/R(THETA=0)=0.08 UPW=7 M/S TURBULENT

REX = 0.51124E 06 REM = 1365. REH = 520.
XVO = -147.42 CM DEL2 = 0.300 CM DEH2 = 0.114 CM
UPW = 7.00 M/S DEL99= 2.699 CM DELT99 = 1.613 CM
VISC = 0.15391E-04 M2/S DEL1 = 0.432 CM UPW = 7.00 M/S
PORT = 4 H = 1.440 VISC = 0.15381E-04 M2/S
XLOC = -35.05 CM CF/2 = 0.20816E-02 TINF = 22.82 DEG C
DENS = 1.18 KG/M3 TPLATE = 38.57 DEG C

Y(CM)	Y/DEL	U(M/S)	U/UP	Y+	U+	CF/2	T(DEG C)
0.048	0.018	2.87	0.410	10.0	9.00	0.001589	31.40
0.074	0.027	3.42	0.488	15.3	10.70	0.001806	29.79
0.099	0.037	3.83	0.547	20.6	11.98	0.001972	28.81
0.150	0.056	4.25	0.606	31.1	13.29	0.002056	27.47
0.201	0.074	4.53	0.647	41.7	14.19	0.002105	26.72
0.248	0.092	4.71	0.673	51.6	14.76	0.002116	26.24
0.323	0.120	4.84	0.692	67.0	15.16	0.002060	25.65
0.374	0.139	4.97	0.710	77.7	15.56	0.002069	25.36
0.448	0.166	5.14	0.734	92.9	16.08	0.002088	25.01
0.549	0.203	5.26	0.751	114.0	16.45	0.002060	24.60
0.675	0.250	5.49	0.784	140.1	17.19	0.002109	24.21
0.801	0.297	5.60	0.800	166.3	17.54	0.002095	23.89
1.004	0.372	5.86	0.836	208.5	18.33	0.002145	23.53
1.207	0.447	6.07	0.867	250.5	18.99	0.002187	23.28
1.486	0.550	6.31	0.900	308.4	19.74	0.002231	23.06
1.739	0.644	6.47	0.924	361.0	20.25	0.002254	22.97
2.247	0.833	6.79	0.969	466.3	21.25	0.002321	22.87
2.754	1.020	6.94	0.991	571.6	21.73	0.002313	22.84
3.769	1.397	7.00	1.000	782.4	21.92	0.002200	22.84
4.531	1.679	7.00	1.000	940.6	21.92	0.002119	22.84

Y(CM)	Y+	U(M/S)	T(DEG C)	TBAR	1-TBAR
0.0140	2.90	0.83	37.34	0.078	0.922
0.0394	8.17	2.34	32.09	0.412	0.588
0.0648	13.44	3.23	30.13	0.536	0.464
0.1156	23.99	3.96	28.17	0.661	0.339
0.1664	34.53	4.34	27.13	0.726	0.274
0.2172	45.08	4.60	26.51	0.766	0.234
0.2934	60.90	4.79	25.83	0.809	0.191
0.3442	71.44	4.90	25.51	0.829	0.171
0.4204	87.26	5.08	25.12	0.854	0.146
0.5220	108.35	5.22	24.68	0.882	0.118
0.6490	134.71	5.44	24.27	0.908	0.092
0.7760	161.07	5.58	23.93	0.930	0.070
0.9792	203.25	5.83	23.55	0.954	0.046
1.1824	245.43	6.04	23.29	0.970	0.030
1.4618	303.43	6.28	23.06	0.985	0.015
1.7158	356.15	6.45	22.96	0.991	0.009
2.2238	461.60	6.77	22.86	0.998	0.002
2.7318	567.05	6.93	22.82	1.000	0.000
3.3668	698.86	6.98	22.82	1.000	0.000

RUN 011380 *** CURVATURE RIG *** NASA-NAG-3-3 STANTON NUMBER DATA

TADB= 22.95 DEG C UREF= 7.00 M/S TINF= 22.93 DEG C
RHO= 1.178 KG/M3 VISC= 0.15393E-04 M2/S XVO= -147.3 CM
CP= 1014. J/KGK PR= 0.717

STANTON RUN DEL99/R(THETA=0)=0.08 UPW=7M/S K=0.0 TURBULENT

PLATE	X (CM)	UPW (M/S)	K	REXVO	TO DEG C	STANTON NO	REENTH	DST	DST(%)	DREEN
1	-61.3	7.00	0.000E 00	0.39099E 06	36.65	0.30762E-02		0.347E-03	11.296	
2	-58.7	7.00	0.000E 00	0.40288E 06	37.84	0.41987E-02		0.150E-03	3.574	
3	-56.1	7.00	0.000E 00	0.41478E 06	38.09	0.40432E-02		0.138E-03	3.422	
4	-53.5	7.00	0.000E 00	0.42655E 06	38.25	0.38321E-02		0.135E-03	3.510	
5	-50.9	7.00	0.000E 00	0.43845E 06	37.81	0.33413E-02		0.111E-03	3.323	
6	-48.3	7.00	0.000E 00	0.45034E 06	38.48	0.34930E-02		0.124E-03	3.554	
7	-45.7	7.00	0.000E 00	0.46224E 06	38.62	0.33405E-02		0.117E-03	3.489	
8	-43.0	7.00	0.000E 00	0.47413E 06	38.61	0.32290E-02		0.112E-03	3.471	
9	-40.4	7.00	0.000E 00	0.48591E 06	38.63	0.32710E-02		0.113E-03	3.461	
10	-37.8	7.00	0.000E 00	0.49781E 06	38.68	0.31471E-02		0.110E-03	3.490	
11	-35.2	7.00	0.000E 00	0.50970E 06	38.73	0.31567E-02	0.53840E 03	0.110E-03	3.494	23.
12	-32.6	7.00	0.000E 00	0.52159E 06	38.73	0.30094E-02	0.57517E 03	0.106E-03	3.518	23.
13	-30.0	7.00	0.000E 00	0.53349E 06	38.67	0.30082E-02	0.61296E 03	0.105E-03	3.491	23.
14	-27.4	7.00	0.000E 00	0.54527E 06	38.69	0.30778E-02	0.64835E 03	0.108E-03	3.513	23.
15	-24.8	7.00	0.000E 00	0.55716E 06	38.71	0.30520E-02	0.68391E 03	0.106E-03	3.488	23.
16	-22.2	7.00	0.000E 00	0.56906E 06	38.74	0.30272E-02	0.71884E 03	0.108E-03	3.555	23.
17	-19.5	7.00	0.000E 00	0.58095E 06	38.44	0.28511E-02	0.76756E 03	0.985E-04	3.455	23.
18	-16.9	7.00	0.000E 00	0.59273E 06	38.65	0.29441E-02	0.79124E 03	0.104E-03	3.541	23.
19	-14.3	7.00	0.000E 00	0.60462E 06	38.75	0.29846E-02	0.82173E 03	0.105E-03	3.535	23.
20	-11.7	7.00	0.000E 00	0.61652E 06	38.62	0.29574E-02	0.86394E 03	0.103E-03	3.485	23.
21	-9.1	7.00	0.000E 00	0.62841E 06	38.64	0.28311E-02	0.89710E 03	0.992E-04	3.503	23.
22	-6.5	7.00	0.000E 00	0.64031E 06	38.77	0.28053E-02	0.92311E 03	0.995E-04	3.546	23.
23	-3.9	7.00	0.000E 00	0.65209E 06	38.84	0.28737E-02	0.95289E 03	0.101E-03	3.518	23.
24	-1.3	7.00	0.000E 00	0.66398E 06	38.92	0.26773E-02	0.98080E 03	0.983E-04	3.672	23.
CURVE BEGINS										
25	2.4	6.31	-0.773E-05	0.61331E 06	38.83	0.24397E-02	0.10306E 04	0.115E-03	4.710	21.
26	7.3	6.20	-0.837E-06	0.62317E 06	38.83	0.23791E-02	0.10781E 04	0.901E-04	3.786	21.
27	12.4	6.07	-0.113E-05	0.62957E 06	38.82	0.23431E-02	0.11271E 04	0.893E-04	3.812	20.
28	17.4	6.00	-0.587E-06	0.64211E 06	38.85	0.22002E-02	0.11700E 04	0.892E-04	4.055	20.
29	22.5	6.00	0.000E 00	0.66191E 06	38.94	0.21276E-02	0.12063E 04	0.883E-04	4.149	20.
30	27.6	6.00	0.000E 00	0.68161E 06	39.01	0.19218E-02	0.12417E 04	0.867E-04	4.509	20.
31	32.6	6.00	0.000E 00	0.70142E 06	38.93	0.18269E-02	0.12850E 04	0.867E-04	4.744	20.
32	37.7	6.00	0.000E 00	0.72112E 06	39.02	0.17711E-02	0.13136E 04	0.859E-04	4.851	20.
33	42.8	6.11	0.848E-06	0.75391E 06	39.04	0.16635E-02	0.13472E 04	0.843E-04	5.068	21.
34	47.8	6.00	-0.693E-06	0.76072E 06	38.99	0.16171E-02	0.13841E 04	0.855E-04	5.285	20.
35	52.9	5.97	-0.281E-06	0.77616E 06	39.02	0.15784E-02	0.14128E 04	0.855E-04	5.418	20.
36	58.0	6.00	0.275E-06	0.80022E 06	39.00	0.15373E-02	0.14456E 04	0.850E-04	5.529	20.
37	63.0	6.04	0.305E-06	0.82493E 06	39.08	0.14521E-02	0.14685E 04	0.835E-04	5.752	21.
38	68.1	6.07	0.266E-06	0.84938E 06	39.12	0.12424E-02	0.14916E 04	0.784E-04	6.315	21.
RECOVERY BEGINS										
39	72.0	6.07	0.000E 00	0.86450E 06	39.23	0.14320E-02	0.14979E 04	0.643E-04	4.489	21.
40	74.6	6.07	0.000E 00	0.87481E 06	39.16	0.15339E-02	0.15200E 04	0.674E-04	4.394	21.
41	77.2	6.07	0.000E 00	0.88513E 06	39.25	0.17057E-02	0.15282E 04	0.737E-04	4.321	21.
42	79.8	6.07	0.000E 00	0.89544E 06	39.25	0.17218E-02	0.15458E 04	0.741E-04	4.302	21.
43	82.4	6.07	0.000E 00	0.90566E 06	39.19	0.18579E-02	0.15697E 04	0.769E-04	4.139	21.
44	85.0	6.07	0.000E 00	0.91597E 06	39.23	0.18232E-02	0.15851E 04	0.793E-04	4.347	21.
45	87.6	6.07	0.000E 00	0.92629E 06	39.24	0.17817E-02	0.16023E 04	0.758E-04	4.255	21.
46	90.2	6.07	0.000E 00	0.93660E 06	39.09	0.19231E-02	0.16356E 04	0.770E-04	4.005	21.
47	92.8	6.07	0.000E 00	0.94682E 06	39.09	0.18514E-02	0.16560E 04	0.770E-04	4.159	21.
48	95.4	6.07	0.000E 00	0.95713E 06	39.04	0.19522E-02	0.16801E 04	0.803E-04	4.113	21.
49	98.1	6.07	0.000E 00	0.96745E 06	39.07	0.18906E-02	0.16970E 04	0.797E-04	4.215	21.
50	100.7	6.07	0.000E 00	0.97776E 06	39.11	0.19550E-02	0.17128E 04	0.825E-04	4.222	21.
51	103.3	6.07	0.000E 00	0.98807E 06	39.01	0.19918E-02	0.17432E 04	0.808E-04	4.058	21.
52	105.9	6.07	0.000E 00	0.99829E 06	39.08	0.19887E-02	0.17560E 04	0.829E-04	4.166	21.
53	108.5	6.07	0.000E 00	0.10086E 07	39.02	0.20607E-02	0.17843E 04	0.833E-04	4.041	21.
54	111.1	6.07	0.000E 00	0.10189E 07	39.04	0.20335E-02	0.18024E 04	0.845E-04	4.156	21.
55	113.7	6.07	0.000E 00	0.10292E 07	38.85	0.21117E-02	0.18454E 04	0.831E-04	3.935	21.
56	116.4	6.07	0.000E 00	0.10395E 07	39.02	0.21157E-02	0.18473E 04	0.873E-04	4.127	21.
57	118.9	6.07	0.000E 00	0.10498E 07	39.03	0.20527E-02	0.18677E 04	0.851E-04	4.145	21.
58	121.6	6.07	0.000E 00	0.10601E 07	38.87	0.21059E-02	0.19082E 04	0.851E-04	4.039	21.
59	124.2	6.07	0.000E 00	0.10704E 07	38.84	0.20947E-02	0.19330E 04	0.858E-04	4.098	21.
60	126.8	6.07	0.000E 00	0.10807E 07	38.63	0.20734E-02	0.19798E 04	0.820E-04	3.955	21.
61	129.4	6.07	0.000E 00	0.10910E 07	38.83	0.20358E-02	0.19769E 04	0.912E-04	4.481	21.
62	132.0	6.07	0.000E 00	0.11012E 07	38.37	0.17375E-02	0.20541E 04	0.130E-03	7.508	21.

UNCERTAINTY IN REX=12518.

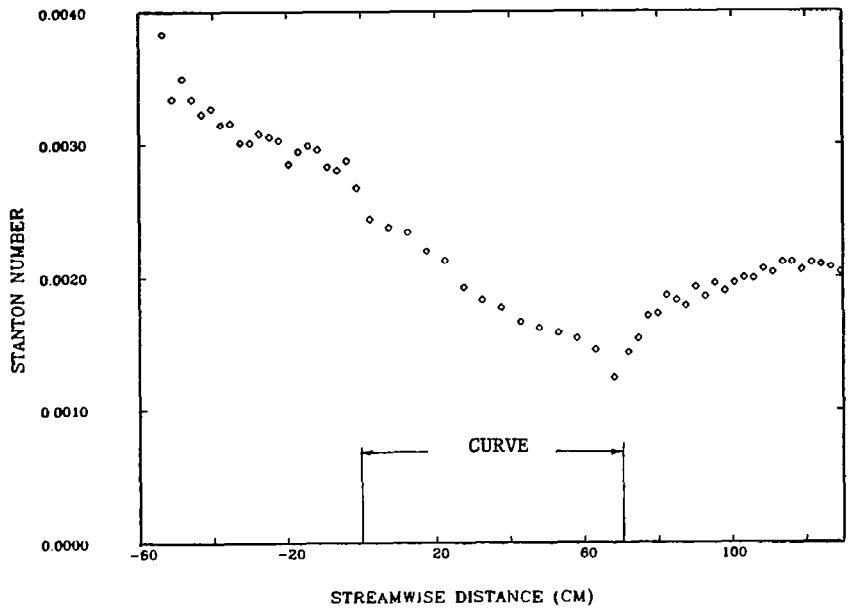

Fig. G-9. Case 011380: Stanton number versus streamwise distance.

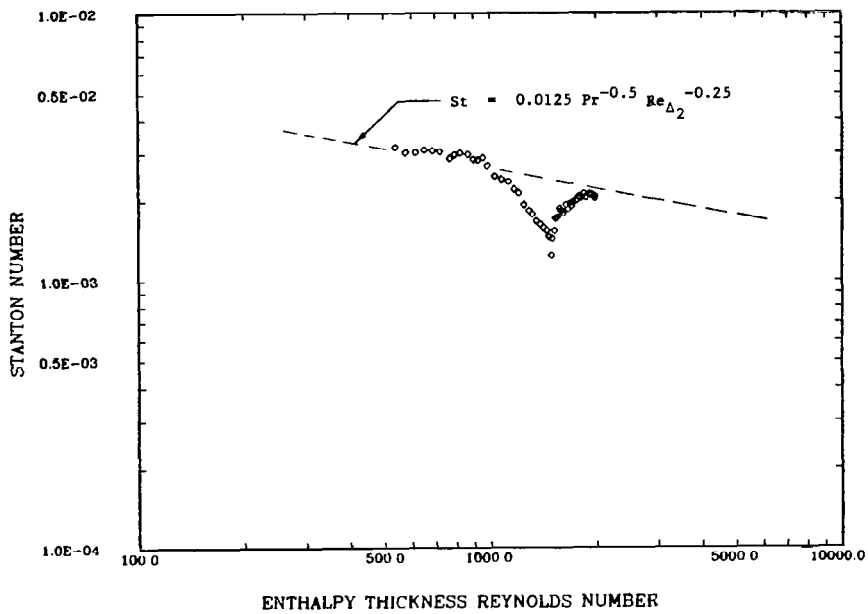

Fig. G-10. Case 011380: Stanton number versus enthalpy thickness Reynolds number.

RUN 113079 *** CURVATURE RIG *** NASA-NAG-3-3 STANTON NUMBER DATA

TADB= 23.43 DEG C UREF= 14.52 M/S TINF= 23.33 DEG C
RHO= 1.189 KG/M3 VISC= 0.15305E-04 M2/S XVO= -118.7 CM
CP= 1011. J/KGK PR= 0.715

STANTON RUN DEL99/R(THETA=0)=0.05 DEH2/R(THETA=0)=0.0 TURBULENT

PLATE	X (CM)	UPW (M/S)	K	REXVO	TO DEG C	STANTON NO	REENTH	DST	DST(%)	DREEN
1	-61.3	14.52	0.000E 00	0.54471E 06	23.33					
2	-58.7	14.52	0.000E 00	0.56953E 06	23.32					
3	-56.1	14.52	0.000E 00	0.59436E 06	23.32					
4	-53.5	14.52	0.000E 00	0.61895E 06	23.33					
5	-50.9	14.52	0.000E 00	0.64378E 06	23.34					
6	-48.3	14.52	0.000E 00	0.66861E 06	23.36					
7	-45.7	14.52	0.000E 00	0.69343E 06	23.36					
8	-43.0	14.52	0.000E 00	0.71826E 06	23.38					
9	-40.4	14.52	0.000E 00	0.74285E 06	23.39					
10	-37.8	14.52	0.000E 00	0.76768E 06	23.40					
11	-35.2	14.52	0.000E 00	0.79250E 06	23.42					
12	-32.6	14.52	0.000E 00	0.81733E 06	23.46					
13	-30.0	14.52	0.000E 00	0.84216E 06	23.49					
14	-27.4	14.52	0.000E 00	0.86675E 06	23.47					
15	-24.8	14.52	0.000E 00	0.89157E 06	23.53					
16	-22.2	14.52	0.000E 00	0.91640E 06	23.61					
17	-19.5	14.52	0.000E 00	0.94123E 06	23.65					
18	-16.9	14.52	0.000E 00	0.96582E 06	23.69					
19	-14.3	14.52	0.000E 00	0.99064E 06	23.72					
20	-11.7	14.52	0.000E 00	0.10155E 07	23.70					
21	-9.1	14.52	0.000E 00	0.10403E 07	23.64					
22	-6.5	14.52	0.000E 00	0.10651E 07	23.49					
23	-3.9	14.52	0.000E 00	0.10897E 07	23.22					
24	-1.3	14.52	0.000E 00	0.11145E 07	22.68					
CURVE BEGINS										
25	2.4	14.60	0.142E-06	0.11550E 07	37.43	0.37250E-02	0.83741E 02	0.260E-03	6.972	0.
26	7.3	14.59	-0.106E-07	0.12011E 07	37.56	0.28531E-02	0.23565E 03	0.130E-03	4.552	7.
27	12.4	14.45	-0.200E-06	0.12377E 07	37.59	0.27202E-02	0.36855E 03	0.124E-03	4.549	8.
28	17.4	14.40	-0.749E-07	0.12809E 07	37.61	0.24689E-02	0.49196E 03	0.114E-03	4.600	9.
29	22.5	14.42	0.212E-07	0.13301E 07	37.62	0.23397E-02	0.60654E 03	0.108E-03	4.613	10.
30	27.6	14.44	0.424E-07	0.13805E 07	37.61	0.22120E-02	0.71609E 03	0.103E-03	4.632	10.
31	32.6	14.49	0.627E-07	0.14327E 07	37.64	0.21405E-02	0.81893E 03	0.100E-03	4.665	11.
32	37.7	14.50	0.209E-07	0.14821E 07	37.70	0.20914E-02	0.91780E 03	0.983E-04	4.693	11.
33	42.8	14.52	0.311E-07	0.15325E 07	37.71	0.20312E-02	0.10163E 04	0.956E-04	4.699	12.
34	47.8	14.45	-0.105E-06	0.15728E 07	37.70	0.19820E-02	0.11135E 04	0.940E-04	4.734	12.
35	52.9	14.44	-0.106E-07	0.16197E 07	37.68	0.19253E-02	0.12083E 04	0.910E-04	4.718	13.
36	58.0	14.50	0.730E-07	0.16735E 07	37.68	0.17970E-02	0.12986E 04	0.868E-04	4.820	13.
37	63.0	14.61	0.164E-06	0.17352E 07	37.65	0.16921E-02	0.13853E 04	0.822E-04	4.847	13.
38	68.1	14.64	0.405E-07	0.17872E 07	37.66	0.15025E-02	0.14622E 04	0.750E-04	4.983	14.
RECOVERY BEGINS										
39	72.0	14.60	-0.812E-07	0.18185E 07	37.70	0.16708E-02	0.15160E 04	0.589E-04	3.524	14.
40	74.6	14.55	-0.120E-06	0.18380E 07	37.51	0.17257E-02	0.15783E 04	0.592E-04	3.431	14.
41	77.2	14.50	-0.142E-06	0.18563E 07	37.83	0.17605E-02	0.15861E 04	0.627E-04	3.561	14.
42	79.8	14.45	-0.143E-06	0.18745E 07	37.87	0.17002E-02	0.16239E 04	0.602E-04	3.541	14.
43	82.4	14.40	-0.146E-06	0.18923E 07	37.84	0.17717E-02	0.16701E 04	0.618E-04	3.487	14.
44	85.0	14.44	0.123E-06	0.19227E 07	37.91	0.17183E-02	0.17051E 04	0.615E-04	3.581	14.
45	87.6	14.48	0.102E-06	0.19523E 07	37.92	0.16934E-02	0.17467E 04	0.601E-04	3.549	14.
46	90.2	14.52	0.101E-06	0.19820E 07	37.75	0.17735E-02	0.18099E 04	0.616E-04	3.473	14.
47	92.8	14.55	0.101E-06	0.20116E 07	37.63	0.17286E-02	0.18676E 04	0.605E-04	3.502	14.
48	95.4	14.57	0.399E-07	0.20385E 07	37.62	0.18127E-02	0.19141E 04	0.636E-04	3.507	14.
49	98.1	14.58	0.398E-07	0.20655E 07	37.61	0.17348E-02	0.19589E 04	0.611E-04	3.525	14.
50	100.7	14.58	0.000E 00	0.20904E 07	37.73	0.18075E-02	0.19863E 04	0.646E-04	3.574	14.
51	103.3	14.58	0.000E 00	0.21153E 07	37.63	0.18184E-02	0.20459E 04	0.632E-04	3.476	14.
52	105.9	14.58	0.000E 00	0.21400E 07	37.75	0.18104E-02	0.20741E 04	0.643E-04	3.553	14.
53	108.5	14.58	0.000E 00	0.21650E 07	37.67	0.18329E-02	0.21308E 04	0.640E-04	3.491	14.
54	111.1	14.58	0.000E 00	0.21899E 07	37.69	0.18033E-02	0.21729E 04	0.646E-04	3.582	14.
55	113.7	14.58	0.000E 00	0.22148E 07	37.38	0.18380E-02	0.22662E 04	0.627E-04	3.411	15.
56	116.4	14.59	0.199E-07	0.22408E 07	37.67	0.18626E-02	0.22654E 04	0.665E-04	3.569	15.
57	118.9	14.59	0.000E 00	0.22655E 07	37.67	0.18004E-02	0.23100E 04	0.642E-04	3.567	15.
58	121.6	14.59	0.000E 00	0.22905E 07	37.44	0.18030E-02	0.23923E 04	0.631E-04	3.499	15.
59	124.2	14.59	0.000E 00	0.23154E 07	37.42	0.17963E-02	0.24415E 04	0.646E-04	3.596	15.
60	126.8	14.59	0.000E 00	0.23404E 07	37.02	0.18127E-02	0.25556E 04	0.617E-04	3.404	15.
61	129.4	14.59	0.000E 00	0.23653E 07	37.40	0.17850E-02	0.25305E 04	0.666E-04	3.730	15.
62	132.0	14.59	0.000E 00	0.23900E 07	37.10	0.15729E-02	0.26284E 04	0.824E-04	5.236	15.

UNCERTAINTY IN REX=12534.

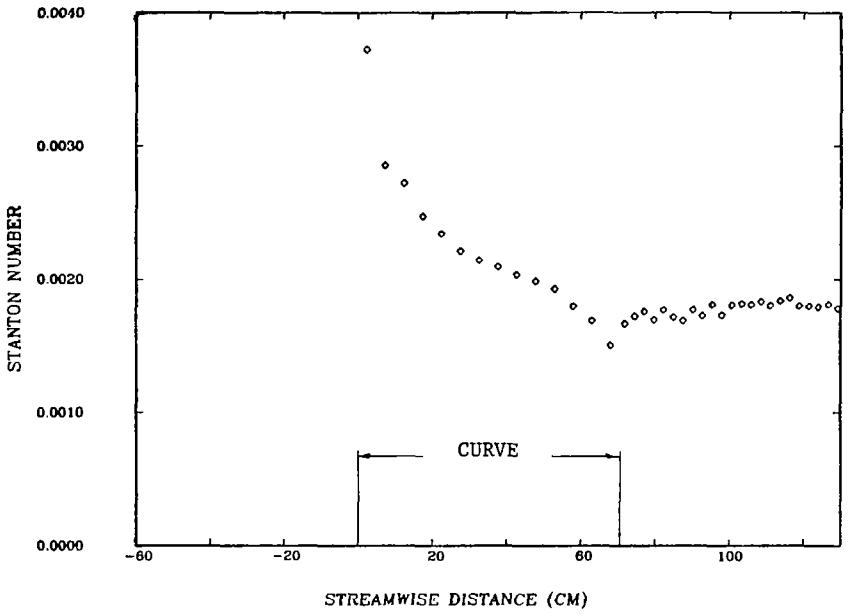

Fig. G-11. Case 113079: Stanton number versus streamwise distance.

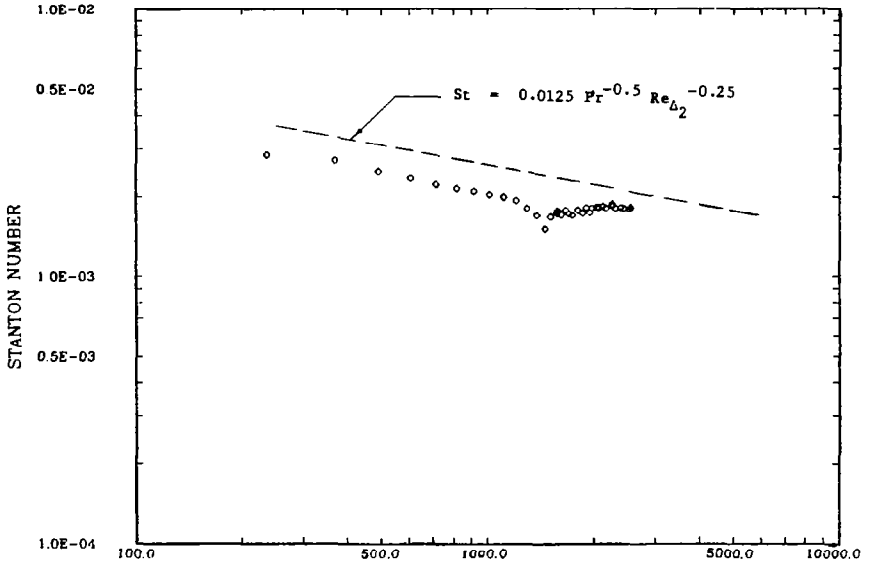

Fig. G-12. Case 113079: Stanton number versus enthalpy thickness Reynolds number.

RUN 030280 *** CURVATURE RIG *** NASA-NAG-3-3 STANTON NUMBER DATA

TADB= 21.78 DEG C UREF= 14.46 M/S TINF= 21.69 DEG C
RHO= 1.187 KG/M3 VISC= 0.15245E-04 M2/S XVO= -118.6 CM
CP= 1012. J/KGK PR= 0.716

STANTON RUN DEL99/R(THETA=0)=0.05 DEH2/R(THETA=90 DEG)=0.0 TURBULEN

PLATE	X (CM)	UPW (M/S)	K	REXVO	TO DEG C	STANTON NO	REENTH	DST	DST(Z)	DREEN
1	-61.3	14.46	0.000E 00	0.54348E 06	21.59					
2	-58.7	14.46	0.000E 00	0.56830E 06	21.57					
3	-56.1	14.46	0.000E 00	0.59311E 06	21.57					
4	-53.5	14.46	0.000E 00	0.61769E 06	21.57					
5	-50.9	14.46	0.000E 00	0.64250E 06	21.57					
6	-48.3	14.46	0.000E 00	0.66732E 06	21.57					
7	-45.7	14.46	0.000E 00	0.69213E 06	21.57					
8	-43.0	14.46	0.000E 00	0.71695E 06	21.57					
9	-40.4	14.46	0.000E 00	0.74153E 06	21.57					
10	-37.8	14.46	0.000E 00	0.76634E 06	21.57					
11	-35.2	14.46	0.000E 00	0.79116E 06	21.57					
12	-32.6	14.46	0.000E 00	0.81597E 06	21.57					
13	-30.0	14.46	0.000E 00	0.84079E 06	21.59					
14	-27.4	14.46	0.000E 00	0.86536E 06	21.53					
15	-24.8	14.46	0.000E 00	0.89018E 06	21.55					
16	-22.2	14.46	0.000E 00	0.91500E 06	21.55					
17	-19.5	14.46	0.000E 00	0.93981E 06	21.55					
18	-16.9	14.46	0.000E 00	0.96439E 06	21.57					
19	-14.3	14.46	0.000E 00	0.98920E 06	21.57					
20	-11.7	14.46	0.000E 00	0.10140E 07	21.59					
21	-9.1	14.46	0.000E 00	0.10388E 07	21.57					
22	-6.5	14.46	0.000E 00	0.10637E 07	21.59					
23	-3.9	14.46	0.000E 00	0.10882E 07	21.61					
24	-1.3	14.46	0.000E 00	0.11130E 07	21.63					
CURVE BEGINS										
25	2.4	14.46	0.000E 00	0.11477E 07	21.57					
26	7.3	14.46	0.000E 00	0.11942E 07	21.65					
27	12.4	14.46	0.000E 00	0.12424E 07	21.65					
28	17.4	14.46	0.000E 00	0.12904E 07	21.69					
29	22.5	14.46	0.000E 00	0.13386E 07	21.68					
30	27.6	14.46	0.000E 00	0.13865E 07	21.69					
31	32.6	14.46	0.000E 00	0.14347E 07	21.68					
32	37.7	14.46	0.000E 00	0.14826E 07	21.68					
33	42.8	14.46	0.000E 00	0.15308E 07	21.70					
34	47.8	14.46	0.000E 00	0.15790E 07	21.70					
35	52.9	14.46	0.000E 00	0.16269E 07	21.77					
36	58.0	14.46	0.000E 00	0.16751E 07	21.92					
37	63.0	14.46	0.000E 00	0.17231E 07	22.46					
38	68.1	14.46	0.000E 00	0.17713E 07	24.67					
RECOVERY BEGINS										
39	72.0	14.53	0.135E-06	0.18167E 07	35.73	0.31153E-02	0.38771E 02	0.170E-03	5.444	0.
40	74.6	14.49	-0.120E-06	0.18361E 07	36.89	0.28238E-02	0.10942E 03	0.955E-04	3.381	2.
41	77.2	14.44	-0.142E-06	0.18545E 07	37.83	0.26441E-02	0.17045E 03	0.905E-04	3.424	3.
42	79.8	14.39	-0.143E-06	0.18727E 07	38.05	0.24651E-02	0.23113E 03	0.825E-04	3.348	3.
43	82.4	14.34	-0.146E-06	0.18904E 07	38.15	0.24480E-02	0.29007E 03	0.815E-04	3.328	4.
44	85.0	14.38	0.123E-06	0.19208E 07	38.27	0.23435E-02	0.34691E 03	0.791E-04	3.376	4.
45	87.6	14.42	0.102E-06	0.19504E 07	38.34	0.22721E-02	0.40243E 03	0.766E-04	3.372	4.
46	90.2	14.45	0.101E-06	0.19801E 07	38.20	0.23210E-02	0.46259E 03	0.772E-04	3.324	4.
47	92.8	14.49	0.101E-06	0.20097E 07	38.10	0.22349E-02	0.52221E 03	0.745E-04	3.335	5.
48	95.4	14.50	0.399E-07	0.20366E 07	38.11	0.23248E-02	0.57831E 03	0.777E-04	3.343	5.
49	98.1	14.52	0.398E-07	0.20635E 07	38.15	0.22064E-02	0.63328E 03	0.738E-04	3.346	5.
50	100.7	14.52	0.000E 00	0.20884E 07	38.36	0.22526E-02	0.68058E 03	0.767E-04	3.405	5.
51	103.3	14.52	0.000E 00	0.21134E 07	38.27	0.22365E-02	0.74009E 03	0.743E-04	3.321	5.
52	105.9	14.52	0.000E 00	0.21380E 07	38.45	0.22291E-02	0.78762E 03	0.756E-04	3.391	5.
53	108.5	14.52	0.000E 00	0.21629E 07	38.39	0.22309E-02	0.84609E 03	0.745E-04	3.338	6.
54	111.1	14.52	0.000E 00	0.21879E 07	38.45	0.21792E-02	0.89781E 03	0.748E-04	3.432	6.
55	113.7	14.53	0.199E-07	0.22139E 07	38.07	0.21943E-02	0.97314E 03	0.717E-04	3.268	6.
56	116.4	14.53	0.000E 00	0.22388E 07	38.47	0.22077E-02	0.10042E 04	0.755E-04	3.421	6.
57	118.9	14.53	0.000E 00	0.22635E 07	38.50	0.21188E-02	0.10564E 04	0.723E-04	3.413	6.
58	121.6	14.53	0.000E 00	0.22884E 07	38.22	0.21184E-02	0.11265E 04	0.710E-04	3.352	6.
59	124.2	14.53	0.000E 00	0.23133E 07	38.18	0.21110E-02	0.11821E 04	0.727E-04	3.444	6.
60	126.8	14.53	0.000E 00	0.23383E 07	37.66	0.20999E-02	0.12723E 04	0.684E-04	3.258	7.
61	129.4	14.53	0.000E 00	0.23632E 07	38.15	0.21076E-02	0.12858E 04	0.747E-04	3.546	7.
62	132.0	14.53	0.000E 00	0.23879E 07	37.82	0.18014E-02	0.13610E 04	0.948E-04	5.262	7.

UNCERTAINTY IN REX=12528.

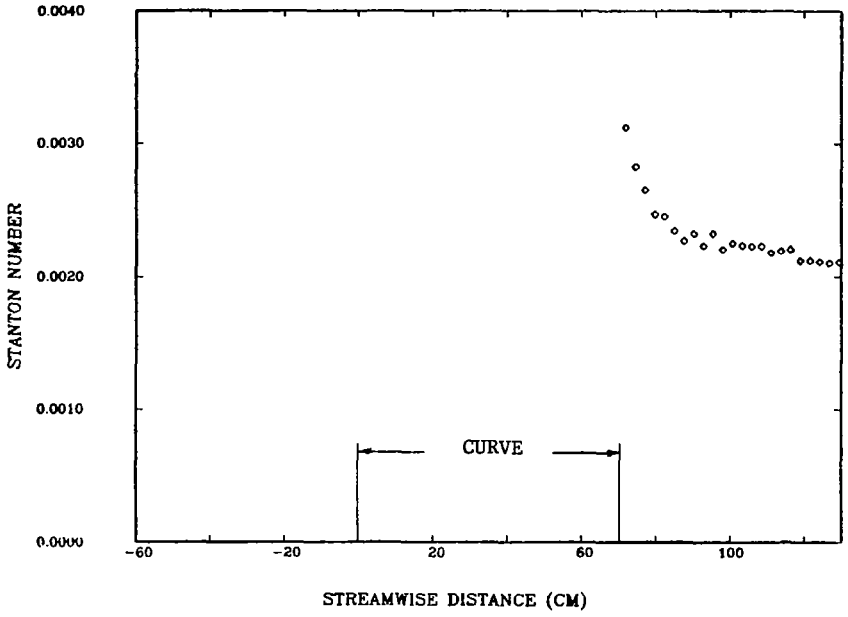

Fig. G-13. Case 030280: Stanton number versus streamwise distance.

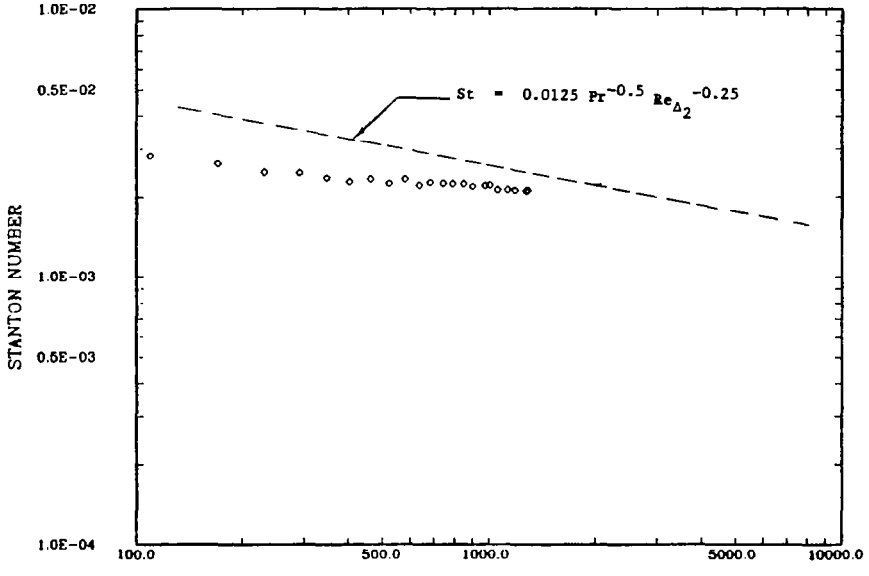

Fig. G-14. Case 030280: Stanton number versus enthalpy thickness Reynolds number.

010680 STARTING PROFILE AT X=-35 CM UPW=7 M/S LATE TRANSITIONAL

REX	= 0.21762E 06	REM	= 689.	REH	= 222.		
XVO	= -82.63 CM	DEL2	= 0.151 CM	DEH2	= 0.049 CM		
UPW	= 7.01 M/S	DEL99	= 1.028 CM	DELT99	= 0.593 CM		
VISC	= 0.15317E-04 M2/S	DEL1	= 0.366 CM	UPW	= 7.00 M/S		
PORT	= 4	H	= 2.431	VISC	= 0.15291E-04 M2/S		
XLOC	= -35.05 CM	CF/2	= 0.18677E-02	TINF	= 22.64 DEG C		
DENS	= 1.19 KG/M3			TPLATE	= 39.12 DEG C		

Y(CM)	Y/DEL	U(M/S)	U/UP	Y+	U+	CF/2	T(DEG C)	Y(CM)	Y+	U(M/S)	T(DEG C)	TBAR	1-TBAR
0.048	0.047	1.39	0.198	9.6	4.58	0.000496	35.54	0.0140	2.76	0.40	37.82	0.079	0.921
0.074	0.072	1.48	0.211	14.6	4.87	0.000460	34.32	0.0394	7.78	1.13	36.00	0.189	0.811
0.099	0.096	1.65	0.236	19.6	5.46	0.000493	33.24	0.0648	12.80	1.44	34.70	0.268	0.732
0.150	0.146	1.89	0.270	29.6	6.25	0.000530	31.14	0.1156	22.84	1.73	32.54	0.399	0.601
0.201	0.195	2.24	0.320	39.7	7.39	0.000637	29.23	0.1664	32.88	2.00	30.47	0.525	0.475
0.252	0.245	2.71	0.388	49.7	8.97	0.000821	27.58	0.2172	42.92	2.39	28.64	0.636	0.364
0.328	0.319	3.37	0.482	64.8	11.14	0.001099	25.51	0.2934	57.99	3.08	26.29	0.778	0.222
0.379	0.368	3.85	0.549	74.8	12.71	0.001323	24.59	0.3442	68.03	3.53	25.14	0.848	0.152
0.455	0.442	4.50	0.643	89.9	14.87	0.001650	23.64	0.4204	83.09	4.21	23.91	0.923	0.077
0.556	0.541	5.31	0.758	110.0	17.54	0.002085	23.01	0.5220	103.17	5.04	23.09	0.972	0.028
0.683	0.665	6.10	0.871	135.1	20.15	0.002525	22.75	0.6490	128.27	5.89	22.76	0.992	0.008
0.804	0.782	6.60	0.942	159.0	21.81	0.002787	22.69	0.7760	153.37	6.49	22.68	0.998	0.002
1.003	0.976	6.91	0.987	198.3	22.83	0.002868	22.66	0.9792	193.53	6.87	22.65	1.000	0.000
1.204	1.172	6.97	0.995	238.1	23.03	0.002792	22.66	1.1824	233.70	6.97	22.64	1.000	0.000
1.484	1.443	7.00	1.000	293.3	23.13	0.002683	22.66						

RUN 010680 *** CURVATURE RIG *** NASA-NAG-3-3 STANTON NUMBER DATA

TADB= 22.95 DEG C UREF= 7.00 M/S TINF= 22.93 DEG C
RHO= 1.187 KG/M3 VISC= 0.15318E-04 M2/S XVO= -81.5 CM
CP= 1011. J/KGK PR= 0.715

STANTON RUN UPW=7M/S LATE TRANSITIONAL

PLATE	X (CM)	UPW (M/S)	K	REXVO	TO DEG C	STANTON NO	REENTH	DST	DST(%)	DREEN
1	-61.3	7.00	0.000E 00	0.92406E 05	37.71	0.99772E-03		0.308E-03	30.892	
2	-58.7	7.00	0.000E 00	0.10437E 06	38.75	0.24263E-02		0.946E-04	3.899	
3	-56.1	7.00	0.000E 00	0.11633E 06	38.97	0.23270E-02		0.856E-04	3.681	
4	-53.5	7.00	0.000E 00	0.12817E 06	39.06	0.22278E-02		0.844E-04	3.790	
5	-50.9	7.00	0.000E 00	0.14013E 06	38.69	0.20842E-02		0.742E-04	3.558	
6	-48.3	7.00	0.000E 00	0.15209E 06	39.19	0.21013E-02		0.810E-04	3.854	
7	-45.7	7.00	0.000E 00	0.16405E 06	39.29	0.20142E-02		0.766E-04	3.801	
8	-43.0	7.00	0.000E 00	0.17602E 06	39.23	0.20125E-02		0.755E-04	3.751	
9	-40.4	7.00	0.000E 00	0.18786E 06	39.19	0.20769E-02		0.773E-04	3.721	
10	-37.8	7.00	0.000E 00	0.19982E 06	39.18	0.20716E-02		0.778E-04	3.756	
11	-35.2	7.00	0.000E 00	0.21178E 06	39.14	0.21933E-02	0.23489E 03	0.812E-04	3.704	2.
12	-32.6	7.00	0.000E 00	0.22374E 06	39.08	0.21690E-02	0.26183E 03	0.809E-04	3.730	2.
13	-30.0	7.00	0.000E 00	0.23570E 06	38.95	0.22967E-02	0.29063E 03	0.841E-04	3.662	3.
14	-27.4	7.00	0.000E 00	0.24755E 06	38.83	0.24893E-02	0.32125E 03	0.905E-04	3.634	3.
15	-24.8	7.00	0.000E 00	0.25951E 06	38.78	0.26115E-02	0.35283E 03	0.935E-04	3.582	3.
16	-22.2	7.00	0.000E 00	0.27147E 06	38.71	0.27488E-02	0.38632E 03	0.995E-04	3.619	3.
17	-19.5	7.00	0.000E 00	0.28343E 06	38.35	0.27733E-02	0.42828E 03	0.969E-04	3.492	3.
18	-16.9	7.00	0.000E 00	0.29527E 06	38.46	0.29416E-02	0.45936E 03	0.105E-03	3.555	3.
19	-14.3	7.00	0.000E 00	0.30724E 06	38.46	0.31091E-02	0.49536E 03	0.110E-03	3.533	3.
20	-11.7	7.00	0.000E 00	0.31920E 06	38.27	0.31841E-02	0.53913E 03	0.111E-03	3.483	3.
21	-9.1	7.00	0.000E 00	0.33116E 06	38.20	0.31507E-02	0.57941E 03	0.109E-03	3.462	3.
22	-6.5	7.00	0.000E 00	0.34312E 06	38.37	0.31465E-02	0.61067E 03	0.111E-03	3.530	4.
23	-3.9	7.00	0.000E 00	0.35496E 06	38.38	0.32987E-02	0.64852E 03	0.115E-03	3.474	4.
24	-1.3	7.00	0.000E 00	0.36692E 06	38.47	0.31311E-02	0.68334E 03	0.112E-03	3.561	4.
CURVE BEGINS										
25	2.4	6.31	-0.768E-05	0.34571E 06	38.60	0.27310E-02	0.72571E 03	0.166E-03	6.080	4.
26	7.3	6.21	-0.832E-06	0.36000E 06	38.60	0.26846E-02	0.77982E 03	0.146E-03	5.440	4.
27	12.4	6.07	-0.112E-05	0.37226E 06	38.73	0.26912E-02	0.82771E 03	0.148E-03	5.487	5.
28	17.4	6.00	-0.564E-06	0.38784E 06	38.75	0.25112E-02	0.87896E 03	0.141E-03	5.597	5.
29	22.5	6.00	0.000E 00	0.40776E 06	38.76	0.23480E-02	0.92655E 03	0.135E-03	5.745	6.
30	27.6	6.00	0.000E 00	0.42757E 06	38.82	0.21542E-02	0.96840E 03	0.130E-03	6.032	6.
31	32.6	6.00	0.000E 00	0.44748E 06	38.76	0.20541E-02	0.10136E 04	0.126E-03	6.130	6.
32	37.7	6.00	0.000E 00	0.46729E 06	38.72	0.19465E-02	0.10561E 04	0.122E-03	6.263	6.
33	42.8	6.11	0.843E-06	0.49574E 06	38.82	0.18843E-02	0.10889E 04	0.121E-03	6.383	7.
34	47.8	6.00	-0.888E-06	0.50711E 06	38.79	0.18645E-02	0.11281E 04	0.121E-03	6.468	7.
35	52.9	5.97	-0.279E-06	0.52405E 06	38.78	0.18396E-02	0.11658E 04	0.120E-03	6.496	7.
36	58.0	6.00	0.273E-06	0.54683E 06	38.86	0.17587E-02	0.11959E 04	0.119E-03	6.746	7.
37	63.0	6.04	0.303E-06	0.57010E 06	38.70	0.15242E-02	0.12416E 04	0.111E-03	7.261	7.
38	68.1	6.07	0.264E-06	0.59330E 06	38.76	0.12585E-02	0.12646E 04	0.101E-03	7.988	8.
RECOVERY BEGINS										
39	72.0	6.07	0.000E 00	0.60851E 06	38.88	0.16142E-02	0.12734E 04	0.698E-04	4.325	8.
40	74.6	6.07	0.000E 00	0.61868E 06	38.79	0.17419E-02	0.12983E 04	0.730E-04	4.189	8.
41	77.2	6.07	0.000E 00	0.62925E 06	38.94	0.18675E-02	0.13048E 04	0.789E-04	4.223	8.
42	79.8	6.07	0.000E 00	0.63962E 06	38.95	0.18587E-02	0.13230E 04	0.783E-04	4.210	8.
43	82.4	6.07	0.000E 00	0.64990E 06	38.90	0.19616E-02	0.13473E 04	0.803E-04	4.092	8.
44	85.0	6.07	0.000E 00	0.66027E 06	38.93	0.19267E-02	0.13646E 04	0.821E-04	4.261	8.
45	87.6	6.07	0.000E 00	0.67064E 06	38.98	0.18553E-02	0.13801E 04	0.784E-04	4.225	8.
46	90.2	6.07	0.000E 00	0.68101E 06	38.84	0.20038E-02	0.14119E 04	0.798E-04	3.981	8.
47	92.8	6.07	0.000E 00	0.69128E 06	38.83	0.19256E-02	0.14335E 04	0.794E-04	4.125	8.
48	95.4	6.07	0.000E 00	0.70166E 06	38.79	0.20217E-02	0.14576E 04	0.827E-04	4.092	8.
49	98.1	6.07	0.000E 00	0.71203E 06	38.81	0.19624E-02	0.14763E 04	0.819E-04	4.173	8.
50	100.7	6.07	0.000E 00	0.72240E 06	38.87	0.20285E-02	0.14913E 04	0.851E-04	4.196	8.
51	103.3	6.07	0.000E 00	0.73277E 06	38.78	0.20452E-02	0.15209E 04	0.828E-04	4.050	8.
52	105.9	6.07	0.000E 00	0.74304E 06	38.85	0.20481E-02	0.15357E 04	0.849E-04	4.145	8.
53	108.5	6.07	0.000E 00	0.75342E 06	38.78	0.21054E-02	0.15634E 04	0.850E-04	4.039	8.
54	111.1	6.07	0.000E 00	0.76379E 06	38.81	0.20655E-02	0.15826E 04	0.861E-04	4.167	8.
55	113.7	6.07	0.000E 00	0.77416E 06	38.59	0.21687E-02	0.16261E 04	0.849E-04	3.917	8.
56	116.4	6.07	0.000E 00	0.78453E 06	38.79	0.21398E-02	0.16283E 04	0.887E-04	4.146	8.
57	118.9	6.07	0.000E 00	0.79480E 06	38.79	0.20765E-02	0.16493E 04	0.862E-04	4.152	8.
58	121.6	6.07	0.000E 00	0.80518E 06	38.63	0.21122E-02	0.16877E 04	0.856E-04	4.055	8.
59	124.2	6.07	0.000E 00	0.81555E 06	38.63	0.20894E-02	0.17102E 04	0.864E-04	4.135	8.
60	126.8	6.07	0.000E 00	0.82592E 06	38.41	0.20899E-02	0.17553E 04	0.830E-04	3.971	8.
61	129.4	6.07	0.000E 00	0.83629E 06	38.58	0.20380E-02	0.17573E 04	0.916E-04	4.492	8.
62	132.0	6.07	0.000E 00	0.84656E 06	38.13	0.17261E-02	0.18281E 04	0.130E-03	7.526	8.

UNCERTAINTY IN REX=23225.

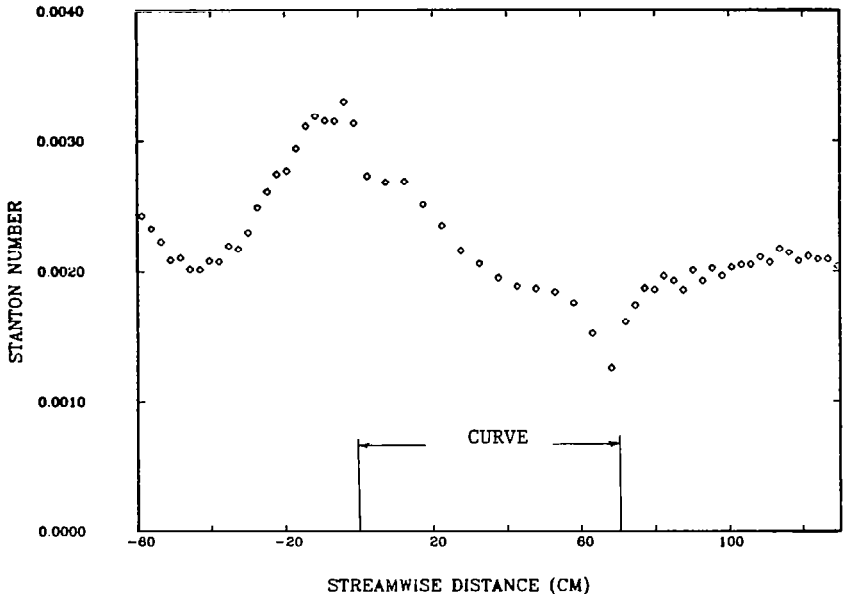

Fig. G-15. Case 010680: Stanton number versus streamwise distance.

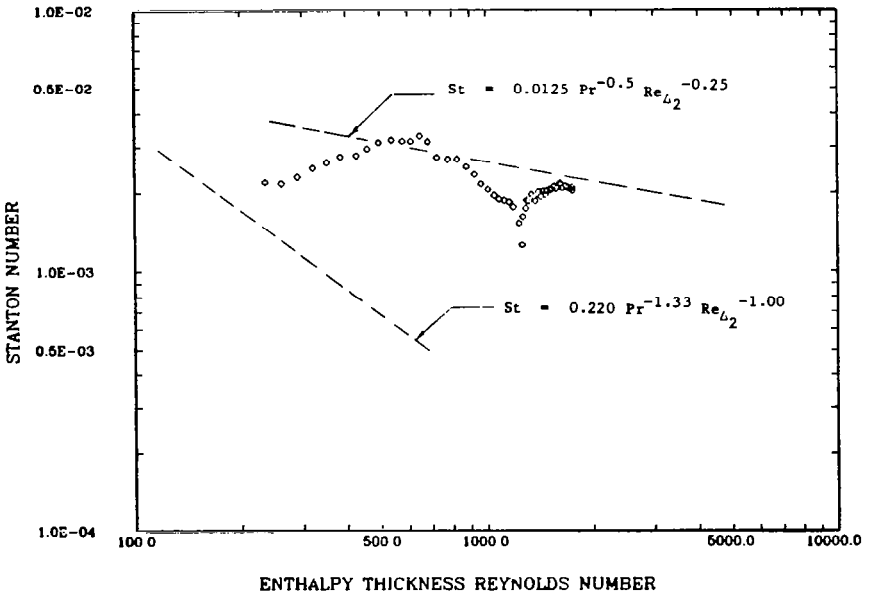

Fig. G-16. Case 010680: Stanton number versus enthalpy thickness Reynolds number.

012480 STARTING PROFILES UPW=5.2 M/S TRANSITIONAL B.L. AT THETA=0

REX = 0.18995E 06	REM = 618.	REH = 217.
XVO = -91.07 CM	DEL2 = 0.182 CM	DEH2 = 0.064 CM
UPW = 5.16 M/S	DEL99= 1.291 CM	DELT99 = 0.896 CM
VISC = 0.15226E-04 M2/S	DEL1 = 0.485 CM	UPW = 5.16 M/S
PORT = 4	H = 2.662	VISC = 0.15234E-04 M2/S
XLOC = -35.05 CM	CF/2 = 0.42870E-03	TINF = 22.76 DEG C
DENS = 1.19 KG/M3		TPLATE = 40.12 DEG C

Y(CM)	Y/DEL	U(M/S)	U/UP	Y+	U+	CF/2	T(DEG C)	Y(CM)	Y+	U(M/S)	T(DEG C)	TBAR	1-TBAR
0.048	0.037	0.32	0.062	3.4	2.97	0.000099	37.83	0.0140	0.98	0.09	39.64	0.028	0.972
0.074	0.057	0.60	0.117	5.2	5.63	0.000206	36.80	0.0394	2.76	0.26	38.21	0.110	0.890
0.099	0.077	0.71	0.137	7.0	6.62	0.000233	35.85	0.0648	4.55	0.50	37.14	0.172	0.828
0.150	0.116	0.96	0.186	10.5	8.96	0.000320	34.02	0.1156	8.11	0.79	35.24	0.281	0.719
0.201	0.156	1.22	0.237	14.1	11.45	0.000429	32.28	0.1664	11.68	1.04	33.43	0.386	0.614
0.252	0.195	1.54	0.299	17.7	14.45	0.000584	30.67	0.2172	15.25	1.33	31.74	0.483	0.517
0.328	0.254	1.96	0.380	23.0	18.37	0.000804	28.43	0.2934	20.60	1.77	29.38	0.619	0.381
0.379	0.293	2.24	0.433	26.6	20.91	0.000959	27.19	0.3442	24.16	2.05	27.98	0.700	0.300
0.455	0.352	2.64	0.512	31.9	24.74	0.001212	25.67	0.4204	29.51	2.46	26.23	0.801	0.199
0.556	0.431	3.18	0.616	39.1	29.74	0.001574	24.31	0.5220	36.65	3.00	24.58	0.895	0.105
0.683	0.529	3.77	0.730	48.0	35.28	0.002003	23.46	0.6490	45.56	3.61	23.57	0.953	0.047
0.810	0.628	4.29	0.830	56.9	40.11	0.002399	23.11	0.7760	54.48	4.15	23.15	0.978	0.022
1.008	0.780	4.83	0.935	70.7	45.15	0.002797	22.91	0.9792	68.75	4.75	22.92	0.991	0.009
1.206	0.934	5.05	0.979	84.7	47.28	0.002906	22.84	1.1824	83.01	5.03	22.83	0.996	0.004
1.484	1.150	5.15	0.998	104.2	48.19	0.002863	22.79	1.4618	102.63	5.14	22.78	0.999	0.001
1.738	1.346	5.16	1.000	122.0	48.31	0.002773	22.78	1.7158	120.46	5.16	22.77	1.000	0.000

RUN 012480 *** CURVATURE RIG *** NASA-NAG-3-3 STANTON NUMBER DATA

TADB= 22.68 DEG C UREF= 5.16 M/S TINF= 22.67 DEG C
RHO= 1.193 KG/M3 VISC= 0.15225E-04 M2/S XVO= -86.4 CM
CP= 1011. J/KGK PR= 0.715

STANTON RUN UPW=5.2M/S TRANSITIONAL B.L. AT THETA=0.

PLATE	X (CM)	UPW (M/S)	K	REXVO	TO DEG C	STANTON NO	REENTH	DST	DST(%)	DREEN
1	-61.3	5.16	0.000E 00	0.84896E 05	38.58	0.28255E-03		0.380E-03	134.390	
2	-58.7	5.16	0.000E 00	0.93767E 05	39.57	0.23105E-02		0.986E-04	4.269	
3	-56.1	5.16	0.000E 00	0.10264E 06	39.78	0.21689E-02		0.874E-04	4.029	
4	-53.5	5.16	0.000E 00	0.11142E 06	39.86	0.20780E-02		0.855E-04	4.116	
5	-50.9	5.16	0.000E 00	0.12029E 06	39.66	0.18766E-02		0.747E-04	3.979	
6	-48.3	5.16	0.000E 00	0.12916E 06	40.04	0.18790E-02		0.809E-04	4.306	
7	-45.7	5.16	0.000E 00	0.13803E 06	40.12	0.17859E-02		0.763E-04	4.271	
8	-43.0	5.16	0.000E 00	0.14690E 06	40.12	0.17289E-02		0.742E-04	4.291	
9	-40.4	5.16	0.000E 00	0.15569E 06	40.07	0.17819E-02		0.750E-04	4.210	
10	-37.8	5.16	0.000E 00	0.16456E 06	40.08	0.17446E-02		0.749E-04	4.294	
11	-35.2	5.16	0.000E 00	0.17343E 06	40.09	0.18011E-02	0.22500E 03	0.765E-04	4.247	2.
12	-32.6	5.16	0.000E 00	0.18230E 06	40.07	0.17531E-02	0.24105E 03	0.753E-04	4.294	2.
13	-30.0	5.16	0.000E 00	0.19117E 06	40.01	0.17968E-02	0.25754E 03	0.760E-04	4.231	2.
14	-27.4	5.16	0.000E 00	0.19996E 06	39.94	0.18921E-02	0.27499E 03	0.797E-04	4.210	2.
15	-24.8	5.16	0.000E 00	0.20883E 06	39.92	0.19215E-02	0.29217E 03	0.789E-04	4.106	2.
16	-22.2	5.16	0.000E 00	0.21770E 06	39.93	0.19602E-02	0.30921E 03	0.816E-04	4.160	2.
17	-19.5	5.16	0.000E 00	0.22657E 06	39.74	0.19435E-02	0.32993E 03	0.789E-04	4.057	2.
18	-16.9	5.16	0.000E 00	0.23535E 06	39.81	0.20196E-02	0.34613E 03	0.828E-04	4.102	2.
19	-14.3	5.16	0.000E 00	0.24422E 06	39.81	0.21495E-02	0.36452E 03	0.862E-04	4.012	2.
20	-11.7	5.16	0.000E 00	0.25309E 06	39.69	0.21368E-02	0.38599E 03	0.855E-04	4.000	2.
21	-9.1	5.16	0.000E 00	0.26197E 06	39.62	0.22050E-02	0.40681E 03	0.864E-04	3.919	2.
22	-6.5	5.16	0.000E 00	0.27084E 06	39.69	0.22207E-02	0.42465E 03	0.890E-04	4.007	2.
23	-3.9	5.16	0.000E 00	0.27962E 06	39.62	0.24638E-02	0.44736E 03	0.951E-04	3.860	2.
24	-1.3	5.16	0.000E 00	0.28849E 06	39.59	0.24984E-02	0.47006E 03	0.993E-04	3.976	3.
CURVE BEGINS										
25	2.4	5.20	0.541E-06	0.30295E 06	39.64	0.24261E-02	0.49926E 03	0.128E-03	5.274	3.
26	7.3	5.22	0.239E-06	0.32097E 06	39.79	0.21919E-02	0.53363E 03	0.973E-04	4.437	3.
27	12.4	5.19	-0.372E-06	0.33623E 06	39.85	0.22369E-02	0.57013E 03	0.953E-04	4.262	3.
28	17.4	5.17	-0.133E-06	0.35263E 06	39.69	0.21189E-02	0.61307E 03	0.955E-04	4.507	4.
29	22.5	5.17	0.115E-07	0.36997E 06	39.73	0.21412E-02	0.64859E 03	0.954E-04	4.455	4.
30	27.6	5.19	0.161E-06	0.38823E 06	39.78	0.20637E-02	0.68293E 03	0.943E-04	4.569	4.
31	32.6	5.21	0.190E-06	0.40688E 06	39.75	0.19462E-02	0.71934E 03	0.936E-04	4.808	4.
32	37.7	5.21	0.709E-07	0.42469E 06	39.78	0.19722E-02	0.75227E 03	0.935E-04	4.743	4.
33	42.8	5.18	-0.336E-06	0.43953E 06	39.82	0.18351E-02	0.78349E 03	0.934E-04	5.088	4.
34	47.8	5.20	0.207E-06	0.45848E 06	39.72	0.18591E-02	0.82037E 03	0.935E-04	5.030	5.
35	52.9	5.20	-0.343E-07	0.47546E 06	39.70	0.17918E-02	0.85263E 03	0.932E-04	5.201	5.
36	58.0	5.22	0.205E-06	0.49458E 06	39.72	0.18193E-02	0.88327E 03	0.927E-04	5.096	5.
37	63.0	5.26	0.442E-06	0.51589E 06	39.71	0.15850E-02	0.91416E 03	0.908E-04	5.731	5.
38	68.1	5.28	0.215E-06	0.53546E 06	39.71	0.14240E-02	0.94056E 03	0.859E-04	6.035	5.
RECOVERY BEGINS										
39	72.0	5.26	-0.210E-06	0.54723E 06	39.70	0.16386E-02	0.95937E 03	0.728E-04	4.441	5.
40	74.6	5.26	0.000E 00	0.55627E 06	39.63	0.18122E-02	0.97922E 03	0.783E-04	4.321	5.
41	77.2	5.26	0.000E 00	0.56532E 06	39.72	0.20041E-02	0.99104E 03	0.854E-04	4.263	5.
42	79.8	5.26	0.000E 00	0.57436E 06	39.75	0.19821E-02	0.10073E 04	0.851E-04	4.296	5.
43	82.4	5.26	0.000E 00	0.58332E 06	39.68	0.21321E-02	0.10301E 04	0.880E-04	4.129	5.
44	85.0	5.26	0.000E 00	0.59236E 06	39.73	0.20809E-02	0.10463E 04	0.897E-04	4.310	5.
45	87.6	5.26	0.000E 00	0.60140E 06	39.78	0.19952E-02	0.10615E 04	0.855E-04	4.284	5.
46	90.2	5.26	0.000E 00	0.61045E 06	39.64	0.21553E-02	0.10887E 04	0.872E-04	4.044	5.
47	92.8	5.26	0.000E 00	0.61940E 06	39.63	0.20538E-02	0.11086E 04	0.860E-04	4.189	5.
48	95.4	5.26	0.000E 00	0.62845E 06	39.61	0.21596E-02	0.11290E 04	0.901E-04	4.170	5.
49	98.1	5.26	0.000E 00	0.63749E 06	39.61	0.20998E-02	0.11482E 04	0.889E-04	4.232	5.
50	100.7	5.26	0.000E 00	0.64653E 06	39.67	0.21526E-02	0.11632E 04	0.919E-04	4.267	5.
51	103.3	5.26	0.000E 00	0.65558E 06	39.60	0.21629E-02	0.11875E 04	0.895E-04	4.136	6.
52	105.9	5.26	0.000E 00	0.66453E 06	39.67	0.21541E-02	0.12024E 04	0.912E-04	4.233	6.
53	108.5	5.26	0.000E 00	0.67357E 06	39.60	0.21983E-02	0.12265E 04	0.909E-04	4.136	6.
54	111.1	5.26	0.000E 00	0.68262E 06	39.63	0.21568E-02	0.12445E 04	0.918E-04	4.258	6.
55	113.7	5.26	0.000E 00	0.69166E 06	39.43	0.22653E-02	0.12790E 04	0.909E-04	4.012	6.
56	116.4	5.26	0.000E 00	0.70070E 06	39.62	0.22150E-02	0.12844E 04	0.942E-04	4.254	6.
57	118.9	5.26	0.000E 00	0.70966E 06	39.63	0.21515E-02	0.13035E 04	0.915E-04	4.252	6.
58	121.6	5.26	0.000E 00	0.71870E 06	39.49	0.21815E-02	0.13339E 04	0.910E-04	4.170	6.
59	124.2	5.26	0.000E 00	0.72775E 06	39.48	0.21531E-02	0.13540E 04	0.915E-04	4.249	6.
60	126.8	5.26	0.000E 00	0.73679E 06	39.27	0.21567E-02	0.13909E 04	0.877E-04	4.067	6.
61	129.4	5.26	0.000E 00	0.74583E 06	39.48	0.20906E-02	0.13926E 04	0.963E-04	4.605	6.
62	132.0	5.26	0.000E 00	0.75479E 06	39.09	0.17259E-02	0.14427E 04	0.139E-03	8.061	6.

UNCERTAINTY IN REX=17225.

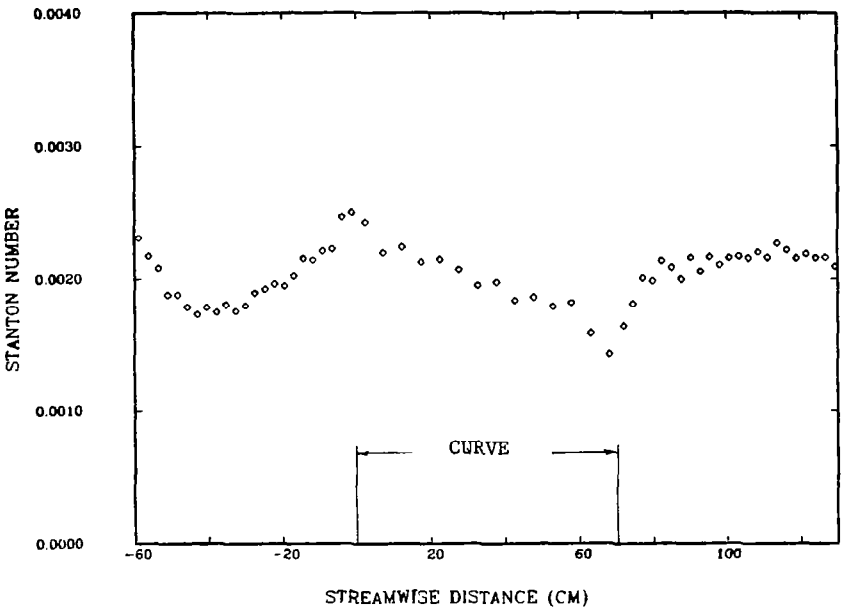

Fig. G-17. Case 012480: Stanton number versus streamwise distance.

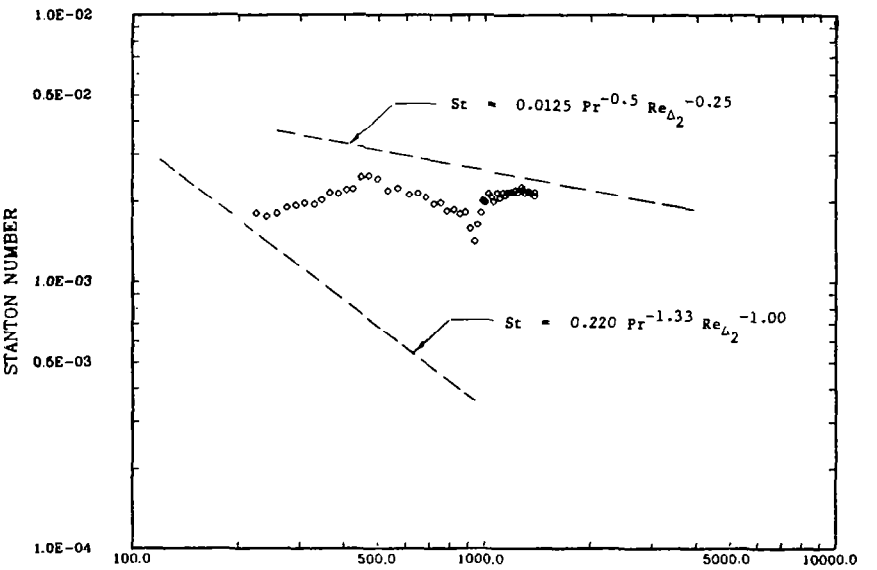

Fig. G-18. Case 012480: Stanton number versus enthalpy thickness Reynolds number.

062880 STARTING PROFILES UPW=12.3M/S EARLY TRANSITIONAL B.L. AT THETA=0

REX = 0.23589E 06	REM = 322.	REH = 359.
XVO = -65.71 CM	DEL2 = 0.042 CM	DEH2 = 0.047 CM
UPW = 12.36 M/S	DEL99= 0.306 CM	DELT99 = 0.341 CM
VISC = 0.16062E-04 M2/S	DEL1 = 0.112 CM	UPW = 12.36 M/S
PORT = 4	H = 2.682	VISC = 0.16078E-04 M2/S
XLOC = -35.05 CM	CF/2 = 0.68213E-03	TINF = 30.65 DEG C
DENS = 1.15 KG/M3		TPLATE = 43.22 DEG C

Y(CM)	Y/DEL	U(M/S)	U/UP	Y+	U+	CF/2	T(DEG C)	Y(CM)	Y+	U(M/S)	T(DEG C)	TBAR	1-TBAR
0.048	0.158	3.20	0.259	9.7	9.90	0.000695	39.98	0.0140	2.81	0.92	42.11	0.088	0.912
0.053	0.175	3.51	0.284	10.7	10.87	0.000690	39.69	0.0190	3.83	1.26	41.83	0.111	0.889
0.059	0.191	3.80	0.307	11.8	11.77	0.000683	39.41	0.0241	4.85	1.59	41.48	0.138	0.862
0.069	0.224	4.54	0.367	13.8	14.06	0.000695	38.86	0.0343	6.89	2.27	40.81	0.192	0.808
0.079	0.258	5.05	0.409	15.8	15.65	0.000674	38.26	0.0444	8.93	2.94	40.20	0.240	0.760
0.089	0.291	5.66	0.458	17.9	17.53	0.000669	37.69	0.0546	10.97	3.57	39.62	0.286	0.714
0.104	0.341	6.48	0.524	20.9	20.07	0.000654	36.86	0.0698	14.03	4.60	38.78	0.353	0.647
0.114	0.374	7.06	0.571	23.0	21.87	0.000649	36.32	0.0800	16.08	5.12	38.19	0.400	0.600
0.130	0.424	7.88	0.637	26.0	24.40	0.000639	35.59	0.0952	19.14	5.99	37.33	0.468	0.532
0.150	0.490	8.81	0.713	30.1	27.30	0.000618	34.66	0.1156	23.22	7.12	36.24	0.555	0.445
0.175	0.573	9.85	0.797	35.2	30.52	0.000591	33.65	0.1410	28.32	8.40	35.03	0.652	0.348
0.201	0.656	10.65	0.862	40.3	32.99	0.000558	32.80	0.1664	33.43	9.48	33.93	0.739	0.261
0.239	0.781	11.49	0.930	48.0	35.61	0.000506	31.87	0.2045	41.08	10.73	32.64	0.841	0.159
0.276	0.903	12.00	0.971	55.5	37.19	0.000457	31.39	0.2426	48.74	11.54	31.74	0.913	0.087
0.332	1.087	12.30	0.995	66.8	38.10	0.000389	30.92	0.3061	61.50	12.16	30.98	0.973	0.027
0.379	1.239	12.36	1.001	76.2	38.31	0.000343	30.79	0.3569	71.70	12.33	30.76	0.991	0.009
0.481	1.571	12.36	1.000	96.6	38.30	0.000270	30.71	0.4585	92.12	12.36	30.66	0.999	0.001
								0.5220	104.88	12.36	30.66	0.999	0.001

RUN 062880 *** CURVATURE RIG *** NASA-NAG-3-3 STANTON NUMBER DATA

TADB= 30.53 DEG C UREF= 12.35 M/S TINF= 30.46 DEG C
RHO= 1.151 KG/M3 VISC= 0.16060E-04 M2/S XVO= -29.9 CM
CP= 1014. J/KGK PR= 0.715

STANTON RUN EARLY TRANSITIONAL B.L. AT THETA=0

PLATE	X (CM)	UPW (M/S)	K	REXVO	TO DEG C	STANTON NO	REENTH	DST	DST(%)	DREEN
1	-61.3	12.30	0.000E 00	-0.24096E 06	39.74	0.36192E-02		0.239E-03	6.615	
2	-58.7	12.30	0.000E 00	-0.22092E 06	41.51	0.27816E-02		0.111E-03	4.003	
3	-56.1	12.30	0.000E 00	-0.20087E 06	42.12	0.22536E-02		0.860E-04	3.815	
4	-53.5	12.30	0.000E 00	-0.18103E 06	42.46	0.19004E-02		0.743E-04	3.909	
5	-50.9	12.30	0.000E 00	-0.16098E 06	42.34	0.15105E-02		0.578E-04	3.828	
6	-48.3	12.30	0.000E 00	-0.14094E 06	42.84	0.14956E-02		0.610E-04	4.076	
7	-45.7	12.32	0.501E-07	-0.12102E 06	43.04	0.13252E-02		0.543E-04	4.098	
8	-43.0	12.32	0.000E 00	-0.10095E 06	43.10	0.12086E-02		0.500E-04	4.139	
9	-40.4	12.33	0.505E-07	-0.81165E 05	43.15	0.11768E-02		0.489E-04	4.153	
10	-37.8	12.34	0.498E-07	-0.61142E 05	43.23	0.10857E-02		0.466E-04	4.293	
11	-35.2	12.35	0.497E-07	-0.41079E 05	43.28	0.10711E-02	0.37026E 03	0.459E-04	4.288	8.
12	-32.6	12.35	0.000E 00	-0.20955E 05	43.32	0.97732E-03	0.38945E 03	0.433E-04	4.435	8.
13	-30.0	12.35	0.000E 00	-0.83047E 03	43.31	0.96160E-03	0.40935E 03	0.423E-04	4.400	8.
14	-27.4	12.35	0.000E 00	0.19099E 05	43.35	0.96397E-03	0.42734E 03	0.434E-04	4.500	8.
15	-24.8	12.35	0.000E 00	0.39223E 05	43.37	0.92860E-03	0.44585E 03	0.412E-04	4.440	8.
16	-22.2	12.35	0.000E 00	0.59347E 05	43.38	0.91568E-03	0.46401E 03	0.413E-04	4.512	8.
17	-19.5	12.35	0.000E 00	0.79471E 05	43.28	0.86528E-03	0.48542E 03	0.391E-04	4.522	8.
18	-16.9	12.35	0.000E 00	0.99400E 05	43.37	0.84673E-03	0.49931E 03	0.393E-04	4.646	8.
19	-14.3	12.35	0.000E 00	0.11952E 06	43.44	0.83518E-03	0.51332E 03	0.388E-04	4.648	8.
20	-11.7	12.35	0.000E 00	0.13965E 06	43.41	0.80760E-03	0.53116E 03	0.378E-04	4.676	8.
21	-9.1	12.35	0.000E 00	0.15977E 06	43.46	0.75206E-03	0.54481E 03	0.361E-04	4.804	8.
22	-6.5	12.35	0.000E 00	0.17990E 06	43.49	0.75082E-03	0.55856E 03	0.366E-04	4.870	8.
23	-3.9	12.35	0.000E 00	0.19983E 06	43.46	0.79427E-03	0.57531E 03	0.377E-04	4.752	8.
24	-1.3	12.35	0.000E 00	0.21995E 06	43.43	0.82875E-03	0.59275E 03	0.411E-04	4.958	8.
CURVE BEGINS										
25	2.4	12.35	0.000E 00	0.24809E 06	43.49	0.89963E-03	0.61407E 03	0.821E-04	9.101	8.
26	7.3	12.42	0.131E-06	0.28722E 06	43.47	0.71522E-03	0.64563E 03	0.652E-04	9.094	9.
27	12.4	12.35	-0.128E-06	0.32487E 06	43.39	0.64506E-03	0.67630E 03	0.643E-04	9.943	9.
28	17.4	12.35	0.000E 00	0.36375E 06	43.27	0.64922E-03	0.70770E 03	0.641E-04	9.839	9.
29	22.5	12.34	-0.386E-07	0.40222E 06	43.27	0.69558E-03	0.73420E 03	0.675E-04	9.672	9.
30	27.6	12.38	0.895E-07	0.44259E 06	43.23	0.70052E-03	0.76383E 03	0.672E-04	9.569	9.
31	32.6	12.39	0.254E-07	0.48223E 06	43.15	0.75352E-03	0.79695E 03	0.702E-04	9.289	9.
32	37.7	12.39	0.000E 00	0.52122E 06	43.15	0.75405E-03	0.82646E 03	0.706E-04	9.334	10.
33	42.8	12.36	-0.639E-07	0.55902E 06	43.09	0.81046E-03	0.86125E 03	0.736E-04	9.055	10.
34	47.8	12.35	-0.256E-07	0.59752E 06	43.01	0.84086E-03	0.89869E 03	0.739E-04	8.756	10.
35	52.9	12.37	0.385E-07	0.63734E 06	42.98	0.92793E-03	0.93559E 03	0.770E-04	8.271	10.
36	58.0	12.43	0.138E-06	0.68015E 06	42.92	0.93318E-03	0.97708E 03	0.764E-04	8.169	11.
37	63.0	12.52	0.173E-06	0.72424E 06	42.76	0.10370E-02	0.10286E 04	0.789E-04	7.583	11.
38	68.1	12.52	0.000E 00	0.76384E 06	42.63	0.88109E-03	0.10776E 04	0.718E-04	8.132	11.
RECOVERY BEGINS										
39	72.0	12.51	-0.327E-07	0.79297E 06	42.43	0.11902E-02	0.11249E 04	0.507E-04	4.259	11.
40	74.6	12.48	-0.121E-06	0.81135E 06	42.29	0.13048E-02	0.11631E 04	0.546E-04	4.188	11.
41	77.2	12.45	-0.121E-06	0.82964E 06	42.38	0.14834E-02	0.11830E 04	0.620E-04	4.179	11.
42	79.8	12.42	-0.122E-06	0.84782E 06	42.27	0.16447E-02	0.12252E 04	0.665E-04	4.041	11.
43	82.4	12.39	-0.125E-06	0.86569E 06	42.16	0.18581E-02	0.12722E 04	0.733E-04	3.943	11.
44	85.0	12.39	0.000E 00	0.88587E 06	42.07	0.19826E-02	0.13206E 04	0.780E-04	3.936	11.
45	87.6	12.35	-0.124E-06	0.90379E 06	42.05	0.20155E-02	0.13627E 04	0.788E-04	3.909	11.
46	90.2	12.35	0.000E 00	0.92391E 06	41.90	0.21730E-02	0.14233E 04	0.827E-04	3.804	11.
47	92.8	12.35	0.000E 00	0.94384E 06	41.81	0.21309E-02	0.14777E 04	0.820E-04	3.847	11.
48	95.4	12.35	0.000E 00	0.96396E 06	41.78	0.22783E-02	0.15256E 04	0.875E-04	3.840	11.
49	98.1	12.35	-0.249E-07	0.98360E 06	41.79	0.21991E-02	0.15693E 04	0.850E-04	3.864	11.
50	100.7	12.35	0.000E 00	0.10037E 07	41.89	0.22731E-02	0.16009E 04	0.886E-04	3.900	12.
51	103.3	12.35	0.000E 00	0.10238E 07	41.82	0.22720E-02	0.16561E 04	0.866E-04	3.813	12.
52	105.9	12.35	0.000E 00	0.10437E 07	41.92	0.22636E-02	0.16868E 04	0.878E-04	3.879	12.
53	108.5	12.35	0.000E 00	0.10639E 07	41.88	0.22704E-02	0.17387E 04	0.870E-04	3.833	12.
54	111.1	12.35	0.000E 00	0.10840E 07	41.90	0.22249E-02	0.17794E 04	0.869E-04	3.905	12.
55	113.7	12.35	0.000E 00	0.11041E 07	41.71	0.22219E-02	0.18542E 04	0.841E-04	3.785	12.
56	116.4	12.35	0.000E 00	0.11242E 07	41.92	0.22638E-02	0.18650E 04	0.886E-04	3.913	12.
57	118.9	12.35	0.000E 00	0.11441E 07	41.92	0.21717E-02	0.19096E 04	0.852E-04	3.923	12.
58	121.6	12.35	0.000E 00	0.11642E 07	41.73	0.21796E-02	0.19860E 04	0.842E-04	3.865	12.
59	124.2	12.35	0.000E 00	0.11843E 07	41.70	0.21749E-02	0.20339E 04	0.857E-04	3.939	12.
60	126.8	12.35	0.000E 00	0.12045E 07	41.42	0.21479E-02	0.21296E 04	0.814E-04	3.791	12.
61	129.4	12.34	-0.249E-07	0.12240E 07	41.72	0.21491E-02	0.21157E 04	0.876E-04	4.077	12.
62	132.0	12.34	0.000E 00	0.12439E 07	41.51	0.18259E-02	0.21937E 04	0.105E-03	5.769	12.

UNCERTAINTY IN REX=19538.

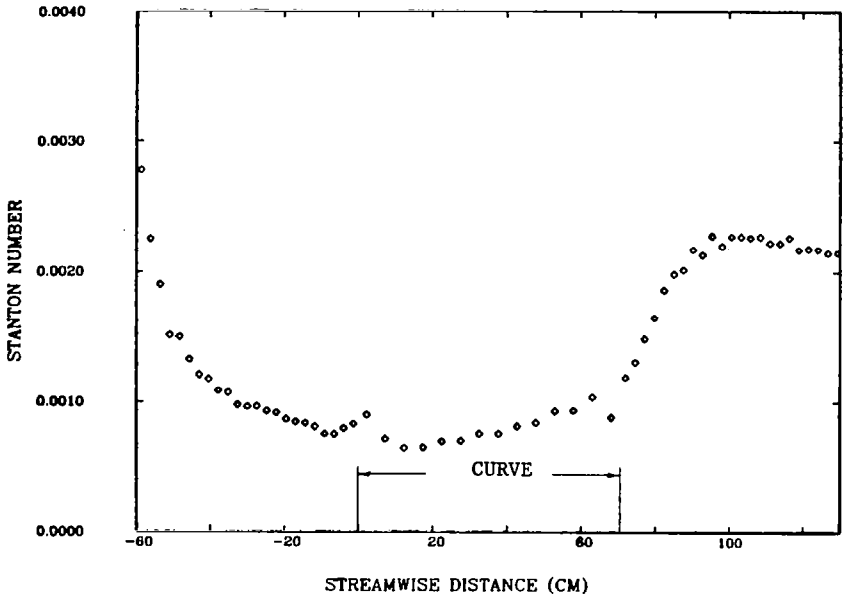

Fig. G-19. Case 062880: Stanton number versus streamwise distance.

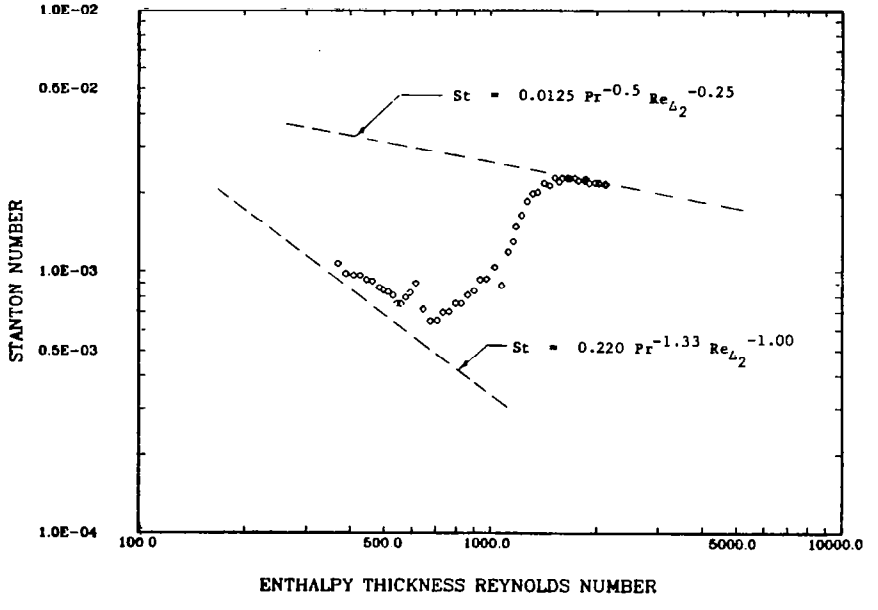

Fig. G-20. Case 062880: Stanton number versus enthalpy thickness Reynolds number.

062580 STARTING PROFILES UPW=7M/S VERY EARLY TRANSITIONAL B.L.; THETA=0

REX	= 0.12896E 06	REM	= 238.	REH	= 288.		
XVO	= -63.20 CM	DEL2	= 0.052 CM	DEH2	= 0.063 CM		
UPW	= 7.05 M/S	DEL99	= 0.411 CM	DELT99	= 0.426 CM		
VISC	= 0.15381E-04 M2/S	DEL1	= 0.141 CM	UPW	= 7.05 M/S		
PORT	= 4	H	= 2.712	VISC	= 0.15421E-04 M2/S		
XLOC	= -35.05 CM	CF/2	= 0.89985E-03	TINF	= 24.45 DEG C		
DENS	= 1.18 KG/M3			TPLATE	= 39.55 DEG C		

Y(CM)	Y/DEL	U(M/S)	U/UP	Y+	U+	CF/2	T(DEG C)	Y(CM)	Y+	U(M/S)	T(DEG C)	TBAR	1-TBAR
0.048	0.118	1.40	0.199	6.6	6.64	0.000900	36.82	0.0140	1.92	0.41	38.87	0.045	0.955
0.053	0.130	1.58	0.224	7.3	7.47	0.000916	36.53	0.0190	2.62	0.55	38.57	0.065	0.935
0.059	0.142	1.71	0.243	8.0	8.10	0.000906	36.24	0.0241	3.32	0.70	38.16	0.092	0.908
0.069	0.167	1.98	0.281	9.4	9.38	0.000894	35.67	0.0343	4.71	1.00	37.72	0.121	0.879
0.079	0.192	2.32	0.330	10.8	11.00	0.000913	35.11	0.0444	6.11	1.29	37.04	0.166	0.834
0.089	0.216	2.63	0.373	12.2	12.44	0.000915	34.55	0.0546	7.50	1.61	36.46	0.204	0.796
0.104	0.253	3.00	0.426	14.3	14.21	0.000893	33.72	0.0698	9.60	2.02	35.60	0.261	0.739
0.114	0.278	3.28	0.466	15.7	15.54	0.000889	33.19	0.0800	10.99	2.36	35.05	0.298	0.702
0.130	0.315	3.72	0.528	17.8	17.59	0.000888	32.42	0.0952	13.09	2.78	34.19	0.355	0.645
0.150	0.365	4.25	0.603	20.6	20.12	0.000878	31.39	0.1156	15.88	3.32	33.12	0.425	0.575
0.175	0.426	4.81	0.683	24.1	22.76	0.000850	30.17	0.1410	19.37	4.02	31.84	0.510	0.490
0.201	0.488	5.37	0.763	27.6	25.43	0.000829	29.09	0.1664	22.86	4.61	30.55	0.596	0.404
0.239	0.581	5.94	0.843	32.8	28.09	0.000770	27.69	0.2045	28.10	5.43	28.92	0.704	0.296
0.277	0.673	6.42	0.912	38.1	30.40	0.000719	26.66	0.2426	33.33	5.98	27.54	0.795	0.205
0.339	0.825	6.82	0.967	46.6	32.25	0.000622	25.41	0.3061	42.06	6.61	25.89	0.905	0.095
0.383	0.930	6.92	0.982	52.6	32.75	0.000561	25.01	0.3569	49.04	6.86	25.14	0.954	0.046
0.481	1.172	7.04	0.999	66.3	33.31	0.000452	24.53	0.4585	63.00	7.01	24.55	0.993	0.007
0.545	1.327	7.05	1.001	75.0	33.36	0.000400	24.47	0.5220	71.73	7.05	24.46	1.000	0.000
								0.6490	89.18	7.05	24.46	1.000	0.000

RUN 062580 *** CURVATURE RIG *** NASA-NAG-3-3 STANTON NUMBER DATA

TADB= 24.03 DEG C UREF= 7.04 M/S TINF= 24.01 DEG C
RHO= 1.184 KG/M3 VISC= 0.15380E-04 M2/S XVO= -15.0 CM
CP= 1012. J/KGK PR= 0.715

STANTON RUN VERY EARLY TRANSITIONAL B.L. AT THETA=0

PLATE	X (CM)	UPW (M/S)	K	REXVO	TO DEG C	STANTON NO	REENTH	DST	DST(%)	DREEN
1	-61.3	7.04	0.000E 00	-0.21210E 06	35.73	0.45641E-02		0.367E-03	8.043	
2	-58.7	7.04	0.000E 00	-0.20012E 06	37.84	0.36884E-02		0.147E-03	3.984	
3	-56.1	7.04	0.000E 00	-0.18815E 06	38.49	0.29993E-02		0.111E-03	3.692	
4	-53.5	7.04	0.000E 00	-0.17629E 06	38.86	0.25253E-02		0.959E-04	3.799	
5	-50.9	7.04	0.000E 00	-0.16431E 06	38.77	0.19919E-02		0.742E-04	3.726	
6	-48.3	7.04	0.000E 00	-0.15234E 06	39.30	0.19399E-02		0.782E-04	4.033	
7	-45.7	7.04	0.000E 00	-0.14036E 06	39.47	0.17496E-02		0.704E-04	4.024	
8	-43.0	7.04	0.000E 00	-0.12839E 06	39.54	0.15778E-02		0.649E-04	4.112	
9	-40.4	7.04	0.000E 00	-0.11653E 06	39.58	0.15393E-02		0.634E-04	4.120	
10	-37.8	7.04	0.000E 00	-0.10455E 06	39.66	0.14116E-02		0.606E-04	4.292	
11	-35.2	7.04	0.000E 00	-0.92578E 05	39.73	0.13776E-02	0.29657E 03	0.595E-04	4.321	12.
12	-32.6	7.04	0.000E 00	-0.80602E 05	39.76	0.12742E-02	0.31185E 03	0.567E-04	4.449	12.
13	-30.0	7.04	0.000E 00	-0.68627E 05	39.78	0.12325E-02	0.32639E 03	0.551E-04	4.468	12.
14	-27.4	7.04	0.000E 00	-0.56767E 05	39.82	0.12299E-02	0.34026E 03	0.564E-04	4.588	12.
15	-24.8	7.04	0.000E 00	-0.44792E 05	39.82	0.11864E-02	0.35475E 03	0.534E-04	4.504	12.
16	-22.2	7.04	0.000E 00	-0.32816E 05	39.85	0.11719E-02	0.36820E 03	0.539E-04	4.595	12.
17	-19.5	7.04	0.000E 00	-0.20841E 05	39.76	0.11014E-02	0.38389E 03	0.510E-04	4.627	12.
18	-16.9	7.04	0.000E 00	-0.89816E 04	39.84	0.10697E-02	0.39490E 03	0.512E-04	4.784	12.
19	-14.3	7.04	0.000E 00	0.29938E 04	39.91	0.10551E-02	0.40589E 03	0.505E-04	4.783	12.
20	-11.7	7.04	0.000E 00	0.14969E 05	39.88	0.10299E-02	0.41910E 03	0.496E-04	4.816	12.
21	-9.1	7.04	0.000E 00	0.26945E 05	39.91	0.96593E-03	0.43030E 03	0.476E-04	4.929	12.
22	-6.5	7.04	0.000E 00	0.38920E 05	39.96	0.93881E-03	0.44026E 03	0.480E-04	5.113	12.
23	-3.9	7.04	0.000E 00	0.50760E 05	39.91	0.99847E-03	0.45331E 03	0.492E-04	4.929	12.
24	-1.3	7.04	0.000E 00	0.62755E 05	39.88	0.10227E-02	0.46615E 03	0.539E-04	5.271	12.
CURVE BEGINS										
25	2.4	7.07	0.236E-06	0.79815E 05	39.84	0.88748E-03	0.48279E 03	0.105E-03	11.792	12.
26	7.3	7.12	0.302E-06	0.10305E 06	39.71	0.70520E-03	0.50490E 03	0.822E-04	11.619	12.
27	12.4	7.07	-0.297E-06	0.12569E 06	39.71	0.62371E-03	0.52029E 03	0.817E-04	13.061	12.
28	17.4	7.02	-0.283E-06	0.14796E 06	39.52	0.65615E-03	0.54164E 03	0.821E-04	12.475	12.
29	22.5	7.01	-0.653E-07	0.17089E 06	39.48	0.67262E-03	0.55836E 03	0.851E-04	12.606	12.
30	27.6	7.00	-0.659E-07	0.19364E 06	39.42	0.69016E-03	0.57616E 03	0.855E-04	12.354	12.
31	32.6	7.00	0.000E 00	0.21677E 06	39.48	0.68524E-03	0.59003E 03	0.883E-04	12.841	12.
32	37.7	6.99	-0.662E-07	0.23941E 06	39.40	0.68583E-03	0.60863E 03	0.871E-04	12.662	12.
33	42.8	6.99	0.000E 00	0.26250E 06	39.49	0.69805E-03	0.62134E 03	0.911E-04	12.996	12.
34	47.8	6.99	0.000E 00	0.28559E 06	39.41	0.76707E-03	0.64134E 03	0.909E-04	11.811	12.
35	52.9	7.01	0.131E-06	0.30951E 06	39.43	0.94081E-03	0.66035E 03	0.964E-04	10.209	13.
36	58.0	7.06	0.319E-06	0.33517E 06	39.37	0.83136E-03	0.68361E 03	0.929E-04	11.134	13.
37	63.0	7.11	0.293E-06	0.36087E 06	39.30	0.96652E-03	0.70832E 03	0.975E-04	10.052	13.
38	68.1	7.09	-0.147E-06	0.38305E 06	39.15	0.76353E-03	0.73556E 03	0.871E-04	11.379	13.
RECOVERY BEGINS										
39	72.0	7.08	-0.559E-07	0.40033E 06	39.16	0.11965E-02	0.75097E 03	0.565E-04	4.725	13.
40	74.6	7.08	-0.823E-07	0.41197E 06	39.04	0.13565E-02	0.77210E 03	0.609E-04	4.492	13.
41	77.2	7.07	-0.825E-07	0.42359E 06	39.16	0.14621E-02	0.78292E 03	0.662E-04	4.528	13.
42	79.8	7.06	-0.828E-07	0.43518E 06	39.10	0.15790E-02	0.80426E 03	0.688E-04	4.355	13.
43	82.4	7.05	-0.838E-07	0.44663E 06	39.00	0.17805E-02	0.82974E 03	0.742E-04	4.165	13.
44	85.0	7.05	-0.833E-07	0.45817E 06	38.93	0.18891E-02	0.85563E 03	0.785E-04	4.158	13.
45	87.6	7.04	-0.835E-07	0.46969E 06	38.95	0.18986E-02	0.87739E 03	0.783E-04	4.124	13.
46	90.2	7.04	0.417E-07	0.48190E 06	38.76	0.21399E-02	0.91270E 03	0.829E-04	3.872	13.
47	92.8	7.05	0.420E-07	0.49402E 06	38.69	0.21082E-02	0.94212E 03	0.835E-04	3.962	13.
48	95.4	7.05	0.000E 00	0.50600E 06	38.62	0.22995E-02	0.97298E 03	0.898E-04	3.903	13.
49	98.1	7.05	0.416E-07	0.51825E 06	38.61	0.22746E-02	0.10016E 04	0.893E-04	3.926	13.
50	100.7	7.05	0.000E 00	0.53024E 06	38.68	0.23672E-02	0.10244E 04	0.938E-04	3.962	13.
51	103.3	7.05	0.415E-07	0.54251E 06	38.58	0.24167E-02	0.10597E 04	0.926E-04	3.831	13.
52	105.9	7.05	0.000E 00	0.55439E 06	38.65	0.24326E-02	0.10836E 04	0.950E-04	3.905	13.
53	108.5	7.06	0.414E-07	0.56667E 06	38.58	0.25005E-02	0.11182E 04	0.956E-04	3.825	13.
54	111.1	7.06	0.000E 00	0.57868E 06	38.60	0.24698E-02	0.11469E 04	0.968E-04	3.919	13.
55	113.7	7.06	0.414E-07	0.59098E 06	38.37	0.25498E-02	0.11949E 04	0.951E-04	3.730	13.
56	116.4	7.06	0.000E 00	0.60299E 06	38.58	0.25388E-02	0.12084E 04	0.995E-04	3.919	13.
57	118.9	7.06	0.000E 00	0.61488E 06	38.56	0.24619E-02	0.12398E 04	0.963E-04	3.912	13.
58	121.6	7.06	0.000E 00	0.62689E 06	38.38	0.24978E-02	0.12852E 04	0.959E-04	3.841	13.
59	124.2	7.06	0.000E 00	0.63890E 06	38.35	0.24839E-02	0.13173E 04	0.974E-04	3.922	13.
60	126.8	7.06	0.000E 00	0.65092E 06	38.08	0.24828E-02	0.13726E 04	0.928E-04	3.738	13.
61	129.4	7.06	0.413E-07	0.66326E 06	38.36	0.24256E-02	0.13749E 04	0.101E-03	4.145	13.
62	132.0	7.06	0.000E 00	0.67516E 06	38.05	0.19539E-02	0.14310E 04	0.140E-03	7.189	14.

UNCERTAINTY IN REX=11627.

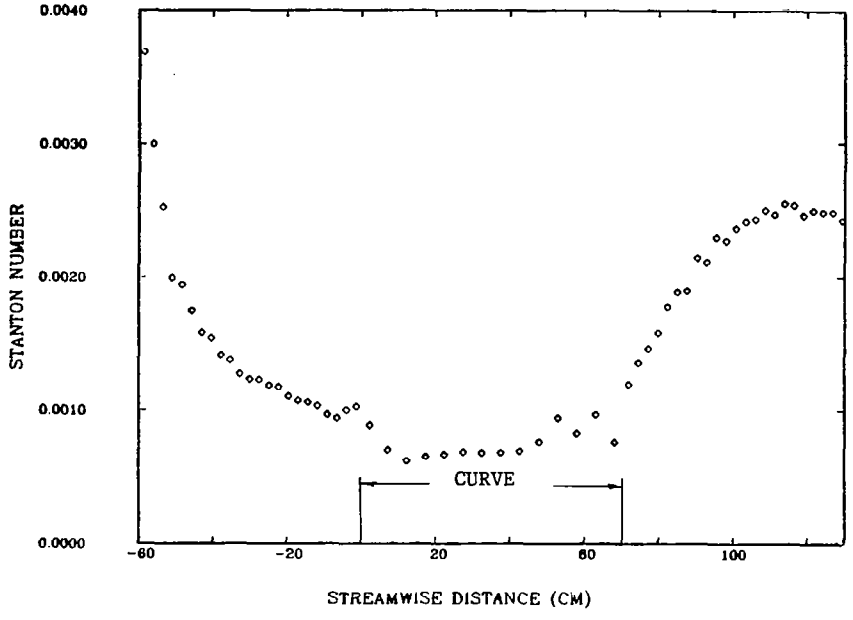

Fig. G-21. Case 062580: Stanton number versus streamwise distance.

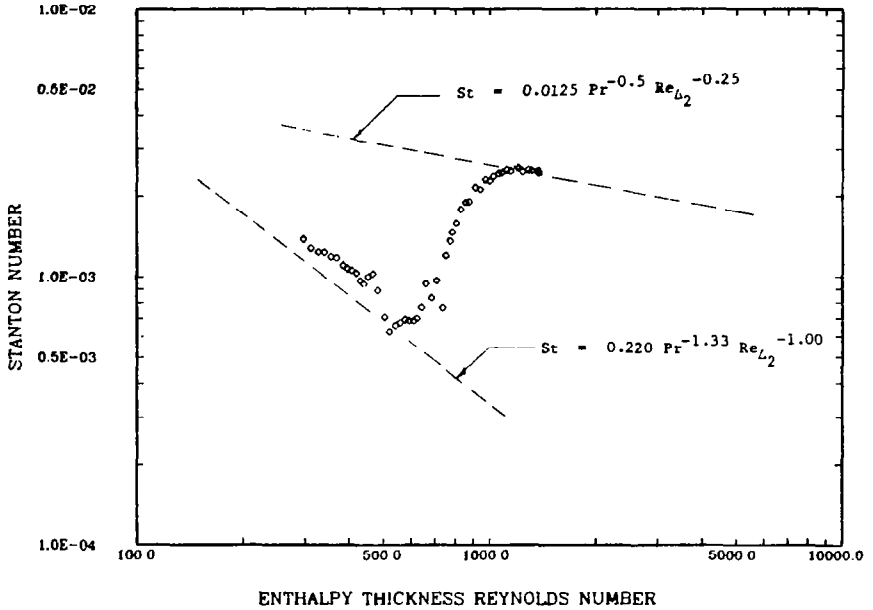

Fig. G-22. Case 062580: Stanton number versus enthalpy thickness Reynolds number.

060980 STARTING PROFILES UPW=3.5M/S TRANSITIONAL B.L. AT THETA=0

REX	= 0.47913E 05	REM	= 145.	REH	= 171.		
XVO	= -55.83 CM	DEL2	= 0.063 CM	DEH2	= 0.074 CM		
UPW	= 3.54 M/S	DEL99	= 0.456 CM	DELT99	= 0.589 CM		
VISC	= 0.15336E-04 M2/S	DEL1	= 0.180 CM	UPW	= 3.54 M/S		
PORT	= 4	H	= 2.849	VISC	= 0.15428E-04 M2/S		
XLOC	= -35.05 CM	CF/2	= 0.13310E-02	TINF	= 24.26 DEG C		
DENS	= 1.18 KG/M3			TPLATE	= 39.68 DEG C		

Y(CM)	Y/DEL	U(M/S)	U/UP	Y+	U+	CF/2	T(DEG C)
0.048	0.106	0.50	0.142	4.1	3.88	0.001270	37.55
0.053	0.117	0.60	0.169	4.5	4.62	0.001369	37.40
0.059	0.128	0.68	0.193	4.9	5.29	0.001430	37.12
0.069	0.151	0.71	0.200	5.8	5.48	0.001262	36.49
0.079	0.173	0.88	0.250	6.6	6.86	0.001377	35.99
0.089	0.195	0.94	0.266	7.5	7.30	0.001298	35.53
0.104	0.229	1.10	0.311	8.8	8.52	0.001293	34.86
0.114	0.251	1.19	0.337	9.6	9.23	0.001277	34.43
0.130	0.285	1.41	0.398	10.9	10.91	0.001332	33.82
0.150	0.329	1.62	0.457	12.6	12.53	0.001322	32.99
0.175	0.385	1.91	0.541	14.7	14.83	0.001338	31.96
0.201	0.441	2.21	0.626	16.9	17.17	0.001353	31.01
0.239	0.524	2.55	0.721	20.1	19.76	0.001309	28.93
0.277	0.608	2.85	0.807	23.3	22.11	0.001263	27.77
0.340	0.747	3.19	0.902	28.6	24.72	0.001149	26.29
0.391	0.858	3.36	0.950	32.9	26.04	0.001054	25.58
0.486	1.066	3.53	0.999	40.9	27.38	0.000892	24.72
0.549	1.206	3.54	1.002	46.2	27.46	0.000791	24.53

Y(CM)	Y+	U(M/S)	T(DEG C)	TBAR	1-TBAR
0.0140	1.17	0.14	38.90	0.050	0.950
0.0190	1.60	0.20	38.63	0.068	0.932
0.0241	2.03	0.25	38.45	0.080	0.920
0.0343	2.88	0.35	37.82	0.121	0.879
0.0444	3.74	0.46	37.67	0.130	0.870
0.0546	4.59	0.62	37.36	0.150	0.850
0.0698	5.87	0.73	36.41	0.212	0.788
0.0800	6.73	0.89	35.94	0.242	0.758
0.0952	8.01	1.01	35.24	0.288	0.712
0.1156	9.72	1.21	34.38	0.343	0.657
0.1410	11.86	1.52	33.37	0.409	0.591
0.1664	13.99	1.81	32.30	0.479	0.521
0.2045	17.20	2.25	30.87	0.571	0.429
0.2426	20.40	2.58	28.72	0.711	0.289
0.3061	25.74	3.01	26.96	0.825	0.175
0.3569	30.01	3.24	25.97	0.889	0.111
0.4585	38.56	3.48	24.81	0.964	0.036
0.5220	43.90	3.54	24.58	0.979	0.021
0.6490	54.58	3.54	24.32	0.996	0.004
0.7760	65.26	3.54	24.29	0.998	0.002
0.9030	75.94	3.54	24.27	0.999	0.001
1.1570	97.31	3.54	24.26	1.000	0.000

RUN 060980 *** CURVATURE RIG *** NASA-NAG-3-3 STANTON NUMBER DATA

TADB= 24.03 DEG C UREF= 3.49 M/S TINF= 24.03 DEG C
RHO= 1.183 KG/M3 VISC= 0.15406E-04 M2/S XVO= -23.1 CM
CP= 1011. J/KGK PR= 0.714

STANTON RUN UPW=3.5M/S TRANSITIONAL B.L. AT THETA=0

PLATE	X (CM)	UPW (M/S)	K	REXVO	TO DEG C	STANTON NO	REENTH	DST	DST(%)	DREEN
1	-61.3	3.49	0.000E 00	-0.86600E 05	30.33	0.65263E-02		0.753E-03	11.532	
2	-58.7	3.49	0.000E 00	-0.80670E 05	35.41	0.67406E-02		0.427E-03	6.328	
3	-56.1	3.49	0.000E 00	-0.74740E 05	37.49	0.52956E-02		0.249E-03	4.709	
4	-53.5	3.49	0.000E 00	-0.68868E 05	38.41	0.45032E-02		0.197E-03	4.378	
5	-50.9	3.49	0.000E 00	-0.62938E 05	38.64	0.33661E-02		0.145E-03	4.317	
6	-48.3	3.49	0.000E 00	-0.57009E 05	39.18	0.32011E-02		0.148E-03	4.620	
7	-45.7	3.49	0.000E 00	-0.51079E 05	39.35	0.27510E-02		0.130E-03	4.733	
8	-43.0	3.49	0.000E 00	-0.45149E 05	39.25	0.24072E-02		0.123E-03	5.105	
9	-40.4	3.49	0.000E 00	-0.39277E 05	38.69	0.23645E-02		0.115E-03	4.855	
10	-37.8	3.49	0.000E 00	-0.33347E 05	39.43	0.21870E-02		0.119E-03	5.449	
11	-35.2	3.49	0.000E 00	-0.27418E 05	39.69	0.20987E-02	0.17489E 03	0.110E-03	5.231	25.
12	-32.6	3.49	0.000E 00	-0.21488E 05	39.77	0.18858E-02	0.18572E 03	0.102E-03	5.432	25.
13	-30.0	3.49	0.000E 00	-0.15558E 05	39.82	0.18127E-02	0.19617E 03	0.100E-03	5.521	25.
14	-27.4	3.49	0.000E 00	-0.96862E 04	39.73	0.19098E-02	0.20832E 03	0.104E-03	5.453	25.
15	-24.8	3.49	0.000E 00	-0.37565E 04	39.74	0.17890E-02	0.21905E 03	0.981E-04	5.483	25.
16	-22.2	3.49	0.000E 00	0.21733E 04	39.73	0.18113E-02	0.22983E 03	0.995E-04	5.492	25.
17	-19.5	3.49	0.000E 00	0.81030E 04	39.66	0.17466E-02	0.24144E 03	0.965E-04	5.523	25.
18	-16.9	3.49	0.000E 00	0.13975E 05	39.70	0.17476E-02	0.25108E 03	0.980E-04	5.607	25.
19	-14.3	3.49	0.000E 00	0.19905E 05	39.76	0.17621E-02	0.26063E 03	0.979E-04	5.557	25.
20	-11.7	3.49	0.000E 00	0.25835E 05	39.69	0.18403E-02	0.27243E 03	0.997E-04	5.419	25.
21	-9.1	3.49	0.000E 00	0.31764E 05	39.66	0.18243E-02	0.28376E 03	0.983E-04	5.386	25.
22	-6.5	3.49	0.000E 00	0.37694E 05	39.67	0.17848E-02	0.29418E 03	0.992E-04	5.556	25.
23	-3.9	3.49	0.000E 00	0.43566E 05	39.62	0.19357E-02	0.30614E 03	0.103E-03	5.337	25.
24	-1.3	3.49	0.000E 00	0.49496E 05	39.58	0.20037E-02	0.31669E 03	0.112E-03	5.585	25.
CURVE BEGINS										
25	2.4	3.54	0.151E-05	0.58532E 05	39.79	0.18043E-02	0.33023E 03	0.193E-03	10.680	26.
26	7.3	3.58	0.112E-05	0.70699E 05	39.79	0.13534E-02	0.34799E 03	0.145E-03	10.702	26.
27	12.4	3.54	-0.113E-05	0.81449E 05	39.88	0.13274E-02	0.36175E 03	0.141E-03	10.655	26.
28	17.4	3.54	0.000E 00	0.93054E 05	39.81	0.12472E-02	0.37854E 03	0.142E-03	11.357	26.
29	22.5	3.54	0.000E 00	0.10472E 06	39.90	0.14020E-02	0.39184E 03	0.142E-03	10.123	26.
30	27.6	3.49	-0.113E-05	0.11484E 06	39.99	0.17525E-02	0.40784E 03	0.145E-03	8.298	26.
31	32.6	3.49	0.000E 00	0.12635E 06	40.07	0.17863E-02	0.42611E 03	0.145E-03	8.132	26.
32	37.7	3.54	0.109E-05	0.13959E 06	40.10	0.21702E-02	0.44655E 03	0.147E-03	6.763	26.
33	42.8	3.54	0.000E 00	0.15125E 06	40.15	0.21997E-02	0.47261E 03	0.147E-03	6.671	26.
34	47.8	3.49	-0.113E-05	0.16084E 06	40.12	0.24902E-02	0.50050E 03	0.151E-03	6.069	26.
35	52.9	3.49	0.000E 00	0.17229E 06	39.97	0.26354E-02	0.53489E 03	0.154E-03	5.838	26.
36	58.0	3.49	0.000E 00	0.18381E 06	39.91	0.27854E-02	0.56832E 03	0.155E-03	5.580	26.
37	63.0	3.49	0.000E 00	0.19526E 06	39.92	0.26665E-02	0.59949E 03	0.154E-03	5.784	26.
38	68.1	3.54	0.109E-05	0.20945E 06	39.96	0.24904E-02	0.62818E 03	0.145E-03	5.828	26.
RECOVERY BEGINS										
39	72.0	3.54	0.220E-06	0.21868E 06	39.59	0.30090E-02	0.66532E 03	0.135E-03	4.473	26.
40	74.6	3.55	0.321E-06	0.22513E 06	39.49	0.31474E-02	0.68804E 03	0.141E-03	4.478	26.
41	77.2	3.56	0.319E-06	0.23161E 06	39.67	0.32383E-02	0.69953E 03	0.148E-03	4.580	26.
42	79.8	3.56	0.317E-06	0.23811E 06	39.69	0.31922E-02	0.71822E 03	0.146E-03	4.560	26.
43	82.4	3.57	0.318E-06	0.24457E 06	39.66	0.33096E-02	0.73908E 03	0.149E-03	4.490	26.
44	85.0	3.58	0.313E-06	0.25111E 06	39.67	0.32636E-02	0.75841E 03	0.150E-03	4.594	26.
45	87.6	3.58	0.234E-06	0.25756E 06	39.74	0.30767E-02	0.77443E 03	0.142E-03	4.618	27.
46	90.2	3.58	0.000E 00	0.26364E 06	39.62	0.33021E-02	0.79956E 03	0.145E-03	4.403	27.
47	92.8	3.58	0.000E 00	0.26967E 06	39.60	0.31249E-02	0.82034E 03	0.142E-03	4.538	27.
48	95.4	3.58	0.000E 00	0.27575E 06	39.60	0.32856E-02	0.83958E 03	0.149E-03	4.532	27.
49	98.1	3.58	0.000E 00	0.28184E 06	39.63	0.31778E-02	0.85795E 03	0.146E-03	4.594	27.
50	100.7	3.58	-0.235E-06	0.28751E 06	39.71	0.31856E-02	0.87239E 03	0.149E-03	4.672	27.
51	103.3	3.57	-0.395E-06	0.29289E 06	39.65	0.32069E-02	0.89504E 03	0.146E-03	4.542	26.
52	105.9	3.56	-0.401E-06	0.29817E 06	39.71	0.31837E-02	0.91117E 03	0.148E-03	4.635	26.
53	108.5	3.55	-0.400E-06	0.30349E 06	39.66	0.32658E-02	0.93367E 03	0.148E-03	4.544	26.
54	111.1	3.54	-0.403E-06	0.30877E 06	39.67	0.32098E-02	0.95214E 03	0.149E-03	4.648	26.
55	113.7	3.54	-0.406E-06	0.31403E 06	39.51	0.33078E-02	0.98184E 03	0.147E-03	4.452	26.
56	116.4	3.53	-0.409E-06	0.31925E 06	39.67	0.32624E-02	0.99107E 03	0.152E-03	4.667	26.
57	118.9	3.52	-0.416E-06	0.32438E 06	39.69	0.31414E-02	0.10088E 04	0.148E-03	4.699	26.
58	121.6	3.51	-0.415E-06	0.32954E 06	39.56	0.32227E-02	0.10360E 04	0.148E-03	4.599	26.
59	124.2	3.50	-0.418E-06	0.33467E 06	39.58	0.31727E-02	0.10542E 04	0.149E-03	4.692	26.
60	126.8	3.49	-0.422E-06	0.33976E 06	39.36	0.32440E-02	0.10877E 04	0.145E-03	4.475	26.
61	129.4	3.49	0.000E 00	0.34569E 06	39.57	0.30569E-02	0.10918E 04	0.155E-03	5.070	26.
62	132.0	3.49	0.000E 00	0.35157E 06	39.20	0.24816E-02	0.11346E 04	0.223E-03	8.974	26.

UNCERTAINTY IN REX= 5757.

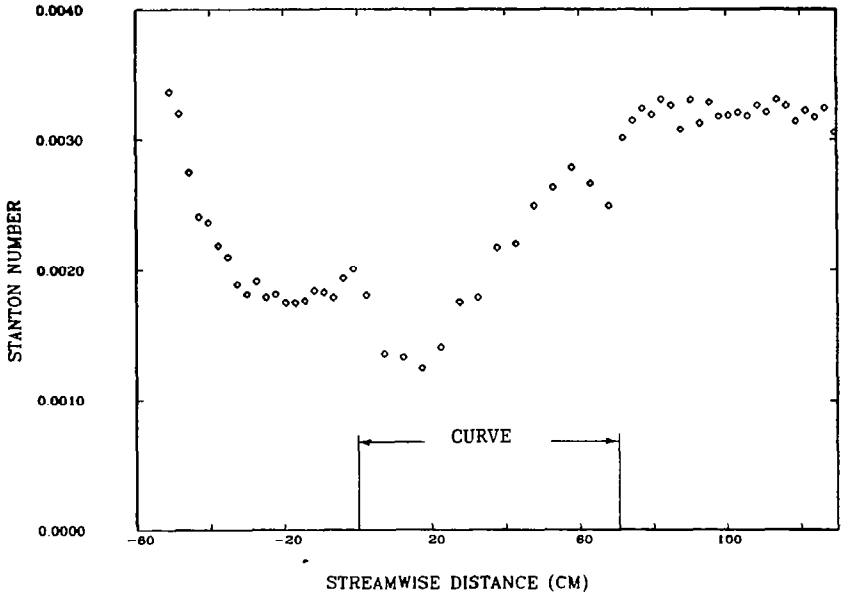

Fig. G-23. Case 060980: Stanton number versus streamwise distance.

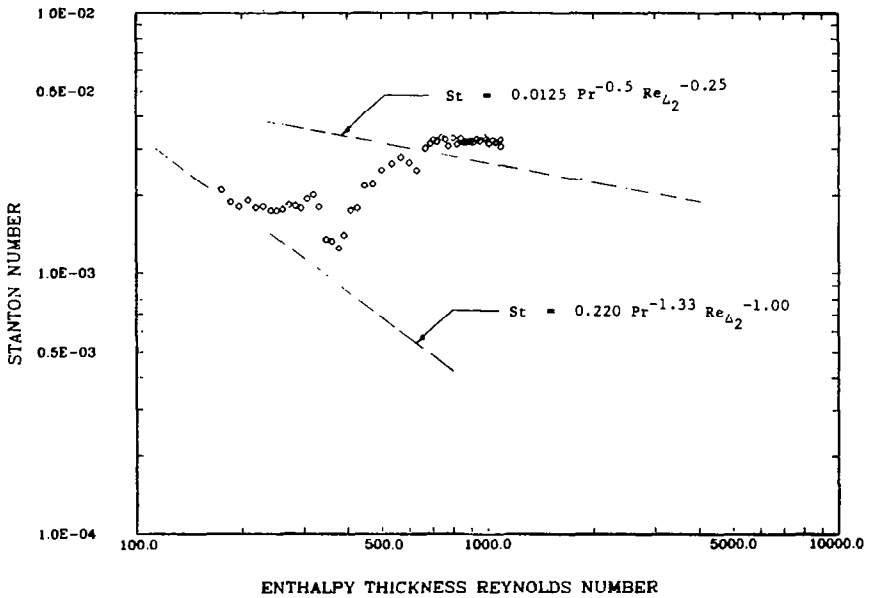

Fig. G-24. Case 060980: Stanton number versus enthalpy thickness Reynolds number.

042280 START PROFILE DEL99/R(THETA=0)=0.05 UPW(PREPLATE)=13M/S K=0.57E-6

REX	= 0.68227E 06	REM	= 1719.	REH	= 755.		
XVO	= -112.95 CM	DEL2	= 0.196 CM	DEH2	= 0.086 CM		
UPW	= 13.33 M/S	DEL99=	1.725 CM	DELT99	= 1.204 CM		
VISC	= 0.15218E-04 M2/S	DEL1	= 0.292 CM	UPW	= 13.35 M/S		
PORT	= 4	H	= 1.486	VISC	= 0.15278E-04 M2/S		
XLOC	= -35.05 CM	CF/2	= 0.18928E-02	TINF	= 22.49 DEG C		
DENS	= 1.19 KG/M3			TPLATE	= 37.34 DEG C		

Y(CM)	Y/DEL	U(M/S)	U/UP	Y+	U+	CF/2	T(DEG C)	Y(CM)	Y+	U(M/S)	T(DEG C)	TBAR	1-TBAR
0.048	0.028	6.41	0.481	18.4	11.06	0.001628	29.01	0.0140	5.32	1.85	32.79	0.306	0.694
0.074	0.043	7.53	0.565	28.1	12.99	0.001857	27.86	0.0394	15.00	5.22	29.50	0.528	0.472
0.099	0.058	8.07	0.605	37.8	13.92	0.001906	27.19	0.0648	24.68	7.14	28.07	0.624	0.376
0.150	0.087	8.64	0.648	57.1	14.90	0.001901	26.26	0.1156	44.04	8.25	26.74	0.714	0.286
0.201	0.116	8.99	0.675	76.5	15.51	0.001878	25.68	0.1664	63.39	8.76	25.99	0.764	0.236
0.250	0.145	9.33	0.700	95.4	16.10	0.001889	25.27	0.2172	82.75	9.11	25.49	0.798	0.202
0.324	0.188	9.73	0.730	123.5	16.77	0.001897	24.78	0.2934	111.79	9.56	24.93	0.835	0.165
0.374	0.217	9.96	0.747	142.6	17.17	0.001907	24.53	0.3442	131.14	9.82	24.64	0.855	0.145
0.449	0.260	10.31	0.773	171.1	17.77	0.001936	24.20	0.4204	160.18	10.17	24.28	0.880	0.120
0.549	0.319	10.66	0.800	209.4	18.38	0.001958	23.82	0.5220	198.89	10.56	23.87	0.907	0.093
0.676	0.392	11.08	0.831	257.5	19.11	0.001996	23.47	0.6490	247.28	10.99	23.49	0.933	0.067
0.802	0.465	11.47	0.860	305.6	19.77	0.002039	23.19	0.7760	295.67	11.39	23.19	0.953	0.047
1.005	0.583	12.01	0.901	382.8	20.72	0.002107	22.88	0.9792	373.10	11.94	22.86	0.975	0.025
1.207	0.700	12.49	0.937	459.9	21.54	0.002169	22.72	1.1824	450.53	12.43	22.67	0.987	0.013
1.485	0.861	12.96	0.973	565.9	22.36	0.002218	22.59	1.4618	556.99	12.92	22.54	0.996	0.004
1.738	1.008	13.20	0.991	662.3	22.77	0.002218	22.56	1.7158	653.77	13.18	22.50	0.999	0.001
2.246	1.302	13.35	1.001	855.8	23.01	0.002145	22.55	2.2238	847.34	13.34	22.49	1.000	-0.000
								2.7318	1040.91	13.33	22.50	0.999	0.001

RUN 042280 *** CURVATURE RIG *** NASA-NAG-3-3 STANTON NUMBER DATA

TADB= 22.28 DEG C UREF= 13.34 M/S TINF= 22.20 DEG C
RHO= 1.189 KG/M3 VISC= 0.15253E-04 M2/S XVO= -113.0 CM
CP= 1011. J/KGK PR= 0.715

STANTON RUN DEL99/R(THETA=0.0)=0.05 UPW(PREPLATE)=13M/S K=0.57E-6

PLATE	X (CM)	UPW (M/S)	K	REXVO	TO DEG C	STANTON NO	REENTH	DST	DST(%)	DREEN
1	-61.3	13.34	0.000E 00	0.45206E 06	34.89	0.34503E-02		0.217E-03	6.293	
2	-58.7	13.34	0.000E 00	0.47493E 06	36.27	0.37068E-02		0.127E-03	3.413	
3	-56.1	13.34	0.000E 00	0.49780E 06	36.60	0.35638E-02		0.118E-03	3.304	
4	-53.5	13.34	0.000E 00	0.52045E 06	36.83	0.33725E-02		0.114E-03	3.390	
5	-50.9	13.34	0.000E 00	0.54332E 06	36.12	0.29778E-02		0.949E-04	3.186	
6	-48.3	13.34	0.000E 00	0.56620E 06	37.08	0.31163E-02		0.106E-03	3.396	
7	-45.7	13.34	0.000E 00	0.58907E 06	37.28	0.29763E-02		0.993E-04	3.336	
8	-43.0	13.34	0.000E 00	0.61194E 06	37.27	0.28799E-02		0.953E-04	3.310	
9	-40.4	13.34	0.000E 00	0.63459E 06	37.38	0.28774E-02		0.956E-04	3.323	
10	-37.8	13.34	0.000E 00	0.65746E 06	37.41	0.27900E-02		0.925E-04	3.316	
11	-35.2	13.34	0.000E 00	0.68033E 06	37.52	0.27767E-02	0.78892E 03	0.926E-04	3.334	1.
12	-32.6	13.34	0.000E 00	0.70321E 06	37.49	0.26564E-02	0.85225E 03	0.886E-04	3.336	2.
13	-30.0	13.34	0.000E 00	0.72608E 06	37.42	0.26462E-02	0.91689E 03	0.877E-04	3.314	2.
14	-27.4	13.34	0.000E 00	0.74873E 06	37.51	0.26708E-02	0.97177E 03	0.892E-04	3.341	3.
15	-24.8	13.34	0.000E 00	0.77160E 06	37.59	0.26342E-02	0.10276E 04	0.879E-04	3.336	3.
16	-22.2	13.34	0.000E 00	0.79447E 06	37.60	0.26223E-02	0.10870E 04	0.888E-04	3.386	3.
17	-19.5	13.34	0.000E 00	0.81735E 06	37.13	0.25175E-02	0.11790E 04	0.823E-04	3.270	4.
18	-16.9	13.34	0.000E 00	0.84000E 06	37.44	0.26063E-02	0.12136E 04	0.875E-04	3.358	4.
19	-14.3	13.34	0.000E 00	0.86287E 06	37.60	0.26232E-02	0.12607E 04	0.882E-04	3.363	4.
20	-11.7	13.34	0.000E 00	0.88574E 06	37.44	0.25784E-02	0.13331E 04	0.857E-04	3.322	4.
21	-9.1	13.34	0.000E 00	0.90861E 06	37.41	0.24662E-02	0.13934E 04	0.818E-04	3.316	5.
22	-6.5	13.34	0.000E 00	0.93148E 06	37.61	0.24819E-02	0.14313E 04	0.833E-04	3.356	5.
23	-3.9	13.34	0.000E 00	0.95413E 06	37.70	0.25487E-02	0.14800E 04	0.851E-04	3.340	5.
24	-1.3	13.34	0.000E 00	0.97701E 06	37.73	0.24257E-02	0.15340E 04	0.822E-04	3.388	5.
CURVE BEGINS										
25	2.4	13.83	0.105E-05	0.10461E 07	37.68	0.19964E-02	0.16127E 04	0.103E-03	5.158	6.
26	7.3	14.08	0.396E-06	0.11107E 07	37.88	0.18970E-02	0.16798E 04	0.848E-04	4.463	7.
27	12.4	14.33	0.363E-06	0.11782E 07	38.09	0.18727E-02	0.17469E 04	0.928E-04	4.947	7.
28	17.4	14.64	0.428E-06	0.12519E 07	38.02	0.17615E-02	0.18440E 04	0.865E-04	4.903	8.
29	22.5	15.00	0.482E-06	0.13332E 07	38.00	0.17148E-02	0.19347E 04	0.844E-04	4.911	9.
30	27.6	15.40	0.499E-06	0.14195E 07	38.01	0.16742E-02	0.20203E 04	0.826E-04	4.923	10.
31	32.6	15.87	0.548E-06	0.15154E 07	38.07	0.16105E-02	0.21000E 04	0.799E-04	4.949	10.
32	37.7	16.38	0.562E-06	0.16181E 07	38.07	0.15835E-02	0.21890E 04	0.783E-04	4.933	11.
33	42.8	16.87	0.512E-06	0.17229E 07	38.05	0.15760E-02	0.22810E 04	0.774E-04	4.902	12.
34	47.8	17.33	0.456E-06	0.18279E 07	38.12	0.15610E-02	0.23631E 04	0.772E-04	4.937	13.
35	52.9	17.81	0.447E-06	0.19370E 07	38.04	0.15668E-02	0.24688E 04	0.759E-04	4.832	13.
36	58.0	18.42	0.534E-06	0.20651E 07	38.15	0.15188E-02	0.25466E 04	0.743E-04	4.880	14.
37	63.0	19.23	0.649E-06	0.22200E 07	38.15	0.14421E-02	0.26437E 04	0.716E-04	4.952	15.
38	68.1	19.87	0.476E-06	0.23596E 07	37.93	0.13339E-02	0.27757E 04	0.655E-04	4.903	16.
RECOVERY BEGINS										
39	72.0	20.31	0.422E-06	0.24632E 07	37.55	0.15360E-02	0.29158E 04	0.516E-04	3.358	17.
40	74.6	20.31	0.000E 00	0.24981E 07	37.32	0.15553E-02	0.30133E 04	0.515E-04	3.313	17.
41	77.2	20.31	0.000E 00	0.25329E 07	37.72	0.16061E-02	0.29899E 04	0.552E-04	3.437	17.
42	79.8	20.31	0.000E 00	0.25678E 07	37.72	0.15765E-02	0.30438E 04	0.534E-04	3.389	17.
43	82.4	20.31	0.000E 00	0.26023E 07	37.69	0.16237E-02	0.31057E 04	0.547E-04	3.368	17.
44	85.0	20.31	0.000E 00	0.26371E 07	37.72	0.16000E-02	0.31557E 04	0.546E-04	3.414	17.
45	87.6	20.31	0.000E 00	0.26719E 07	37.73	0.15852E-02	0.32100E 04	0.540E-04	3.406	17.
46	90.2	20.31	0.000E 00	0.27068E 07	37.56	0.16496E-02	0.33009E 04	0.553E-04	3.351	17.
47	92.8	20.31	0.000E 00	0.27413E 07	37.45	0.15888E-02	0.33816E 04	0.536E-04	3.374	17.
48	95.4	20.31	0.000E 00	0.27761E 07	37.43	0.16818E-02	0.34426E 04	0.567E-04	3.373	17.
49	98.1	20.31	0.000E 00	0.28110E 07	37.44	0.16054E-02	0.34967E 04	0.543E-04	3.384	17.
50	100.7	20.31	0.000E 00	0.28458E 07	37.58	0.16781E-02	0.35216E 04	0.574E-04	3.421	17.
51	103.3	20.31	0.000E 00	0.28806E 07	37.50	0.16650E-02	0.35994E 04	0.558E-04	3.352	17.
52	105.9	20.31	0.000E 00	0.29151E 07	37.62	0.16805E-02	0.36297E 04	0.572E-04	3.404	17.
53	108.5	20.31	0.000E 00	0.29500E 07	37.56	0.16782E-02	0.37021E 04	0.565E-04	3.367	17.
54	111.1	20.31	0.000E 00	0.29848E 07	37.60	0.16547E-02	0.37505E 04	0.569E-04	3.439	17.
55	113.7	20.31	0.000E 00	0.30196E 07	37.26	0.16408E-02	0.38898E 04	0.543E-04	3.308	17.
56	116.4	20.31	0.000E 00	0.30545E 07	37.59	0.17004E-02	0.38632E 04	0.584E-04	3.433	17.
57	118.9	20.31	0.000E 00	0.30890E 07	37.60	0.16313E-02	0.39196E 04	0.560E-04	3.433	18.
58	121.6	20.31	0.000E 00	0.31238E 07	37.31	0.16317E-02	0.40502E 04	0.549E-04	3.365	18.
59	124.2	20.31	0.000E 00	0.31587E 07	37.29	0.16281E-02	0.41138E 04	0.563E-04	3.459	18.
60	126.8	20.31	0.000E 00	0.31935E 07	36.82	0.15995E-02	0.43002E 04	0.526E-04	3.291	18.
61	129.4	20.31	0.000E 00	0.32283E 07	37.27	0.16382E-02	0.42243E 04	0.580E-04	3.543	18.
62	132.0	20.31	0.000E 00	0.32628E 07	37.00	0.14449E-02	0.43546E 04	0.680E-04	4.708	18.

UNCERTAINTY IN REX=11258.

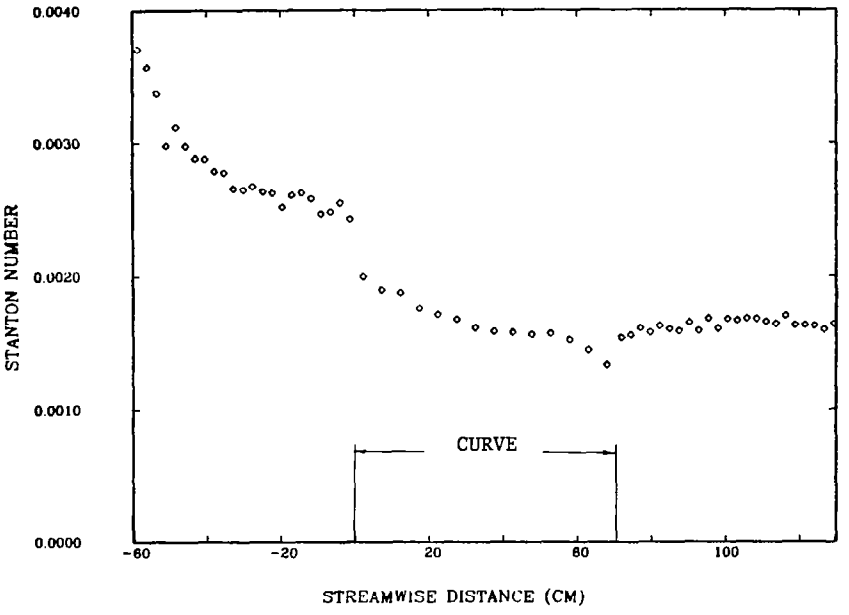

Fig. G-25. Case 042280: Stanton number versus streamwise distance.

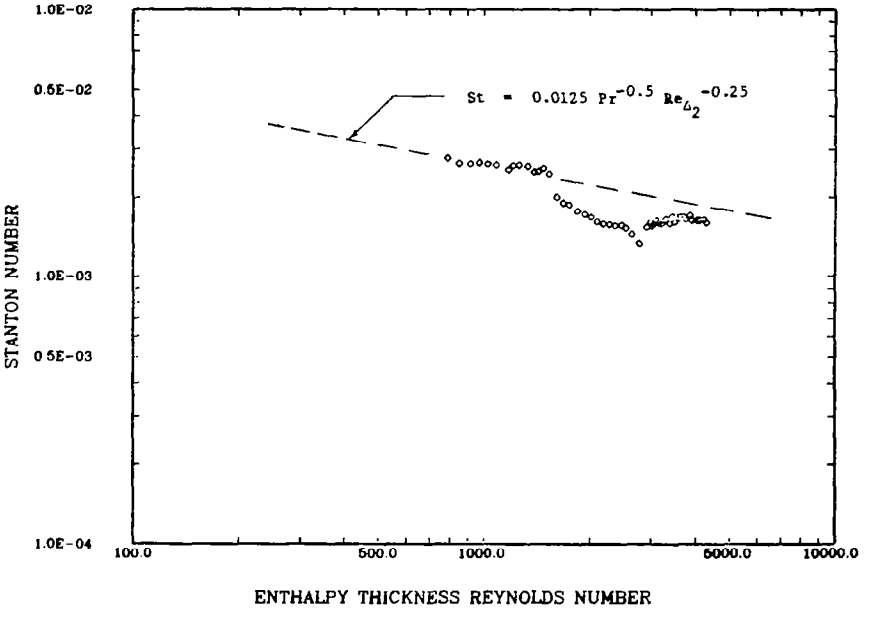

Fig. G-26. Case 042280: Stanton number versus enthalpy thickness Reynolds number.

051080 STARTING PROFILES DEL99/R(THETA=0)=0.05 K=1.25E-6

REX = 0.29659E 06		REM = 883.					REH = 565.				
XVO = -85.26 CM		DEL2 = 0.149 CM					DEH2 = 0.096 CM				
UPW = 9.05 M/S		DEL99= 1.460 CM					DELT99 = 1.319 CM				
VISC = 0.15319E-04 M2/S		DEL1 = 0.229 CM					UPW = 9.06 M/S				
PORT = 4		H = 1.529					VISC = 0.15353E-04 M2/S				
XLOC = -35.05 CM		CF/2 = 0.23124E-02					TINF = 22.54 DEG C				
DENS = 1.18 KG/M3							TPLATE = 38.40 DEG C				
Y(CM)	Y/DEL	U(M/S)	U/UP	Y+	U+	CF/2	T(DEG C)	Y(CM)	Y+	U(M/S)	T(DEG C)	TBAR	1-TBAR
0.048	0.033	4.50	0.498	13.7	10.35	0.001976	30.38	0.0140	3.97	1.30	35.38	0.190	0.810
0.074	0.051	5.32	0.588	21.0	12.23	0.002254	28.66	0.0394	11.18	3.67	31.14	0.458	0.542
0.099	0.068	5.66	0.626	28.2	13.02	0.002276	27.73	0.0648	18.40	5.03	28.98	0.594	0.406
0.150	0.103	6.12	0.677	42.6	14.07	0.002291	26.56	0.1156	32.83	5.81	27.11	0.712	0.288
0.201	0.138	6.39	0.706	57.0	14.68	0.002265	25.88	0.1664	47.26	6.21	26.28	0.764	0.236
0.250	0.172	6.65	0.734	71.1	15.27	0.002279	25.43	0.2172	61.69	6.47	25.66	0.803	0.197
0.325	0.223	6.92	0.765	92.3	15.90	0.002279	24.90	0.2934	83.33	6.80	25.09	0.839	0.161
0.375	0.257	7.13	0.788	106.6	16.38	0.002311	24.64	0.3442	97.76	7.00	24.77	0.860	0.140
0.450	0.308	7.39	0.816	127.8	16.98	0.002347	24.30	0.4204	119.40	7.28	24.41	0.883	0.117
0.550	0.377	7.69	0.850	156.3	17.67	0.002396	23.92	0.5220	148.26	7.61	23.98	0.909	0.091
0.676	0.463	8.01	0.885	191.9	18.40	0.002447	23.58	0.6490	184.33	7.94	23.62	0.932	0.068
0.802	0.549	8.26	0.913	227.7	18.99	0.002483	23.29	0.7760	220.41	8.21	23.31	0.952	0.048
1.004	0.688	8.61	0.951	285.1	19.78	0.002534	23.00	0.9792	278.13	8.57	23.00	0.972	0.028
1.205	0.826	8.82	0.975	342.4	20.28	0.002540	22.82	1.1824	335.84	8.80	22.82	0.983	0.017
1.484	1.017	8.96	0.991	421.6	20.60	0.002494	22.64	1.4618	415.20	8.95	22.62	0.995	0.005
1.738	1.190	9.03	0.998	493.6	20.76	0.002443	22.59	1.7158	487.35	9.03	22.57	0.998	0.002
2.245	1.538	9.06	1.001	637.8	20.81	0.002324	22.56	2.2238	631.64	9.05	22.54	1.001	-0.001
2.753	1.886	9.06	1.001	782.1	20.81	0.002228	22.58	2.7318	775.94	9.06	22.55	1.000	0.000
								3.2398	920.23	9.05	22.55	1.000	0.000

051080 VELOCITY PROFILE K=1.25E-6 THETA=52.5 DEG. S=40.8 CM

REX = 0.18836E 06 REM = 614.

XVO = 20.08 CM DEL2 = 0.068 CM
UPW = 13.75 M/S DEL99= 0.936 CM
VISC = 0.15199E-04 M2/S DEL1 = 0.111 CM
PORT = 4 H = 1.642
XLOC = 40.89 CM CF/2 = 0.28298E-02
DENS = 1.19 KG/M3

Y(CM)	Y/DEL	U(M/S)	U/UP	Y+	U+	CF/2
0.048	0.052	6.96	0.507	23.3	9.51	0.001752
0.074	0.079	8.87	0.646	35.5	12.13	0.002299
0.099	0.106	10.07	0.734	47.7	13.77	0.002612
0.125	0.133	10.82	0.789	60.0	14.79	0.002768
0.175	0.187	11.61	0.847	84.4	15.86	0.002843
0.223	0.239	12.03	0.879	107.5	16.44	0.002840
0.270	0.289	12.29	0.899	130.2	16.80	0.002807
0.345	0.368	12.57	0.921	166.1	17.18	0.002747
0.394	0.421	12.70	0.931	189.8	17.36	0.002709
0.470	0.502	12.84	0.943	226.3	17.55	0.002647
0.571	0.610	13.03	0.960	274.8	17.81	0.002597
0.672	0.717	13.13	0.969	323.4	17.95	0.002535
0.824	0.880	13.26	0.982	396.6	18.12	0.002463
1.052	1.123	13.41	0.998	506.3	18.33	0.002382
1.305	1.394	13.37	1.000	628.3	18.27	0.002261
1.432	1.530	13.33	1.000	689.5	18.22	0.002206

RUN 051080 *** CURVATURE RIG *** NASA-NAG-3-3 STANTON NUMBER DATA

TADB= 22.55 DEG C UREF= 9.05 M/S TINF= 22.51 DEG C
RHO= 1.184 KG/M3 VISC= 0.15350E-04 M2/S XVO= -85.3 CM
CP= 1010. J/KGK PR= 0.714

STANTON RUN DEL99/R(THETA=0)=0.05 UPW(PREPLATE)=9.0 M/S K=1.25E-6

PLATE	X (CM)	UPW (M/S)	K	REXVO	TO DEG C	STANTON NO	REENTH	DST	DST(%)	DREEN
1	-61.3	9.05	0.000E 00	0.14167E 06	37.36	0.21119E-02		0.259E-03	12.255	
2	-58.7	9.05	0.000E 00	0.15710E 06	38.35	0.31740E-02		0.113E-03	3.551	
3	-56.1	9.05	0.000E 00	0.17253E 06	38.35	0.32894E-02		0.111E-03	3.381	
4	-53.5	9.05	0.000E 00	0.18781E 06	38.37	0.33287E-02		0.116E-03	3.485	
5	-50.9	9.05	0.000E 00	0.20324E 06	37.63	0.31549E-02		0.102E-03	3.245	
6	-48.3	9.05	0.000E 00	0.21867E 06	38.38	0.33696E-02		0.117E-03	3.477	
7	-45.7	9.05	0.000E 00	0.23410E 06	38.46	0.33213E-02		0.113E-03	3.400	
8	-43.0	9.05	0.000E 00	0.24953E 06	38.40	0.32829E-02		0.111E-03	3.373	
9	-40.4	9.05	0.000E 00	0.26481E 06	38.43	0.33378E-02		0.113E-03	3.377	
10	-37.8	9.05	0.000E 00	0.28024E 06	38.46	0.32268E-02		0.109E-03	3.386	
11	-35.2	9.05	0.000E 00	0.29567E 06	38.53	0.32191E-02	0.58953E 03	0.109E-03	3.398	12.
12	-32.6	9.05	0.000E 00	0.31109E 06	38.52	0.30792E-02	0.63826E 03	0.105E-03	3.407	12.
13	-30.0	9.05	0.000E 00	0.32652E 06	38.49	0.30529E-02	0.68691E 03	0.103E-03	3.387	12.
14	-27.4	9.05	0.000E 00	0.34180E 06	38.56	0.30680E-02	0.73073E 03	0.105E-03	3.416	12.
15	-24.8	9.05	0.000E 00	0.35723E 06	38.60	0.30119E-02	0.77585E 03	0.102E-03	3.400	12.
16	-22.2	9.05	0.000E 00	0.37266E 06	38.63	0.29763E-02	0.82062E 03	0.103E-03	3.460	12.
17	-19.5	9.05	0.000E 00	0.38809E 06	38.26	0.28369E-02	0.88428E 03	0.950E-04	3.350	12.
18	-16.9	9.05	0.000E 00	0.40337E 06	38.53	0.29178E-02	0.91390E 03	0.100E-03	3.439	12.
19	-14.3	9.05	0.000E 00	0.41880E 06	38.65	0.29421E-02	0.95223E 03	0.101E-03	3.436	12.
20	-11.7	9.05	0.000E 00	0.43423E 06	38.53	0.28868E-02	0.10042E 04	0.982E-04	3.403	12.
21	-9.1	9.05	0.000E 00	0.44966E 06	38.51	0.27735E-02	0.10486E 04	0.942E-04	3.397	12.
22	-6.5	9.05	0.000E 00	0.46509E 06	38.70	0.27595E-02	0.10790E 04	0.952E-04	3.451	13.
23	-3.9	9.05	0.000E 00	0.48037E 06	38.74	0.28662E-02	0.11200E 04	0.978E-04	3.414	13.
24	-1.3	9.05	0.000E 00	0.49580E 06	38.78	0.27185E-02	0.11597E 04	0.952E-04	3.502	13.
CURVE BEGINS										
25	2.4	9.44	0.178E-05	0.53940E 06	38.69	0.22586E-02	0.12232E 04	0.805E-04	3.565	13.
26	7.3	9.76	0.105E-05	0.58912E 06	38.68	0.20024E-02	0.12907E 04	0.598E-04	2.988	14.
27	12.4	10.15	0.110E-05	0.64580E 06	38.77	0.18931E-02	0.13496E 04	0.558E-04	2.949	14.
28	17.4	10.59	0.118E-05	0.70910E 06	38.72	0.17360E-02	0.14192E 04	0.531E-04	3.058	15.
29	22.5	11.15	0.133E-05	0.78361E 06	38.79	0.16366E-02	0.14771E 04	0.502E-04	3.068	16.
30	27.6	11.79	0.136E-05	0.86735E 06	38.88	0.14819E-02	0.15308E 04	0.467E-04	3.150	17.
31	32.6	12.52	0.136E-05	0.96234E 06	38.89	0.13773E-02	0.15926E 04	0.440E-04	3.195	18.
32	37.7	13.31	0.131E-05	0.10664E 07	38.98	0.12657E-02	0.16439E 04	0.409E-04	3.233	19.
33	42.8	14.11	0.119E-05	0.11778E 07	38.99	0.11740E-02	0.17031E 04	0.385E-04	3.277	20.
34	47.8	14.99	0.114E-05	0.13002E 07	39.01	0.10884E-02	0.17593E 04	0.360E-04	3.310	22.
35	52.9	15.89	0.105E-05	0.14309E 07	39.09	0.10738E-02	0.18104E 04	0.342E-04	3.183	23.
36	58.0	16.96	0.109E-05	0.15836E 07	39.06	0.94768E-03	0.18747E 04	0.317E-04	3.341	25.
37	63.0	18.49	0.130E-05	0.17870E 07	39.00	0.93669E-03	0.19463E 04	0.296E-04	3.158	27.
38	68.1	20.02	0.111E-05	0.20014E 07	38.96	0.80338E-03	0.20152E 04	0.259E-04	3.227	29.
RECOVERY BEGINS										
39	72.0	20.20	0.179E-06	0.20702E 07	39.03	0.95742E-03	0.20498E 04	0.347E-04	3.620	29.
40	74.6	20.28	0.115E-06	0.21130E 07	38.71	0.10366E-02	0.21247E 04	0.361E-04	3.478	30.
41	77.2	20.36	0.114E-06	0.21561E 07	38.82	0.11826E-02	0.21482E 04	0.419E-04	3.544	30.
42	79.8	20.44	0.113E-06	0.21995E 07	38.64	0.12442E-02	0.22144E 04	0.434E-04	3.488	30.
43	82.4	20.52	0.112E-06	0.22427E 07	38.40	0.13838E-02	0.22936E 04	0.475E-04	3.431	30.
44	85.0	20.60	0.110E-06	0.22866E 07	38.24	0.14536E-02	0.23669E 04	0.502E-04	3.451	30.
45	87.6	20.68	0.109E-06	0.23306E 07	38.13	0.14990E-02	0.24350E 04	0.516E-04	3.439	30.
46	90.2	20.76	0.107E-06	0.23749E 07	37.84	0.16236E-02	0.25371E 04	0.547E-04	3.372	30.
47	92.8	20.84	0.107E-06	0.24191E 07	37.63	0.16100E-02	0.26295E 04	0.546E-04	3.390	31.
48	95.4	20.92	0.105E-06	0.24639E 07	37.53	0.17433E-02	0.27054E 04	0.590E-04	3.387	31.
49	98.1	20.92	0.000E 00	0.24995E 07	37.45	0.16999E-02	0.27820E 04	0.575E-04	3.381	31.
50	100.7	20.98	0.781E-07	0.25423E 07	37.55	0.18005E-02	0.28250E 04	0.616E-04	3.423	31.
51	103.3	21.04	0.775E-07	0.25853E 07	37.42	0.18083E-02	0.29159E 04	0.606E-04	3.349	31.
52	105.9	21.12	0.103E-06	0.26305E 07	37.53	0.18310E-02	0.29586E 04	0.623E-04	3.401	31.
53	108.5	21.17	0.760E-07	0.26738E 07	37.46	0.18398E-02	0.30397E 04	0.619E-04	3.362	31.
54	111.1	21.23	0.754E-07	0.27173E 07	37.49	0.18123E-02	0.30980E 04	0.622E-04	3.431	31.
55	113.7	21.23	0.000E 00	0.27535E 07	37.14	0.17891E-02	0.32372E 04	0.592E-04	3.308	31.
56	116.4	21.31	0.994E-07	0.27998E 07	37.47	0.18637E-02	0.32300E 04	0.639E-04	3.427	32.
57	118.9	21.39	0.993E-07	0.28460E 07	37.46	0.17870E-02	0.32995E 04	0.612E-04	3.423	32.
58	121.6	21.48	0.121E-06	0.28953E 07	37.16	0.17764E-02	0.34326E 04	0.597E-04	3.361	32.
59	124.2	21.56	0.960E-07	0.29423E 07	37.11	0.17707E-02	0.35080E 04	0.611E-04	3.452	32.
60	126.8	21.63	0.950E-07	0.29895E 07	36.60	0.17352E-02	0.36988E 04	0.570E-04	3.283	32.
61	129.4	21.63	0.000E 00	0.30264E 07	37.11	0.17833E-02	0.36314E 04	0.628E-04	3.520	32.
62	132.0	21.63	0.000E 00	0.30629E 07	36.88	0.15944E-02	0.37503E 04	0.711E-04	4.462	32.

UNCERTAINTY IN REX= 8658.

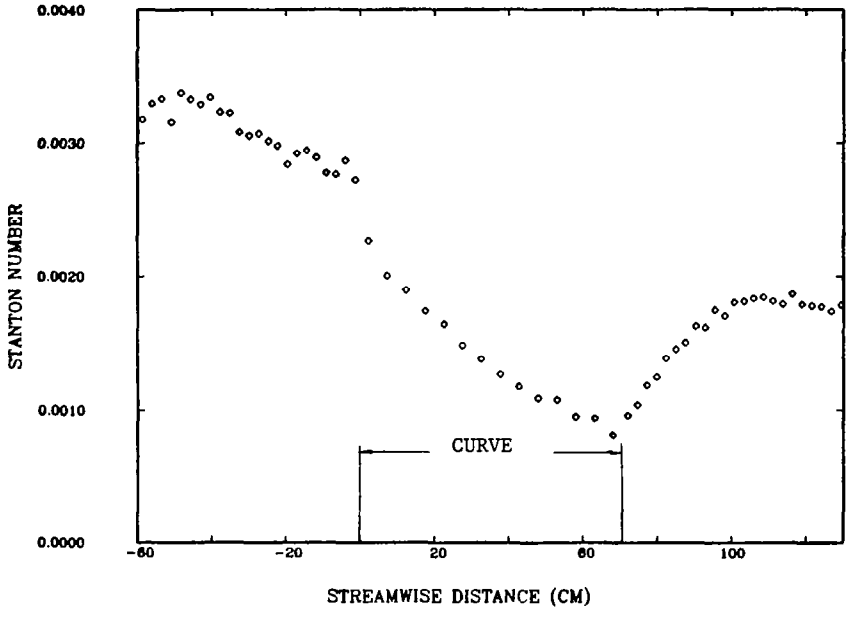

Fig. G-27. Case 051080: Stanton number versus streamwise distance.

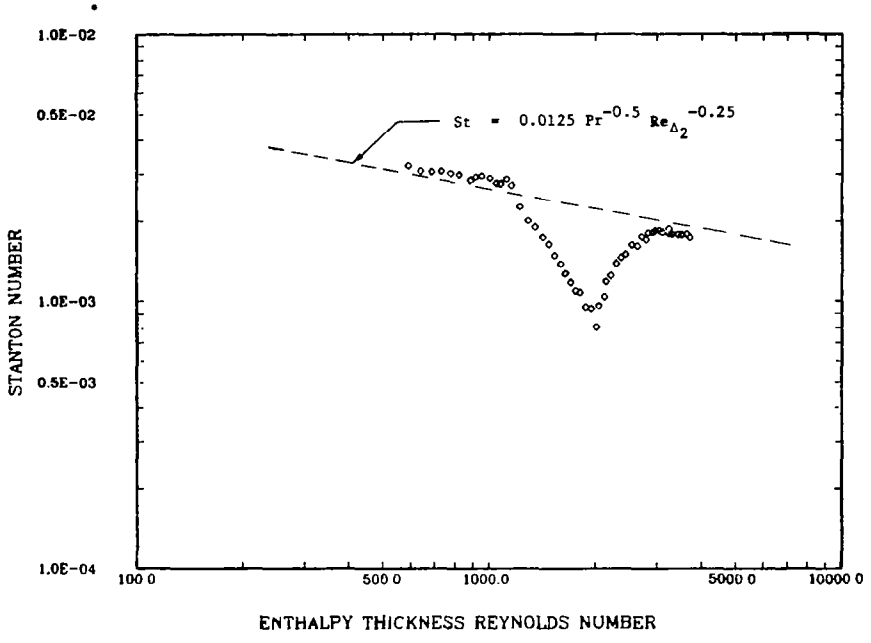

Fig. G-28. Case 051080: Stanton number versus enthalpy thickness Reynolds number.

Appendix H

Modifications to STAN5 for Convex Curvature Predictions

The following listing shows the modifications made to STAN5 [1] to account for convex curvature effects. This version of the program was used to make the predictions of Figs. 4-2 through 4-17. New programming is listed, bracketed with the preceding and following lines of the original STAN5 program (lines with identification on right side).

```
      C.....                                                                    MAIN0150
      C..... THIS PROGRAM HAS BEEN MODIFIED FOR CONVEX CURVATURE
      C..... USING THE GILLIS MODEL WITH THE SIMON CHANGES
      C..... SEE THE TWO THESES FOR DETAILS
      C..... LATEST REVISION    ******* SEPTEMBER  1980 ********
    1       INTEGER GEOM,FLUID,SOURCE(5),SPACE,BODFOR,OUTPUT,TYPBC              MAIN0160

            3/ADD/RBOM(54),OMD(54),ROMD(54),ITKE,CBC(100),CEFF(54),CLAG,CURV,   MAIN0290
            4CW,PL(54),SKIN(100),STANT(100),XPLOT(100),REENTH(100),IPLOT,XSTART
    3        DIMENSION AMEF(5),AMIF(5)                                          MAIN0300
    4        DIMENSION FPP(100),AFPP(100),BFPP(100),CFPP(100)                   MAIN0310
    5        CALL STARTG('GENIL*',0.)
      C.....                                                                    MAIN0311

    7         NIND=0                                                           MAIN0340
    8         IPLOT=0
    9         NPLOT=0
   10       5 KERROR=0                                                         MAIN0350
   11         DO 7 I=1,100
   12         SKIN(I)=0.0
   13         STANT(I)=0.0
   14         XPLOT(I)=0.0
   15         REENTH(I)=0.0
   16       7 CONTINUE
   17         NIND=NIND+1                                                      MAIN0360

   19         IF(KERROR.GT.0)GO TO  1000                                       MAIN0390
   20         XSTART=X(1)
   21         DO 8 M=2,NXBC
   22         IF (CBC(M) .LT. -1.0E-6 .AND. CBC(M-1) .GT. -1.0E-6) XSTART=X(M)
   23       8 CONTINUE
      C ------------------------------------------------------- STEP5 ----MAIN0400

   30         AUXM2=AUX2(M-1)+(AUX2(M)-AUX2(M-1))*(XU-X(M-1))/(X(M)-X(M-1))    MAIN0470
      C       **************************************************
      C       CURVATURE MODIFICATION, INTERP. WALL RADIUS
   31         CW=CBC(M-1)+(CBC(M)-CBC(M-1))*(XU-X(M-1))/(X(M)-X(M-1))
      C       **************************************************
   32         IF (KEX.EQ.1) AME=AMIE                                           MAIN0480
```

```
290         H=DEL1/DEL2                                                    MAIN3490
291         BXX=DEL1
292         REM=DEL2*UGU*RHG/VISG                                          MAIN3500
345         CALL OUT                                                       MAIN4120
346         SKIN(IPLOT)=CF2
347         STANT(IPLOT)=ST(1)
348         IF (ST(1) .LT. 1.0E-6) STANT(IPLOT)=1.0
349         XPLOT(IPLOT)=(XU-XSTART)*30.48
350         REENTH(IPLOT)=REH
351       561 CONTINUE
352         IF(LVAR.GT.1)GO TO  1000                                       MAIN4130
359         AUXM2=AUX2(M-1)+(AUX2(M)-AUX2(M-1))*(XD-X(M-1))/(X(M)-X(M-1))  MAIN4250
      C     ************************************************
      C     CURVATURE MODIFICATION, INTERP. WALL RADIUS
360         CW=CBC(M-1)+(CBC(M)-CBC(M-1))*(XU-X(M-1))/(X(M)-X(M-1))
361         SP(2)=ABS(CBC(M))
      C     ************************************************
      C.....IF IT IS DESIRED TO INTRODUCE THE WALL BOUNDARY CONDITION AS  MAIN4260
382         GO TO 15                                                       MAIN4590
383      1000 CONTINUE
384         IF (NPLOT .EQ. 1) CALL PICTRG(0.0)
385         CALL SETSMG(23,0.0)
386         CALL SETSMG(24,0.0)
387         CALL SUBJEG(-60.,0.0,130.0,0.004)
388         CALL SETSMG(130,0.01)
389         CALL SETSMG(131,0.01)
390         CALL SETSMG(132,1.0)
391         CALL CSETG('DUPLEX*')
392         CALL GRAPHG('*',1,IPLOT,XPLOT,STANT,0,'STREAMWISE DISTANCE (CM)*'
           1,'STANTON NUMBER, CF/2*','*')
393         CALL LINESG('DASH*',IPLOT,XPLOT,SKIN)
394         CALL PICTRG(0.0)
395         CALL SETSMG(23,1.0)
396         CALL SETSMG(24,1.0)
397         CALL CSETG('DUPLEX*')
398         CALL SUBJEG(200.,0.0005,5000.0,0.005)
399         CALL SETSMG(133,2.0)
400         CALL SETSMG(134,2.0)
401         CALL GRAPHG('*',1,IPLOT,REENTH,STANT,0,'ENTHALPY THICKNESS REYNOLD
           1S NUMBER*','STANTON NUMBER*','*')
402         NPLOT=1
403         IF(NIND.LT.NUMRUN)GO TO 5                                      MAIN4600
404         CALL EXITG
405         STOP                                                           MAIN4610
```

```
     3/ADD/RBOM(54),OMD(54),ROMD(54),ITKE,CBC(100),CEFF(54),CLAG,CURV,  STEP0150
     4CW,PL(54),SKIN(100),STANT(100),XPLOT(100),REENTH(100),IPLOT,XSTART
C.....                                                                  STEP0160
```

```
     3/ADD/RBOM(54),OMD(54),ROMD(54),ITKE,CBC(100),CEFF(54),CLAG,CURV,  AUX00150
     4CW,PL(54),SKIN(100),STANT(100),XPLOT(100),REENTH(100),IPLOT,XSTART
1224      DIMENSION DV(54),SHR(54),STAB(54),VELGRD(54),TPL(54)          AUX00160
```

```
1232      YPUT=RHW*UTAU/VISW                                            AUX00240
1233      KTHRU=0
1234      IF (INTG.GT.1) GO TO 10                                       AUX00250
```

```
1236      IF (MODE.EQ.2) KOUNT=1                                        AUX00270
      C   ************************************************************
      C   CURVATURE MODIFICATION -- GUESS INITIAL VALUES OF PARAMETERS
1237      SLT=YL
1238      DISSHR=BXX
1239      ALAM=SLT-DISSHR
1240      PLAM=ALAM
1241      P2LAM=PLAM
1242      P3LAM=P2LAM
1243      ISLT=N
1244      REMS=REM
      C   ************************************************************
1245    1 RAVG=R(1)                                                     AUX00280
```

```
      C.....                                                            AUX00610
1270   10 KTHRU=KTHRU+1
1271      DO 89  I=2,NP1                                                AUX00620
```

```
      C.....COMPUTE MIXING LENGTH                                       AUX01000
      C   ************************************************************
      C   CURVATURE MODIFICATION TO WAKE MIXING LENGTH
1301      ALAMA=ALAM
1302      IF (XU .LT. XSTART) ALAMA=0.85*YL
```

```
1303          IF(INTG.LT.27) ALAMA=.85*YL
1304       30 AL=ALMG*ALAMA*1.1765                                          AUX01010
1305          ALMAX=AL
      C       ************************************************************
1306          IF (KASE.EQ.1.AND.YM.LT.AL/AK) AL=AK*YM                       AUX01020

1314       35 EMUT=RHOAV*AL*AL*ABS((U(I+1)-U(I))/(Y(I+1)-Y(I)))*DV(I)*DV(I)  AUX01060
1315          PL(I)=AL/YL
1316          SP(2)=BXX
1317          SP(3)=SLT
1318          IF(K2.NE.2.OR.KASE.EQ.2)GO TO 36                              AUX01090

             1(Y(I+1)-Y(I)))/(GC*TAUW)                                      AUX01240
1332          TPL(I)=ABS(EMU(I)*(U(I+1)-U(I))/(Y(I+1)-Y(I)))/(GC*TAUW)
1333          VELGRD(I)=(U(I+1)-U(I))/(Y(I+1)-Y(I))
1334          IF (NPH.EQ.0) GO TO 89                                        AUX01250

1357       80 PREF(J,I)=0.5*(PR(J,I+1)+PR(J,I))                             AUX01560
1358       88 CONTINUE
1359       89 CONTINUE
1360          Y12=0.00
1361          YCRIT=0.0
1362          IF(CW.GE.-1.0E-6) GO TO 91
1363          SCRIT=0.25*((-CW*YL)**0.33)
1364          DO 90 I=2,NP1
1365          VELGRD(I)=(U(I)-U(I-1))/(Y(I)-Y(I-1))
1366          STAB(I)=CW*U(I)/VELGRD(I)
1367          IF(STAB(I).GT.-SCRIT) GO TO 90
1368          Y12=(-SCRIT-STAB(I-1))/(STAB(I)-STAB(I-1))
1369          YCRIT=Y12*(Y(I)-Y(I-1))+Y(I-1)
1370          GO TO 91
1371       90 CONTINUE
1372       91 P3LAM=P2LAM
1373          P2LAM=PLAM
1374          PLAM=SLT-DISSHR
1375          NPSHR=NP1-1
1376          TAUMAX=0.0
1377          DO 92  I=3,NPSHR
1378       92 IF(TPL(I).GT.TAUMAX) TAUMAX=TPL(I)
1379          CNTR=0.65
1380          BAND=0.25
1381       93 KLUNK=0
1382          NFIT=0
1383          SUM1=0.0
1384          SUM2=0.0
1385          SUM3=0.0
1386          SUM4=0.0
1387          DO 94 I=1,NPSHR
1388          UPPER=(CNTR+BAND)*TAUMAX
```

```
1389          ALOWR=(CNTR-BAND)*TAUMAX
1390          IF(KLUNK.GT.0) GO TO 94
1391          NSRC=NP1-I
1392          IF(TPL(NSRC).GE.(0.93*TAUMAX)) KLUNK=1
1393          IF(TPL(NSRC).GT.UPPER.OR.TPL(NSRC).LT.ALOWR) GO TO 94
1394          NFIT=NFIT+1
1395          SUM1=SUM1+Y(NSRC)
1396          SUM2=SUM2+TPL(NSRC)
1397          SUM3=SUM3+TPL(NSRC)*Y(NSRC)
1398          SUM4=SUM4+TPL(NSRC)*TPL(NSRC)
1399       94 CONTINUE
1400          IF (NFIT .EQ. 0) GO TO 98
1401          ANUM=SUM3-(SUM1*SUM2/NFIT)
1402          DENUM=SUM4-(SUM2*SUM2/NFIT)
1403          IF(DENUM.LE.0.0) WRITE(6,96) (I,Y(I),U(I),TPL(I), I=1,NPSHR)
1404          IF(BAND.GT.0.50) GO TO 100
1405          IF(DENUM.GT.0.0.AND.NFIT.GT.2) GO TO 100
1406       96 FORMAT(2X,I3,4X,F9.5,4X,F7.2,4X,F7.4)
1407       98 BAND=BAND*1.25
1408          GO TO 93
1409      100 YE=(SUM1-SUM2*(ANUM/DENUM))/NFIT
1410          IF(INTG.GT.19.AND.INTG.LT.30) WRITE(6,97) (I,Y(I),U(I),
             1TPL(I),VELGRD(I),PL(I), I=1,NPSHR)
1411       97 FORMAT(2X,I3,4X,F9.5,4X,F7.2,4X,F7.4,4X,F7.0,4X,F7.4)
1412      102 CONTINUE
1413          SLT=YE
1414          WRITE(6,111) YE,YCRIT,SLT,CW
1415          IF (CW .GE. -1.0E-6  .OR. YCRIT .LT. 1.0E-6) GO TO 107
1416          SLT=YCRIT
1417          IF (YE .LE. YCRIT) GO TO 107
1418          ACO=2.00
1419          SLTR=1.0-ACO*((YE/YCRIT)-1.0)
1420          IF (SLTR .LT. 0.33) SLTR=0.33
1421          SLT=SLTR*YCRIT
1422          WRITE (6,111) YE,YCRIT,SLT,CW
1423      111 FORMAT (1X,'DELSL FROM SHEAR STRESS PROFILE =',F10.5
             1,10X,'DELSL FROM SCRIT=',F10.5,'DELSL IN MIXING LENGTH ='
             2,F10.5,'CW= ',F10.5)
1424      107 IF(SLT.GT.1.2*YL) SLT=1.2*YL
          C      FIND NEW DELTASTAR BASED ON SHEAR LAYER THICKNESS
          C       FIND NEW EDGE VELOCITY
1425          KSLT=0
1426          DO 103 I=2,NP1
1427          IF(KSLT.EQ.0.AND.Y(I).GT.SLT) ISLT=I
1428          IF(Y(I).GT.SLT) KSLT=1
1429      103 CONTINUE
1430          IF(KSLT.EQ.0) GO TO 105
1431          USLT=UGU
1432          DISSHR=(1.-U(2)/USLT)*(Y(2)/2)
1433          DMOMT=(U(2)/USLT)*DISSHR
1434          ISLT1=ISLT-1
1435          DO 104 I=3,ISLT1
1436          DISSHR=DISSHR+((1.-U(I-1)/USLT)+(1.-U(I)/USLT))
             1*(Y(I)-Y(I-1))/2.
1437          DMT1=(U(I)/USLT)*(1.-(U(I)/USLT))
1438          DMT2=(U(I-1)/U(ISLT))*(1.-(U(I-1)/U(ISLT)))
1439      104 DMOMT=DMOMT+(DMT1+DMT2)*(Y(I)-Y(I-1))/2.
1440          DISSHR=DISSHR+(1.-U(ISLT1)/USLT)*(SLT-Y(ISLT1))/2.
1441          DMINC=(U(ISLT1)/USLT)*(1.-U(ISLT1)/USLT)*(SLT-Y(ISLT1))/2.
1442          DMOMT=DMOMT+DMINC
1443          REMS=DMOMT*USLT*RHO(1)/VISCO(1)
1444      105 IF(KSLT.EQ.0) DISSHR=BXX
1445          ALAM=SLT-DISSHR
1446          IF(INTG.GT.0.AND.INTG.LT.299) WRITE(6,106) INTG,SLT,DISSHR,
             1YL,NFIT,REMS,ALMAX,KTHRU
1447      106 FORMAT(1X,'INTG =',I4,3X,'SLT =',F8.5,3X,'DISSHR =',F8.5,3X,
             1'DEL99=',F7.4,3X,'KFIT=',I2,4X,'REMS=',F7.2,4X,'LMAX=',F7.4,
             22X,'KTHRU=',I3)
1448          IF(ABS(ALAM-P2LAM).LE.(0.05*YL)) ALAM=(PLAM+ALAM)/2.
1449      108 CONTINUE
1450          DO 110 I=2,NP1                                          AUX01600
```

```
     2/CN/AXX,BXX,CXX,DXX,EXX,K1,K2,K3,SP(54),AUX1(100),AUX2(100),YPMAX OUT00140
     3/ADD/RBOM(54),OMD(54),ROMD(54),ITKE,CBC(100),CEFF(54),CLAG,CURV,
     4CW,PL(54),SKIN(100),STANT(100),XPLOT(100),REENTH(100),IPLOT,XSTART
C.....                                                                 OUT00150
```

```
C.....PROPERLY, IT MUST BE THE LAST EQUATION SOLVED.                   OUT00240
1512       IF(INTG.GT.29.AND.INTG.LT.39) SPACE=1
1513       IF(INTG.GT.39) SPACE=10
1514       IF(INTG.GT.29.AND.INTG.LT.39) KSPACE=1
1515       IF(INTG.GT.39) KSPACE=10
1516       IF(INTG.GT.59.AND.INTG.LT.70) SPACE=1
1517       IF(INTG.GT.70) SPACE=10
1518       IF(INTG.GT.59.AND.INTG.LT.70) KSPACE=1
1519       IF(INTG.GT.70) KSPACE=10
1520       IF(KIN.NE.1)GO TO 600                                       OUT00250
```

```
1559       WRITE(6,284)NINTG,XU,UGU,CAY,FAM,REM,CF2,H,REH,STA,F(1,1),CPL,AME OUT00640
1560       IPLOT=IPLOT+1
1561       IF(K1.GT.10)WRITE(6,286)(SP(I),I=1,5),G,BTA                 OUT00650
```

```
     2/CN/AXX,BXX,CXX,DXX,EXX,K1,K2,K3,SP(54),AUX1(100),AUX2(100),YPMAX INPU0140
     3/ADD/RBOM(54),OMD(54),ROMD(54),ITKE,CBC(100),CEFF(54),CLAG,CURV,
     4CW,PL(54),SKIN(100),STANT(100),XPLOT(100),REENTH(100),IPLOT,XSTART
C.....                                                                 INPU0150
```

```
C (DECIMAL NUMBERS, IN THE FORM OF A TABLE.)                           INPU2140
C     ***************************************************
C          CURVATURE MODIFICATION, READ WALL CURVATURE
1817    90 READ(5,580) X(M),RW(M),AUX1(M),AUX2(M),CBC(M)               INPU2150
C     ***************************************************
C.....                                                                 INPU2160
```

```
      C ***********************************************************************INPU3500
      C (DECIMAL NUMBERS)
1854        READ(5,580) CLAG,CURV
      C.....
      C  CLAG IS THE CONSTANT IN THE EFFECTIVE CURVATURE LAG EQUATION.
      C  RECOMMENDED VALUE IS 3.3, CURV IS THE MIXING LENGTH MODIFICATION
      C  CONSTANT, RECOMMENDED VALUE IS 8.
      C  ***************************************************************
      C (DECIMAL NUMBERS)                                                  INPU3510
1880        READ(5,580) GC,CJ,AXX,BXX,CXX,DXX,EXX                          INPU4010
1881        CXX=CURV
1882        AXX=CLAG
          C.....                                                           INPU4020
```

1. Report No.	2. Government Accession No.	3. Recipient's Catalog No.
NASA CR-3510		

4. Title and Subtitle	5. Report Date
TURBULENT BOUNDARY LAYER HEAT TRANSFER EXPERIMENTS: CONVEX CURVATURE EFFECTS INCLUDING INTRODUCTION AND RECOVERY	February 1982
	6. Performing Organization Code

7. Author(s)	8. Performing Organization Report No.
T. W. Simon, R. J. Moffat, J. P. Johnston, and W. M. Kays	HMT-32
	10. Work Unit No.

9. Performing Organization Name and Address	11. Contract or Grant No.
Stanford University Department of Mechanical Engineering Stanford, California 94305	NSG-3124 and NAG 3-3
	13. Type of Report and Period Covered

12. Sponsoring Agency Name and Address	13. Type of Report and Period Covered
	Contractor Report
National Aeronautics and Space Administration Washington, D.C. 20546	14. Sponsoring Agency Code
	505-32-2B

15. Supplementary Notes

Final report. Project Manager, Raymond E. Gaugler, Aerothermodynamics and Fuels Division, NASA Lewis Research Center, Cleveland, Ohio 44135.

16. Abstract

Measurements have been made of the heat transfer rate through turbulent and transitional boundary layers on an isothermal, convexly curved wall and downstream flat plate. The effect of convex curvature on the fully turbulent boundary layer was a reduction of the local Stanton numbers 20 to 50% below those predicted for a flat wall was under the same circumstances. The recovery of the heat transfer rates on the downstream flat wall was extremely slow. After 60 cm of recovery length, the Stanton number was still typically 15 to 20% below the flat-wall predicted value. Various effects important in the modeling of curved flows were studied separately. These are: (1) the effect of initial boundary layer thickness, (2) the effect of freestream velocity, (3) the effect of freestream acceleration, (4) the effect of unheated starting length, and (5) the effect of the maturity of the boundary layer. An existing curvature-prediction model was tested against this broad heat transfer data base to determine where it could appropriately be used for heat transfer predictions.

17. Key Words (Suggested by Author(s))	18. Distribution Statement
Boundary layer Curvature Turbulence modeling	Unclassified - unlimited STAR Category 34

19. Security Classif. (of this report)	20. Security Classif. (of this page)	21. No. of Pages	22. Price*
Unclassified	Unclassified	214	A10

* For sale by the National Technical Information Service, Springfield, Virginia 22161

NASA-Langley, 1982